MEDI-BED VOL 2

Energy, Entropy and Quantum Tunneling of Protons and Electrons in Brain Mitochondria: Relation to Mitochondrial Impairment in Aging-Related Human Brain Diseases and Therapeutic Measures

James P Bennett Jr [1,*], Isaac G Onyango [2]

Abstract

Adult human brains consume a disproportionate amount of energy substrates (2–3% of body weight; 20–25% of total glucose and oxygen). Adenosine triphosphate (ATP) is a universal energy currency in brains and is produced by oxidative phosphorylation (OXPHOS) using ATP synthase, a nano-rotor powered by the proton gradient generated from proton-coupled electron transfer (PCET) in the multi-complex electron transport chain (ETC). ETC catalysis rates are reduced in brains from humans with neurodegenerative diseases (NDDs). Declines of ETC function in NDDs may result from combinations of nitrative stress (NS)–oxidative stress (OS) damage; mitochondrial and/or nuclear genomic mutations of ETC/OXPHOS genes; epigenetic modifications of ETC/OXPHOS genes; or defects in importation or assembly of ETC/OXPHOS proteins or complexes, respectively; or alterations in mitochondrial dynamics (fusion, fission, mitophagy). Substantial free energy is gained by direct O_2-mediated oxidation of NADH. Traditional ETC mechanisms require separation between O_2 and electrons flowing from NADH/$FADH_2$ through the ETC. Quantum tunneling of electrons and much larger protons may

facilitate this separation. Neuronal death may be viewed as a local increase in entropy requiring constant energy input to avoid. The ATP requirement of the brain may partially be used for avoidance of local entropy increase. Mitochondrial therapeutics seeks to correct deficiencies in ETC and OXPHOS.

Keywords: mitochondria, electron transport chain, oxidative phosphorylation, ATP, brain energy metabolism, neurodegenerative diseases, oxidative stress, nitrative stress

1. Introduction

A 70 kg human adult nominally makes ~70 kg of adenosine triphosphate (ATP) per 24 h. Under conditions of normal oxygen availability, most of this ATP is made in mitochondria by oxidative phosphorylation (OXPHOS) of energy substrates directly or indirectly created by solar photons through photosynthesis. This amount of ATP (8.31×10^{25} molecules/24 h) requires ~20.8×10^{25} electrons/24 h to be passed through the mitochondrial electron transport chain (ETC), when ~2.5 electrons are required for each ATP generated by ATP synthase under normal coupling. If the adult brain, which comprises 2–3% of body weight, but consumes at least ~20% of molecular oxygen and energy substrates [1], contains on average 86 billion (86×10^9) neurons [2], and if each neuron contains 1000 mitochondria (likely an overestimate), then each neuronal mitochondrion in the brain must pass on average 1.40×10^7 electrons/s to maintain ATP production. This estimation is based on glucose utilization/oxygen consumption being split 1–1 between neurons and nonneuronal cells in the brain and is not corrected for glial generation of lactate (from glucose) and neuronal metabolism of glial lactate.

If each neuronal mitochondrion has 10^4 ETC macrocomplexes (“respirasome”; likely an overestimate) along the inner membrane cristae, then each ETC macrocomplex passes ~1400 electrons/s (0.0007 s·electron^{-1}) and at least ~7000 protons/s (0.00014 s·proton^{-1}) to maintain ATP production. (Note that this estimate of proton translocation rate (1.4×10^{-4} s/proton) is comparable to the lower estimate (0.35×10^{-4} s) of proton tunneling time through an AT base pair in DNA at room temperature [3,4].) These calculations represent lower-limit averages with debatable assumptions (i.e., likely more protons are translocated), and they do not include corrections for electron or proton leakage/scavenging, variations in coupling between electron flow and ATP synthesis, variations in substrate availability, or other conditions of mitochondrial “health”.

What is apparent from these average estimates of electron and proton velocities (*momenta*, if particle masses are also considered) is that Nature has designed in mitochondria efficient and stereotyped mechanisms for controlling electron and proton flow to transform potential energies of solar photon-derived small molecules acquired by photosynthesis into ATP. One intriguing but unresolved question is whether mitochondria ultimately represent an organelle mediating a transition between quantum and classical behaviors of electrons and protons. Again, note that several-fold more protons are pumped than electrons are passed to maintain ATP production.

The ETC/OXPHOS process in mitochondria is therefore critical to energy metabolism in the brain. The mitochondrial ETC/OXPHOS process is also damaged during human aging, mainly as

a result of consuming so much oxygen, leading to “oxidative stress”. Such damage is particularly meaningful for brain energy metabolism and may account for the increased incidence of degenerative brain diseases associated with aging.

2. Quantum Tunneling of Protons and Electrons in Mitochondria

Electrons (mass = 9.11×10^{-28} gm) and protons (mass = 1.67×10^{-24} gm) are both quantum entities that are best described as waves existing in probabilistic vector spaces (“quantum fields”) with “spin” one-half and are either elementary particles (electrons) or composed of quarks (protons) in the standard model. These “waves” become “particles” upon certain types of detection, potentially explaining the wave–particle duality universally observed in quantum entities since their descriptions in the early 20th century (see [5]).

According to the Heisenberg uncertainty principle, the locations and momenta of electrons and protons cannot be precisely known at the same time, at least when moving through empty space. Yet contemporary descriptions of mitochondrial function appear to violate this principle, and it is critical that the momentum-location constraints on electrons and protons be kept in mind as mitochondrial ETC activity is analyzed.

It is likely, though not proven, that proton pumping (mitochondrial proton-coupled electron transfer (PCET)) occurs in Complex I through protein subunits separable from those mediating electron transport [6]. These proton-pumping complexes appear to be composed of the seven hydrophobic Complex I subunits coded by the mitochondrial genome (mtDNA) [6]. If this formulation is correct, then damage/mutations to mtDNA (at least to the seven Complex I subunits) will selectively affect proton pumping rates and not directly alter ETC catalytic rates.

Although the electron acceptor molecule (ubiquinone) for electron flow in Complex I is well characterized, there does not appear to be a separate proton acceptor molecule in the intermembrane space, other than water molecules. Because the downstream ATP synthase rotor head (for OXPHOS) appears to accept only protons (not hydrated protons, [7]), this situation begs the question of how pumped protons are “protected” from hydration by water molecules in the mitochondrial intermembrane space. (Note that proton solvation by water is very energetically favorable with Free energy ~266 kcal/mol.). Perhaps there exists an as of yet unknown proton acceptor molecule in the intermembrane space (other than water) with different thermodynamics of proton binding? An alternative mechanism proposed by Leone, et al. [7] is that the rotor arms of ATP synthase operate using a gradient of un-hydrated protons bound to carboxylate anions, with water molecules separately bound to the rotor arms.

3. Decoherence

It is debatable as to whether decoherence occurs to a significant degree in mitochondria. Stated simplistically, decoherence (loss of “quantum-ness”) occurs when there is interaction of quantum

entities with non-quantum, classical macroscopic objects such that quantum behavior is reduced or lost [8]. Mitochondria may properly be considered macroscopic entities; whether Complex I iron–sulfur centers with low energy molecular orbitals that are separated by 14 angstroms or less, and thus form "wires" for conducting electrons, meet the same criterion is debatable. The addition of nearby water molecules arranged in tandem appears to provide a pathway for electron tunneling through these wires, which reduces activation energies (thus increasing rates) but theoretically has no effect on the energetics of electron movement ([9] and references therein).

Tunneling is the phenomenon of quantum entities appearing to pass through energy barriers due to their wave properties and small (nonzero) probabilities (wave function (Ψ^2)) of existing on either side of barriers defining an energy well [10] (also, see Figure 1). Tunneling is considered to be a quantum phenomenon; thus, if decoherence is dominant in mitochondrial ETC function, then tunneling is less probable. Contrarily stated, the greater the quantum-ness of ETC behavior, the greater the probability that tunneling may occur.

Figure 1.

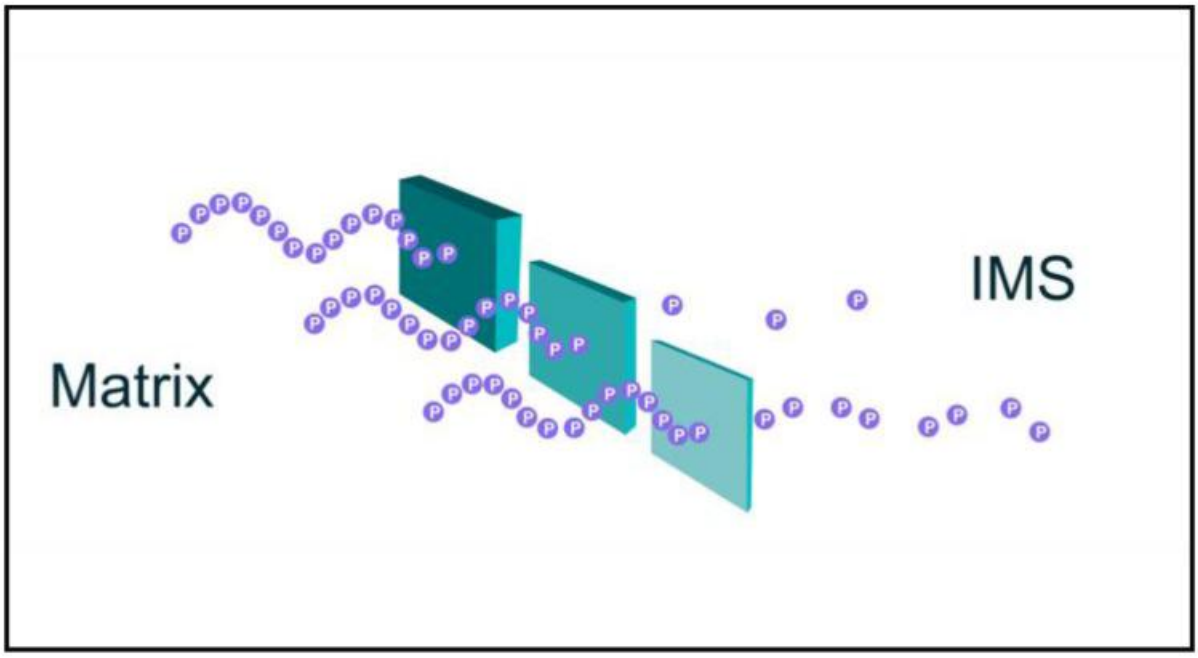

Cartoon of proton tunneling. Protons pumped from the mitochondrial matrix into the intermembrane space (IMS) must overcome electrostatic repulsion of other protons (already in the IMS?) and likely avoid "irreversible" solvation by water. These are but two of likely several energy barriers that protons must overcome, and "quantum tunneling" may provide a mechanism to overcome energy barriers experienced by protons moving into the IMS and increase rates of proton pumping.

Shown in Figure 1 are protons (purple spheres) moving as a sine wave through barriers of variable thickness. Mathematically, quantum tunneling may be viewed as follows: Let ***P*** be the probability of a particle with mass ***m*** and energy ***E*** passing through a barrier with energy ***V***:

$$\boldsymbol{P} = \exp\left(-4 \times \boldsymbol{\alpha} \times \pi h \times \sqrt{2} \times \boldsymbol{m} \times (\boldsymbol{V} - \boldsymbol{E})\right) \quad (1$$

where $\boldsymbol{V}$ is the energy of the potential barrier, $\boldsymbol{E}$ is the kinetic energy possessed by the particle, $\boldsymbol{\alpha}$ is the thickness of the barrier, $\boldsymbol{m}$ is mass of the particle (in the case of protons, mass = 1.67×10^{-24} gm), and h is Plank's constant (6.626×10^{-34} $m^2 \cdot kg/s$). (Above taken from ChemLibre Texts: https://chem.libretexts.org/Bookshelves/Physical_and_Theoretical_Chemistry_Textbook_Maps/Supplemental_Modules_(Physical_and_Theoretical_Chemistry/Quantum_Mechanics/02._Fundamental_Concepts_of_Quantum_Mechanics/Tunneling (accessed on 21 February 2021)). (The above are taken from [9]).

By this formula, decreasing barrier thickness ($\boldsymbol{\alpha}$) will increase the probability of tunneling through an energy barrier. This is presented in Figure 1.

Electron tunneling in Complex I was recently reviewed [9] (and references therein). Proton tunneling has been described in laboratory experiments, typically performed at very cold temperatures and high pressures [11]. Proton tunneling in mitochondrial ETC has not been described but has been proposed to occur through hydrogen bonds in replicating DNA molecules as a mechanism of spontaneous DNA mutation [3]. Proton tunneling may also occur in the "Grotthuss" mechanism of "proton jumping", whereby protons move through a hydrogen bond network of adjacent water molecules [12,13].

PCET [14] has been proposed (at least in X-ray resolved crystals of bacterial Complex I) to occur by the combination of electrostatic charge-mediated conformational change in tertiary structure of proton channels following reduction of ubiquinone [15,16]. By this "action at a distance" mechanism, channels in proton-pumping Complex I subunits (see Figure 2) are opened as a result of two electron reduction of ubiquinone following attachment of NADH to its binding site in the matrix side of Complex I and oxidation of NADH to NAD+ with reduction of attached FMN cofactor, followed by passage of the two resulting electrons to ubiquinone to form ubiquinol.

Figure 2.

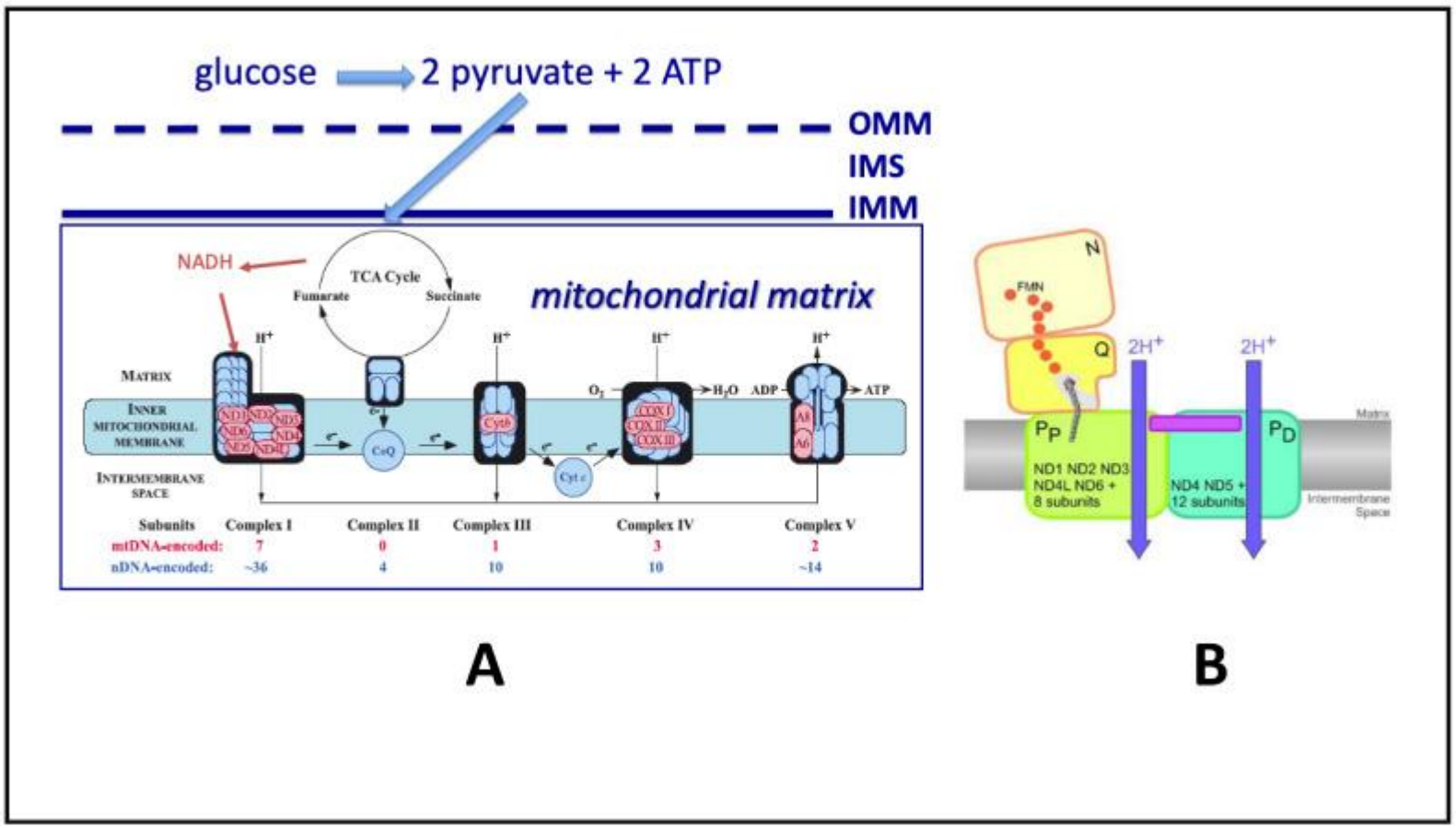

Overview of Mitochondrial Electron Transport Chain ETC/Oxidative Phosphorylation (OXPHOS) and ATP Production. (A). (left) Linear representation of the mitochondrial ETC/OXPHOS system. Shown are the 5 mitochondrial complexes involved in ETC/OXPHOS. In pink are the 13 individual protein subunits derived by transcription of mtDNA genes (usually maternally derived) and translated in the mitochondrial matrix. In blue are the protein subunits derived from nDNA (paternally and maternally derived) that are synthesized in the cytosol and imported into mitochondria. Mammals are now thought to have a total of 45 subunits in Complex I (7 from mtDNA, 38 from nDNA). In the brain, glucose is believed to be the major carbon energy source that is transformed to ATP. In other tissues, mitochondria can metabolize fatty acids and amino acids. Glucose (6 carbons) is broken down outside of mitochondria into 2

pyruvate molecules (3 carbons each) by glycolysis, and the resulting pyruvate is imported into the mitochondrial matrix by specific pyruvate carrier proteins that span the relatively protein-rich outer mitochondrial membrane (OMM), the intermembrane space (IMS), and the relatively lipid-rich inner mitochondrial membrane (IMM). Once in the matrix, pyruvate is oxidatively decarboxylated by the tricarboxylic acid cycle (TCA cycle), yielding reducing electrons that in pairs reduce the electron carrier NAD^+ to NADH. NADH is subsequently oxidized back to NAD^+ at Complex I (thus its name, *NADH-NAD oxidoreductase*) and transfers its two electrons to flavin mononucleotide (FMN) that is embedded in the hydrophilic (matrix) arm of Complex I. FMN then passes these two electrons through the Fe–S centers of Complex I to reduce the electron carrier ubiquinone to ubiquinol. This reaction provides the initial free energy that is used for proton pumping. Ubiquinol is reoxidized to ubiquinone at Complex III, where a separate electron carrier in the IMS, cytochrome C, is reduced. Reduced cytochrome C is reoxidized at Complex IV, giving up electrons that participate in the reduction of molecular oxygen to water. Protons are pumped into the IMS at Complexes I, III, and IV (none at Complex II, now regarded as a component of the TCA cycle), and the resulting proton gradient is used to drive ATP production by Complex V. (B). (right) Cartoon showing separate ETC and proton-pumping components of Complex I (taken from Figure 6 of [6]). Shown are the embedded FMN moiety and the nine Fe–S centers that pass electrons through Complex I (orange circles), leading to reduction of ubiquinone to ubiquinol. Additionally shown are the proposed separate proton-pumping subunits of Complex I that consist of proximal (P_P) and distal (P_D) subunits that are both believed to be located primarily in the lipid IMM and are in turn composed of the 7 hydrophobic proteins coded by mtDNA and 8 or 12 proteins coded by nDNA, respectively. Proton tunneling into the IMS may occur at these sites.

The energetics of ubiquinone reduction theoretically drive the translocation of protons across the inner membrane through proton channels in Complex I subunits “opened” by ubiquinone reduction, but a simpler proton tunneling mechanism may be operative and contribute to the overall PCET rate of Complex I (please also see [6,15,16,17]). Note that the proposal of proton tunneling does not change the bioenergetics, which depend on the free energy of ubiquinone reduction to ubiquinol, but proton tunneling could lower activation energy of proton passage and thus increase the rate of proton pumping. Ubiquinone reduction-induced conformational changes (“action at a distance”) and proton tunneling could synergistically work together to induce Complex I proton displacement, such that proton pumping would not be rate limiting in Complex I PCET. (Please see Figure 2 for a current model of Complex I subunits mediating proton pumping).

Which mechanism might be affected in neurodegenerative diseases (NDDs) (if either mechanism is even operative) is unknown. The possibility should also be considered that proton pumping is not directly affected by NDD pathobiology, and that the major deficit leading to a reduced rate of ATP synthesis is lowering of electron transport rate. Finally, we are aware of no data supporting or refuting the existence of electron quantum tunneling in the other ETC complexes (beyond Complex I, which has been crystallized) and no data supporting or refuting the existence of proton quantum tunneling in any ETC Complex.

4. Entropy and Neurodegeneration

Whatever origin of the observable universe hypothesis one subscribes to, all can agree that the cosmological evidence supports the ongoing expansion of the observable universe with a resulting steady increase in entropy. Earlier thermodynamic theorists (such as Clausius) describing the varying forms of this "Second Law of Thermodynamics" developed the concept that the entropy in the Universe may remain constant but is more likely constantly increased, regardless of what happens locally.

The human brain and its ~86 billion neurons display a marked (increase in order)/(decrease in disorder) that represents thermodynamically a decrease in entropy of cellular molecules. In fact, all cells, and life forms themselves, represent a reduction in molecular entropy; from this perspective, cell and organismal death can be viewed as an (inevitable) increase in molecular entropy.

Might neurodegeneration and neuronal death also be viewed as a local increase in entropy, driven ultimately by a reduction in energy input, whatever the "genesis" cause(s) of the bioenergetic deficit? By this paradigm, neuronal death and its attendant increase in molecular entropy would be thermodynamically favored, independent of whether it occurred during "life" or after organismal "death". If occurring during life, then a clinical phenotype is generated that can be discerned (i.e., loss of cognitive capacity in Alzheimer's disease (AD); loss of smooth voluntary movement in Parkinson's disease (PD); loss of muscle mass and appearance of weakness in amyotrophic lateral sclerosis (ALS), etc.).

If this paradigm is true, then prevention of neuronal death (in NDDs) can be viewed as a thermodynamic problem with potential thermodynamic solutions. For example, energy input, which is already disproportionately elevated in adult human brain, could be increased by processes that stimulate mitochondrial energy transformation and ATP synthesis. One could also attempt to increase synaptogenesis and size/interactions of neuronal networks (which should also reduce neuronal molecular entropy). However, we wish to note that no reported therapeutic strategies derived from the above thermodynamic hypothesis of neuronal death have yet been published.

5. Oxidative Phosphorylation (OXPHOS) Alterations in NDDs

OXPHOS is an evolved process in which electron flow through the ETC is coupled to proton translocation from the mitochondrial matrix to the intermembrane space, creating a proton and pH gradient between the mitochondrial matrix and intermembrane space. The resulting proton gradient is used to rotate the arm of ATP synthase, an evolutionarily old enzyme [18] that appears to require non-hydrated protons to operate [7] (see above). As discussed previously, this PCET may utilize proton tunneling and/or structural alterations in proton-pumping subunits of the ETC (at least for Complex I).

Because electron flow (at least in Complex I) is believed to use a tunneling mechanism (for discussion see [9] and references therein), structural alterations to proteins critical to electron tunneling may result in reduced rates of electron flow, leading to reduced rates of proton

pumping and ATP synthesis. This could result in a bioenergetic deficiency state, based on maintaining a minimum rate of ATP synthesis necessary for neuronal functions (see above). By this mechanism, proton pumping (PCET) would not be mechanistically impaired per se, just reduced in rate.

In NDDs variable reductions in ETC rates at one or more specific complexes have been described. Epigenetic modifications potentially responsible for these reductions include pre-transcriptional changes to genes such as gene methylation and histone modifications that affect gene promoter or repressor activities. Epigenetic alterations have been described in amyotrophic lateral sclerosis (ALS, [19]), Parkinson's disease (PD, [20,21,22,23,24,25,26,27,28]), and Alzheimer's disease (AD, [19,20,21,22,25,28,29,30,31,32,33,34,35]). In many studies, cell or animal models of NDDs are utilized, with the understanding that similar phenomena may occur in the more common sporadic forms of each NDD.

Reductions in bioenergetics may also derive from nitrative damage to proteins, particularly to nitration of tyrosine residues by peroxynitrite anion ($ONOO^-$). So-called "nitrative stress", which is frequently found in models that demonstrate "oxidative stress", have been described in ALS [36,37,38,39,40,41,42,43], AD [36,37,40,44,45,46,47,48,49,50,51,52,53,54,55], and PD [36,37,40,42,44,53,55,56,57,58,59,60,61,62,63,64,65,66,67,68,69,70,71,72,73] tissues.

Oxidative stress (OS) is the condition where production rates of oxidizing species exceed rates of inactivation. Oxidizing species may damage lipids, nucleic acids, and proteins and thus are potentially toxic to cells and energy production at several levels. Because most molecular oxygen is utilized by mitochondria for ETC activity (and is reduced to water), mitochondria are particularly susceptible to OS. OS damage has been described in ALS [74,75], AD [31,35,44,45,50,52,53,55,76,77,78,79,80,81,82,83,84,85,86,87,88,89], and PD [24,36,53,55,56,57,60,62,63,64,65,66,67,71,77,90,91,92,93,94,95,96,97] tissues and models.

6. Summary of ETC-OXPHOS

The human brain has disproportionately elevated (~10-fold, relative to mass) energy substrate and oxygen consumption rates. These elevated metabolic rates in brain likely depend on electron and proton tunneling in mitochondria, although neither of these processes has been conclusively demonstrated to occur. Mitochondria can be viewed as transitional organelles that bridge the quantum world of very small wave-particle behavior and the classical world of decoherent larger, more macroscopic structures such as cells.

Photosynthesis yields both the small molecules that directly or indirectly drive mitochondrial electron transport and the toxic by-product (molecular oxygen) that is an excellent electron acceptor (oxidant) for terrestrial life. The highly electrophilic nature of molecular oxygen requires "protection" of reducing equivalents (as mainly NADH) and competes with ETC thermodynamics to yield oxygen free radicals. These free radicals must be detoxified or they will damage cellular constituents (proteins, lipids, nucleic acids) and can combine in several ways with other molecules to yield nitrogen–oxygen toxins ("nitrative stress").

Protons pumped into the intermembrane space theoretically require protection from thermodynamically favorable hydration, since non-hydrated protons appear to be favored for driving the ATP synthase rotor [7]. How this occurs is presently unknown but may require anatomic proximity of ATP synthase rotor proton-binding sites to proton-pumping sites or an as yet unknown proton solvation system other than water alone. An alternative mechanism presented by Leone et al., involves carboxylate protonation (by non-hydrated protons) and binding of water (from hydronium ions) to ATP synthase [7]. By this mechanism, hydrated protons could drive ATP synthase, but the H_3O^+ ions would dissociate rapidly into H^+ and H_2O that would separately bind to ATP synthase.

These massive energy transformation systems appear to be damaged in neurodegenerative diseases (NDDs), at least in terms of ease of detecting epigenetic alterations/oxidative stress damage/nitrative stress damage. The result could be a reduction in neuronal ATP synthesis rate, with neuronal dysfunction leading to emergence of early clinical phenotypes and an ultimate increase in entropy following neuronal death or even autophagic digestion of organelles (i.e., mitophagy).

Nature was tasked with producing large quantities of ATP that are used by neurons for many purposes, including the lifetime (usually over many decades) maintenance of nondividing state and recharging of neuronal potentials where rapid potential swings are necessary for functions of both individual neurons and neuronal networks. A truly remarkable system resulted, which appears to fade as organisms age and accumulate biochemical damages over a lifetime. Whether these aging phenomena can be more successfully controlled and the burden of NDD reduced are future challenges to mitochondrial therapeutics.

7. Brain Mitochondrial Therapeutics

The human brain is one of several tissues that are “non-mitotic”, meaning that the majority of its cells do not undergo cell division during most of the organism’s lifetime. In fact, entering the cell cycle is considered a lethal event for mature neurons, compared to “mitotic” cells of mesodermal and endodermal origins that regularly die, divide, and are thus replaced.

Even in non-mitotic neurons, mitochondria undergo their own cycles of DNA (mitochondrial DNA, mtDNA) replication. While the mechanistic details of mtDNA replication remain debated, all agree that mtDNA replication is independent of host cell division in both non-mitotic (should be small or nonexistent) and mitotic tissues.

We have yet to learn how mtDNA replication is regulated, although some knowledge exists about the molecules and their hierarchy of control for mtDNA replication. For instance, mtDNA replication utilizes a DNA polymerase specially synthesized by nuclear genes for mtDNA replication, coded for by host cells (DNA polymerase gamma) and imported into mitochondria. There appear to be multiple copies of mtDNA within each mitochondrion, but it remains unclear how that number is regulated. Additionally, not all copies of mtDNA within each mitochondrion, and thus within each cell, are necessarily identical, a condition known as heteroplasmy. In

addition, mtDNA appears to have a higher mutation rate than does nuclear DNA, ascribed to both the relative lack of protective proteins and limited DNA repair mechanisms.

The thirteen genes encoded by mtDNA (all for ETC/OXPHOS function) are believed to be translated within the mitochondrial matrix using a genetic code similar to but not identical with the code used in nuclear DNA–nuclear mRNA translation. Special mitochondrial chaperone proteins (again provided by the host cell) appear to assist assembly of the ETC/OXPHOS complexes that are characterized by many nuclear DNA-encoded subunits and lesser numbers of more hydrophobic mtDNA-encoded subunits. Again, several of the regulatory proteins for mtDNA transcription (synthesized from nuclear DNA genes and imported into mitochondria) are known, but the complete details of regulation of mtDNA transcription and translation/assembly into functioning ETC/OXPHOS complexes remain unclear.

Mitochondrial therapeutics strategies, in terms of ATP production, are difficult to implement currently, due mainly to ignorance about details of how mitochondria within brain neurons (and many other cell types) regulate/are regulated in terms of ETC/OXPHOS and thus ATP production capacities. Several approaches can be discussed, and this list is by no means complete:

- Correction of mtDNA mutations
- Correction of mtRNA and/or mitochondrial mRNA errors
- Increase in mitochondrial mass leading to increased ETC/OXPHOS capacity to make ATP
- Prevention of epigenetic, nitrative stress (NS) and oxidative stress (OS) damage to ETC/OXPHOS genes or proteins

The above potential strategies relate solely to mitochondrial ETC/OXPHOS function and not directly to regulation of mitochondrial calcium signaling or cell death initiation, important mitochondrial functions not addressed in this review.

7.1. Correction of mtDNA Mutations

The development of rapid and relatively inexpensive “next-generation” DNA sequencing has allowed the development of “3-parent babies” as a viable strategy for prevention of mtDNA-transmitted mutations. If precautions are taken to screen out mitochondrial “pseudogenes” (stretches of nuclear DNA containing variable amounts of mtDNA sequences [98]), then specific mtDNA mutations can be defined in oocytes of mothers who have given birth to a child with a mtDNA mutation-derived disease. Because the mother’s oocytes may contain variable proportions of mutant compared to wild-type mtDNA (recall heteroplasmy), and because maternal transmission of mtDNA is the rule, implantation and growth of oocytes containing only wild-type mtDNA and both maternal and paternal nuclear genomes is now possible with mitochondrial replacement therapy. This can be accomplished by transferring the maternal meiotic nuclear spindle into a donor oocyte that contains only wild-type mtDNA (and has its own nuclear meiotic spindle removed), followed by fertilization with paternal sperm. This technique is referred to as maternal spindle transfer (MST). An alternative approach is to fertilize

a donor oocyte with paternal sperm, then remove the paternal-donor pronuclei and replace them with pre-fusion maternal and paternal pronuclei. This approach is known as pronuclei transfer (PNT). See [99] for details. These approaches to a 3-parent baby have been developed, discussed, and implemented in the UK by the Newcastle group [99,100,101,102,103,104] and by the Mitalipov group at Oregon Health Sciences University [100,105,106,107,108,109,110,111,112,113,114,115,116,117,118,119].

7.2. Correction of mtRNA and/or Mitochondrial mRNA Errors

The mtDNA genome contains 13 sequences/genes for ETC/OXPHOS proteins that are made in the mitochondrial matrix, 22 tRNA sequences for ribosomal protein synthesis, and 2 rRNA's that assist in making ETC/OXPHOS proteins from mtDNA genome sequences (that first must be transcribed into mtRNAs). Many of the mtDNA mutational errors that impact translation of mtRNA sequences are mutations in one or more of the tRNA genes in circular mtDNA [120,121]. In addition, it remains unclear how mitochondria maintain an adequate supply of tRNAs needed for synthesis of multiple proteins [122]. Post-transcriptional mt-tRNA gene modifications may also play a role in mitochondrial RNA-based diseases [123].

There are several published reports of correcting mt-tRNA mutation defects, usually by rescuing the respiratory phenotypes of cells harboring specific mt-tRNA mutations (for example, see [124]). These are successful but appear to be restricted to specific mutations, although a more "generic" approach has been reported [125]. This approach utilizes the mitochondrial importation of wild-type tRNAs fused with a mitochondrial importation signal. Using this approach, the authors were able to partially correct metabolic abnormalities of cybrid cells carrying mutations for MELAS (mitochondrial encephalopathy lactic acidosis and stroke) or MERRF (mitochondrial encephalopathy and ragged red fiber disease) [125].

7.3. Increase in Mitochondrial Mass Leading to Increased ETC/OXPHOS Capacity to Make ATP

Mitochondrial mass is controlled by the processes of mitochondrial biogenesis (also known as mitobiogenesis, increases mitochondrial mass) and mitochondrial autophagy (also known as mitophagy, decreases mitochondrial mass). Both processes are important for maintaining overall neuronal and cellular bioenergetic function, are operative under normal circumstances, and can be impaired in certain disease phenotypes. Several key pathways are known for mitobiogenesis [126,127,128,129,130,131,132,133,134,135,136,137,138,139,140,141,142,143,144,145,146,147,148,149,150,151,152,153,154,155,156,157,158,159,160,161,162,163,164,165,166,167,168,169,170,171,172,173,174,175,176,177,178,179,180,181,182,183,184,185,186,187,188,189,190,191,192,193,194,195,196,197,198,199,200,201,202,203,204,205,206,207,208,209,210,211,212,213,214,215,216,217,218] and mitophagy [56,61,64,93,139,145,151,163,192,194,195,205,209,213,219,220,221,222,223,224,225,226,227,228,229,230,231,232,233,234,235,236,237,238,239,240,241,242,243,244,245,246,247,248]. The reader is directed to comprehensive reviews of these two important subjects (for mitobiogenesis: [129,130,136,164,167,192,193], and [211]; for mitophagy: [226,233], and [243]).

An obvious question relates to increasing mass of mitochondria containing damaged mtDNA. There are at least two related issues to consider. First, increasing mass of impaired mtDNA-containing mitochondria may improve bioenergetics for the host cell, which is a desired therapeutic goal. The same argument can be applied to cells containing mutated nuclear DNA coding for mitochondrial genes. Second, it remains unclear whether stimulation of mitobiogenesis (or manipulation of mitophagy) will yield net positive or negative effects on cells harboring a heterogenous collection of mitochondria. It must be remembered that effects on peripheral tissues do not necessarily extend into brain tissues.

It is likely that such experiments will need to be tested on an individual's cells before being applied to that individual. Stimulating mitobiogenesis or manipulating mitophagy could be performed on white blood cells or muscle cells, both readily accessible tissues that are mitotic and non-mitotic, respectively. Improvements in respiration or ATP synthesis rates can be assayed in response to several agents.

7.4. Prevention of Epigenetic, Nitrative Stress (NS) and Oxidative Stress (OS) Damage to ETC/OXPHOS Genes (Epigenetics) or Proteins (NS and OS)

This final approach represents decades of investigation by many scientists, is potentially applicable to both specific clinical phenotypes and the broad area of aging, and likely will continue to be popular in the future. Mitochondrial respiration, particularly in brain neurons and generally throughout the body, suffers from taking place in environments with relatively high levels of oxygen molecules and oxygen–nitrogen adducts (such as peroxynitrite anion, ONOO-), or nitric oxide (NO) itself). In addition, it remains unclear how the > 80 genes responsible for mitochondrial proteins of the ETC and OXPHOS systems are regulated by epigenetics, but recent studies suggest that this does occur and that mitochondrial metabolism can affect nuclear epigenetics [107,249,250,251,252].

There have been many attempts to develop therapies directed toward reduction of OS and/or NS. The most promising utilize molecules that are either organic cations at physiological pH, such as pramipexole [253,254], or are attached to "inactive" organic cationic groups such as triphenylphosphonium (TPP) [255,256,257,258] or rhodamine [256,259,260,261,262]. The underlying concepts are that by virtue of lipophilicity, such potential therapeutics can pass through cell and mitochondrial membranes, and the cationic nature suggests that such molecules will be concentrated into the relatively negative mitochondrial matrix (a result of proton pumping).

The OS/NS scavenging molecules must have intrinsic activity and their concentration into the mitochondrial matrix adds organelle specificity. It is striking that the capacity of mitochondrially-targeted ROS and RNS ultimately derive from proton pumping across the inner membrane (responsible for the mitochondria membrane potential), which may involve several mechanisms of PCET, including proton tunneling.

Both NS and OS have been reduced in brain and specifically human disease models [39,50,52,53,55,56,67,76,78,80,84,91,94,95,96,257,262] by such approaches. This therapeutic area appears to be popular in attempting to improve mitochondrial bioenergetics in nervous tissues, as well as other organs.

8. Conclusions

Mitochondria have evolved, likely from protobacterial precursors through endosymbiosis [263], and now inhabit cells of almost all terrestrial and marine plants and animals, including humans. In addition to their critical roles in modulating cellular calcium signaling and cell death initiation, mitochondria through ETC/OXPHOS appear to supply most of the substantial daily ATP requirement for humans. Adult human brain has a ~10-fold disproportionate (relative to mass) ATP production rate and depends on the stereotyped movement of reducing electrons down an energy gradient in the ETC and conservation of this ETC energy decrease by proton displacement across the mitochondrial inner membrane. This electron movement and proton displacement, however they occur, must respect quantum mechanical constraints.

Both electrons moving through the ETC and proton displacement from the matrix to the intermembrane space (IMS) may utilize quantum tunneling in addition to other mechanisms. It is not yet clear whether tunneling occurs at all, but it is a theoretically appealing mechanism for quantum entities to pass through energy barriers and reduce activation energies (thus increasing rates of proton transfer).

Mitochondria must likely segregate electrons from electrophilic molecular oxygen and protons from solvation by water. How these feats are accomplished remains unclear, but our daily ATP requirements likely require these biochemical gymnastics. Mitochondria may represent a necessary transitional organelle between the quantum world of elementary particles and energy-releasing catabolism of molecules created from absorbed solar-derived photons. Decoherence (loss of quantum-ness) may assist ATP production in mitochondria, and theoretically its presence may vary with energy needs.

Many neurodegenerative diseases (NDDs) afflicting humans may be viewed thermodynamically as increases in molecular entropy during life of the organism as neurons die. Such local entropy increases may arise from decreased neuronal energy production traceable to decline of OXPHOS rates. OXPHOS rates in turn depend on availability of intact ATP synthase complexes and (likely) non-hydrated protons in the intermembrane space or at the proton-binding sites of the ATP synthase rotor.

Mitochondrial therapeutics can address bioenergetic deficiencies at multiple levels, from epigenetic changes in mitochondrial and/or nuclear genomes, through measures to reduce post-translational damage to ETC/OXPHOS proteins. Many such approaches have been/are being developed, and optimism exists for varied solutions to the human problems of mitochondrial ETC/OP dysfunction in NDDs.

Acknowledgments

I.G.O. was supported by the international Clinical Research Center, St. Anne's University Hospital, CZ-6569i Brno, Czech Republic.

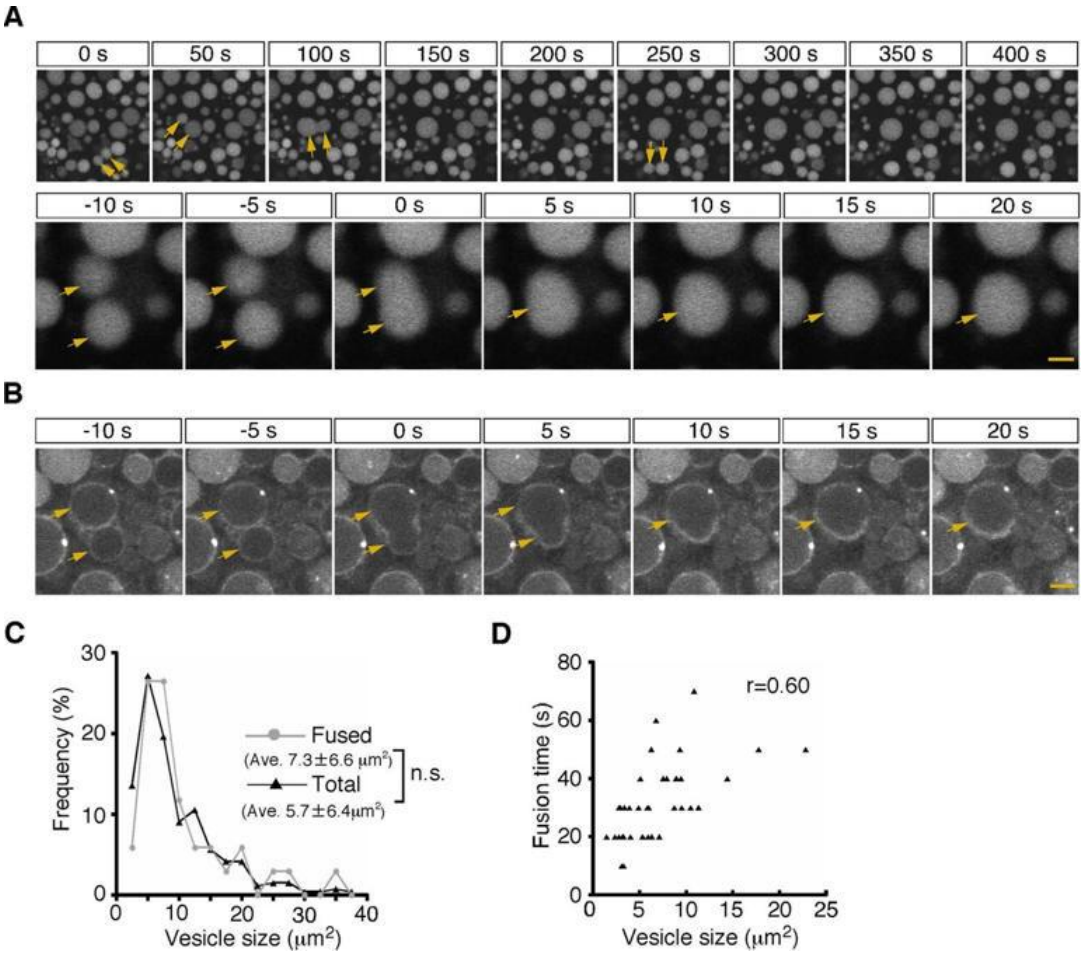

Researchers discover two vesicle fusion mechanisms while studying vesicle movement in living cells

Homotypic fusion between late endosomes. (A) Time-lapse imaging of endocytic vesicles in VE cells. (B) By labeling of VE cells with FM1-43, the fusion process of the cell membranes in zone 2 was observed. (C) Histograms showing the size distribution of total late endosomes (black line, n = 265) and the late endosomes that underwent homotypic fusion (gray line, n = 37). (D) Correlation between the size of the late endosomes that underwent homotypic fusion and the time required for completion of fusion. Credit: eLife (2024). DOI: 10.7554/eLife.95999© Provided by Phys.org

Cells intake substances from the outside world by encapsulating them in vesicles called endosomes, which are subsequently transported throughout the cell. During the transport process, vesicles fuse with other intracellular organelles. However, observing this process is challenging in many cells due to their small size and the complexity of underlying regulatory mechanisms.

In a new study published in *eLife*, the researchers focused on the outermost visceral endoderm cells of mouse embryos. By labeling endosomes with fluorescent markers, they successfully observed the fusion process under a microscope.

They identified two distinct modes of endosomal fusion: homotypic fusion, where two endosomes fuse rapidly to form a single vesicle, and heterotypic fusion, in which lysosomes slowly absorb endosomes.

In addition, a mathematical analysis of the vesicle fusion process using a mechanical model of the vesicle membrane revealed that the vesicle size determines the fusion mode: homotypic fusion occurs in small vesicles and heterotypic fusion happens in large ones. Moreover, the application of fluctuating forces to the vesicle membrane facilitated homotypic fusion even in large vesicles.

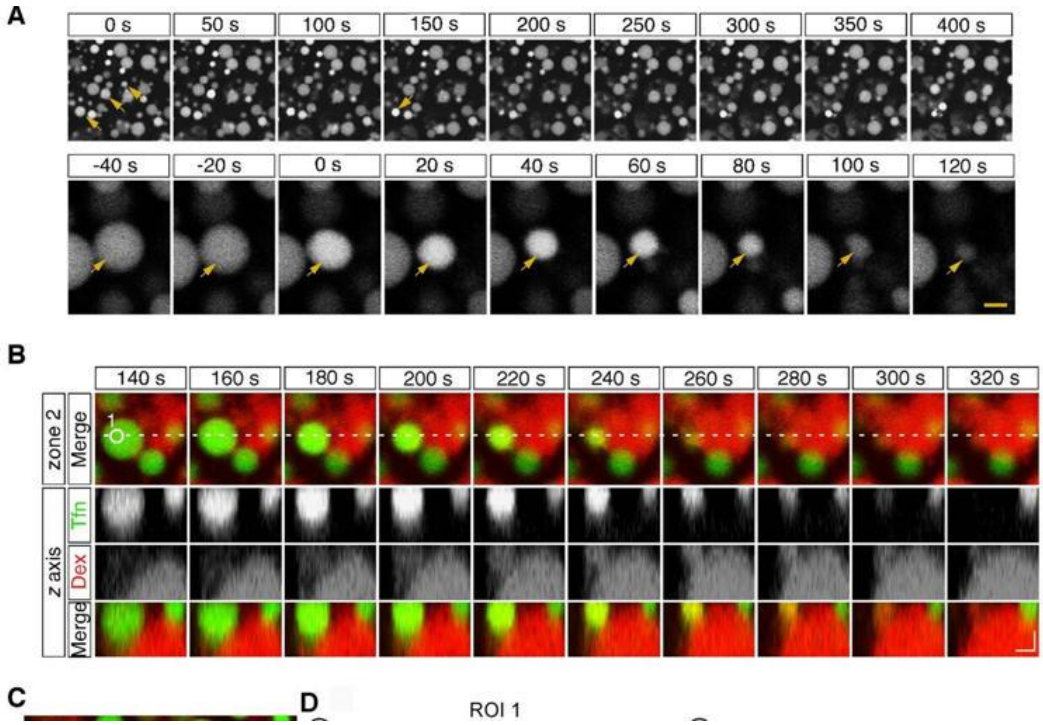

Heterotypic fusion between late endosomes and lysosomes. (A) Time-lapse imaging of VE cells. After 15 min of pulse-labeling with Alexa 488-transferrin, heterotypic fusion of late endosomes was observed: they shrank gradually and disappeared from the focal plane (arrows). (B) Time-lapse imaging of late endosomes in VE cells. (C and D) Time course of the fluorescence intensity. (E) Electron microscopic image showing pore formation between a late endosome (LE) and a lysosome (Ly). (F) Correlation between the size of late endosomes that underwent heterotypic fusion and the time required for completion of fusion. (G) Histograms showing the size distribution of late endosomes at 5 min and 15 min. Credit: eLife (2024). DOI: 10.7554/eLife.95999© Provided by Phys.org

The binding of endosomes to the cytoskeletal protein called actin, which is believed to generate these fluctuating forces, appears to promote homotypic fusion. Furthermore, cofilin, which promotes actin turnover, and myosin, which interacts with actin, were crucial for vesicle fusion.

Using this observation system, the researchers expect to elucidate the regulatory mechanisms controlling the processes of intracellular vesicle fusion and trafficking.

More information: Seiichi Koike et al, Actin dynamics switches two distinct modes of endosomal fusion in yolk sac visceral endoderm cells, *eLife* (2024). DOI: 10.7554/eLife.95999

Provided by University of Tsukuba

Transcranial Low-Level Laser (Light) Therapy for Brain Injury

Connor Thunshelle [1,,2], Michael R Hamblin [2,,3,,4,✉]
PMCID: PMC5180077 PMID: 28001759

Abstract

Background: Low-level laser therapy (LLLT) or photobiomodulation (PBM) is a possible treatment for brain injury, including traumatic brain injury (TBI). ***Methods:*** We review the fundamental mechanisms at the cellular and molecular level and the effects on the brain are discussed. There are several contributing processes that have been proposed to lead to the beneficial effects of PBM in treating TBI such as stimulation of neurogenesis, a decrease in inflammation, and neuroprotection. Both animal and clinical trials for ischemic stroke are outlined. A number of articles have shown how transcranial LLLT (tLLLT) is effective at increasing memory, learning, and the overall neurological performance in rodent models with TBI. ***Results:*** Our laboratory has conducted three different studies on the effects of tLLLT on mice with TBI. The first studied pulsed against continuous laser irradiation, finding that 10 Hz pulsed was the best. The second compared four different wavelengths, discovering only 660 and 810 nm to have any effectiveness, whereas 732 and 980 nm did not. The third looked at varying regimens of daily laser treatments (1, 3, and 14 days) and found that 14 laser

applications was excessive. We also review several studies of the effects of tLLLT on neuroprogenitor cells, brain-derived neurotrophic factor and synaptogenesis, immediate early response knockout mice, and tLLLT in combination therapy with metabolic inhibitors. ***Conclusions:*** Finally, some clinical studies in TBI patients are covered.
Keywords: : traumatic brain injury, photobiomodulation, stroke, low-level laser therapy, brain disorders

Introduction

TRAUMATIC BRAIN INJURY (TBI) can include skull fracture, intracranial hemorrhage, elevated intracranial pressure, and/or cerebral contusion. Unlike stroke, the prevalence of which is tied with an increasing age of onset, TBI is much more common in younger populations. Not only does TBI have a large impact on the healthcare industry but also causes severe socioeconomic problems throughout the world. Every year in the United States, there are nearly 2 million head injuries resulting in 283,000 hospitalizations, 53,000 of which lead to death.[1–3] Consequently, Americans living with TBI-related disabilities cost an estimated $56 billion yearly.[4] In 2001, the World Health Organization (WHO) projected that within 5 years, motor vehicle accidents, one of the largest causes of TBI, would be ranked just behind ischemic heart disease and unipolar major depression as a cause of morbidity and mortality.[5]

Although the understanding of the pathophysiology underlying the damage following severe brain injury has improved, current treatment options remain limited.[6] The processes and mechanisms that underlie TBI are incredibly complex and are still not well understood. After the initial impact, multiple pathways are activated that result in secondary injury, which can spread throughout the brain. These injury processes may include inflammation, an ionic imbalance, excitotoxic damage, oxidative stress, increased vascular permeability, and mitochondrial dysfunction.[7] In turn, these secondary injuries result in brain edema and an increase in intracranial pressure. These physiological changes and disruptions cause neuronal death and a spread of ischemic necrosis, while worsening motor and cognitive impairment follows. Researchers and clinicians should prioritize efforts to improve the outcome and treatment options for TBI patients.[8]

Recently, transcranial low-level laser therapy (tLLLT) or photobiomodulation (PBM) has garnered a greater interest as an alternative to existing approaches to treat TBI as the search for conventional therapeutic treatments has been relatively unsuccessful. There are a number of articles showing the beneficial effects of tLLLT such as reducing brain damage and recovery times in stroke models. These promising results may soon lead to tLLLT becoming a more widely used treatment for TBI.

Mechanisms of tLLLT

The discussion of tLLLT has moved past its biological effects into a search for how light energy—specifically from lasers or light-emitting diodes (LED)—works at the cellular

and organism levels. With a wide range of different applications of LLLT, it is necessary to find and understand the optimal parameters for each. Heat absorption, one of several unlikely mechanistic explanations for tLLLT, is closely tied to the use of lasers, but because the lasers used in tLLLT do not meaningfully raise brain temperature, photothermal effects from light energy do not play a significant role in explaining the benefits of tLLLT. Rather, photochemistry is becoming the accepted hypothesis for explaining the biological effects of light absorption in cells and tissues.[9] These effects rely on the absorption of light by chromophores within cells to produce the many biological effects such as an increase of adenosine triphosphate (ATP), DNA, and RNA, release of nitric oxide (NO), cytochrome c oxidase (CCO) activity, a regulation of reactive oxygen species (ROS), and changes to the organelle membrane activity in mitochondria.[10–14] In order for the photons to effectively reach their target area, the penetration of light through the tissue must be maximized by choosing an appropriate wavelength. This “optical window” ranges from 600 nm to 1200 nm, involving almost exclusively, red and near-infrared (NIR) light.[15]

Mitochondria are the most important cellular organelles to study, when trying to understand the cellular response of LLLT. Conventionally known as the “powerhouse of the cell,” mitochondria not only supply the cell with energy but are also involved in cellular signaling, cell differentiation, cell death, along with cellular metabolism and proliferation. Complex IV on the mitochondrial inner membrane, or CCO, is considered to be the crucial chromophore in the cellular response to LLLT as shown by the action spectra (a plot of the rate of the physiological activity plotted against wavelength of light).[16,17] CCO is a large protein complex with two copper and two iron centers.[18] The way in which light interacts and ultimately affects CCO is not precisely known, but will certainly involve a complex series of interactions that will result in a change in redox states. LLLT produces a shift toward higher oxidation in the overall cell redox potential[11,17] and briefly increases the level of ROS.[19,20] This change in the redox state of the mitochondria regulates several transcription factors. These include redox factor-1 (Ref-1), cAMP response element (CREB), activator protein 1 (AP-1), p53, nuclear factor kappa B (NF-κB), hypoxia-inducible factor (HIF-1), and HIF-like factor. The activation and regulation of redox-sensitive genes and transcription factors are thought to be caused by ROS induced from LLLT.[19] An important feature of LLLT is its biphasic dose–response curve.[21,22] This can be explained in other terms: a small amount of light can be good, more may lose the beneficial effect, and too much light may be harmful. This effect can be explained by two of the LLLT signaling mediators, ROS[12] and NO.[14] Both of these species can have positive effects at low concentration, but can have adverse effects at a high concentration.

tLLLT may cause a separation (photodissociation) between NO and CCO.[13,23] Normally, cellular respiration is downregulated when NO binds with CCO and inhibits it from binding to the Fe and Cu centers. The NO displaces the oxygen from CCO, thus decreasing cellular respiration and decreasing the production rate of ATP.[10] Therefore, by breaking NO from CCO, LLLT is able to prevent this inhibition from occurring. In turn, both ATP levels and blood flow increase (NO is a vasodilator).[24] With an increase in

blood flow, improved oxygenation is found in damaged areas of the brain. Figure 1 depicts the molecular mechanisms and signaling pathways that are thought to occur post-LLLT.

FIG. 1.

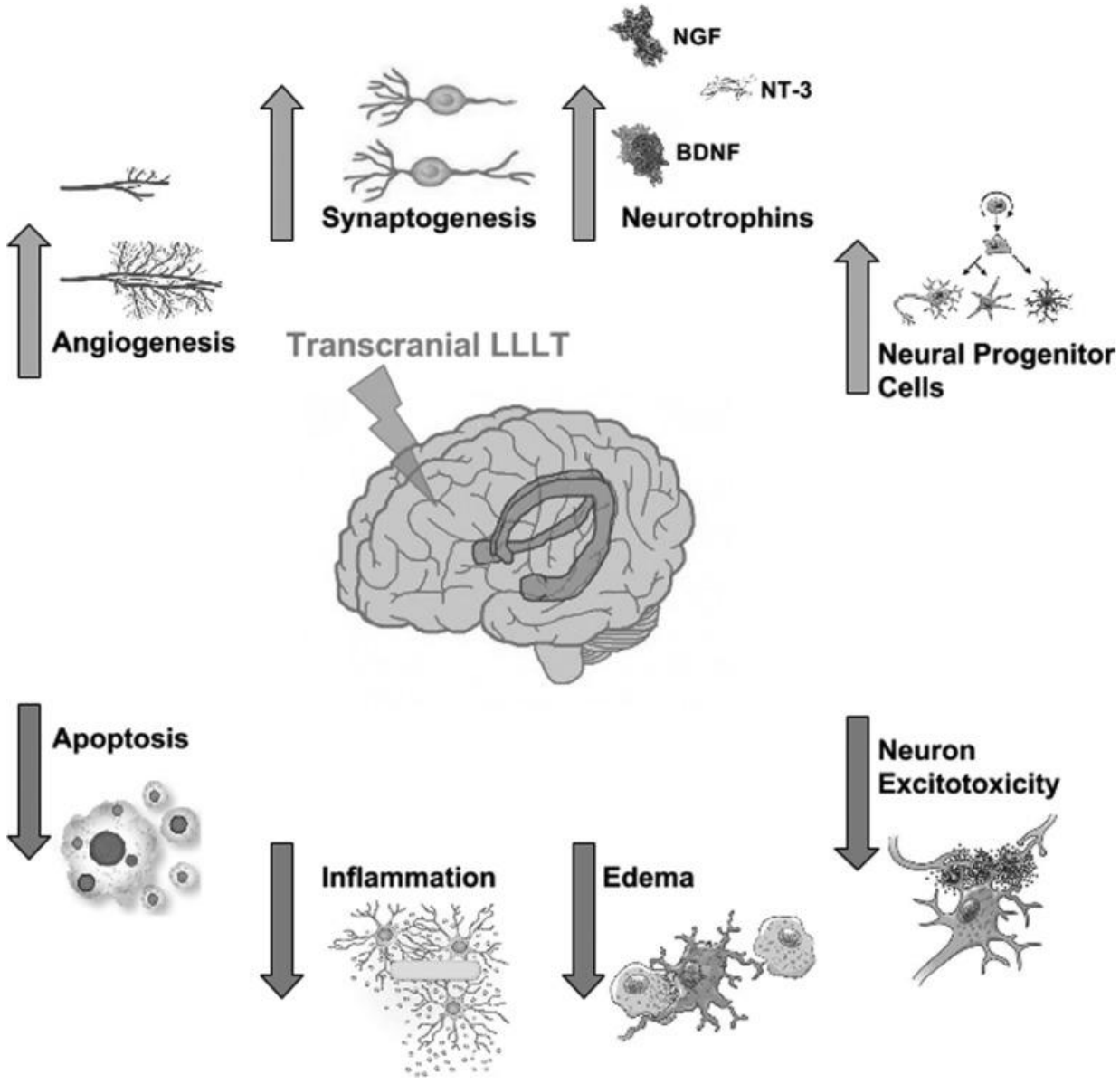

Molecular mechanisms of transcranial LLLT. Light passes through the scalp and skull, where it is then absorbed by cytochrome c oxidase in the mitochondrial respiratory chain of the cortical neurons in the brain. Cell signaling and messenger molecules are upregulated as a result of stimulated mitochondrial activity, including ROS, NO, and ATP. These signaling molecules activate transcription factors, including NF-κB and AP-1, which enter the nucleus and cause transcription of a range of new gene products. AP-1, activator protein 1; ATP, adenosine triphosphate; BDNF, brain-derived

neurotrophic factor; LLLT, low-level laser therapy; NF-κB, nuclear factor kappa B; NGF, nerve growth factor; NO, nitric oxide; ROS, reactive oxygen species.

When using LLLT as a method to treat disorders of the brain, more specific mechanisms need to be closely examined. Brain-specific functional mechanisms of tLLLT for TBI are illustrated in Fig. 2. The cytoprotective effects of LLLT are thought to prevent injured neurons from dying and reduce the number of neuronal cells undergoing death as has been shown for toxins such as cyanide,[25] tetrodotoxin,[26] and methanol.[27] This protective effect may include several mediators such as Bcl2, heat shock proteins,[28] survivin,[29] and superoxide dismutase.[30] The decrease of proinflammatory mediators from dendritic cells[31] along with the increase in anti-inflammatory mediators [interleukin (IL)-10 and transforming growth factor β][32] is thought to cause the anti-inflammatory effect of LLLT.[33,34]

FIG. 2.

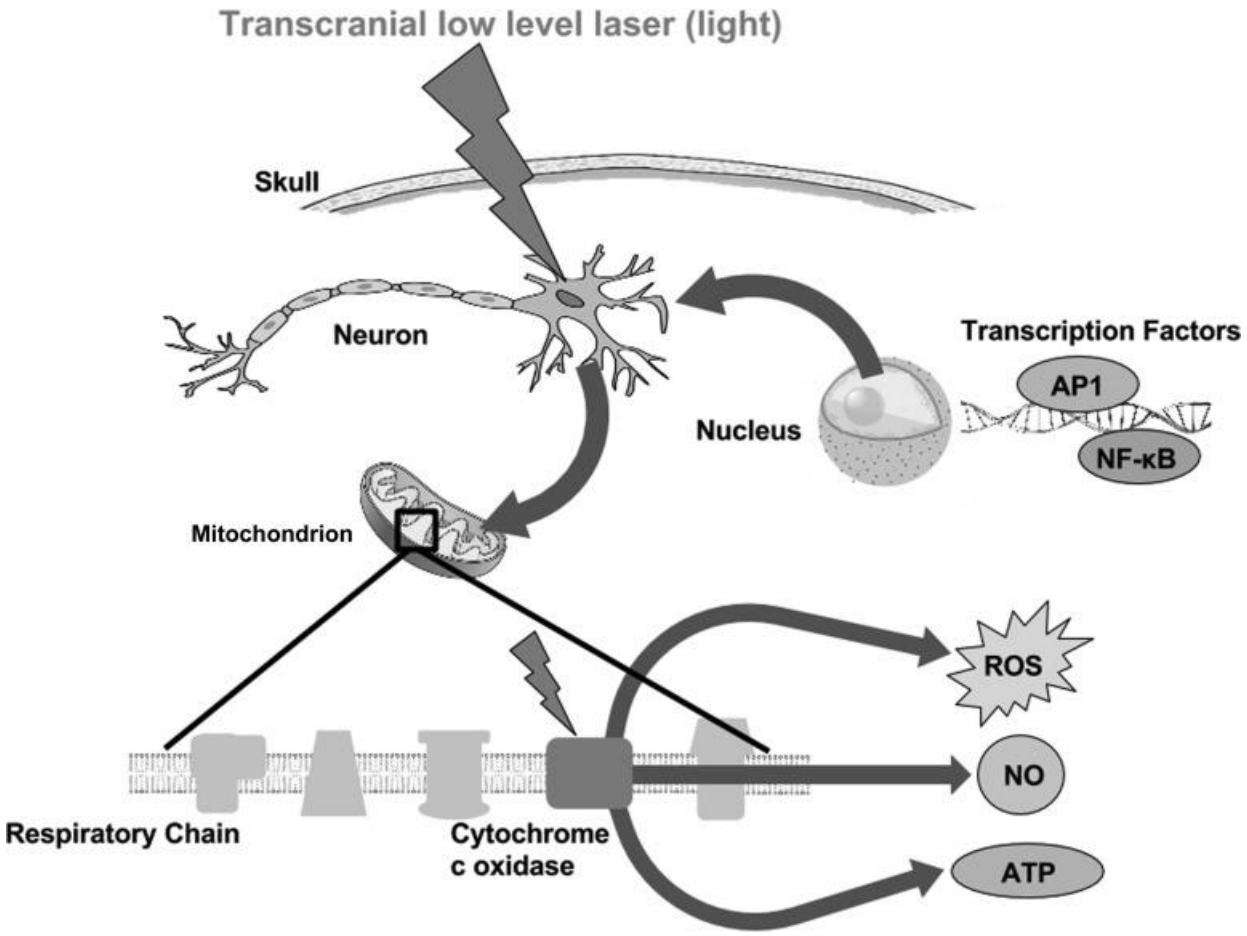

Functional mechanisms of transcranial LLLT. The gene transcription process described in Fig. 1 can lead to decreases in neuronal apoptosis and excitotoxicity, and lessening of inflammation and edema, which will help reduce progressive brain damage. Increases in angiogenesis and expression of neurotrophins leading to activation of

neural progenitor cells, and increased synaptogenesis may all contribute to the brain repairing itself from damage sustained in the trauma.

Last, neurogenesis and neuroplasticity (synaptogenesis) may both be other mechanisms that contribute to the beneficial effects of tLLLT in the brain.[35] These processes are initiated by the increase in neurotrophin expression as in brain-derived neurotrophic factor (BDNF) and nerve growth factor.

tLLLT for Stroke and TBI

Apart from ischemic heart disease, stroke is the leading cause of death worldwide. The approved treatment for stroke is to apply tissue plasminogen activator within 3 h of stroke onset.[36,37] Although this method is very effective at clearing blood clots, the small time window that exists for effective treatment diminishes the ability to treat most patients. Because of this short time frame, other treatment options for stroke victims must be considered.

Low-level laser therapy (LLLT) has been investigated as an alternative treatment for stroke, and LLLT has been shown to have a neuroprotective effect,[38,39] while regulating several biological processes.[40–42] Light can penetrate several tissues, including both the scalp and skull, and reach into the brain. Several clinical and preclinical studies have shown that this process can lead to an improved recovery from stroke.[43] In these studies, stroke was induced in rat and rabbit models and showed that intervention by tLLLT within 24 h could have meaningful beneficial effects. For the rat models, stroke was induced by permanent middle cerebral artery occlusion by insertion of a filament into the carotid artery or by craniotomy.[44,45] Stroke induction in the rabbit models were induced by the small clot embolic model by injecting a microclot made from blood from a donor rabbit.[46] These studies along with the treatments and results are listed in Table 1.

TABLE 1.

REPORTS OF TRANSCRANIAL LOW-LEVEL LASER THERAPY USED FOR STROKE IN ANIMAL MODELS

Subject	*Stroke model*	*Parameters*	*Effect*	*References*
Rat	MCAO	660 nm; 8.8 mW; 2.64 J/cm^2; pulse frequency of 10 kHz; Laser applied at cerebrum at 1, 5, and 10 min	Suppression of NOS activity and upregulation of TGF-β1	44
Rat	MCAO	808 nm; 7.5 mW/cm^2; 0.9 J/cm^2; 3.6 J/cm^2 at cortical surface; CW and pulse wave at 70 Hz, 4 mm diameter	Administration of LLLT 24 h after stroke onset induced functional benefit and neurogenesis induction	45
Rabbit	RSCEM	808 ± 5 nm; 7.5 W/cm^2, 2-min duration 3 h after stroke and 25 mW/cm^2 10-min duration 1 or 6 h after stroke	Improved behavioral performance and durable effect after LLLT within 6 h from stroke onset	46

Subject	*Stroke model*	*Parameters*	*Effect*	*References*
Rat	MCAO	808 nm; 0.5 mW/cm^2; 0.9 J/cm^2 on brain 3 mm dorsal to the eye and 2 mm anterior to the ear	LLLT applied at different locations on the skull improved neurological function after acute stroke	47
Rabbit	RSCEM	808 nm; 7.5 mW/cm^2; 0.9 J/cm^2; 3.6 J/cm^2 at cortical surface; CW; 300 min; pulse at 1 kHz, 2 min at 100 Hz	LLLT administered 6 h after embolic stroke resulted in clinical improvements in rabbits	48

CW, continuous wave; LLLT, low-level laser therapy; MCAO, middle cerebral artery occlusion; NOS, nitric oxide synthase; RSCEM, rabbit small clot embolic model; TGF-β1, transforming growth factor β1.

Clinical trial for stroke	*No. of subjects*	*Eligibility criteria*	*Parameters of treatment*	*Effect*	*References*
NEST-1	120	Patients: between 40 and 85 years of age; clinical diagnosis of ischemic stroke; measurable neurological deficit; NeuroThera Laser System within 24 h of stroke onset. 79 cases received the Real and 41 received the Sham.	808 nm; 700 mW/cm^2 on shaved scalp with cooling; 1 J/cm^2 at cortical surface; 20 predetermined location 2 min each.	Greater improvement in the Real-treated group, but not in the Sham-treated group ($p < 0.05$, NIH Stroke Severity Scale).	49
			10 placements on the left and right side of the head (regardless of the side of the stroke); no midline placements.		
NEST-2	660	Patients: between 40 and 90 years of age; clinical diagnosis of ischemic	808 nm; 700 mW/cm^2 on shaved scalp with cooling; 1 J/cm^2 at	Beneficial results ($p < 0.04$) were found for the moderate and	50

Clinical trial for stroke	*No. of subjects*	*Eligibility criteria*	*Parameters of treatment*	*Effect*	*References*
		stroke within 24 h of onset; NIH stroke scale of 7–22.	cortical surface; 20 predetermined location 2 min each as described for NEST-1.	moderate-severe (but not for the severe) stroke patients. Mortality and adverse event rates were not adversely affected by TLT.	
		331 cases received Real tLLLT and 327 received Sham tLLLT			
NEST-3	1000	Patients: between 40 and 80 years of age; clinical diagnosis of ischemic stroke within 24 h of onset; NIH stroke scale of 7–17	808 nm; 700 mW/cm^2 on shaved scalp with cooling; 1 J/cm^2 at cortical surface; 20 predetermined location 2 min each as described for NEST-1 and NEST-2	The study was terminated prematurely after 600 (out of 1000) patients by the DSMB due to an expected lack of statistical significance	[54]

Three clinical trials of tLLLT have been conducted in human patients who had suffered from an acute stroke. The first study, NEST-1, enrolled 120 patients between the ages of 40–85 years with a diagnosis of ischemic stroke involving a neurological deficit that could be measured. The purpose of this first clinical trial was to demonstrate the safety and effectiveness of laser therapy for stroke within 24 h.[49] Transcranial PBM significantly improved outcome in human stroke patients, when applied at ~18 h poststroke, over the entire surface of the head (20 points in the 10/20 EEG system) regardless of stroke location.[49] Only one LLLT was administered, and 5 days later, there was significantly greater improvement in the Real- but not in the Sham-treated group ($p < 0.05$, NIH Stroke Severity Scale). This significantly greater improvement was still present at 90 days poststroke, where 70% of the patients treated with Real LLLT had successful outcome, while only 51% of controls did. The second clinical trial, NEST-2, enrolled 660 patients, aged 40–90 years, who were randomly assigned to one of two groups (331 to LLLT, 327 to sham).[50] Beneficial results ($p < 0.04$) were found for the moderate and moderate–severe (but not for the severe) stroke patients, who received the Real laser protocol.[50–52] These results suggest that the overall severity of the individual stroke should be taken into consideration in future studies, and very severe patients are unlikely to recover with any kind of treatment. The last clinical trial, NEST-3, was planned for enrollment of 1000 patients. The study was prematurely terminated by the data safety monitoring board for futility—that is, on an Interim Analysis, no significant difference was observed between those receiving the real intervention versus the sham intervention. If the study had been continued, a lack of statistical significance

would have been expected.[53] The parameters and results for these three clinical trials are listed in Table 2.

TABLE 2.
REPORTS OF TRANSCRANIAL LOW-LEVEL LASER THERAPY USED FOR STROKE IN CLINICAL TRIALS

DSMB, data safety monitoring board; NIH, National Institutes of Health; NEST, NeuroThera Efficacy and Safety Trial; TLT, transcranial laser therapy.

Studies of tLLLT for TBI in Mice

With the success of tLLLT for stroke has come an influx of researchers testing this technique in different animal models of TBI. Oron et al.[55] examined the effects of LLLT for TBI in mice. A weight-drop device was used to induce a closed-head injury in the mice. An 808 nm diode laser with two energy densities (1.2–2.4 J/cm^2 over 2 min of irradiation with 10 and 20 mW/cm^2) was delivered to the head 4 h after TBI was induced. Neurobehavioral function was assessed by the neurological severity score (NSS) with a range of 0 to 10, where the lowest number (0) reflects normal function. There was no significant difference in NSS between the power densities (10 vs. 20 mW/cm^2), nor was there a significant difference between the control and laser-treated group after 24 and 48 h post-TBI. However, there was a significant improvement of a 27% lower NSS in the laser-treated group after 5 days to 4 weeks. The laser-treated group also showed a smaller loss of cortical tissue than the sham group.[55]

Oron et al.[56] then looked at the long-term effects of varying treatments of different therapies administered at varying time points in mice with internal (closed-head) injury. Again, a weight-drop device was used along with an 808 nm Ga-Al-As diode laser with an energy density of 1.2 J/cm^2 (power density of 10 mW/cm^2). Treatments were given at 4, 6, and 8 h postinjury transcranially. Laser treatments at 10 mW/cm^2 at 100 Hz and 600 Hz and continuous wave (CW) 4 h postinjury were conducted in a complementary experiment. For the laser-treated group at 6 h postinjury, the NSS was 3.4 times better (lower) than in the nonirradiated control group. For the laser-treated group at 8 h postinjury, the NSS was 1.8 times better (lower) than the control group. Both groups were evaluated on day 56. The NSS for the all three varying frequency treatments (100 Hz, 600 Hz and CW) had 3.5 times greater difference when compared to the nontreated control group. The mice receiving tLLLT with pulsed wave (PW) at 100 Hz 4 h postinjury made a full recovery (NSS of 0) by day 56. When compared to the control group, the CW and PW laser-treated groups had significant smaller lesion size in the brain.[56]

Khuman et al.[12] demonstrated that tLLLT could improve cognitive function in controlled cortical impact (CCI) mice. The CCI was created by a 3 mm flat-tipped pneumatic piston moving at a velocity of 6 m/sec to a depth of 0.6 mm into the brain exposed by a craniotomy. The mice were assigned to one of two groups: either an open craniotomy

laser-treated group or a transcranial laser-treated group. Within the open craniotomy group, the mice were irradiated with a low-level laser light with a wavelength of 800 nm at varying energy levels (0, 30, 60, 105, 120, and 210 J/cm^2) at 60–80 min post-CCI. The group treated transcranially were exposed to low-level laser light with an energy level of 60 J/cm^2 at varying timing regimens (60–80 min post-CCI, 4 h post-CCI, or once a day for 7 days after CCI). The Morris water maze (MWM) was utilized to assess cognitive function improvement, while motor function was evaluated using the wire grip test. Brain edema, lesion size, and nitrosative stress were also evaluated using a nitrotyrosine ELISA test. Mice in both groups (transcranially or open craniotomy) treated with lasers with an energy level of 60 J/cm^2 showed significant improvements in both the response time to the hidden platform and probe trial performance. An anti-inflammatory effect was also noted in both groups, however, there was no significant difference found in the motor function (days 1–7), lesion size (14 days), brain edema (24 h), and nitrosative stress (24 h) between the LLLT groups and the control.[12]

Quirk et al.[57] evaluated the neuroprotective effects of NIR light using an *in vivo* rodent model of TBI induced by CCI and characterized the changes at the behavioral and biochemical levels. Rats were divided into three different groups: a severe TBI group, a sham surgery group, and a group receiving anesthetization only. Rats in each group were then administered either with or without NIR light. They received two 670 nm LED treatments (5 min, 50 mW/cm^2, 15 J/cm^2) per day for 72 h (biochemical analysis assay) or for 10 days (behavioral assay). During the recovery period, rats were tested for locomotor and behavioral activities using a TruScan device. At the 72-h mark, frozen brain tissue was collected and evaluated for apoptotic markers and measured for reduced glutathione (GSH) levels. Significant differences between TBI with and without NIR (TBI+/−) light and between the sham surgery with and without NIR (S+/−) light were observed. In rats exposed to NIR light, there was a significant decrease in the proapoptotic marker Bax along with a smaller increase in antiapoptotic markers and GSH levels.[57]

Moreira et al.[58] assessed the effects of low-level laser phototherapy following direct cortical cryogenic injury (CI) to the brain of rodents. The rats were irradiated with 780 and 600 nm lasers at energy levels of 3 and 5 J/cm^2. This study found that laser-treated lesions had smaller tissue loss at 6 h, had significantly higher amount of viable neurons at 24 h, and had fewer leukocytes and lymphocytes in first 24 h, while the GFAP staining increased in the control group (but not the tLLLT group) by 14 days. It was concluded that LLLT facilitated wound healing in the brain following CI by controlling brain damage, preventing neuronal death, and reducing severe astrogliosis[58]

Effect of Different Laser Wavelengths in tLLLT for TBI

The following three sections will discuss and summarize studies conducted in our laboratory where we have investigated the use of LLLT to treat TBI in animal models.

Wu et al.[59] explored the effect that varying laser wavelengths of LLLT had on closed-head TBI in mice. Mice were randomly assigned to the LLLT-treated group or the sham group as a control. Closed-head injury was induced by a weight-drop apparatus. To analyze the severity of the TBI, the NSS was measured and recorded. The injured mice were then treated with varying wavelengths of laser (665, 730, 810, or 980 nm) at an energy level of 36 J/cm^2 at 4 h directed onto the scalp. The 665 and 810 nm groups showed significant improvement in NSS when compared to the control group from day 5 to 28. Results are shown in Fig. 3. Conversely, the 730 and 980 nm groups did not show a significant improvement in NSS and these wavelengths did not produce similar beneficial effects as in the 665 and 810 nm LLLT groups.[59] The tissue chromophore CCO is proposed to be responsible for the underlying mechanism that produces the many PBM effects that are the byproduct of LLLT. CCO has absorption bands around 665 and 810 nm, while it has low absorption bands at the wavelength of 730 nm.[23] It should be noted that this particular study found that the 980 nm wavelength did not produce the positive effects as the 665 and 810 nm wavelengths did, but other previous studies did find that the 980 nm wavelength was an active one for LLLT. Wu et al. proposed these dissimilar results may be due to the variance in the energy level, irradiance, and so on between the other studies and this particular study.[59]

FIG. 3.

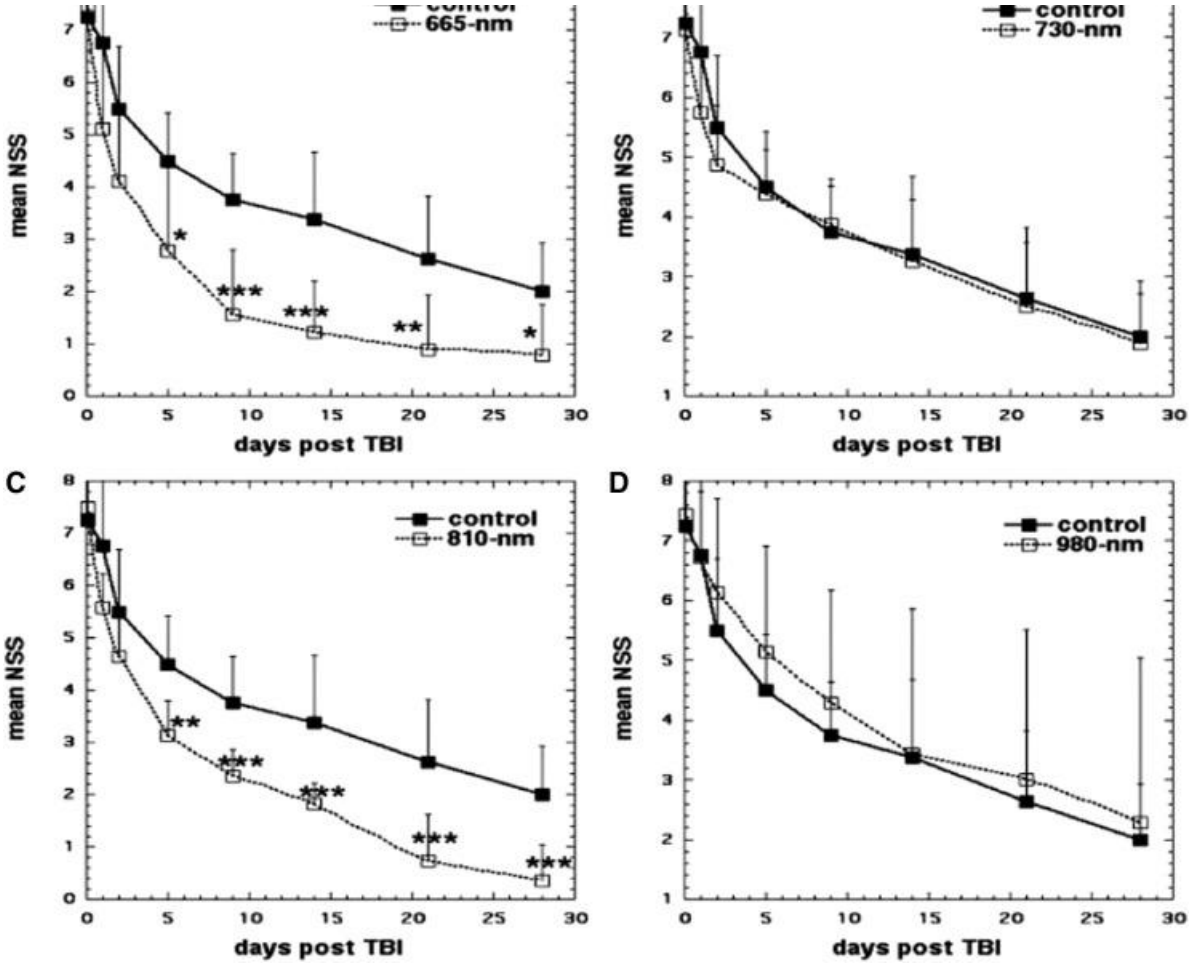

Effect of different wavelengths in tLLLT in closed head TBI in mice. **(A)** Sham-treated control versus 665 nm laser. **(B)** Sham-treated control versus 730 nm laser. **(C)** Sham-treated control versus 810 nm laser. **(D)** Sham-treated control versus 980 nm laser. Points are means of 8–12 mice and bars are SD. *$p < 0.05$; **$p < 0.01$; ***$p < 0.001$ (one-way analysis of variance). NSS, neurological severity score; SD, standard deviation; TBI, traumatic brain injury; tLLLT, transcranial LLLT.

Effect of Pulsing tLLLT for TBI

A number of studies have investigated the best range of parameters for laser treatment (total energy delivered, irradiance, or power density) and the best wavelengths of lasers that should be used in LLLT for the treatment of TBI and other brain disorders. However, a consensus on whether treatment should be given by CW light or PW light, including the parameters for this light, has not been reached. Ando et al.[60] used the 810 nm wavelength parameters from the previous study and varied the pulse modes of the laser in a mouse model of TBI. These modes consisted of either PW laser at 10 Hz or 100 Hz or CW laser. For the mice, TBI was induced with a CCI device by open craniotomy. A single treatment with an 810 nm Ga-Al-As diode laser with a power density of 50 mW/m^2 and an energy density of 36 J/cm^2 was given by tLLLT to the

closed head in mice for a duration of 12 min at 4 h post-CCI. At 48 h to 28 days post-TBI, all laser-treated groups had significant decreases in the measured NSS when compared to the control. Although all laser-treated groups had similar NSS improvement rates up to day 7, the PW 10 Hz group began to show greater improvement beyond this point as seen in Fig. 4. On day 28, the forced swim test for depression and anxiety was used and showed a significant decrease in the immobility time for the PW 10 Hz group. In the tail suspension test, which measures depression and anxiety, there was also a significant decrease in the immobility time on day 28, and (in contrast to the forced swim test) this was also seen on day 1, in the PW 10 Hz group.

FIG. 4.

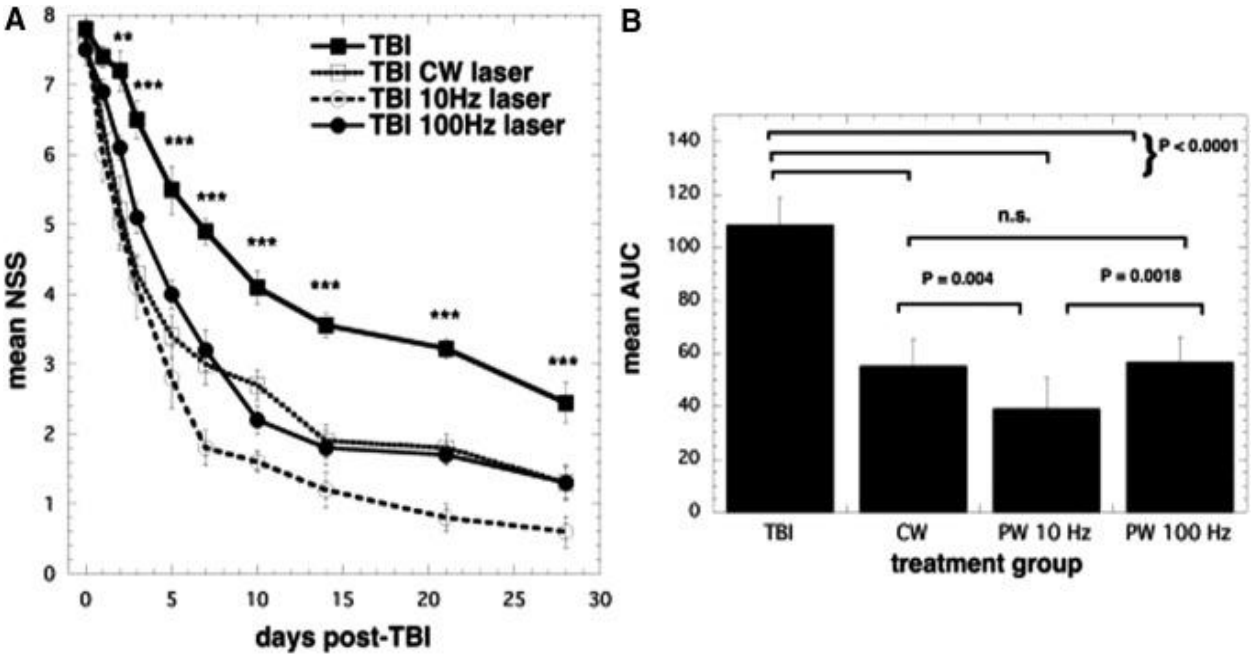

Effects of pulsing in transcranial LLLT for CCI-TBI in mice. **(A)** Time course of NSS of mice with TBI receiving either control (no laser treatment), or 810 nm laser (36 J/cm^2 delivered at 50 mW/cm^2) with a spot size of 0.78 cm^2 in either CW, PW 10 Hz, or PW 100 Hz modes. Results are expressed as mean ± SEM $^{**}p < 0.01$ and $^{***}p < 0.001$ versus the other conditions. **(B)** Mean areas under the NSS time curves in the two-dimensional coordinate system over the 28-day study for the four groups of mice. Results are mean ± SD ($n = 10$). AUC, area under the curve; CCI, controlled cortical impact; CW, continuous wave; n.s., not significant; PW, pulsed wave.

Both these test results indicate an antidepressant effect of tLLLT. It should be noted that severe depression is a major symptom of TBI in human patients. For the PW 10 Hz group on days 15 and 28, the lesion size in the tLLLT-treated TBI mice significantly decreased when compared to the nonlaser-treated control group. These results may suggest a neuroprotective effect of tLLLT. Overall, the beneficial effects of tLLLT for

TBI, including the antidepressant effects, the degree of injury, and the neuroprotective effects, were found to be more effective with the 10 Hz PW frequency compared to both the 100 Hz frequency and the CW. Ando et al. hypothesized that the PW 10 Hz laser irradiation frequency may be the best frequency to affect the entire brain.[60] The pulsed light may have resonance with existing brain waves such as theta waves that oscillate at 4–10 Hz, found in the hippocampus (or a similar region).[62]

Effects of tLLLT Regimen for TBI

Over the whole history of all the reported LLLT studies, there has been found to exist a biphasic dose–response relationship that persists. This applies to not only cell culture studies but also to preclinical studies in animal models and clinical studies of LLLT.[63] Through many previous studies, including the ones discussed above, it is largely accepted that there is an optimal level of energy density and power density and an optimum treatment regimen that is needed to create the most beneficial effects with tLLLT. Choosing suboptimal parameters may lead to a reduction in the beneficial effects and therefore a less than effective treatment, or may even cause negative effects or adverse reactions.[40]

Xuan et al.[64] studied the effectiveness of varying treatment repetition regimens of tLLLT on the neurobehavioral and vestibulomotor function and studied neuroprotection and neurogenesis by histomorphological analysis and histological evidence. They used an 810 nm laser to deliver LLLT to CCI mouse models of TBI. The mice were split into three groups and received tLLLT (CW 810 nm laser, 25 mW/cm^2 power density, 18 J/cm^2 energy density) once at 4 h post-CCI, at 3 total treatments (once a day for 3 days), or at 14 total treatments (once a day for 14 days). They found that tLLLT may have beneficial effects as a treatment of TBI when treated with a single laser treatment and to a greater degree with three laser treatments. These two groups showed significant improvement in the NSS, motion tests, and in the wire grip test. However, in the group given 14 treatments, there was no significant improvement in any area. This article also discussed that using tLLLT (once or thrice) on mice with TBI could lead to improved neural function, smaller lesion size, and could possibly protect against neuronal damage in the brain.[64]

tLLLT Has More Effect on IEX Knockout Mice

Mild injury to the brain can sometimes trigger secondary brain injury that can lead to severe postconcussion syndrome. The mechanism behind these series of events is not well understood. Zhang et al.[65] showed that secondary brain injury occurs to a worse degree in mice that had been genetically engineered to lack “Immediate Early Response” gene X-1 (IEX-1) when exposed to a gentle head impact (this injury is thought to closely resemble mild TBI in humans). This secondary injury could be characterized by widespread leukocyte infiltrates and extensive cell death that lead to large amounts of tissue loss. A similar insult in wild-type mice (mice with intact IEX-1) did not produce any secondary injury. Exposing IEX-1 knockout mice to LLLT 4 h

postinjury suppressed proinflammatory cytokine expression of IL-Iβ and IL-6, but upregulated TNF-α. The lack of IEX-1 decreased ATP production, but exposing the injured brain to LLLT elevated ATP production back to near normal levels. The protective effect of LLLT may be attributed to enhanced ATP production and the regulation of proinflammatory mediators. This new model of IEX knockout mice could be a good tool for investigating the pathways of secondary brain injury as well as the mechanisms behind the beneficial effects of LLLT.[65]

tLLLT in Combination with Metabolic Inhibitors

Vascular damage occurs in injured brains and frequently leads to hypoxia, a result that often explains poor results in the clinic. Dong et al.[66] found that neurons cultured under hypoxia led to high levels of glycolysis, reduced levels of ATP generation, increased formation of ROS, and increased levels of apoptosis. The adverse effects of hypoxia were almost completely reversed after treatment with LLLT. LLLT maintained the mitochondrial membrane potential, constrained cytochrome c leakage in cells succumbing to hypoxia, and protected these cells from apoptosis. The beneficial effects of LLLT were strengthened by combining the treatment with metabolic substrates such as pyruvate and/or lactate, both *in vivo* and *in vitro*. This combinatorial treatment was able to reverse memory and learning deficits in TBI-injured mice back to normal levels as well as leaving the hippocampal region completely protected from tissue loss; a stark contrast to control TBI mice that exhibited severe tissue loss from secondary brain injury. Dong et al. concluded that metabolic modulators could work in concert with LLLT to improve its beneficial effects in tissues that have low energy output, such as injured brain tissue.[66]

tLLLT Increases Neuroprogenitor Cells

Previous studies have shown that treating mice with CCI-induced TBI, with LLLT using an 810-nm laser at 4 h post-TBI, could significantly improve the NSS, while decreasing the lesion size. Xuan et al. hypothesized that tLLLT could improve performance on the MWM for learning and memory and increase neurogenesis in the hippocampus and subventricular zone (SVZ) after CCI TBI in mice.[67] TBI was created by subjecting the mice to a single right lateral CCI using a pneumatic impact device with 3 mm flat-tip rod at a speed of 4.8 m/sec with an impact depth of 2 mm. TBI mice were given one of two treatments: one laser treatment 4 h post-TBI or three daily applications (once per day). Both the 1 day and three daily laser treatment groups showed improvement in neurological performance as measured by the wire grip test and by the motion test especially at 3 and 4 weeks post-TBI. Improvements were found in visible and hidden platform latency and probe tests in MWM at 4 weeks. At 4 days post-TBI, caspase-3 expression was found at lower levels in the region of the lesion and double-stained BrdU-NeuN (neuroprogenitor cells) was increased in the dentate gyrus (DG) of the hippocampus and the SVZ. Xuan et al. suggested that tLLLT may improve TBI both by reducing cell death in the lesion and also by stimulating neurogenesis in the hippocampus and the SVZ.[67]

tLLLT Increases BDNF and Synaptogenesis

Other studies have shown that applying NIR light to the head of animals with TBI improves neurological function, lessens the size of the brain lesion, reduces inflammation in the brain, and stimulates the formation of new neurons. In the study by Xuan et al.,[68] they examined the expression of BDNF levels in CCI-TBI mice treated with tLLLT. CCI-TBI mice were subjected to two treatment regimens: either once 4 h post-TBI or were given three daily applications with 810 nm CW laser with an energy density of 36 J/cm^2 at a power density of 50 mW/cm^2. The NSS improved when compared to the untreated mice on day 14 and improved further by days 21 and 28. The mice given daily treatments for 3 days showed an even greater improvement when compared to the single treatment group. After the mice were sacrificed on days 7 and 28 for analysis, it was found that BDNF was upregulated by laser treatment in the DG of the hippocampus and the SVZ, but not in the perilesional cortex (lesion). A marker of synaptogenesis, Synapsin-1, was up-regulated in the lesion and the SVZ, but not in the DG. Upregulation was seen at day 28 but not at day 7. Xuan et al. found that the benefit of LLLT to the brain is partly mediated by stimulation of BDNF production, which may encourage synaptogenesis. In turn, these benefits of BDNF suggest that tLLLT may have a broader application to neurodegenerative and psychiatric disorders.[68]

tLLLT in Humans with TBI

Based on postmortem observations, transcranial application of NIR light can penetrate through human scalp, skull, meninges, and brain to a depth of ~40 mm (808 nm laser system).[69] An estimated 2–3% of NIR laser light applied transcranially in human cadavers has also been reported at 1–2 cm depth.[70] In 2011, Naeser et al. published two clinical case reports of improved cognition in chronic TBI patients following a series of treatments with red/NIR LEDs applied transcranially.[71] In the first case study, the patient reported that her ability to concentrate on tasks for a longer period of time (time able to work at computer) increased from 20 min to 3 h, she had a better ability to remember what she read, decreased sensitivity when receiving haircuts in the spots where LLLT was applied, and improved mathematical skills after undergoing LLLT. A 500 mW CW red/NIR LED with a power density of 25.8 mW/cm^2 (area of 19.29 cm^2) was applied to the forehead for a typical duration of 10 min (13.3 J/cm^2). After applying the red/NIR LED LLLT treatment, both TBI patients reported an improvement in sleep and a better ability to control their social behavior.[71] Using red/NIR LED cluster heads, each with a power density of 22.2 mW/cm^2 (area of 22.48 cm^2), the second patient had statistically significant improvements compared to prior neuropsychological testing, after 9 months of nightly, self-administered home tLED treatments. She returned to work after 4 months of the tLED treatments, whereas she had been on disability for 5 months before that time. The patient had a two standard deviation (SD) increase in tests of inhibition and inhibition accuracy (9th percentile to 63rd percentile) on the Stroop test for executive function and a one SD increase on the Wechsler Memory scale test for the logical memory test (83rd percentile to 99th percentile).[71]

Both these reported case studies showed significant improvement in the patient's states of wellbeing, despite variability in a number of different areas, including time of injury (2 vs. 7 years) and cause of injury (motor vehicle accident vs. injuries resulting from rugby, sky diving, military deployment, and accidental injury).

Naeser et al.[72] conducted an open protocol study that examined whether scalp application of red and NIR light could improve cognition in patients with chronic, mild traumatic brain injury (mTBI). This study had 11 participants ranging from the age of 26 to 62 years (6 males, 5 females) who had persistent cognitive dysfunction resulting from mTBI. The participants' injuries were caused by motor vehicle accidents, sports-related events, and for one participant, IED blast injury. The tLLLT consisted of 18 sessions (Monday, Wednesday, and Friday for 6 weeks) and started from 10 months to 8 years post-TBI. A total of 11 LED clusters (5.25 cm in diameter, 500 mW, 22.2 mW/cm^2, 13 J/cm^2) were applied for about 10 min per session (5 or 6 LED placements per set, Set A and then Set B, in each session). Neuropsychological testing was performed pre-LED application and 1 week, 1 month, and 2 months after the final treatment. Naeser et al. found that there was a significant positive linear trend observed for the Stroop Test for executive function, in trial 3 inhibition ($p = 0.004$); Stroop, trial 4 inhibition switching ($p = 0.003$); California Verbal Learning Test (CVLT)-II, total trials 1–5 ($p = 0.003$); and CVLT-II, long delay free recall ($p = 0.006$). Improved sleep and fewer post-traumatic stress disorder (PTSD) symptoms, if present beforehand, were observed after treatment. Participants and family members also reported better social function and a better ability to perform interpersonal and occupational activities. Although these results are significant, further placebo-controlled studies will be needed to ensure the reliability of these data.[72]

Nawashiro et al.[61] quantified cerebral blood flow using single-photon emission computed tomography with N-isopropyl-p-iodoamphetamine (IMP-SPECT). In this case study, a single patient who was in a vegetative state following severe head trauma was administered 146 LED treatments over a period of 73 days with a device consisting of a grid of 23 diodes, 820 nm LED, each 13 mW, with a power density of 11.4 mW/cm^2, an energy density of 20.5 J/cm^2, and was held 5 mm from the head for 30 min per treatment. After giving treatments bilaterally to the forehead, a 20% increase in blood flow in the left anterior frontal lobe was observed. It was also noted that the patient showed slight movement in the left arm after treatment.

More controlled clinical studies with much larger numbers of patients will be needed to better understand factors that may affect treatment response following a series of tLLLT treatments with brain injuries of different etiologies (TBI or stroke) and different degrees of severity. Collaboration among researchers will be necessary to achieve consistency of tLLLT treatment protocols and parameters applied, as well as measurement of the effects. For example, data from sophisticated brain imaging techniques before and after a series of tLLLT treatments in a specific patient population could help with understanding brain changes that may be occur following a series of tLLLT treatments with that disorder. Some brain imaging techniques include the following: (1) structural

magnetic resonance imaging (MRI) scans, which could show potential changes in cortical thickness post-tLED—for example, perhaps in the hippocampus areas, if thinning was present pre-tLLLT; (2) diffusion tensor imaging MRI to measure axonal damage in specific pathways before entry and potential changes post-tLED; (3) Task-related functional MRI to measure cortical activation during tasks requiring focused attention and inhibition, including reaction times; (4) resting-state functional connectivity MRI to measure functional connectivity in the intrinsic networks of the brain; and (5) brain imaging to measure changes in regional, cerebral blood flow utilizing PET or IMP-SPECT scans. Improvements observed with these brain imaging techniques would be expected to parallel changes in behavior, such as improved executive function and verbal memory, as well as changes in mental status, including PTSD and depression. The improvements in behavior are also expected to translate into better quality of life for these patients as well as their families. Long-term tLLLT treatments may be necessary to maintain the gains made. These are all factors that require further research.

Conclusions

tLLLT has strong evidence for many beneficial effects on TBI and stroke in both animal models and human patients. Both acute stroke and acute TBI have a growing number of studies being published showing that tLLLT is an effective means of treating both. The many benefits of tLLLT are thought to be based on several different biological mechanisms. Near-infrared PBM functions by improving mitochondrial energy production by stimulating the enzyme CCO and increasing ATP synthesis. Laser therapy can result in neuroprotection and help prevent the spread of brain cell death after injury as shown by the long-term development of smaller lesion areas in mice treated with LLLT, when delivered at 4 h post-TBI. Protection against toxins, increased cellular proliferation, and reduction in apoptosis and anti-inflammatory and antiedema effects may also contribute to the mechanisms that underlie the beneficial effects of PBM. The most exciting prospect is the possibility that tLLLT may stimulate both neurogenesis (the ability of the brain to repair itself) and synaptogenesis (encourage cells to form new synaptic connections). This could lead to the application of tLLLT as a treatment modality for neurodegenerative diseases such as Alzheimer's disease and Parkinson's disease. Well-funded, controlled studies are necessary.

WHAT IS DEEP PENETRATING LIGHT AND HOW DOES IT BENEFIT YOU?

By Aliki Chatzilias, MSc.
Clinical Biochemist/Medical Researcher

Introduction

In the fast-paced world of wellness, the quest for effective therapies never ceases. Deep Penetrating Light (DPL) emerges as a promising contender, offering a beacon of hope for those seeking holistic well-being. Delving into the intricacies of DPL requires a fundamental understanding of its mechanisms and applications.

Understanding Deep Penetrating Light

Definition and Explanation: Deep Penetrating Light, often known as low-level laser therapy (LLLT) or photobiomodulation (PBM), involves the application of low-level lasers or light-emitting diodes (LEDs) to stimulate cellular function. The photons emitted penetrate the skin, triggering biochemical processes that enhance cellular energy production.

Mechanism of Action: At its core, DPL operates through the principle of photobiomodulation, influencing cellular processes at the molecular level. Specific wavelengths of light, typically in the red or near-infrared spectrum, interact with chromophores within cells, initiating a cascade of events that lead to increased ATP production, improved oxygenation, and enhanced cellular repair mechanisms.

Benefits of Deep Penetrating Light

Physical Benefits: The application of DPL manifests a myriad of physical advantages. Enhanced blood circulation, facilitated by vasodilation induced by light exposure, promotes nutrient delivery and waste removal. Additionally, DPL showcases anti-inflammatory properties, alleviating pain and contributing to accelerated tissue repair and regeneration.

Mental and Emotional Benefits: Beyond its physical impacts, DPL exhibits profound effects on mental and emotional well-being. The modulation of neurotransmitters and reduction of oxidative stress contribute to improved mood and stress reduction. Emerging studies also suggest potential applications in addressing mental health conditions, opening new avenues for research.

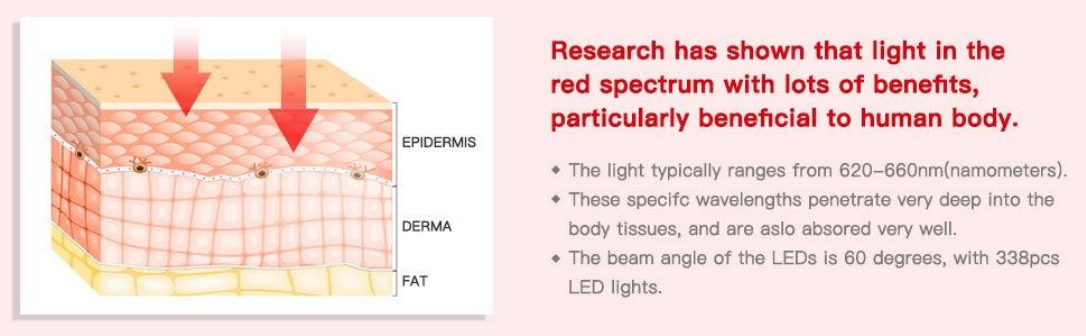

Application in Various Fields: The versatility of DPL finds application in diverse sectors. In the medical realm, it complements traditional treatments for conditions like chronic pain and wound healing. In the beauty and skincare industry, DPL is harnessed for its collagen-stimulating properties, contributing to skin rejuvenation. Moreover, athletes leverage DPL for enhanced recovery and performance.

Devices and Technologies

Overview of Deep Penetrating Light Devices: A spectrum of devices facilitates DPL, ranging from handheld units to larger systems for professional use. Accessibility for home use has surged, enabling individuals to incorporate DPL into their routine with user-friendly devices.

Notable Technologies: Pioneering technologies have propelled DPL into the spotlight. Devices employing targeted wavelengths and advanced delivery mechanisms optimize therapeutic outcomes. Brands at the forefront of innovation continue to refine and enhance DPL technologies, promising more efficient and user-friendly experiences.

Safety Considerations

General Safety Guidelines: While DPL is generally considered safe, adherence to guidelines is paramount. Managing the duration and frequency of exposure prevents overstimulation, and understanding potential side effects ensures a positive experience. It's crucial for users to be aware of contraindications and exercise caution accordingly.

Consultation with Healthcare Professionals: Individuals considering DPL should consult healthcare professionals. A thorough assessment of medical history and existing conditions ensures personalized advice, minimizing risks and maximizing benefits. Collaboration between users and healthcare providers establishes a foundation for safe and effective DPL utilization.

Incorporating Real-Life Examples: Anecdotal evidence amplifies the credibility of DPL. Users across diverse demographics share positive experiences, citing improvements in pain management, skin health, and overall well-being. These narratives provide valuable insights into the varied applications and potential outcomes of DPL.

Future Trends and Research

Ongoing Research: The landscape of DPL is dynamic, with ongoing research unraveling new dimensions. Current studies explore expanded applications, including neurodegenerative diseases and immune system modulation. As the scientific community delves deeper, DPL's potential in shaping future medical interventions becomes increasingly evident.

How to Incorporate Deep Penetrating Light into Your Routine

Practical Tips: Embracing DPL into daily life involves strategic choices. Selecting the right device based on individual needs, understanding optimal exposure times, and establishing a consistent routine are pivotal. A holistic approach considers lifestyle factors, ensuring seamless integration for sustained benefits.

Conclusion

In conclusion, the enigmatic realm of Deep Penetrating Light beckons as a transformative force in the pursuit of wellness. From its profound physiological impacts to its diverse applications, DPL stands at the forefront of cutting-edge therapies. As technology advances and research unfolds, the potential of DPL to shape the future of holistic well-being becomes increasingly tangible.

The Impact of Nootropics on Mitochondrial Health: Improving Energy Production in Brain Cells

Very Big Brain October 3, 2024

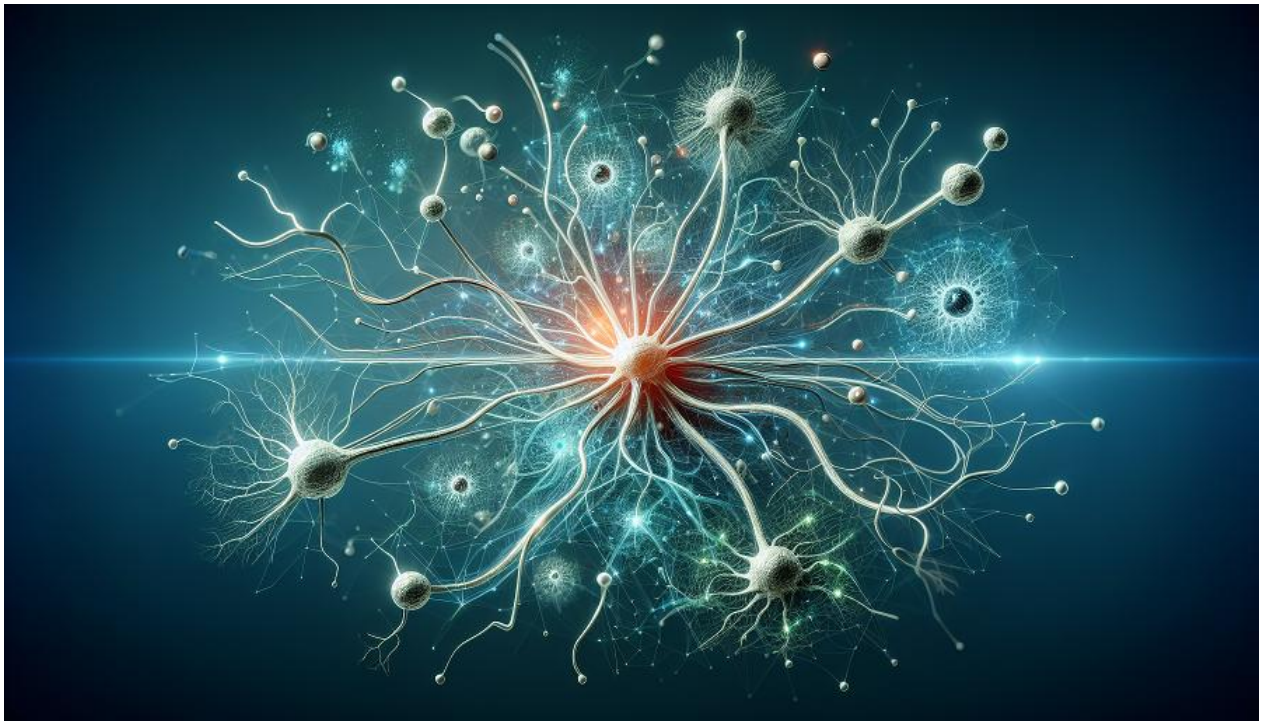

Your brain is a powerhouse, using about 20% of your body's energy to keep you thinking, learning, and functioning throughout the day. But what powers the brain itself? The answer lies in the tiny energy factories inside your cells, known as mitochondria. These microscopic organelles are responsible for producing ATP, the energy currency that fuels brain activity. But as we age, or when we're under stress, mitochondrial function can decline, leading to brain fog, fatigue, and cognitive slowdown. Enter nootropics. These cognitive enhancers might not just sharpen your mind—they can also support mitochondrial health and boost energy production in brain cells.

What Are Mitochondria, and Why Do They Matter for Brain Health?

Mitochondria are often called the “powerhouses” of the cell, and for good reason. These tiny organelles convert nutrients from the food we eat into ATP, a molecule that cells use for energy. The brain, with its high energy demands, relies heavily on healthy mitochondria to keep neurons firing and cognitive processes running smoothly.

When mitochondria aren’t working at full capacity, brain cells don’t get the energy they need. This can lead to mental fatigue, poor concentration, and even contribute to neurodegenerative diseases. Supporting mitochondrial health is crucial for maintaining cognitive performance, especially as we age. This is where nootropics come into play—they can help optimize mitochondrial function, ensuring your brain stays energized and sharp.

How Nootropics Boost Mitochondrial Function

Nootropics don’t just enhance focus or memory—they can also support the very machinery that keeps your brain running. Certain nootropics boost mitochondrial efficiency, protect them from oxidative stress, and even stimulate the production of new mitochondria. Here’s how these cognitive enhancers help keep your brain cells powered up.

Improving Mitochondrial Efficiency

Efficient mitochondria produce more energy with less effort. Nootropics like **Pyrroloquinoline Quinone (PQQ)** improve mitochondrial efficiency by enhancing the processes involved in ATP production. PQQ promotes the creation of new mitochondria in a process called mitochondrial biogenesis, giving your brain more power to work with.

Think of it this way: when your mitochondria are running efficiently, it’s like upgrading an old, sluggish car engine to a shiny new model. Your brain gets more energy with less wear and tear, improving everything from focus to overall cognitive stamina.

Protecting Mitochondria from Oxidative Stress

Oxidative stress is like rust for your brain cells, damaging mitochondria and slowing down energy production. This occurs when free radicals (unstable

molecules) overwhelm your body's ability to neutralize them. Fortunately, some nootropics act as powerful antioxidants, protecting your mitochondria from oxidative damage.

Nootropics like **CoQ10** and **Alpha-Lipoic Acid (ALA)** help scavenge free radicals, reducing oxidative stress and preserving mitochondrial function. By keeping mitochondria healthy, these nootropics can help maintain consistent energy production, preventing brain fatigue and mental fog.

Top Nootropics for Supporting Mitochondrial Health

Now that we understand how nootropics support mitochondrial health, let's take a closer look at some of the best options available. These nootropics can boost energy production in brain cells, protect mitochondria from damage, and even stimulate the growth of new mitochondria.

Pyrroloquinoline Quinone (PQQ)

Pyrroloquinoline Quinone, or PQQ, is one of the most potent nootropics for enhancing mitochondrial function. PQQ not only helps existing mitochondria work more efficiently but also promotes the growth of new ones. This process, known as mitochondrial biogenesis, increases the overall energy production capacity of your brain cells.

PQQ is often used by people looking to combat brain fog, boost mental energy, and improve overall cognitive function. It's like giving your brain a fresh set of batteries, ensuring that you have the energy you need for sustained mental performance.

Coenzyme Q10 (CoQ10)

CoQ10 is a powerful antioxidant that plays a crucial role in energy production within mitochondria. It's essential for converting food into ATP, and it also helps protect mitochondria from oxidative damage. As we age, levels of CoQ10 decline, which can lead to slower cognitive function and fatigue.

Supplementing with CoQ10 helps restore this vital compound, ensuring your brain cells have the energy they need to stay sharp.

Alpha-Lipoic Acid (ALA)

Alpha-Lipoic Acid (ALA) is another antioxidant that supports mitochondrial health by reducing oxidative stress. It works alongside CoQ10 to protect mitochondria from damage while also improving glucose metabolism, which can further enhance brain energy levels. ALA is particularly useful for people looking to maintain cognitive function as they age.

Acetyl-L-Carnitine (ALCAR)

Acetyl-L-Carnitine, or ALCAR, helps transport fatty acids into mitochondria, where they are used to produce energy. ALCAR is well-known for its ability to enhance mental clarity, focus, and energy by supporting mitochondrial function. It's especially beneficial during periods of mental exertion or fatigue, making it a popular choice for students, professionals, and anyone looking to boost their mental stamina.

The Connection Between Mitochondrial Health and Cognitive Performance

Why should you care so much about your mitochondria? The connection between mitochondrial health and cognitive performance is stronger than you might think. When your brain cells are running low on energy, everything from memory to focus can take a hit. By improving mitochondrial function, you can directly boost your cognitive abilities, making it easier to stay focused, think clearly, and process information efficiently.

Mental Fatigue and Mitochondrial Decline

One of the clearest signs of mitochondrial decline is mental fatigue. If your mitochondria aren't producing enough energy, you'll feel mentally exhausted, even if you're not doing anything physically demanding. Nootropics that

support mitochondrial health can help combat this fatigue by ensuring your brain cells have the energy they need to perform at their best.

Memory and Learning

Memory and learning also rely heavily on energy-hungry processes in the brain. By supporting mitochondrial health, nootropics like PQQ and CoQ10 can improve your ability to retain and recall information. This is particularly useful for students or professionals who need to stay sharp and learn new information quickly.

Nootropic Stacks for Mitochondrial Health

For those looking to maximize their mitochondrial support, building a nootropic stack that targets mitochondrial health from multiple angles is a smart approach. Here are a couple of stack ideas that can boost energy production, reduce oxidative stress, and enhance cognitive performance.

Stack 1: PQQ + CoQ10 + ALA

This stack is designed for maximum mitochondrial support. PQQ promotes mitochondrial biogenesis, while CoQ10 and ALA work together to protect mitochondria from oxidative damage and ensure efficient energy production. This combination is perfect for anyone looking to enhance mental energy, focus, and overall brain health.

Stack 2: ALCAR + PQQ + Rhodiola Rosea

If you're looking for a stack that boosts both mental and physical stamina, this combination is ideal. ALCAR supports energy production by transporting fatty acids into mitochondria, PQQ promotes the growth of new mitochondria, and Rhodiola Rosea helps reduce mental fatigue and stress, ensuring that your brain cells stay energized even under pressure.

Can Nootropics Really Improve Mitochondrial Health?

So, can nootropics truly support mitochondrial health and improve brain energy? Absolutely. By boosting mitochondrial efficiency, promoting the creation of new mitochondria, and protecting against oxidative stress, nootropics like PQQ, CoQ10, and ALCAR can have a significant impact on brain cell energy production. Whether you're looking to combat brain fog, enhance focus, or improve memory, supporting mitochondrial health is a crucial step in optimizing cognitive performance.

Incorporating nootropics that target mitochondria into your routine could help keep your brain cells powered up, providing the mental energy you need to tackle whatever comes your way. And in the ever.

Energy transport mechanisms of light-triggered release from nanocarriers

Nadezda Fomina [1], Jagadis Sankaranarayanan [1], Adah Almutairi [1,*]

Abstract

Over the last three decades, a handful of photochemical mechanisms have been applied to a large number of nanoscale assemblies that encapsulate a payload to afford spatio-temporal and remote control over activity of the encapsulated payload. Many of these systems are designed with an eye towards biomedical applications, as spatio-temporal and remote control of bioactivity would advance research and clinical practice. This review covers five underlying photochemical mechanisms that govern the activity of the majority of photoresponsive nanocarriers: 1. photo driven isomerization and oxidation, 2. surface plasmon absorption and photothermal effects, 3. photo driven hydrophobicity changes, 4. photo driven polymer backbone fragmentation and 5. photo driven de-crosslinking. The ways in which these mechanisms have been incorporated into nanocarriers and how they affect release is detailed, as well as the advantages and disadvantages of each system.
Keywords: photochemical, triggered release, light, near infrared, nanocarriers, nanoparticles

1. Introduction

It is well established that nanocarriers in drug delivery offer many advantages over conventional formulation methods. They can minimize degradation of therapeutic agents upon administration, enhance their in vivo efficiency by delivering higher concentrations of drugs to tumor sites, expose the tumors to active drug for longer periods, and prevent undesirable side effects. In addition, these carriers can protect the therapeutic payload from the harsh *in vivo* environment. Furthermore, current studies on

synergistic therapeutic outcomes of combination therapies are better enabled through the use of drug delivery vehicles.

Organic materials, both natural and synthetic, can be used to tailor nanocarriers to provide specific characteristics, including triggered release on demand. The goal of triggered drug delivery is to control the time and place of release of a therapeutic agent to achieve a higher local concentration, reduce overall injected dose, and reduce systemic toxicity.

Various internal and external triggers, such as pH, specific enzymes, temperature, ultrasound, magnetic field and light are being actively explored. Light is especially attractive, as it can be remotely applied with extremely high spatial and temporal precision. Additionally, a broad range of parameters (wavelength, light intensity, duration of exposure, and beam diameter) can be adjusted to modulate release profiles. Radiation in the UV, visible, and near infrared (NIR) regions can be applied *in vivo* to induce drug release. Systems responsive to UV and visible irradiation can be used for topical treatments; radiation below 650 nm cannot penetrate deeper than 1 cm into tissue due to high scattering and absorption by hemoglobin, oxy-hemoglobin, and water . NIR light of 650 – 900 nm (water absorbs wavelengths longer than 900 nm) can penetrate up to 10 cm [1] into living tissue and causes minimal tissue damage at the site of application.

This review focuses on light-triggered release from nanosystems. In this size regime one can passively target diseased tissues like tumors by exploiting the enhanced permeation and retention (EPR) effect while at the same time remotely and actively trigger release via light. The structure of this review reflects different mechanisms by which therapeutic agents may be released from nanocarriers upon light exposure. We cover many different nanocarrier types developed to date, including micelles, polymeric nanoparticles, hollow metal nanoparticles, and liposomes as examples of different triggering mechanisms using various photochemical reactions in order to facilitate release of cargo from the nanocarrier. All reactions lead to a change in the nanocarrier assembly either directly or indirectly, which leads to release of the encapsulated bioactive agent. While other reviews have focused on the photo-triggered release of particular nanocarriers (liposomal systems [2-3], micelles [4-6], etc.) separately, we would like to focus on the mechanism of release rather than the nanocarrier. It should be noted that while the choice of nanocarrier can vary based on the application desired, the photochemistry involved could be applied to multiple materials and the challenges with each mechanism need to be addressed. We have also limited the scope of our review to systems for which release of cargo from nanocarriers has been demonstrated.

2. Mechanisms of light-triggered release from nanocarriers

I. Photoisomerization, photocrosslinking, and photosensitization-induced oxidation

Photoisomerization is a process that involves a conformational change about a bond that is restricted in rotation, usually a double bond. In organic molecules with double bonds, this predominantly involves isomerization from a *trans* orientation to a *cis* form upon irradiation with light. Azobenzenes, which have -N=N- with phenyl rings on either side, are the most commonly used molecules for this purpose. The planar *trans* form of azobenzenes is more hydrophobic than the nonplanar *cis* form, so *cis* azobenzenes form micelles less easily. UV irradiation-induced conversion of azobenzenes to *trans* causes disruption of the assemblies. Azobenzenes are attractive because the isomerization is reversible, which is important in applications that require drug delivery on demand.

The first report of incorporating azobenzene in a nanocarrier system to effect release was reported by Kano et al. in 1980 [7]. In their work they incorporated an amphiphilic azobenzene (C2Azo and C4Azo, Figure 1) moiety along with dipalmitoylphosphatidylcholine (DPPC) at various molar ratios and were able to modulate the release profiles of liposomes based on the azo moiety of choice, the composition of photo-stationary state, and the degree of incorporation in the liposome. They characterized the photoisomerization process via UV spectroscopy by irradiating the *trans* azo compound at 366 nm for 10 seconds. The *trans* compound formed a photo-stationary state with 80% *cis* isomer which reverts back to *trans* when irradiated at >420 nm. They also measured the resulting osmotic shrinkage of the vesicles upon incorporation of azo compound (C2Azo & C4Azo) by measuring the optical density of the solutions. The authors encapsulated bromothymol, a blue dye, in the lipid bilayer of liposomes formulated from DPPC and subsequently showed that the permeation of the dye into water increased with greater incorporation of the *cis* azobenzene moiety (formed by irradiation). In these pioneering studies, percent release and duration of release upon pulsing were not entirely characterized.

Figure 1.

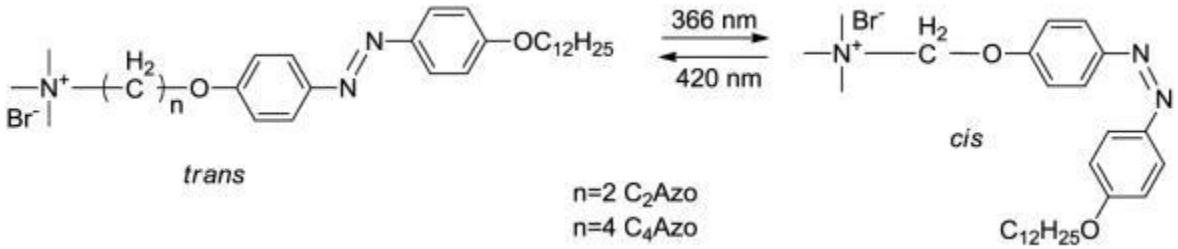

Structure of amphiphatic azobenzene moiety utilized in the study by Kano et al [7].

Since this seminal study there have been numerous publications utilizing this concept. Many systems developed since have incorporated azobenzenes in lipid backbones and formulated liposomes that are photo-responsive [8-13]. The photo-responsiveness of the liposomes arises from the fact that in the *trans* orientation the molecules pack tightly in the bilayer. When irradiated with UV light, they undergo *trans-cis* isomerization, which leads to distortions in the packing of the bilayer and causes the liposomes to become

“leaky,” allowing the encapsulated drugs to be released (Figure 2). Irradiation of azobenzene results in the formation of a photo-stationary state and the composition of this state determines the release rate of the drug. More recently, Smith et al. have used photo-triggerable liposomes to trigger gelation of an alginate solution by releasing calcium chloride upon irradiation with 385 nm light for 1min. Such on demand gelation is important in tissue engineering applications [14].

Figure 2.

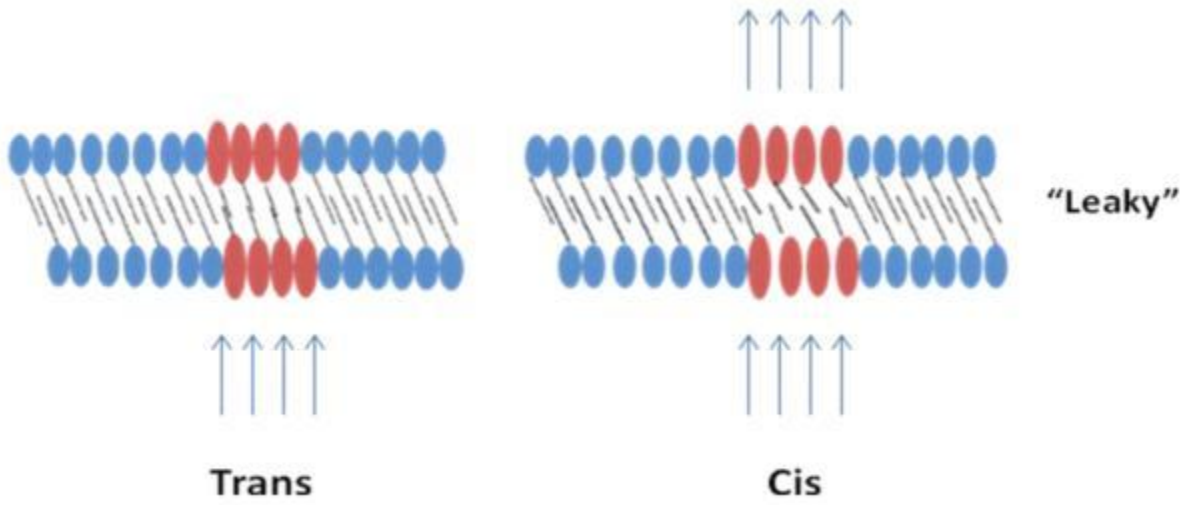

Schematic representation of a cross-section of lipid bilayer packed with *trans*-azobenzenes that photoisomerize upon irradiation into the *cis*-form and cause distortions in the lipid packing.

The photoisomerization concept has also been successfully utilized in preparation of photo-responsive micelles. These systems take advantage of the change in net dipole moment upon switching from the *trans* orientation (no net dipole moment) to the *cis* orientation. This leads to disruption in the hydrophobic-hydrophilic balance of the self-assembled micelles and causes reorganization and subsequent release of encapsulated contents [5].

The first report of utilizing azobenzene to encapsulate a model hydrophobic substance involved an azobenzene-based surfactant, 4-butylazobenzene-4′-(oxyethyl) trimethylammonium bromide (AZTMA). In this preliminary study the authors encapsulated ethylbenzene and showed its release upon irradiation with UV light. They also found the process to be reversible when irradiating with visible light. The authors quantified release by measuring the vapor pressure of ethyl benzene in the headspace, which increased upon irradiation with UV light (260-390nm at 10mW/cm^2) for 2 hrs. They found that at an AZTMA concentration of 5mM, the vapor pressure of ethyl benzene increased to values equivalent to those for pure ethyl benzene, suggesting complete release [15-16].

In later work Wang et al. [17] developed a cationic azobenzene-based surfactant to form an ionomer with a doubly hydrophilic block copolymer of polyethylene glycol and poly acrylic acid (Figure 3A) that self assembled into vesicle like aggregates. They showed that when pyrene sulfonic acid-containing aggregates were irradiated (360 nm) for 300s, the azo benzene underwent photoisomerization leading to release of the dye, as seen by an increase in fluorescence of the solution. When irradiated by visible light (440 nm) for 900s, they observed partial quenching of the solution, leading them to conclude the dye was re-encapsulated. The authors explain the incomplete re-encapsulation upon visible light irradiation as irreversible release of the dye (Figure 3B).

Figure 3.

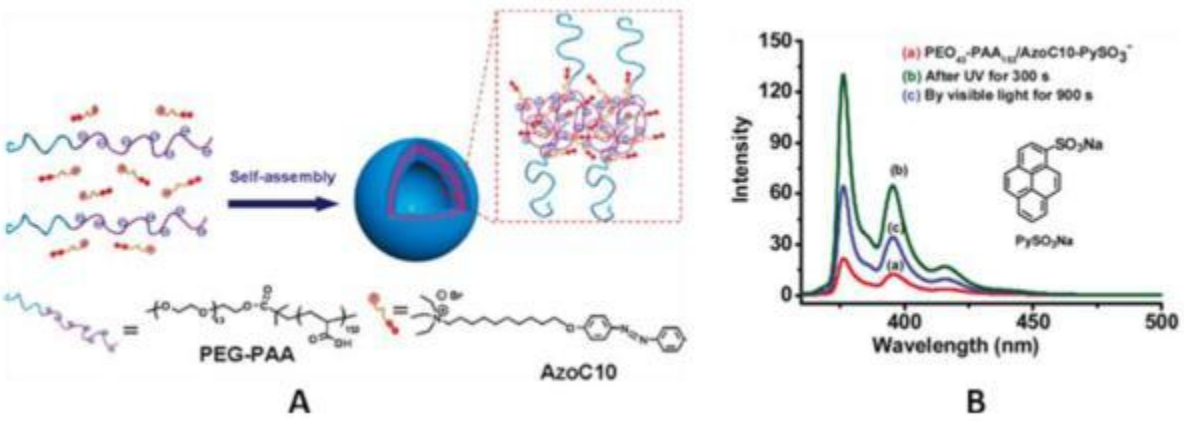

A) Schematic representation of the formation of ionomer vesicles from AzoC10 and PEG-PAA. B) fluorescence emission spectra of pyrene sulfonic acid, a) before, b) after UV, and c) after visible irradiation [17].

Recently, Zhao et al. used this concept in preparing the first macromolecular diblock copolymer micelles [18]. While there have been numerous such reports of azobenzene-based block copolymers for photo-responsive micelles, little has been done towards utilizing these diblock copolymer systems for controlled release applications [5-6, 19-21].

Another area where azobenzenes are used is in making nano-impellers for drug delivery applications. Patnaik et al. [22] made azodextran-based nanogels in which 5% and 10 % of linear dextran moieties were functionalized with a hydrophobic derivative of azobenzene (AD-5 and AD-10, Figure 5). This resulted in the self-assembly of the dextran chains to form nanostructures. The self-assembly is driven by stacking of the flat, linear azobenzene groups. When irradiated at 365 nm, these nanogels undergo photoisomerization, which leads to disruption of stacking and release of the contents. The authors showed that release of model dyes and drugs from AD-5 and AD-10 when irradiated with 365nm is directly proportional to irradiation time (0-300min). They also showed that AD-10 encapsulates and releases more drug than AD-5 due to increased azobenzene content.

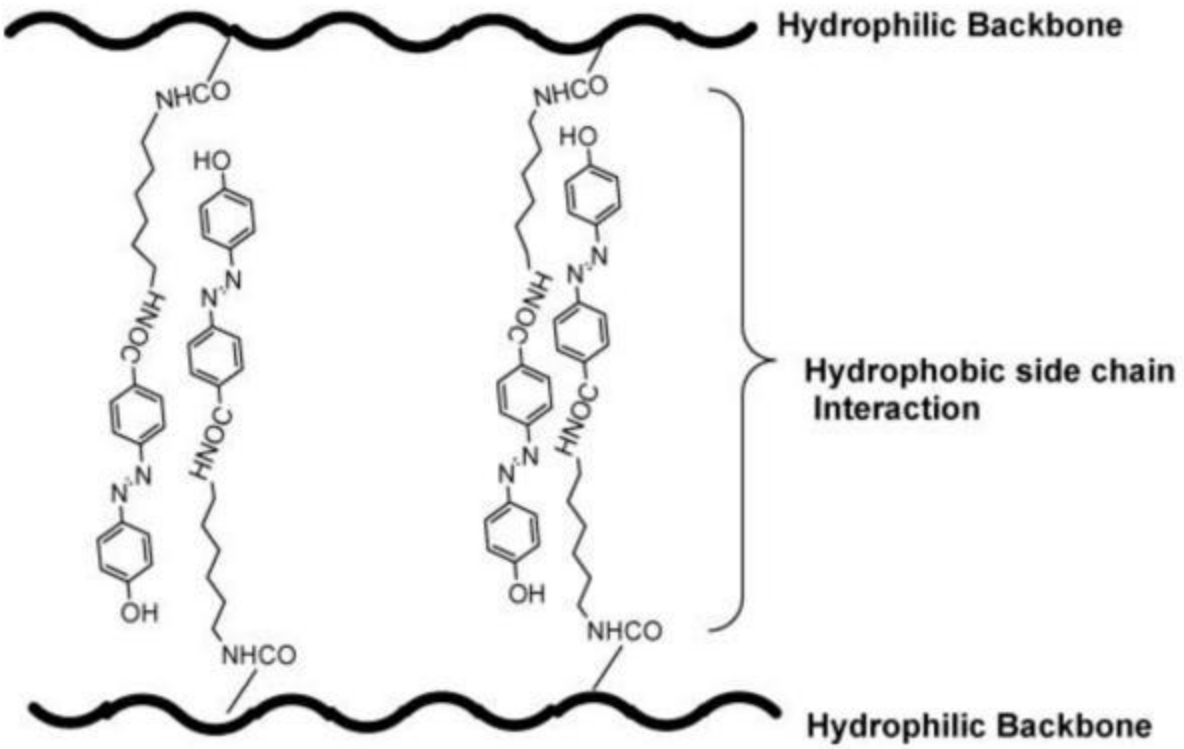

Figure 5.

Schematic representation of non-covalently crosslinked azo-dextran nanogels, AD [22].

Nano-impellers have also been made to form core-shell mesoporous silica structures. Angelos et al. [23] incorporated azobenzene moieties into mesoporous silica particles that function both as impellers and “gatekeepers” to retain the encapsulated drug and release it on demand (Figure 6). The mechanism of release relies on continuous photoisomerization reactions within the particles, resulting in “wagging” of the polymer strands that form the gates of these structures and release. In order to achieve wagging, the particles were irradiated using 9 mW 457 nm light continuously for 1200s. At this wavelength both *cis* and *trans* isomers absorb and photoisomerize with a quantum yield of 0.64 and 0.36, respectively. The released dye was monitored at 540 nm by sampling the solution of particles at one second intervals, which revealed that no dye was released in the absence of irradiation when AzoG1 was used. In comparison, particles formulated with AzoH were leaky even without irradiation. Subsequently, Lu et al. [24] showed that these particles can be used to deliver the anticancer drug camptothecin to cancer cells on demand.

Figure 6.

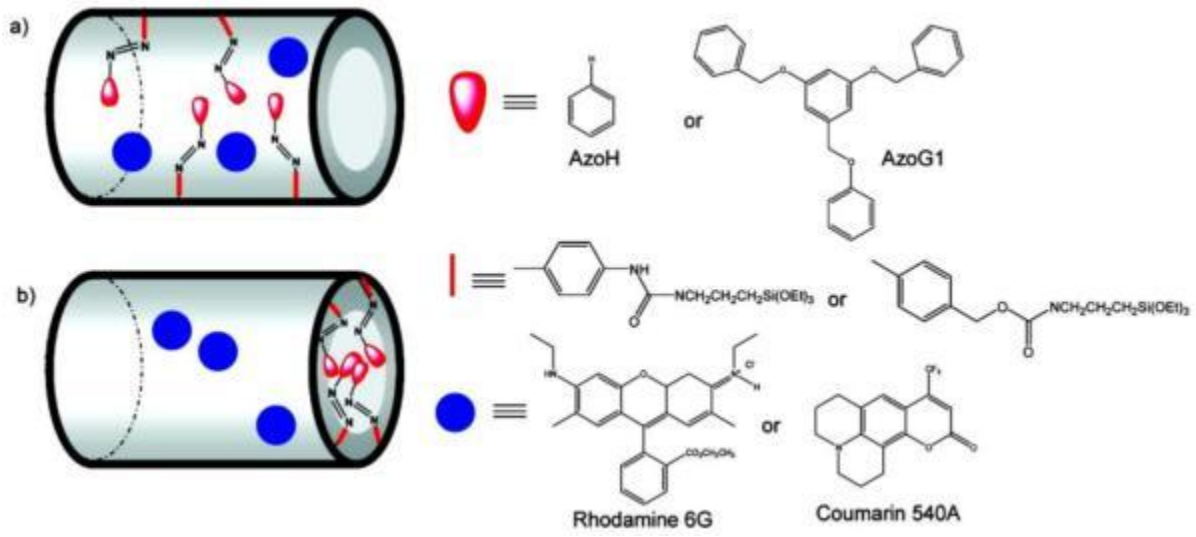

Photoresponsive materials functionalized with azobenzene derivatives. (a) nano-impellers prepared by the co-condensation ethod derivatized with AzoH; (b) triggered release materials prepared by the post-synthesis modification method derivatized with AzoG1 [23].

The major advantage of the azobenzene systems is reversibilty, which may be used to turn the systems on and off and allow dosed release on demand. In spite of their promise, however, systems that rely predominantly on UV irradiation suffer from a lack of translation *in vivo* due to low tissue transparency in the UV region.

Photo-crosslinking or photopolymerization as a means of release might seem counterintuitive, because photo-induced crosslinking is generally used in the formation of nanoparticles. However, this photochemical mechanism can also be used for photo-triggered release. Photo-crosslinking is achieved by irradiating a polymerizable double bond directly or in the presence of a radical initiator/sensitizer. Photopolymerization of double bonds incorporated into the hydrophobic domain of a bilayer causes parts of the bilayer to shrink, disrupting the uniform packaging of the molecules and producing pores in the bilayer, which allows release.

The concept was first realized in liposomes by Regen et al. [25]. Vesicles were formulated with a photo-triggerable (at 254nm) lipid containing two methacrylated phosphatidyl choline derivatives. The resulting vesicles were more stable than non-crosslinked counterparts, which resulted in better circulation. The authors also noted that the leakage rate could be controlled by co-polymerizing the crosslinkable lipids with the homo-polymerizable lipids. Subsequent studies reported systems with modulated rates of release. Some later studies also incorporated sensitizers to absorb at higher wavelengths so that photo-crosslinking could be achieved in the visible region [2-4]. Some recent advances in this area include designing a new class of liposomes containing 1,2 bis-(tricosa-10, 12-dinoyl)-sn-glycero-3-phosphocholine) (DC8,9PC) that

have photo-crosslinkable triple bonds [26]. The authors have shown that these liposomes can be used to deliver doxorubicin (DOX). In addition to performing its cell killing functions, doxorubicin also served as a photosensitizer, resulting in photo-crosslinking of the liposomes upon irradiation at 514 nm. The authors showed that when irradiated with 514 nm (166 mW/cm^2/min) light for 0-7 min, up to a 22% higher release of DOX occurred compared to the non-irradiated samples. This was the first report of a drug being released photochemically from a liposomal formulation (Figure 7).

Figure 7.

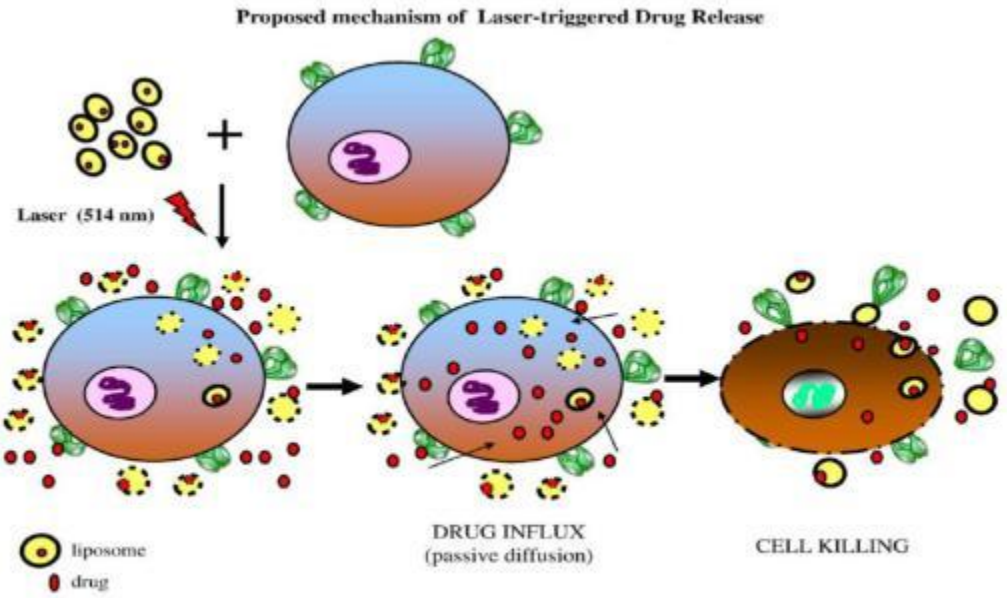

Fig. 5. A Schematic representation of a proposed mechanism of laser-triggered release of entrapped solutes from liposomes. Light treatment of DOX-loaded DPPC:$DC_{8,9}PC$ liposomes results in release of DOX. The effective concentration of the free drug is increased in the vicinity of cells. DOX is subsequently taken up by the cells by passive diffusion leading to improved cell killing.

Schematic representation of the proposed mechanism of laser triggered release of entrapped solutes form liposomes. Light treatment of DOX-loaded DPPC:$DC_{8,9}PC$ liposomes results in release of DOX. The effective concentration of the free drug is increased in the vicinity of cells. DOX is subsequently taken up by cells by passive diffusion leading to improved cell killing. [26]

In addition to liposomes, photocrosslinking has also been used as a means for drug delivery in nanocapsules formulated through layer-by-layer deposition of polymers. Park et al. formulated microcapsules by depositing alternating layers of benzophenone-modified poly-(allylamine hydrochloride) and poly-(sodium-4-styrenesulfonate) on polystyrene particles [27-28]. They subsequently dissolved the polystyrene core in organic solvent to obtain hollow capsules. The benzophenone modified poly-(allylamine hydrochloride) moieties are photocrosslinkable and the release rates of encapsulated molecules from the capsules can be controlled by varying the degree of crosslinking of the poly-(allylamine hydrochloride) layer. It is important to emphasize that this work does not use complete photodegradation as a trigger; rather, it uses photocrosslinking as a means to achieve control over release rates. More recent work on this type of polymers incorporates cinnamic acid derivatives in their backbone. The idea in these

systems is to utilize the [2+2] cycloaddition reaction of *trans* cinnamic acids upon photo-irradiation that results in shrinkage of the nanostructures to expel encapsulated contents (Figure 8). [29-30]

Figure 8.

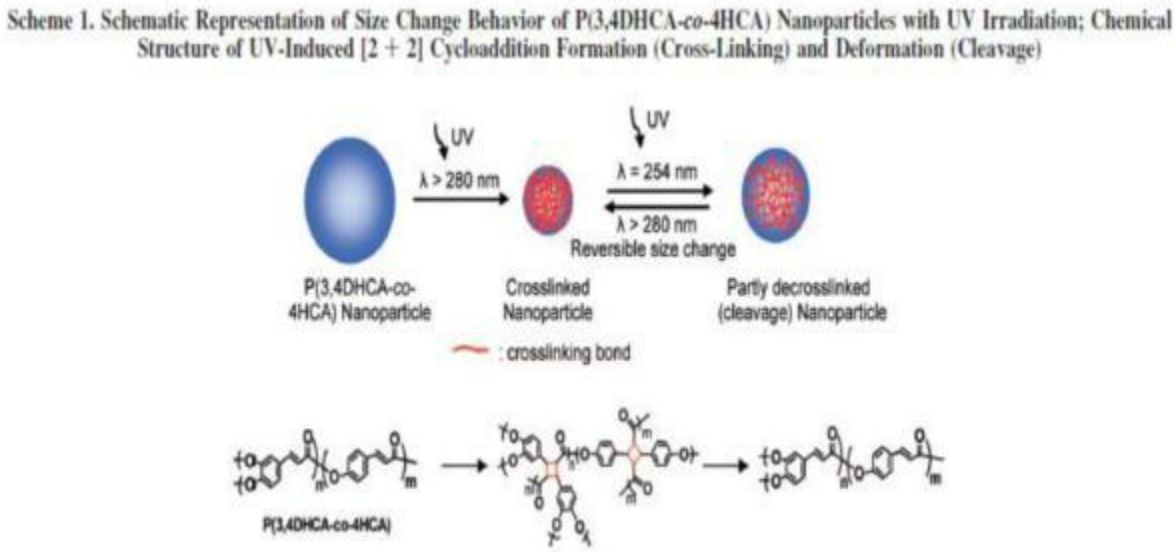

Schematic representation of size change behavior of P(3,4DHCA-co-4HCA) nanoparticles with UV irradiation. Chemical structure of UV-induced [2+2] cycloaddition formation (cross-linking) and deformation (cleavage) [29-30].

Photosensitization-induced oxidation is another photochemical mechanism to impart a change in a nanocarrier through light exposure. Photosensitization-induced oxidation involves generation of a strong oxidizing agent, singlet oxygen, upon illumination of a sensitizer molecule with an appropriate wavelength of light. Singlet oxygen oxidizes plasmogenic lipids and thus causes disruption of biomembranes [31-39]. This mechanism is currently used in photodynamic therapy to disrupt the membrane of cancer cells and induce cell death. The same chemical process can be used to enable photo-controlled release of therapeutic agents from nanocarriers composed of photooxidizable lipids.Lipid photo-oxidation leads to membrane disruption because singlet oxygen formed by irradiation of ZnPc in air leads to the photo-oxidation of the plasmalogen vinyl ether linkage (Fig. 9). [40] The formation of a single-chain surfactant induces a lamellar to hexagonal phase transition, leading to membrane fusion and leakage of the encapsulated content.

Figure 9.

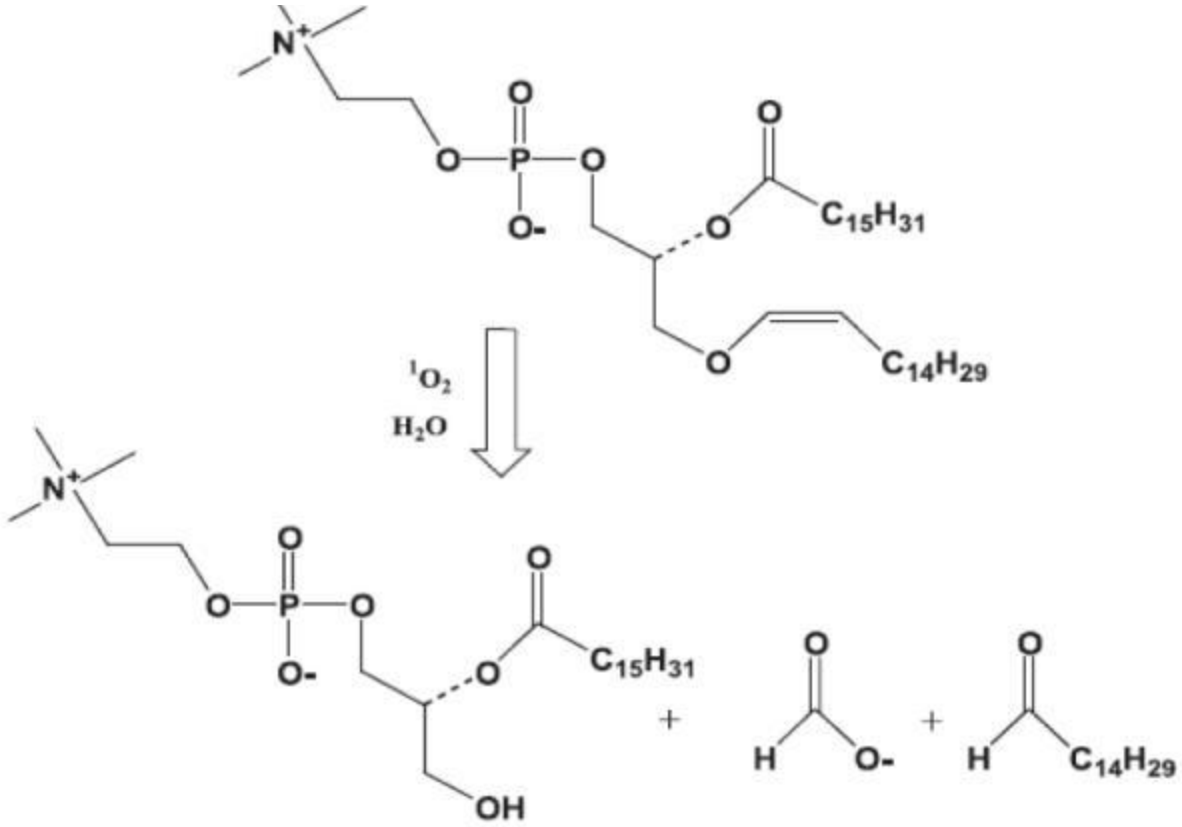

Singlet oxygen mediated photo-oxidation of plasmenylcholine leading to cleavage of vinyl ether linkages [40-41].

The first report of photo-oxidation-controlled release of hydrophilic agents from liposomes was published by Anderson et al. in 1992 [41]. This study demonstrated visible light-triggered release of glucose from liposomes composed of semi-synthetic plasmalogen lipids (1-alk-1′-enyl-2-palmitoyl-*sn*-glycero-3-phosphocholine (PlasPPC)/ 1,2-dipalmitoyl-*sn*-glycero-3-phosphocholine (DPPC) (8:1)) with the photosensitizer zinc phthalocyanine (ZnPc) incorporated within the hydrophobic region of the membrane. Irradiation of air-saturated liposomes with visible light at 37°C for 60 min resulted in release of 62% of encapsulated glucose, twice the amount released in the corresponding dark control experiment.

Several studies utilizing photosensitization to promote endosomal escape of nanoparticles and thus facilitate cargo delivery to the cytosol have appeared in recent years. In this approach light is applied after the particles are endocytosed. Upon irradiation, the photosensitizer encapsulated within the delivery vehicles acts on the lipids that constitute the endosomal membrane, disrupting the lipid bilayer and resulting in the release of particles into cytosol. Berg and coworkers used photosensitizers to mediate endosomal rupture for improved cellular delivery of nucleic acids [42]. Harnessing this mechanism, Kataoka and co-workers reported light-mediated gene delivery to the conjunctival tissue of rats [43].

More recently, Febvay et al. [44] used this approach to achieve cytosolic release of the model cell-impermeable dye Alexa 546 from mesoporous silica nanoparticles internalized by cancer cells. Upon exposure to green light (520 – 570 nm, 500 mW/cm^2) the dye acts as a photosensitizer, producing singlet oxygen, which disrupts the endosomal membrane. An increase in membrane permeability was monitored by increase of the fluorescence of Alexa 546 in the cytosol. FITC-labeled dextran (3 kDa) co-internalized with Alexa 546-loaded silica particles was also successfully released into the cytosol upon light exposure for 2 min.

II. Surface plasmon absorption by gold nanoparticles and photothermal effects

NIR (700-950 nm) is preferable to other types of light for triggering release in biological systems because it can pass through blood and tissue to depths of several inches [1]. However, very few organic chromophores absorb in this region, and even fewer are capable of converting the absorbed energy into a chemical or thermal response that can be used to trigger drug release. A few years ago, gold nanostructures (shells [46-48], particles [49-50], rods [51-52], and cages [53-54]) emerged as useful agents for photothermal therapy after they were shown to have strong absorption in the NIR region (four to five times higher than conventional photo-absorbing dyes [55]) and tunable optical resonances. The strong absorption ensures effective laser therapy at relatively low laser energies, rendering this therapy method minimally invasive.

Gold nanoparticles absorb light efficiently in the visible region due to coherent oscillations of metal conduction band electrons in strong resonance with visible frequencies of light. Photoexcitation of metal nanostructures results in the formation of a heated electron gas that cools rapidly within 1 ps by exchanging energy with the nanoparticle lattice. The nanoparticle lattice, in turn, rapidly exchanges energy with the surrounding medium on the timescale of 100 ps, causing localized heating [56]. This fast energy conversion and dissipation can be achieved by using light radiation with a frequency strongly overlapping with the nanoparticle absorption band. The NIR absorption maximum of metal nanostructures can be modulated by changing their size, shape and aggregation [46, 57-59]. This phenomenon has been widely studied as a stand-alone cancer therapy method since the early 2000s [60] and more recently was adopted to trigger the release of entrapped payload from nanocarriers upon exposure to NIR light. Typically, gold nanostructures are incorporated into polymer capsules along with drug molecules. Energy from NIR light generated by a laser absorbed by gold nanostructures and converted into thermal energy. Spontaneous local heating to temperatures well above 600-800°C [57-58] induces significant thermal and mechanical stress within the system and thus causes rupture of the carrier and subsequent payload release.

The first carrier incorporating gold nanoparticles was reported by Radt et al. [61]. Hollow polyelecrolyte microparticles were prepared by layer-by-layer deposition, incorporating 6

nm gold nanoparticles and lysozyme as a model therapeutic between polymer layers. Lysozyme release was observed upon exposure of the microparticle suspension to laser irradiation for 5 min with short pulses (10 ns) at a frequency of 10 Hz at 1064 nm. The amount of protein released upon light exposure was similar to the amount released from a mechanically crushed control sample.

The major challenge in controlled liposomal drug delivery is to create a system that is sufficiently stable in circulation, yet capable of quickly releasing its contents upon stimulus. Wu et al. [58] reported a liposomal delivery system capable of burst release upon absorption of NIR light by hollow gold nanoparticles. In their construct, gold nanoparticles were either encapsulated within dipalmitoylphosphatidylcholine (DPPC) liposomes or tethered to the surface via a PEG linker. 6-carboxyfluorescein was used as a model drug. Leakage from the liposomes was triggered by 130-fs laser pulses at 800 nm, leading to nearly instantaneous release of payload (71% for encapsulated gold nanoparticles and 93% for nanoparticles tethered to the surface) at laser powers exceeding 2.2 W/cm^2. At this power setting, only a slight increase of the bulk solution temperature was observed (less then 1°C), while local heating was sufficient to anneal the hollow gold nanoparticles into solid nanoparticles, as evident by transmission electron microscopy (TEM). The observed burst release was ascribed to the formation and collapse of vapor microbubbles upon NIR-induced heating of gold nanoparticles. Thus, exposure of gold nanoparticles to femtosecond NIR laser pulses produces an effect similar to ultrasonication.

Oishi et al. [62] created multi-stimuli responsive PEGylated nanogels composed of a PEG shell and a cross-linked thermal-responsive poly[2-(N,N-diethylamino)ethyl methacrylate] core with NIR light-absorbing gold nanoparticles immobilized in the core (Figure 10). The PEAMA core acted as a nanoreactor to produce gold nanoparticles from tetrachloroaurate acid ($HAuCL_4$ (III)) without any additional reducing reagents. 1,3,6,8-pyrenetetrasulfonic acid tetrasodium salt (PSA) was encapsulated into polyion complexes as a fluorescent water-soluble probe. While inside the particles, fluorescence of PSA was low due to self-quenching. Release of PSA in PBS solution (pH 7.4) was triggered by irradiation with an argon laser at 514.5 nm. A gradual increase in PSA fluorescence was observed over 8 min of laser irradiation, corresponding to 26% release. Release of the fluorescent probe from nanogels was due to the efficient heat generation by gold nanoparticles, which caused deprotonation and collapse of the temperature-responsive PEAMA core.

Figure 10.

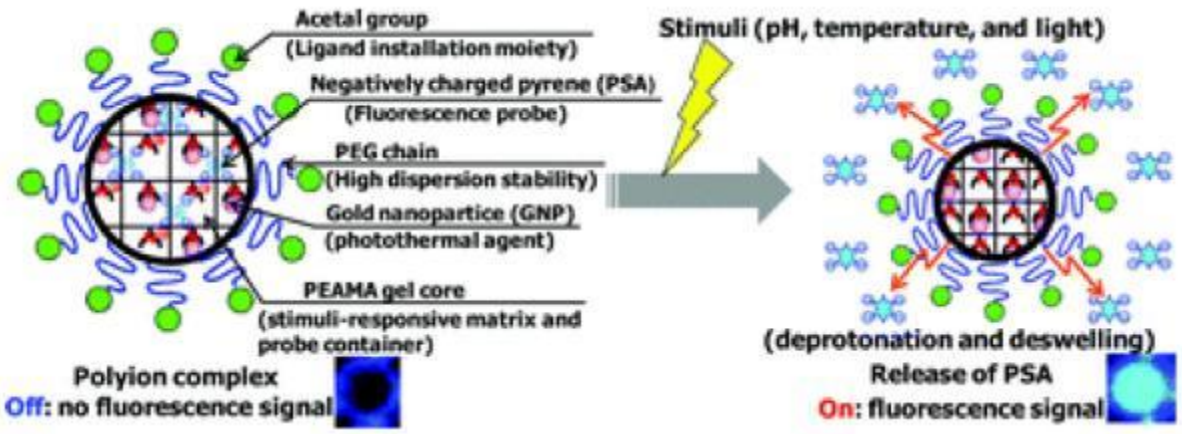

Multi-stimuli responsive PEGylated nanogels composed of a PEG shell and PEAMA core with gold nanoparticles immobilized in the core [62].

Such polyion complex nanoparticles possess great potential as “smart” carriers for delivery of proteins, DNA, and small molecule drugs. Although this particular system cannot be readily translated into *in vivo* systems because of low tissue transparency at 514 nm, it may find applications in tissue engineering and microscopy.

Another example of NIR light-triggered release from a temperature-responsive nanocarrier was published by Wu et al. [63]. Ag/Au bimetallic nanoparticles were coated with a layer of polystyrene to encapsulate the hydrophobic drug curcumin, followed by an outer layer of nonlinear PEG to improve dispersion, circulation stability, and thermal sensitivity in the physiological range. A 70% release of curcumin was achieved upon irradiation with 1.5 W/cm^2 NIR light for 5 min at intervals over 50 hours at 37°C. A similar release profile was observed when the particles were incubated at 41°C for the same time period without irradiation, confirming that the stimulated release is due to thermal sensitivity of the formulated particles triggered by the conversion of NIR energy into thermal energy by the Ag/Au core. Cytotoxicity tests revealed a 4-fold increase in cell killing efficiency of the curcumin-loaded Ag/Au particles compared to free curcumin.

The major concern with gold nanoparticle-mediated light-induced release is stability of the cargo when exposed to the heat generated by the particles upon absorption of NIR energy. Volodkin et al. [59] proposed a solution to this problem by creating gold nanoparticle-liposome assemblies in which the cargo is shielded by a lipid membrane (Figure 11). Large gold nanoparticle aggregates (300 nm) have high cumulative electrostatic charge and attract a large number of liposomes to compensate for their excess charge. The dimensions of the assemblies are controlled by the size and charge of nanoparticles and liposomes as well as their mixing ratio. An additional advantage of this system is higher NIR absorption of aggregated gold nanoparticles compared to single gold nanoparticles.

Figure 11.

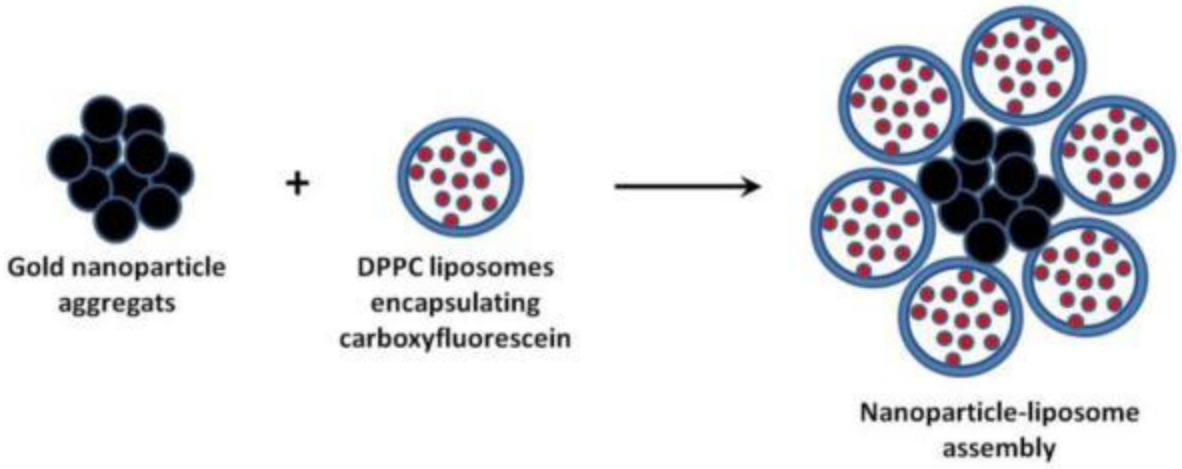

Formation of gold nanoparticle-liposome assemblies for NIR light-triggered release of carboxyfluorescein. [58].

Huschka et al. employed the photothermal response of gold nanoshells to NIR irradiation for light-triggered DNA antisense therapy [64-65]. Strands of DNA molecules were covalently attached to the surface of gold nanoshells at the 5′ end via a Au-thiol bond. A complementary non-thiolated DNA sequence was then bound to each strand to form a double helix. Upon illumination with 800 nm light, the double-stranded DNA was dehybridized, releasing the non-thiolated strand with 50% efficiency [65]. The same group later demonstrated that such constructs may be used for release of various guest molecules that can either intercalate between the adjacent base pairs or bind in the major or minor groove of the DNA double helix (Figure 12) [64]. 4′,6-diamidino-2-phenylindole (DAPI) was used to demonstrate light-induced intracellular release. DAPI fluorescence intensity is low in solution, but increases drastically upon binding to DNA. The release of DAPI from the double-stranded DNA inside living H1299 cancer cells upon irradiation with 800 nm for 5 min (1 W/cm^2) was evidenced by the decrease in fluorescence of unbound DAPI compared to DAPI inside the DNA helix. One hour after irradiation, delivery of released DAPI to the nucleus was evident; fluorescence intensity recovered upon binding to nuclear DNA. Although no apparent temperature increase was observed in the solution containing the nanoparticles, heat-induced damage to the DNA directly attached to the surface of gold nanoparticles remains a possible limitation.

Figure 12.

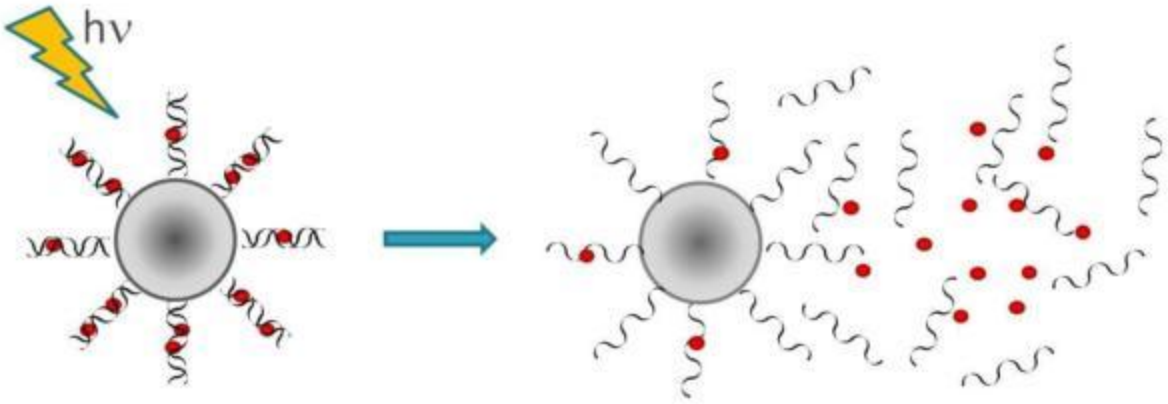

Gold nanoparticles with DNA bound to the surface for NIR light-triggered release [63-64].

Delivery systems that utilize gold nanostructures provide an opportunity to take advantage of a combined effect of photothermal ablation and chemotherapy in a single setting. Such combined treatment has been demonstrated to result in higher cytotoxicity compared with chemo- or photothermal treatment alone [27, 66-67]. You et al. investigated the effect of DOX-loaded PEG-coated hollow gold nanoshells (PEG-HAuNS) for anticancer therapy [67]. Exceptionally high loading of DOX into the outer PEG layer of gold nanoshells (1.7 μg DOX/1μg Au) was achieved. Intracellular release of DOX from PEG-HAuNS was observed upon irradiation with four 3 min pulses of 800 nm (2 W/cm^2 output power) over 2 hours. DOX-loaded PEG-HAuNS enhanced cell killing compared to free DOX at an equivalent concentration or laser-treated HAuNS alone (86.4% vs. 77% and 40.6%, respectively). The same research group also demonstrated laser-induced release of paclitaxel (PAX) from PLGA microspheres incorporating gold nanoshells and enhanced cytotoxicity compared to non-stimulated PAX-containing microspheres or photothermal treatment alone [27].

III. Photochemical hydrophobicity switch

The formation and stability of micelles and other vesicles relies on the hydrophilic to hydrophobic balance within the amphiphilic molecules constituting the aggregates. When amphiphilic molecules become hydrophilic, the micellar system disintegrates, releasing its cargo. Light-induced conversion of amphiphilic molecules to more hydrophilic forms allows remote control over this process.

A large number of organic molecules that undergo structural rearrangements to generate charged (and therefore more hydrophilic) species upon exposure to light have been developed; such rearrangements are termed photochemical reactions. The majority of organic molecules explored for photo-controlled materials applications

respond to UV light. Upon absorption of UV light, these molecules reach an excited state from which they decay non-irradiatively via a chemical transformation. However, some organic chromophores can simultaneously absorb two photons of low-energy NIR light and undergo the same chemical transformation as upon absorption of one photon of high-energy UV light. The phenomenon of two-photon absorption was first theoretically predicted by Maria Goppert-Mayer in the 1930s [68]. The probability of two-photon absorption is generally low and proportional to the square of the intensity of the excitation beam [69]. Therefore, two-photon processes require femtosecond pulsed lasers with high photon density. The first experimental demonstration of two-photon absorption became possible in 1961 soon after the invention of the laser [70]. The efficiency of the two-photon induced chemical transformation is referred to as uncaging action cross-section and is expressed in Goeppert-Mayer units, GM (1 GM = 10^{-50}cm^4 s photon^{-1}) [71]. Incorporation of such light-triggering units into delivery vehicles can be employed for controlled photo-triggered release, eliminating the need for inorganic NIR light-absorbing dopants.

The first micellar system capable of releasing hydrophobic cargo via an NIR light-induced chemical transformation was reported by Goodwin et al. in 2005 [72]. An amphiphilic molecule was constructed by chemically attaching a hydrophobic light-sensitive 2-diazonaphthoquinone (DNQ) to a PEG chain (Figure 13A). This polymer was shown to form micelles above the concentration of 0.15 mg/mL in PBS pH 7.4. Nile Red was encapsulated into the micelles as a reporter dye. Upon irradiation by UV or NIR light (via absorption of one or two photons, respectively), DNQ undergoes a Wolff rearrangement to form a hydrophilic 3-indene carboxylic acid. As a result, the micelles incorporating DNQ dissolve, releasing Nile Red into the aqueous medium, which is evidenced by quenching of the fluorescence of the dye. Over 30 min of irradiation at 795 nm resulted in a 75% decrease in the fluorescence of Nile Red, confirming the dissolution of the micelles. Later, this DNQ-based system was modified by incorporation of dendritic polyester between the PEG and DNQ moieties (Figure 13B), which allowed installation of multiple DNQ molecules per amphiphilic molecule [73]. The new system exhibited lower critical micellar concentration (12 μg/mL) and low cytotoxicity at concentrations as high as 1 mg/mL. However, this stability persisted upon irradiation: irradiation with 795 nm light for 30 min resulted in only a 50% decrease in the fluorescence intensity of encapsulated Nile Red and a decrease in the size of the micelles from 40 to 20 nm.

Figure 13.

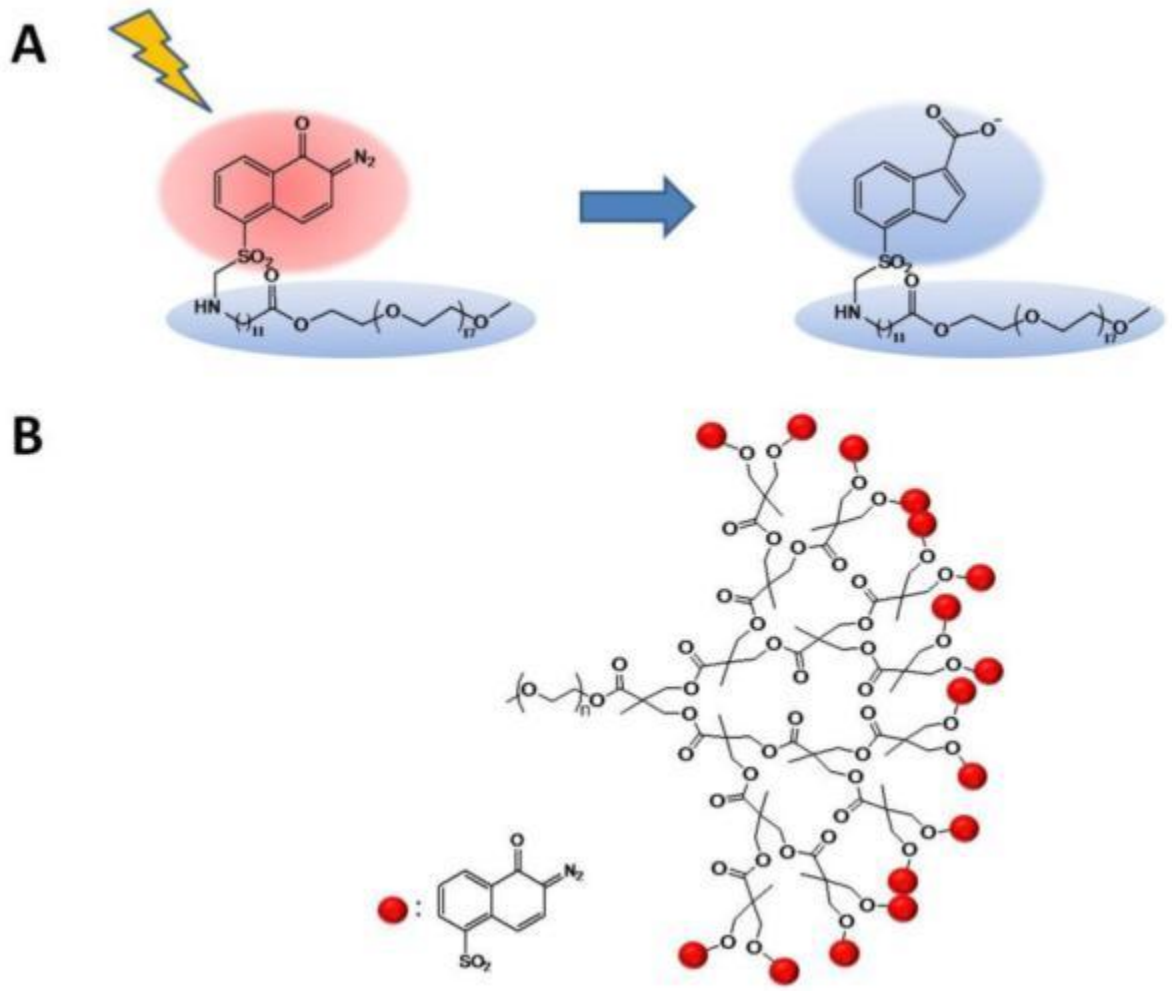

A) Diazonaphthoquinone-based molecules undergoing an amphiphilic to hydrophilic switch upon UV and NIR irradiation. [69] B) DNQ-based system modified by incorporation of dendritic polyester to install multiple DNQ moieties [73].

Micelles formed from amphiphilic block copolymers are being actively studied for photo-controlled release. In these constructs, PEG is usually used as the hydrophilic block, while the hydrophobic block is formed by polymethacrylic acid whose carboxyls are masked by various protecting groups that can be removed upon exposure to light (Figure 14A).

Figure 14.

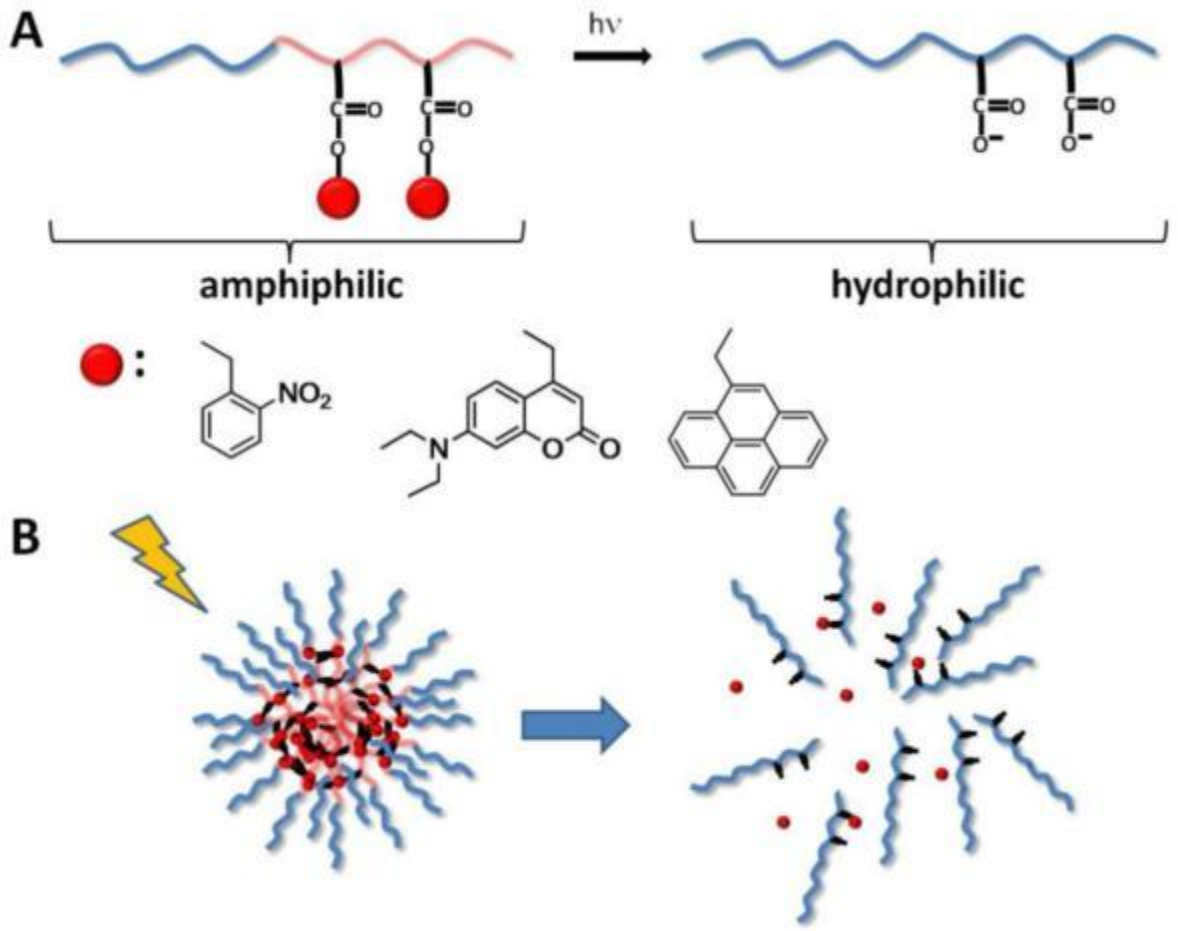

A) Block copolymer with masked carboxyl groups undergoing amphiphilic to hydrophilic switch upon light exposure and examples of light-sensitive protecting groups. (B) Amphiphilic block-copolymer micellar disassembly upon irradiation.

Yue Zhao's group has been studying light-dissociable block-copolymer micelles. Their first system capable of photo-controlled release of hydrophobic small molecules was based on an amphiphilic block copolymer containing the *o*-nitrobenzyl protecting group [74]. Micelles encapsulating Nile Red were formed by first dissolving the polymer and the dye in THF and adding water. Photo-controlled release was induced by irradiating the solution with UV light above 365 nm (145 mW/cm). After 420 seconds of irradiation, the fluorescence of Nile Red decreased by 80%, indicating release of the hydrophobic dye into the aqueous environment. Much faster release was observed at higher irradiation powers (75 sec at 500 mW/cm). The same system was also demonstrated to release Nile Red via two-photon uncaging of the carboxylic groups. The two-photon uncaging cross-section of the *o*-nitrobenzyl group is rather low (0.01 GM [75]); therefore, this process is much slower than the one-photon reaction, requiring irradiation at 700 nm for 210 min to achieve a similar decrease in Nile Red fluorescence.

The [7-(diethylamino)coumarin-4-yl]methyl chromophore (DEACM) has an order of magnitude higher two-photon uncaging cross-section compared to the *o*-nitrobenzyl group and therefore should be more suitable for use in light-activated drug delivery systems. A block copolymer in which the DEACM caging group masked the carboxylic acid groups was reported later by the same group [76]. However, despite the more NIR-sensitive caging group, the observed release of Nile Red from the micelles was slower than in that for the *o*-nitrobenzyl-based system (50% decrease in Nile Red fluorescence after 210 min at 500mW/cm).

Lee et al. described a similar micellar system for light-triggered release via a hydrophobicity switch [77]. In their system, the hydrophobic block is composed of spiropyran-containing polymethacrylate (Figure 15). Unlike in the previously described systems, the switch between the amphiphilic form and the hydrophilic form of the block copolymer is reversible. Thus, irradiation with UV light converts spiropyran into hydrophilic, zwitterionic merocyanine, while exposure to visible light converts it back to the hydrophobic spiro form. The hydrophobic dye coumarin 102 was encapsulated into block copolymer micelles prepared from spiropyran and its release was induced by irradiating the solution of micelles with 365 nm light for 60 min. Similar to Nile Red, coumarin 102 is insoluble in water, so its fluorescence is quenched when the dye was released into aqueous solution. Complete disruption of the micelles after UV irradiation was observed by AFM. Subsequent irradiation of the solution with 620 nm light for 240 min led to reconstitution of the micelles and partial re-encapsulation of coumarin 102, evidenced by AFM and an increase in the fluorescence intensity of the dye.

Figure 15.

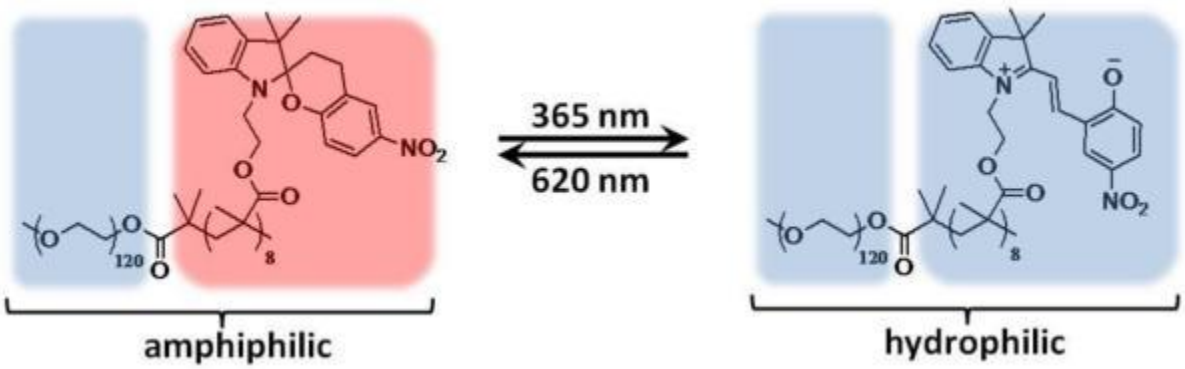

Light-induced hydrophobicity switch of spiropyran-containing block copolymer [74].

Another example of micelles that can be reversibly disrupted was reported by Jiang et al. [78]. Their dual-responsive block copolymer incorporated polyethylene oxide (PEO) as a hydrophilic block and poly(ethoxytriethylene glycol) acrylate-*co*-poly(*o*-nitrobenzyl) acrylate (P(TEGA-*co*-NBA)) as a thermoresponsive hydrophobic block. Above the lower critical solution temperature (LCST) of the P(TEGA-*co*-NBA) block, the copolymer formed micelles encapsulating Nile Red. Upon continuous UV irradiation for 180 min, the *o*-nitrobenzyl groups were cleaved and the LCST of the thermoresponsive block

increased by 11°C, causing dissociation of the micelles. Further increasing the temperature above the LCST of the new thermoresponsive block reconstituted the micelles and re-encapsulated Nile Red.

A molecule that switches from fully hydrophobic to amphiphilic was also used for light-triggered release. Malachite green derivative (Figure 16) was incorporated (4.5 mol%) into the membrane of vesicles composed of phosphatidylcholine [79]. Upon UV exposure, this molecule undergoes photoionization and becomes amphiphilic. This results in a decrease of the total free energy of the system, membrane destabilization and eventual solubilization of the membrane components, leading to release of the encapsulated compounds. 80% of the encapsulated dye (8-aminonaphthalene-1,3,6-trisulphonic acid) was released from the vesicles after 15 min of continuous UV irradiation.

Figure 16.

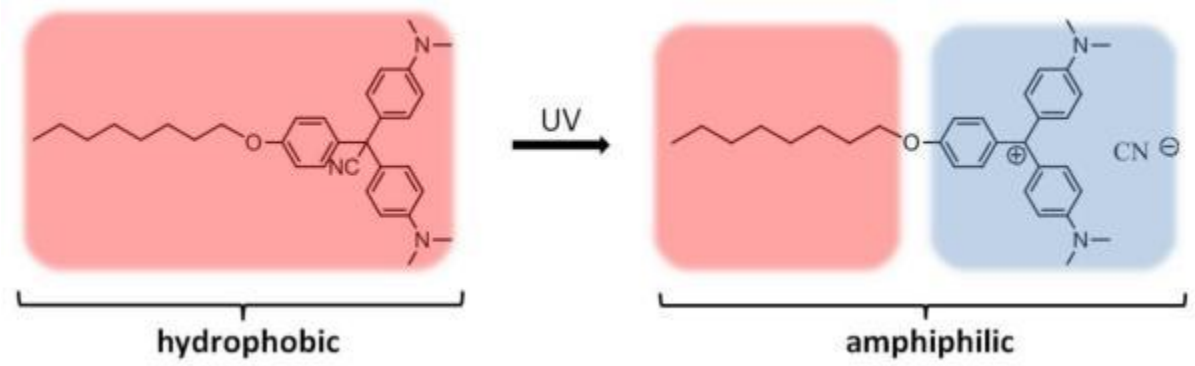

Ionization of Malachite green derivative upon UV light exposure. [76]

Recently, photosensitive polymeric nanoparticles were prepared by self-assembly of oppositely charged polyelectrolytes [80]. Coulomb interactions between the cationic natural polymer chitosan and an anionic photosensitive pyrene derivative resulted in the formation of hydrophobic polymeric particles in aqueous solution, which were loaded with Nile Red. UV irradiation of the particles for 50 sec (1200 mW cm^{-2}) resulted in an 80% decrease in the fluorescence intensity of Nile Red. However, DLS analysis of the particles after UV exposure showed their shrinking in size but neither complete degradation nor dissolution, which would be expected when the polymer turns hydrophilic (Figure 17). This behavior was attributed to the crosslinking of chitosan by butanoic acid generated after the removal of pyrene group. Some Nile Red release was also observed when the particles were exposed to NIR light (808 nm): a 40% decrease in the fluorescence of Nile Red was achieved after 250 min of exposure, owing to low two-photon absorbance of the pyrene derivative.

Figure 17.

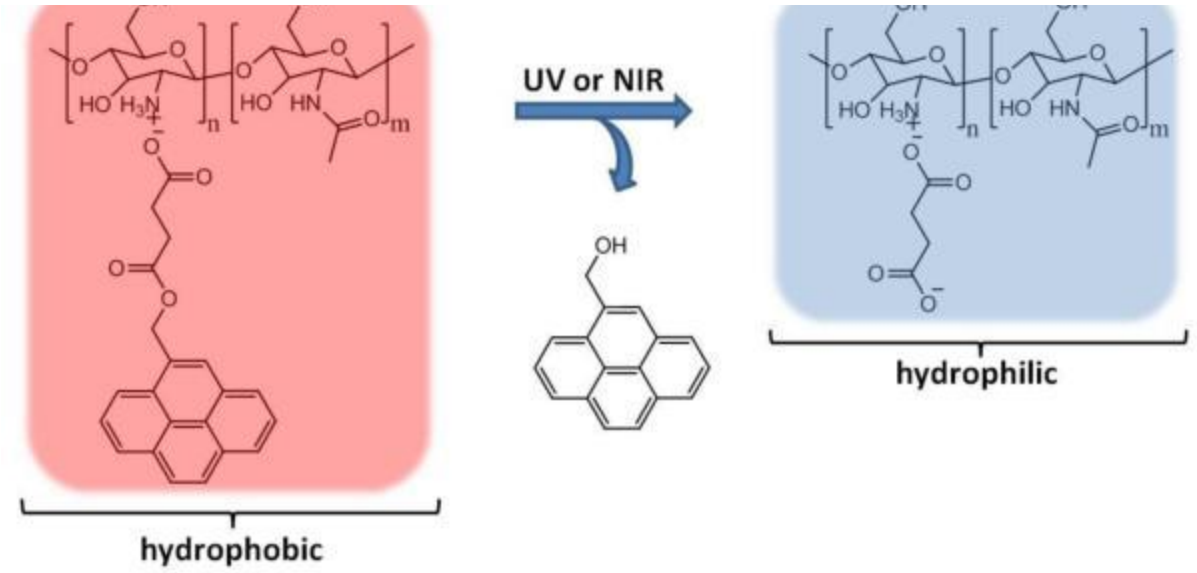

Polyion complex formed between chitosan and pyrene derivative undergoes a hydrophobic to hydrophilic switch upon light exposure [77].

Nanoengineering ion channels to allow optical control is an emerging technology; such channels can be incorporated into liposomes to allow light-triggered release [81]. Channel proteins are excitable pores embedded in cell membranes that, by opening and closing, allow the flow of ions across the membrane. One of these proteins, the mechanosensitive channel of large conductance (MscL) from *Escherichia coli*, was incorporated into liposomes to function as a remotely controlled valve [82]. In order to make MscL responsive to irradiation, a light-sensitive group was installed at the 22nd amino acid. Removal of the triggering group increases the hydrophilic character of the channel pore and opens the valve, allowing cargo release from the liposomes (Figure 18). Two triggering groups, *o*-nitrobenzene and spiropyran, have been used to open the valve irreversibly and reversibly, respectively. A 43% release of calcein from the MscL-containing liposomes was observed after exposure to 366 nm light, while only 10% of calcein diffused from non-irradiated liposomes.

Figure 18.

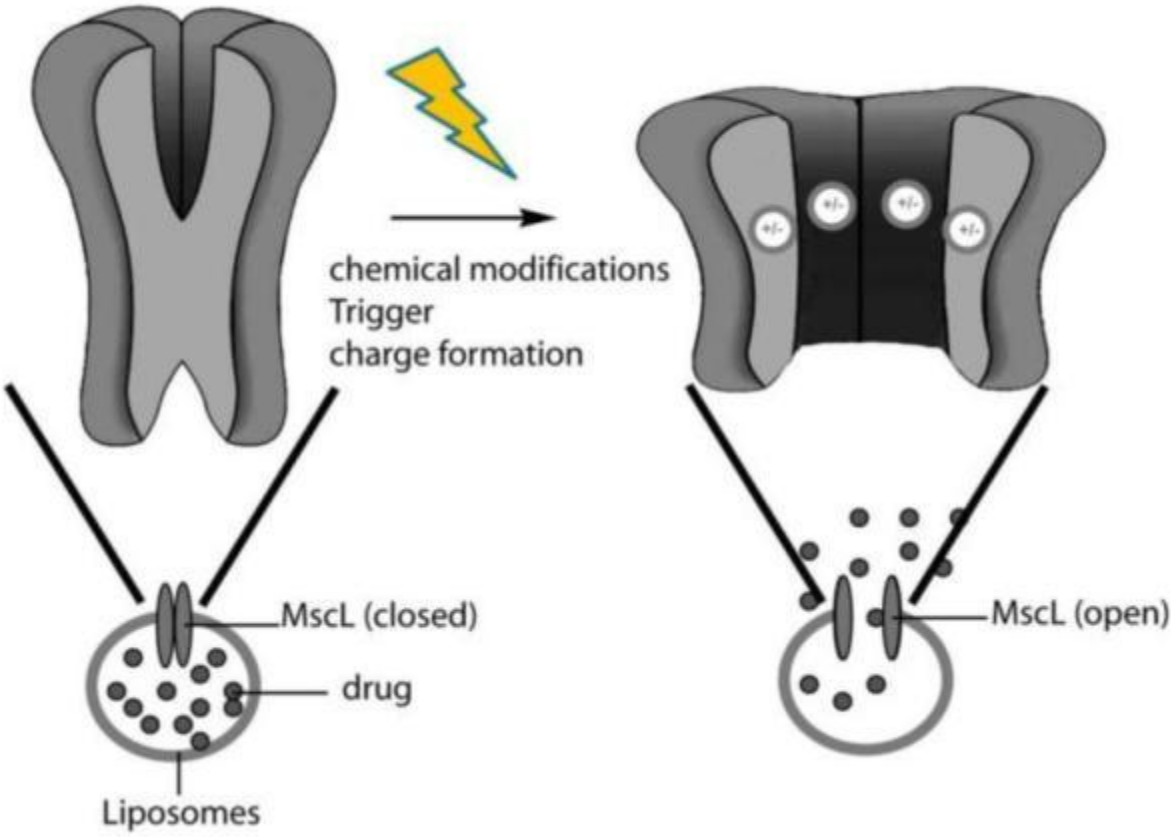

Schematic of triggered liposomal release through an engineered channel protein [78].

Recently, a new way to employ NIR light for triggered release based on lanthanide-doped upconverting nanoparticles (UCNP) has emerged. UCNPs composed of $NaYF_4$ nanocrystals doped with Tm^{3+} and Yb^{3+} act as light-harvesting antennae, sequentially absorbing multiple photons of NIR light and converting it into higher energy UV light [83].

The first example of using UCNPs to induce a chemical reaction was demonstrated by the group of N. Branda, when a 2-phenylbenzofurane photoprotecting group masking acetic acid was conjugated to the surface of UCNPs [84]. Exposure of the NPs to 980 nm continuous wave light (4.37 W, 556 W/cm^{-2}) resulted in photocleavage of the 2-phenylbenzofurane group and release of acetic acid. This process occurred via the conversion of NIR light to UV light, since the 2-phenylbenzofurane group is not cleavable by 980 nm irradiation.

More recently, this strategy was further adapted to induce triggered release from a micellar system by the collaborative efforts of N. Branda and Y. Zhao [85]. Micelles composed of an amphiphilic block copolymer containing *o*-nitrobenzyl photoprotecting groups encapsulating Nile Red (Figure 14) and doped with UCNPs were prepared.

Upon exposure to 980 nm light (5 W, 4 hours), Nile Red release was observed, indicating photocleavage of *o*-nitrobenzyl photo-protecting groups by UV light emitted by the UCNPs and the subsequent hydrophobicity switch and disintegration of the micelles.

The upconversion process happens via sequential absorption of multiple photons and therefore requires 10^4 – 10^7 orders of magnitude lower energy densities compared to simultaneous multi-photon absorption processes [86]. However, the potential toxicity and tissue accumulation of UCNPs should be thoroughly investigated before this technique can be developed for *in vivo* applications.

IV. Polymer backbone photo-degradation

The polymer-based nanocarriers thus far discussed in this review do not degrade into small molecules upon irradiation to effect release. Degradable hydrophobic polymers present an attractive choice as delivery vehicles for therapeutic cargo. Although similar to the hydrophobicity switch mechanism in terms of the chemistry used, the photo-releasing systems described in this section offer the additional advantage of disassembly on both the nanoscale (disintegration of nanocarrier) and the molecular scale (polymer fragmentation). Systems that can degrade into smaller fragments can subsequently be cleared from the body, eliminating any long-term toxicity concerns. Polymers that degrade completely into small molecules via various internal physiological cues like pH, reactive oxygen species, and temperature offer the added advantage of spatio-temporal control. External stimuli, such as ultrasound, light, and magnetic field can also be used to remotely control the release from and final degradation of these delivery vehicles, but have been underutilized. In this regard we have developed the first example of a light degradable polymer that can be formulated into particles for delivery and release of drugs (Figure 19) [87].

Figure 19.

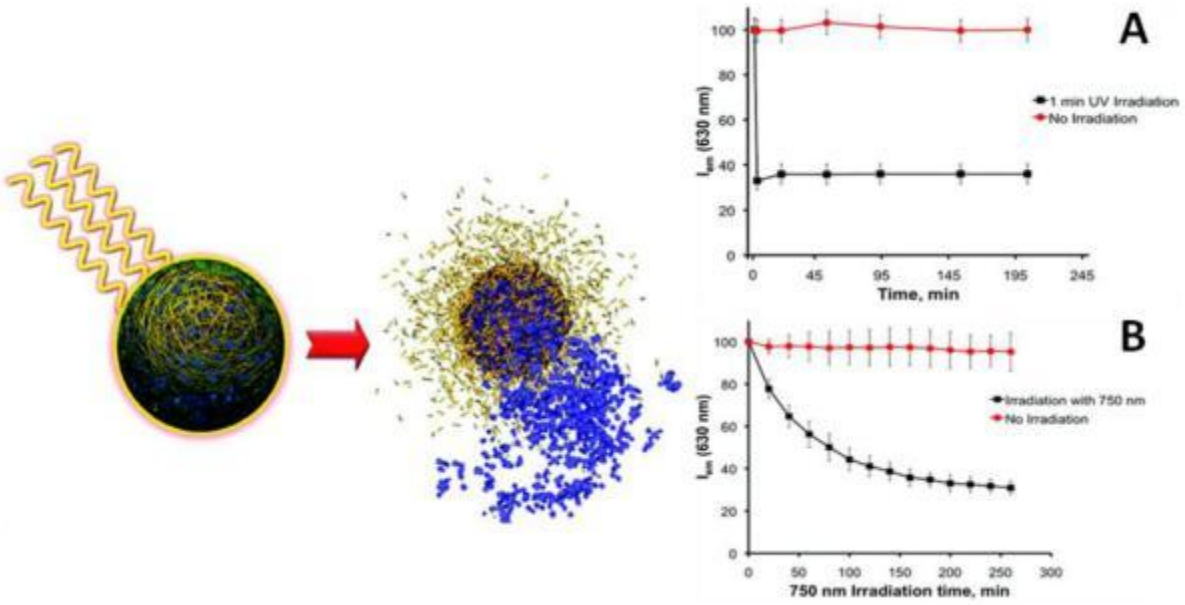

Schematic representation of degradation of polymeric particles by light and release of cargo. Nile Red release from the polymeric particles upon A) UV irradiation at 300-400 nm B) NIR irradiation at 750nm. [87]

The polymer consisted of a quinone-methide-based backbone with pendant N,N-dimethylethylene diamine groups protected with *o*-nitrobenzyl phototriggering groups. A cascade of diamine cyclization and quinone-methide rearrangement is activated when the photo-triggering groups are cleaved by one-photon (350 nm) or two-photon (750 nm) photolysis, resulting in the complete degradation of the polymer backbone into small molecules (Figure 20).

Figure 20.

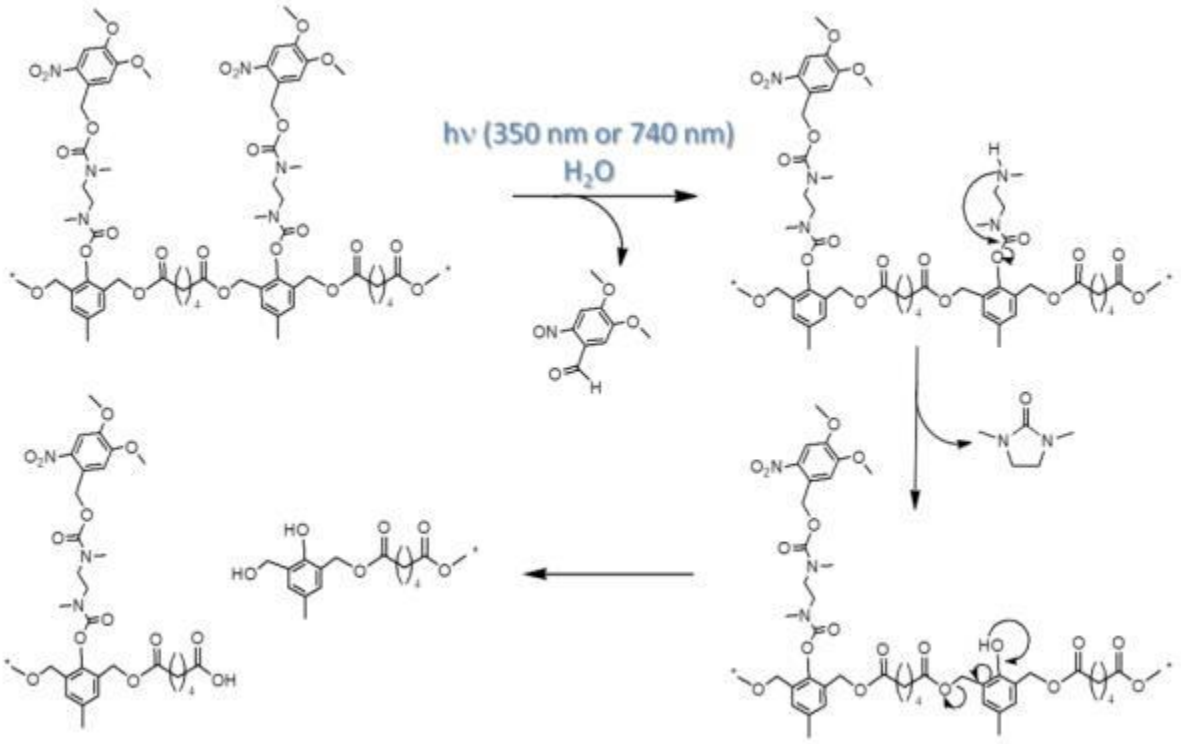

Schematic of quinone-methide-based polymer [83] degradation after cleavage of *o*-nitrobenzyl triggering group with UV or NIR light.

We have shown subsequently that the polymer can be formulated into nanoparticles via standard and commercially viable emulsion techniques that result in regular particle shapes and sizes. Nile Red was encapsulated as a model drug within these particles to allow measurement of release via fluorescence. While UV irradiation causes an almost immediate 67% decrease in fluorescence intensity upon 60 seconds of irradiation, NIR wavelengths result in more gradual decrease (over 250 min) because of the poor two-photon uncaging cross-section of the *o*-nitrobenzyl group (0.01 GM). Ongoing studies currently employ much higher efficiency two-photon uncaging groups [88].

Johnson et al. [89] have adopted a different strategy to release drugs from nanometer sized hydrophobic polymeric systems using light (Figure 21). They have synthesized brush-like nanosystems that have drug covalently bound to the backbone via a photo-degradable *o*-nitrobenzyl moiety. In their synthesis they utilized a “graft-through” strategy, where a norbornene-containing macromonomer is polymerized by ring-opening metathesis polymerization (ROMP) and DOX is then covalently bound to the backbone using “click” chemistry. The linkage also contains the photo-uncaging *o*-nitrobenzyl moiety that can be triggered by UV light to release DOX. Irradiation of these 10 nm nanoassemblies using 365 nm light for up to 10 min resulted in a 70% release of the bound DOX.

Figure 21.

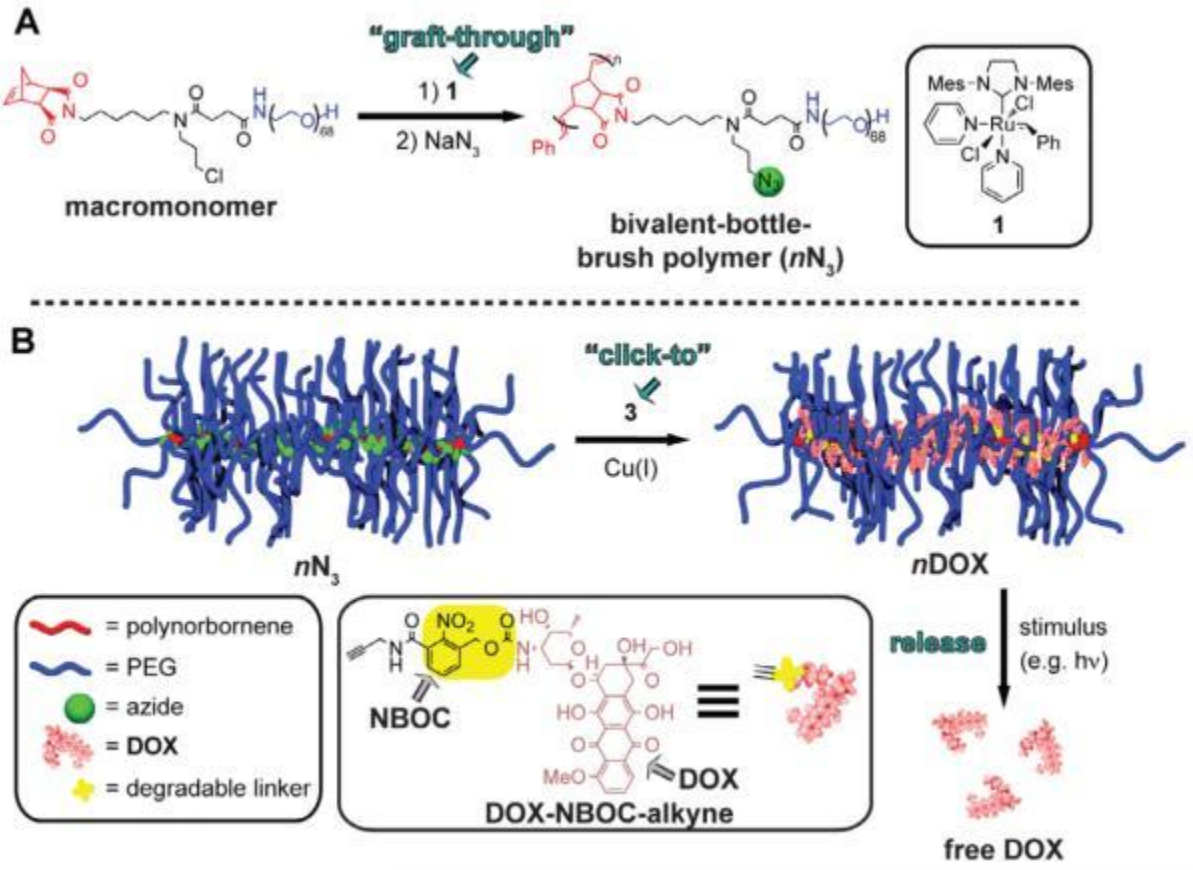

Schematic representation of the “graft-through and “click-to” approach. A) Bivalent macromonomer on which “graft-through” ROMP with catalyst 1 was performed followed by in situ chloride-azide exchange. B) The resulting azido-bivalent-brush polymer functionalized with DOX-alkyne by click chemistry allows controlled release of the anticancer agent doxorubicin (DOX) in response to 365 nm UV light [89].

V. Photo de-crosslinking

A particle may be induced to release its payload by breaking up the light-sensitive crosslinks holding it together, making it more porous. The advantage of this approach is that the light-sensitive moieties remain attached to the polymer after light exposure, thus eliminating the issue of potential toxicity of the photocleavage byproducts.

Reversible photo-crosslinked nanoparticles were prepared by the Zhao group [90]. A water-soluble block copolymer containing a block of PEO and a block of poly(2-(2-methoxyethoxy)ethyl methacrylate-co-4-methyl-(7-(methacryloyl)oxyethyloxy)coumarin), denoted as PEO-b-P(MEOMA-co-CMA), was prepared by atom transfer radical polymerization. The polymer solution was heated above its LCST to form block copolymer micelles, which were then photo-crosslinked by irradiation with light at 320 nm (Figure 22) to induce photo-dimerization of the pendant coumarin groups. Cooling the solution below LCST afforded photo-crosslinked nanogel particles. Nanogel swelling

by 90% was achieved by irradiating the nanoparticles with light of higher energy (254 nm), inducing photocleavage of the coumarin dimers. Repeated crosslinking could be achieved by bringing the nanogel solution temperature above LCST and irradiating with 320 nm light.

Figure 22.

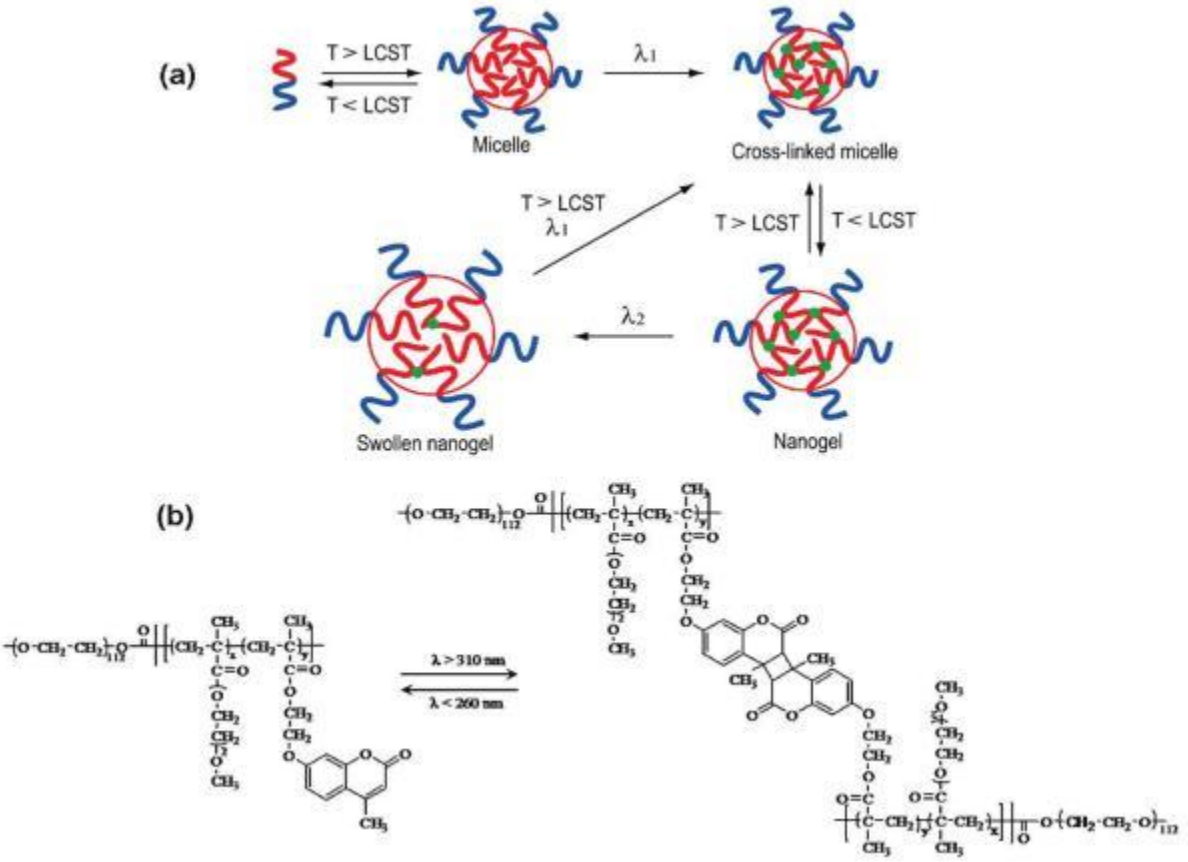

A) Schematic illustration of the preparation and photo-controlled volume change of nanogel [90]. B) Designed diblock copolymer bearing coumarin side groups for the reversible photo-cross-linking reaction.

The rate of cargo release could be controlled by the reversible photo crosslinking and de-crosslinking of the nanogels. Encapsulated dye, dipyridamole, was released slower from the crosslinked nanogels compared to non-crosslinked micelles, demonstrating the possibility of tuning the release rate by controlling the degree of crosslinking. Further, irradiation of the nanogels with 254 nm light for 3 min reduced the crosslinking density, thus significantly increasing the release rate. The de-crosslinking reaction can also be induced through two-photon absorption of visible light (532 nm). [91]

Crosslinked block copolymers containing an *o*-nitrobenzyl group in the crosslinkers were used to form micelles that could be disrupted by UV light via cleavage of the

crosslinks and generation of hydrophilic carboxylic acid moieties (Figure 23) [92]. Nile Red was released from the micelles upon irradiation with 365 nm for 15 min. Such a strategy may be readily adopted for *in vivo* applications by replacing the *o*-nitrobenzyl group with a photosensitive protecting group with a higher two-photon uncaging cross-section.

Figure 23.

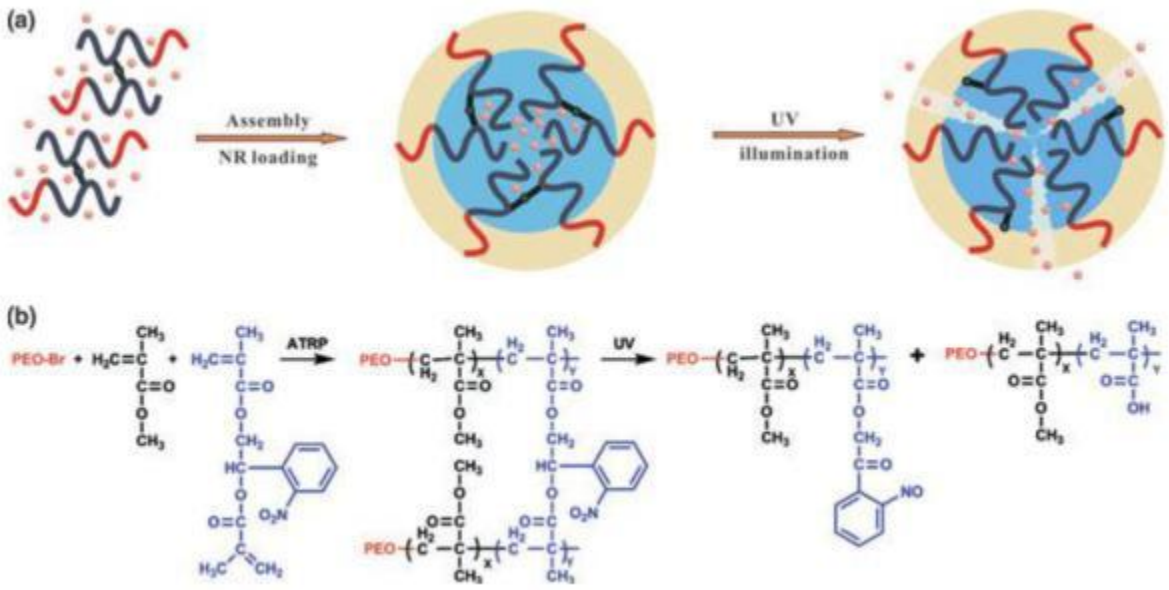

A) Photo-controlled release of encapsulated guest molecules upon light irradiation of polymer micelles. B) Synthesis of photocleavable cross-linked block copolymers and their light-triggered dissociation [92].

3. Conclusions

The use of light as an external stimulus is a promising approach to targeted drug delivery that allows precise control over the place, time, and rate of cargo release. Although the first reports of this concept appeared in the 1980s, significant progress has been made in this area over the past decade. A wide range of nanoscale assemblies have employed a handful of photochemical mechanisms to achieve efficient and reproducible release profiles. Most of the systems developed to date respond most efficiently to UV or visible light. However, these systems will most likely be limited to topical applications, where stimulus penetration is not necessary or undesirable. For such systems, the major concern is the damaging effect of high energy irradiation to tissues, especially at shorter wavelengths. Systems that are sensitive to NIR light, such as surface plasmon absorption by gold particles, upconverting nanoparticles, and NIR chromophores, hold more potential *in vivo* due to the greater depth of penetration of this wavelength of light and the minimal absorption of NIR by endogenous matter. The emerging technology utilizing upconverting nanoparticles is attractive because it does not require expensive high-energy lasers. However, toxicity of these materials and

tissue accumulation remain to be thoroughly investigated. In the case of gold nanoparticles used for photothermal effects, thermal stability of the potential cargo must be considered due to local heat generation. Design and synthesis of more efficient NIR light-absorbing organic chromophores will eliminate the need for inorganic dopants.

Expanding the toolbox of photochemical mechanisms that allow release from nanocarriers would increase the likelihood that an efficient system with little biological risk is developed. Furthermore, there is a need to create systems that degrade into small molecules upon irradiation or completion of function. These fully degradable systems would be desirable for a variety of biomedical applications. A recent review focusing in more depth on the drug delivery aspects of light-sensitive nanocarriers was published in this journal [93]; thus, we chose to address the chemical side of this topic in more depth.

As this field continues to grow, there will be a need for more standardized reporting on the photochemical parameters, such as wavelengths, exposure time, laser power per area, and energies per pulse, that govern these processes. Finally, a systematic method for categorizing the change resulting from irradiation (i.e. swelling, de-crosslinking, full degradation, etc.) will have to be implemented so that the literature may be more easily compared. These efforts will allow the community to make more meaningful conclusions when selecting an appropriate system for biomedical applications.

Figure 4.

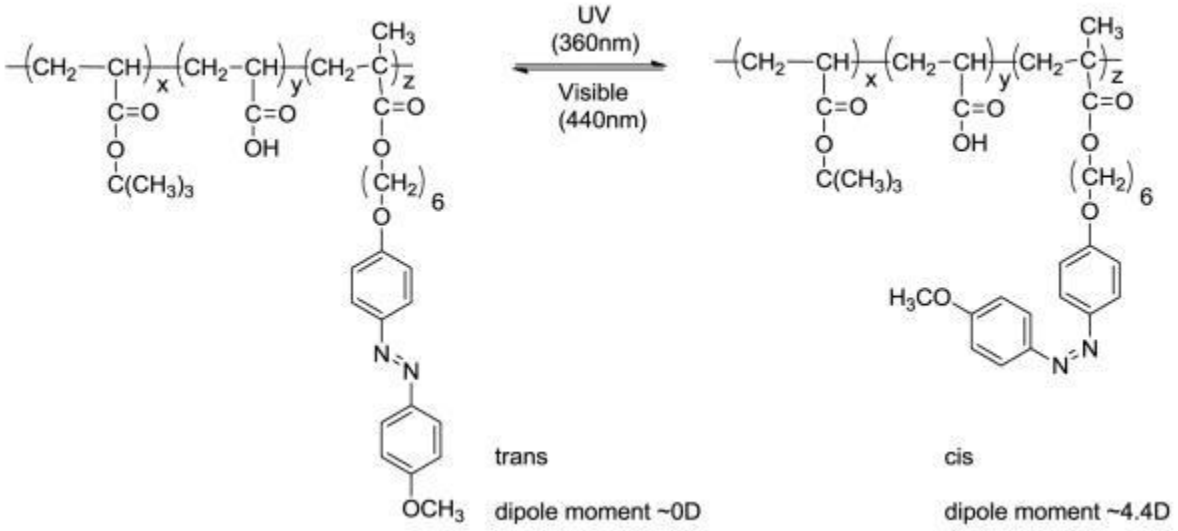

Scheme showing the generation of a net dipole moment on photoisomerization.

Acknowledgements

The authors thank the NIH Director's New Innovator Award (1 DP2 OD006499-01) and King Abdulaziz City for Science and Technology for financially supporting this work.

Telomerase Activation and Rejuvenation of Telomere Length in Stimulated T Cells Derived from Serially Transplanted Hematopoietic Stem Cells

Richard C Allsopp [1], Samuel Cheshier [1], Irving L Weissman [1]

Abstract

Telomeres shorten in hematopoietic cells, including hematopoietic stem cells (HSCs), during aging and after transplantation, despite the presence of readily detectable levels of telomerase in these cells. In T cells, antigenic stimulation has been shown to result in a marked increase in the level of telomerase activity. We now show that stimulation of T cells derived from serially transplanted HSC results in a telomerase-dependent elongation of telomere length to a size similar to that observed in T cells isolated directly from young mice. Southern analysis of telomere length in resting and anti-CD3/CD28 stimulated donor-derived splenic T cells revealed an increase in telomere size by ~7 kb for the population as a whole. Stimulation of donor-derived T cells from recipients of HSCs from telomerase-deficient mice did not result in regeneration of telomere length, demonstrating a dependence on telomerase. Furthermore, clonal anti-CD3/CD28 stimulation of donor-derived T cells followed by fluorescent in situ hybridization (FISH) analysis of telomeric signal intensity showed that telomeres had increased in size by ~50% for all clonal expansions. Together, these results imply that one role for telomerase in T cells may be to renew or extend replicative potential via the rejuvenation of telomere length.

Keywords: T cell, hematopoietic stem cell, transplantation, telomere, mouse

Introduction

Telomeres are genetic elements that are essential for the stability of chromosomal ends. The critical shortening or loss of one or more telomeres leads to the formation of unstable end-to-end fusions and chromosomal instability (1–3). Telomeric chromatin is composed of a number of different telomeric binding proteins and tandem arrays of simple DNA repeats, (TTAGGG)n in mammals (4) ranging in length from <100 bp in ciliates (5) to 5,000–8,000 bp in humans (6–8) and, in some mouse strains, >100,000 bp (9).

The telomerase complex, composed of an essential RNA component (10) and several different protein components including an essential catalytic component (11) is required for the complete replication of telomeres in most dividing eukaryotic cell populations (12). Immortal cell populations, including germ line cells and tumor cell lines, express telomerase and maintain a stable telomere length (2, 13–15). Genetic ablation of the

telomerase RNA gene in yeast (16) and mouse embryonic stem cells (17) or inhibition of telomerase in tumor cell lines (18) leads to the continuous attrition of telomere length as cells divide, culminating in growth arrest and/or cell death. Telomere length also shortens during replicative aging in many types of human somatic cells in which telomerase is repressed (2, 6, 7, 19).

Many mitotically active somatic cells in humans have a finite replicative capacity, up to ~100 population doublings (pd), when grown in vitro. The state of irreversible growth arrest that subsequently ensues is termed replicative senescence (20). Studies have now demonstrated that replicative senescence is the ultimate effect of continuous telomere attrition, as activation of telomerase via ectopic expression of the catalytic component of telomerase, telomerase reverse transcriptase (TERT;* reference 11) in primary cell strains prevents telomere shortening and leads to cell immortalization (19, 21, 22).

A perplexing feature of hematopoietic cells, including hematopoietic stem cells (HSCs), is the presence of readily detectable levels of telomerase activity (23, 24) and yet division of these cells, is accompanied by extensive telomere shortening both in vitro (22, 25) and in vivo (8, 26, 27). It has also recently been shown that the continuous erosion of telomeres and limited replicative capacity observed in long term cultures of T cells from humans (22, 25) can be prevented by the ectopic expression of TERT (22, 28). Thus, for reasons unknown at present, telomerase appears to be present in hematopoietic cells, but not fully functional.

Recently, we have shown that telomere length shortens in HSCs and other hematopoietic cells of donor type during serial transplantation of HSCs in mice (27). We now show that stimulation of splenic T cells isolated from HSC transplant recipients results in a telomerase-dependent restoration of telomere length to a size found in young mice.

Materials and Methods

Mice.

The derivation of the mTR knockout mice and mTERT knockout mice has been described previously (3, 29). The $mTR^{-/-}$ mice and $mTERT^{-/-}$ mice were backcrossed 6 and 4 times, respectively, to the C57Bl/Ka-Thy1.1(Ly5.1) strain at the Stanford University animal facility before use in this study. In all transplant experiments, the Thy1.1/Ly5.1 mice were used as HSC donors and the congenic C57Bl/Ka-Thy1.2(Ly5.2) strain was used as recipients. The initial donor mice and all the recipient mice were 2–3 mo old. The major histocompatibility class I gene promoter ($H2K^b$-GFP) transgenic mice colony was developed and maintained at Stanford University. All mice were bred and maintained on acidified water (pH 2.5).

HSC Detection and Transplantation.

Bone marrow cells were isolated and stained with fluorophor-conjugated antibodies as described previously (27). The antibodies used in the immunofluorescence staining for HSC detection are as described previously (27). The HSC population is defined as c-kit^{hi}Sca-1^{hi} Thy1.1^{lo}lineage^{-}. Whole bone marrow aliquots containing either 100 or 200 HSCs were used in each round of transplantation.

Splenic T Cell Sorting and Stimulation.

Spleens were collected and single cell suspensions prepared followed by lysis of red blood cells using ACK solution (150 mM NH_4Cl, 10 mM $KHCO_3$). Splenocytes were stained with an antibody cocktail (CD3^{PE}, B220^{APC}, Ly5.1^{FITC}, and Ter119^{TR}) in staining media (Hank's balanced salt solution plus 3% fetal bovine serum, pH 7.2) on ice for 30 min. Cells were then washed once and resuspended in staining media containing propidium iodide (0.5 μg/ml). The donor type splenic T cells and splenic T cells from H2K-GFP transgenic mice were defined as (CD3^{hi} B220^{-}Ly5.1^{hi}Ter119^{-}) and (CD3^{hi}B220^{-}), respectively, and were purified by FACS® on a dual-laser Vantage (Becton Dickinson) FACS® machine. Cells were either sorted into growth media (RPMI 1640 plus 10% FBS (GIBCO BRL), glutamine, nonessential amino acids, Pen/Strep, sodium pyruvate, β-mercaptoethanol, mIl-2 (200 U/ml), and CD28 antibody [a kind gift from Dr. Tien Chin, Department of Immunology, Stanford University]) in 24-well plates (mass culture) or 96-well V-bottom plates (oligoclonal culture) precoated with CD3 antibody (BD Biosciences). During oligoclonal culture, cells were split at a 1:2 ratio on days 7, 11, and 14, and donor-derived cells were harvested on day 17.

Detection of Telomerase Activity.

The TRAP assay and quantification of telomerase activity was performed using the TRAP assay kit from Intergen, as described (15) but with following modifications. The final concentration for all dNTPs was 10 mM, and 0.2 μg of TS primer was used per 25 μl reaction.

DNA Isolation and Terminal Restriction Fragment Length Analysis by Field Inversion Gel Electrophoresis.

Splenic T cells were collected for DNA isolation at the time of the initial transplantation and from secondary HSC transplant recipients 4 mo or more post-transplant. The DNA was isolated, digested with restriction enzymes, and subjected to southern analysis of terminal restriction fragment (TRF) length using a field inversion gel electrophoresis *(*FIGE) apparatus as described previously (27). Mean TRF length was calculated as described previously (25).

Fluorescent In Situ Hybridization.

Cells were fixed and telomeres stained with a FITC conjugated peptide nucleic acid telomeric oligomer, $(CCCTAA)_3$ (Applied Biosystems), as described previously (27, 30).

Images were collected and quantitative analysis of the fluorescent signal intensity was performed using a ZEISS confocal microscope. Control slides of unstained cells were used to correct for background fluorescence.

Immunostaining.

The telomerase specific K-370 antibody was used to detect mTERT as described previously (31). Briefly, cells were fixed in methanol, blocked in 10% goat serum, and stained with a 1/500 dilution of the K-370 antibody in 1% serum for 1 h at 37°C. Cells were washed in PBS, and stained with biotin-conjugated anti–rabbit IgG (Vector Laboratories) for 1 h at 37°C. After a brief wash in PBS, cells were stained with Texas Red-conjugated avidin (Sigma-Aldrich) for 1 h at 37°C. Nuclei were stained with Hoechst 33258.

Results

Southern Analysis of Terminal Restriction Fragment Length in Resting and Stimulated T Cells from HSC Recipients.

To assess the effect on telomere length of antigenic stimulation of T cells of donor type from adult mice and HSC transplant recipients, we collected donor-derived splenic T cells by FACS® for anti-CD3/CD28 stimulation in vitro and performed southern analysis of TRF length on the resting and stimulated T cells (Fig. 1) . The TRF length for resting splenic T cells isolated from secondary HSC recipients (mean ~16 kb) was significantly shorter than that observed for resting T cells from young adult mice (mean ~23 kb; $P = 0.005$). 1 wk after anti-CD3/CD28 stimulation, no change in the TRF length was detected for splenic T cells isolated from young adult mice. However, the TRF length of the stimulated splenic T cells isolated from HSC transplant recipients had increased significantly (Fig. 1; $P = 0.002$), to an average size approximately equal to that observed for splenic T cells from young adult mice.

Figure 1.

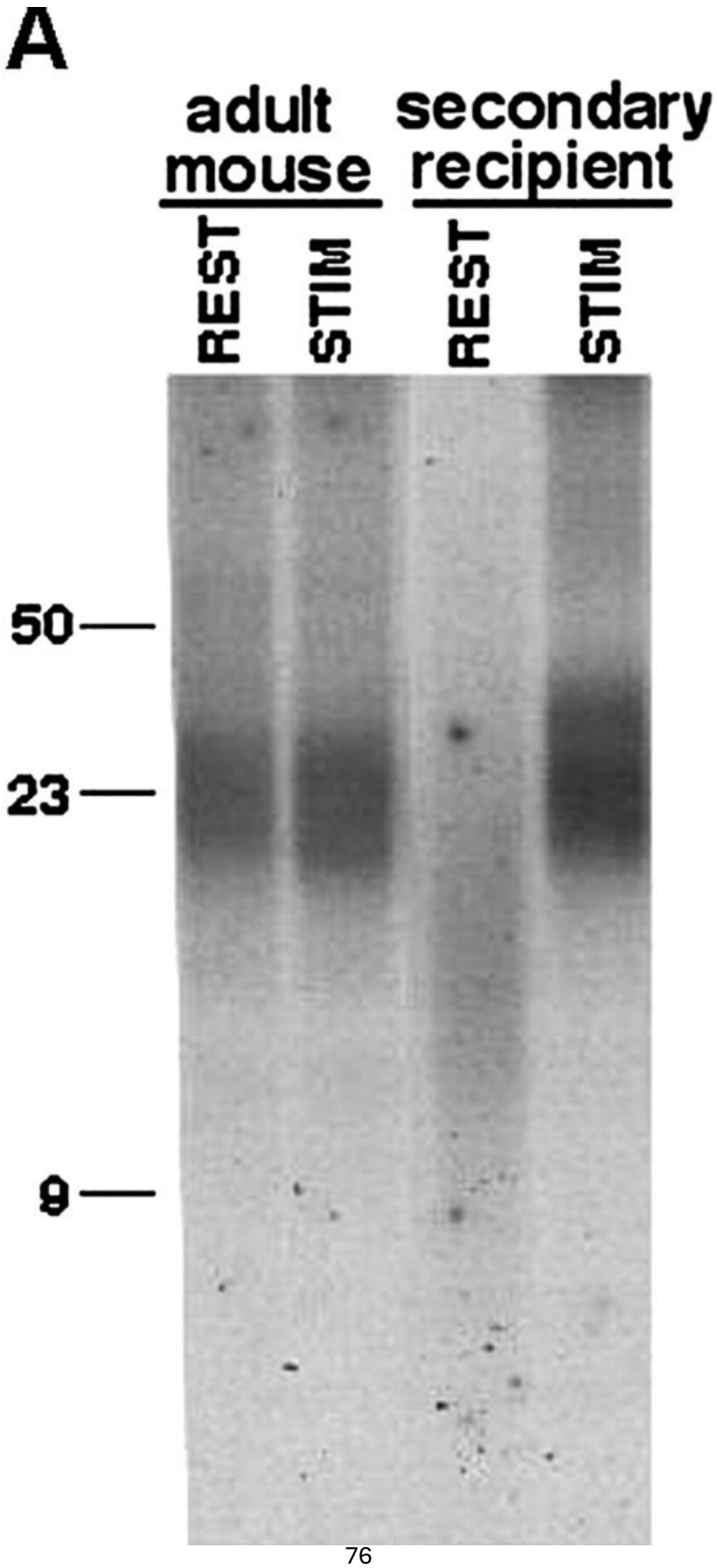
A
adult mouse
secondary recipient
REST
STIM
REST
STIM
50
23
9

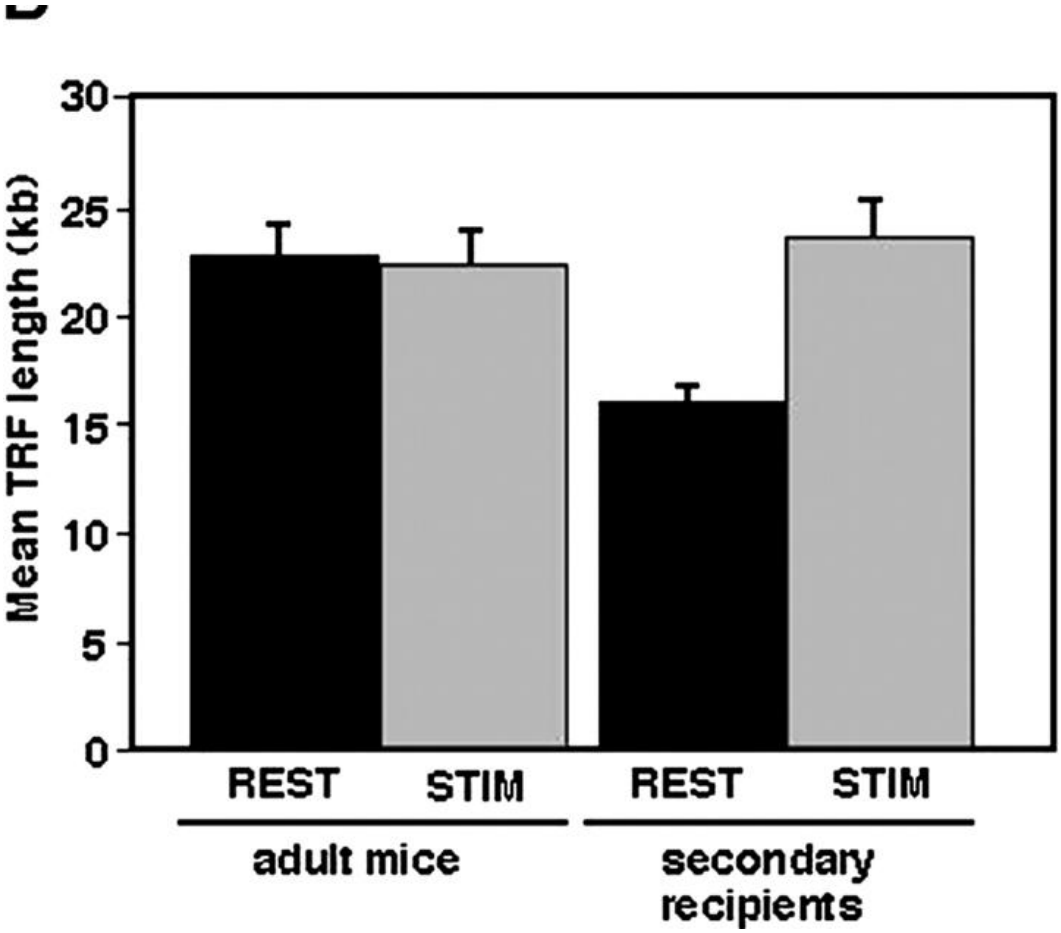

Analysis of TRF length of resting and stimulated donor-derived T cells. (A) Splenic T cells (5×10^4) from young adult mice and secondary HSC recipients were collected via FACS® and either transferred to growth media for stimulation or used for isolation of high molecular weight DNA. Anti-CD3/CD28 stimulated T cells were collected for isolation of DNA after 1–2 wk of growth. The extraction and restriction enzyme digestion of DNA was performed as described previously (reference 27). 1 μg of each DNA sample was resolved in a 0.75% agarose gel by field inversion gel electrophoresis (pulse conditions: 180 V forward; 120 V reverse for 16 h). The gel was dried and the DNA hybridized to a ^{32}P-end labeled telomeric oligomer overnight followed by 3 × 5 min washes at 37°C in 0.35× SSC buffer. Images were collected using a Phosphor-Imager screen. Size of molecular weight standards (kilobases) are shown on the left. REST, resting; STIM, anti-CD3/CD28 stimulated. (B) The mean TRF length was calculated and averaged for all resting and stimulated T cell samples taken from a total of five adult mice and seven secondary recipients. Error bars (standard deviation) and P values (Student's *t* test) are shown.

Activation of Telomerase Is Required for Telomere Length Increase in Stimulated T Cells.

To assess the potential role of telomerase in the restoration of telomere length in stimulated T cells derived from transplanted HSCs, we performed the TRAP assay on resting and anti-CD3/CD28 stimulated splenic T cells (Fig. 2) . Similar to that reported in previous studies (32–35), we observed a large (~45 fold; Fig. 2 B) increase in telomerase activity 2 d after anti-CD3/CD28 stimulation of donor-derived T cells from adult mice and from HSC transplant recipients. No difference in the level of telomerase activity was observed for resting T cells or stimulated T cells isolated from young adult mice as compared with secondary HSC recipients. To begin to assess the mechanism as to how telomerase is activated after antigenic stimulation of T cells, we stained splenic T cells with an antibody to mTERT before and after anti-CD3/CD28 stimulation. TERT appeared to be localized primarily in the cytoplasm of resting cells and in the nucleus of stimulated cells (Fig. 2 C), as previously observed by others (36). To exclude the possibility of nonspecific binding of the mTERT antibody, splenic T cells from mTERT$^{-/-}$ mice were also stained. Only a very faint, nonspecific nuclear signal was observed in both resting mTERT$^{-/-}$ T cells (Fig. 2 C) and activated mTERT$^{-/-}$ T cells (data not depicted).

Figure 2.

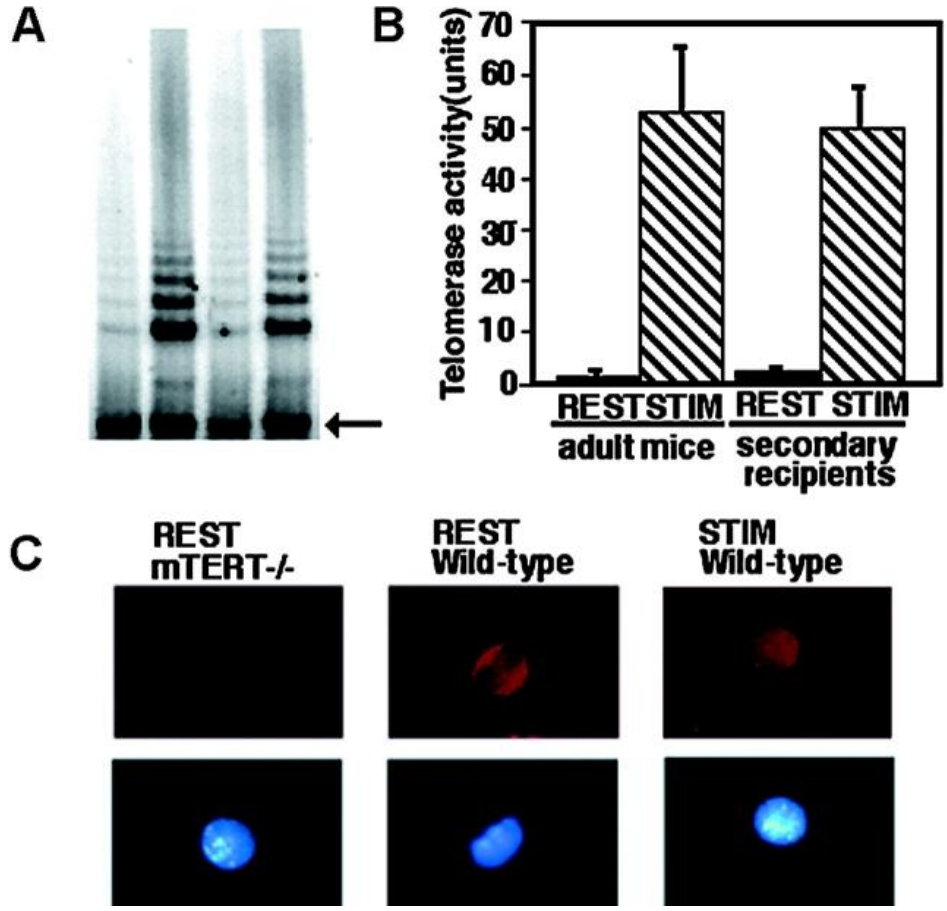

Analysis of telomerase activity in resting and stimulated donor-derived T cells. (A) Splenic T cells (2×10^5) from young adult mice and secondary HSC recipients were collected via FACS® and either lysed in CHAPS buffer for extraction of telomerase, or transferred to growth media for stimulation. After 2 d of growth, anti-CD3/CD28 stimulated splenic T cells were harvested for extraction of telomerase. Telomerase activity was measured for 500 cell equivalents of each sample extract by the TRAP assay. (B) Telomerase activity was measured for resting (REST) and stimulated (STIM) T cells from a total of five adult mice and seven secondary recipients and averaged for all samples. The mean level of activity and error bars (standard deviation) are shown. (C) Analysis of TERT localization in resting and stimulated T cells. Resting and anti-CD3/CD28 stimulated T cells from mTERT wild-type mice and resting T cells from mTERT knockout mice were fixed and stained with an mTERT antibody (top panel). Corresponding Hoechst 33258 staining for each cell is also shown (bottom panel). Original magnification: ×60.

To verify the essential role of telomerase in telomere length rejuvenation after activation of T cells, we analyzed telomere length in T cells from young adult mice and secondary HSC recipients in which the gene encoding the RNA component of telomerase (mTR) was knocked out (3). Telomere length was analyzed using fluorescent in situ hybridization (FISH) as opposed to southern analysis of TRF length due to the large,

heterogeneous, multi-modal nature of the TRFs in this mouse strain (unpublished data). Telomere signal intensity increased after antigenic stimulation of donor-derived T cells from secondary recipients of HSC from $mTR^{+/+}$ mice (Fig. 3 ; P = 0.001), in agreement with the increase in TRF length observed for wild-type C57Bl/Ka Thy1.1 mice (Fig. 1). However, no change in telomere signal intensity was observed following stimulation of donor-derived T cells from secondary recipients of HSCs from $mTR^{-/-}$ mice (Fig. 3), thereby confirming the necessity of telomerase for extension of telomere length.

Figure 3.

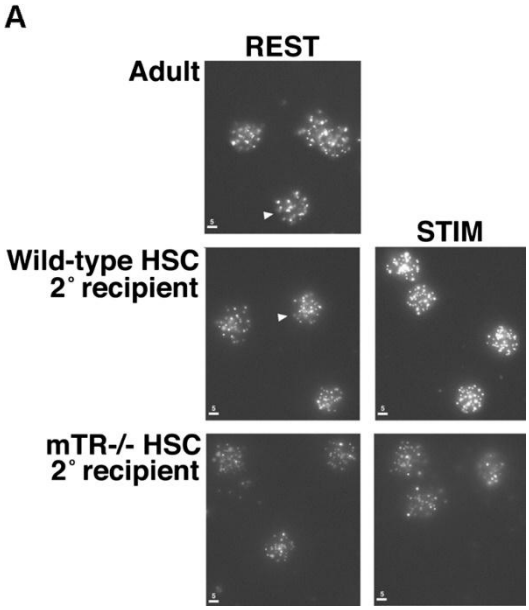

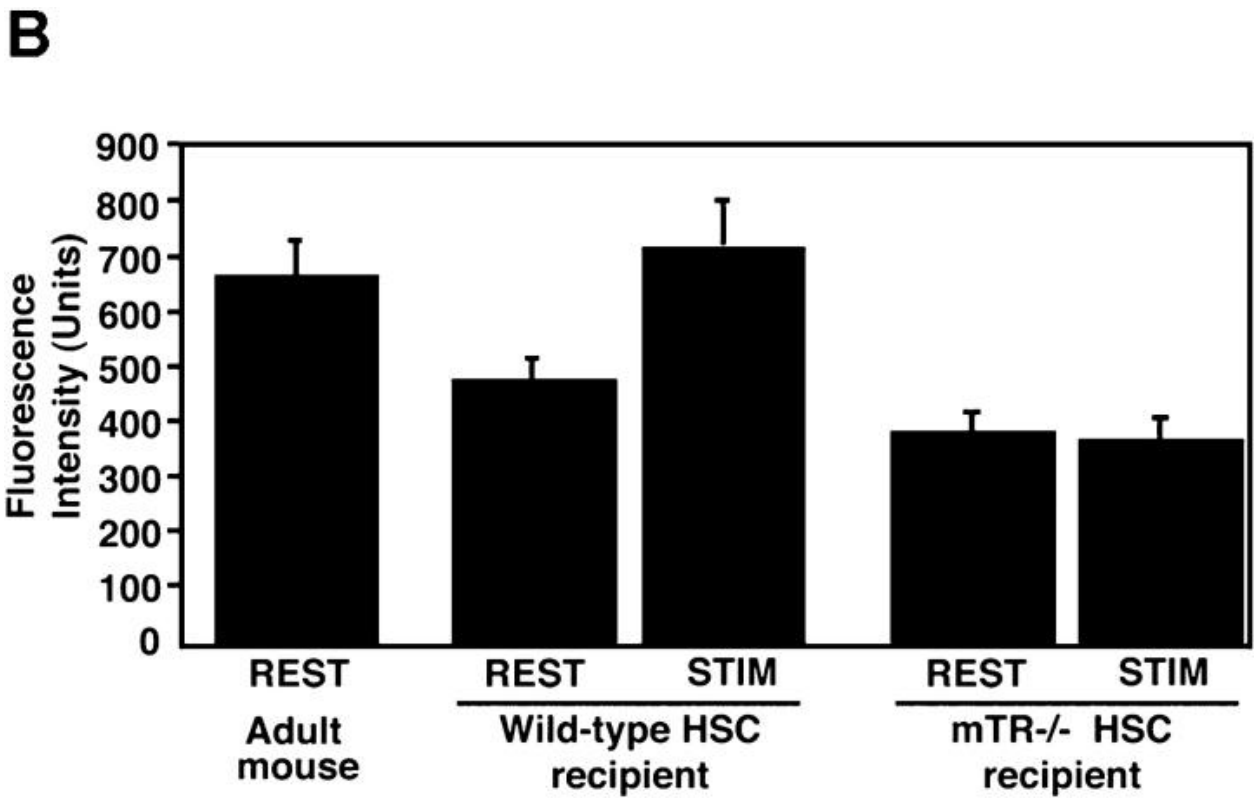

FISH analysis of telomere length in resting and stimulated donor-derived T cells from transplant recipients of HSC from mTR knockout mice. (A) Splenic T cells (5×10^4) from young adult mTR wild-type or knock-out mice and secondary HSC recipients were collected via FACS® and either transferred to growth media for stimulation or fixed. 1 wk after anti-CD3/CD28 stimulation, cells were cytospun onto glass slides and fixed. Telomeres were detected by FISH using a FITC-conjugated peptide nucleic acid telomeric oligomer. Individual interphase nuclei are indicated by arrowheads. Original magnification: ×60. The size scale (μm) is indicated in the bottom left. (B) The fluorescent telomeric signal intensity was calculated and corrected for background for 20 well isolated individual resting or stimulated $mTR^{+/+}$ or $mTR^{-/-}$ donor-derived splenic T cell nuclei. Telomeric signal intensity was also measured for resting splenic T cells from an adult wild-type mouse. The mean fluorescent signal intensity and standard deviation are shown. Telomeric signal intensity increased significantly ($P < 0.005$; Student's *t* test) after stimulation of donor-derived splenic T cells from secondary recipients of $mTR^{+/+}$ HSCs.

Telomere Length Increase in Stimulated T Cells Is Due to Elongation of Short Telomeres by Telomerase, Not Selection of Cells with a Long Telomere Length.

The increase in telomere size in stimulated splenic T cells isolated from HSC transplant recipients could be accounted for by selection of T cells with a long initial telomere length and/or the synthesis of new telomeric DNA after stimulation of T cells with a short initial telomere length. The former possibility implies that there is a rare population of T cells with long telomeres in the spleens of HSC transplant recipients. This population must exist at a frequency of ~10% or less of the reconstituted splenic T cells since we are able to detect two distinct modes of longer and shorter TRFs when DNA from splenic T cells of donor type from adult mice and secondary HSC transplant recipients are mixed at a ratio as low as 1:10 and analyzed for TRF length, but only observe the shorter TRF mode in T cells from secondary recipients (unpublished data). To test for selection of T cells with a long initial telomere length after stimulation, we costimulated 10 pools of 9 T cells from transgenic mice which express GFP throughout the hematopoietic system, plus a single donor-derived T cell from a secondary HSC recipient. 2 1/2 wk after stimulation, cells derived from the secondary HSC recipient T cell were isolated by FACS® for FISH analysis of telomere length (Fig. 4) . For all pools containing cells derived from the secondary recipient (6 of 10), telomere signal intensity increased significantly (~50%), becoming approximately equal to that observed for resting T cells from adult mice (Fig. 4 B). In addition, we also stimulated 10 pools of 10 T cells from an independent secondary HSC recipient and observed a similar increase in telomere signal intensity in all pools (unpublished data). Thus, while we cannot completely exclude the existence of a rare population of T cells with a long initial telomere length, the increase in telomere length following stimulation of donor-derived T cells from HSC transplant recipients is, at least in part if not entirely, a direct result of extension of the shortened telomeres in these cells.

Figure 4.

A

REST

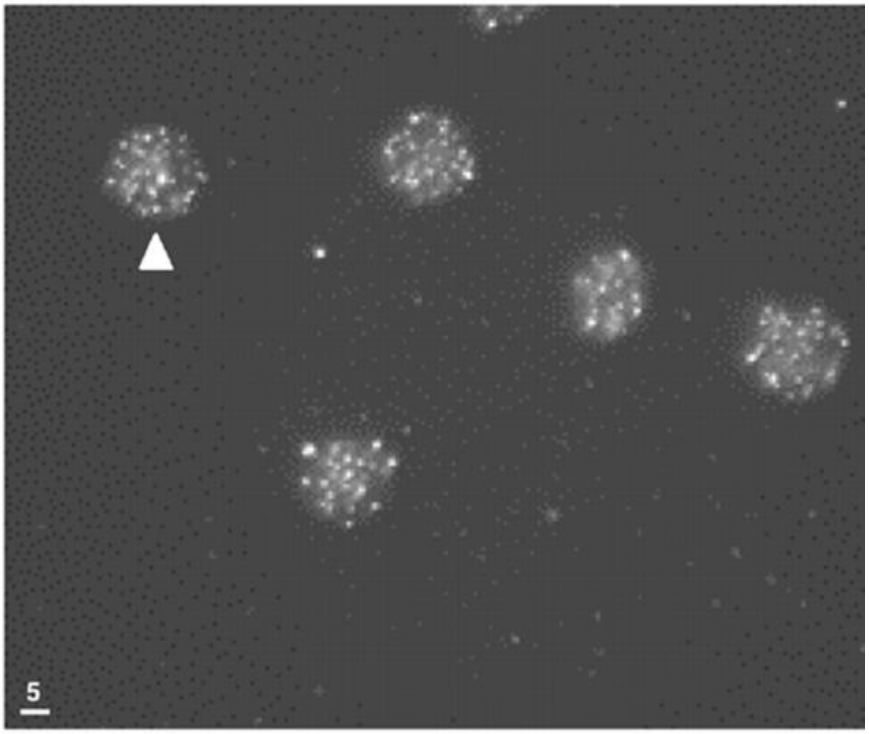

STIM

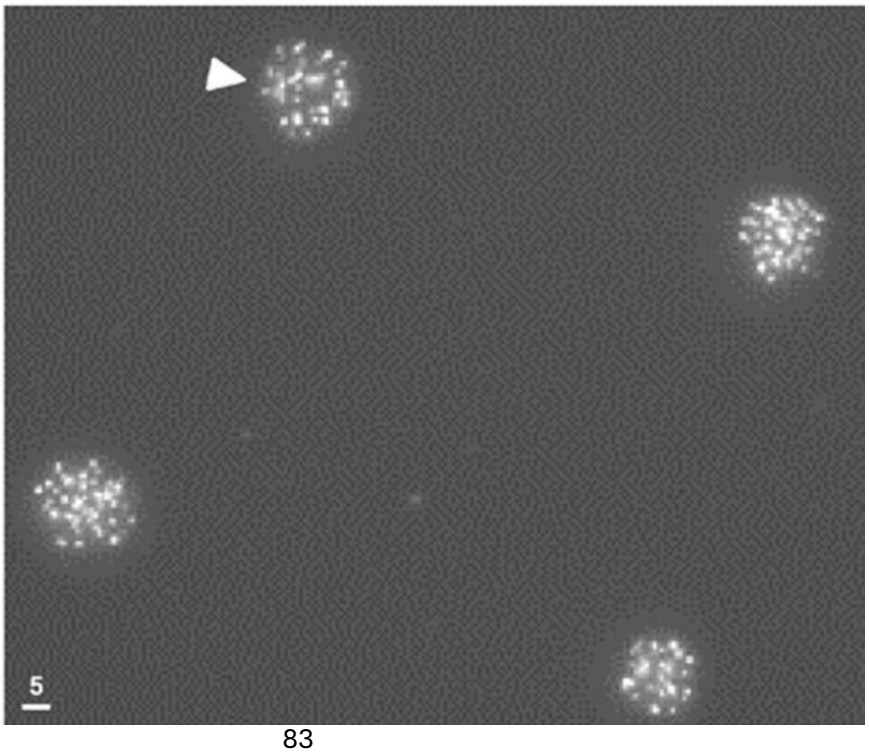

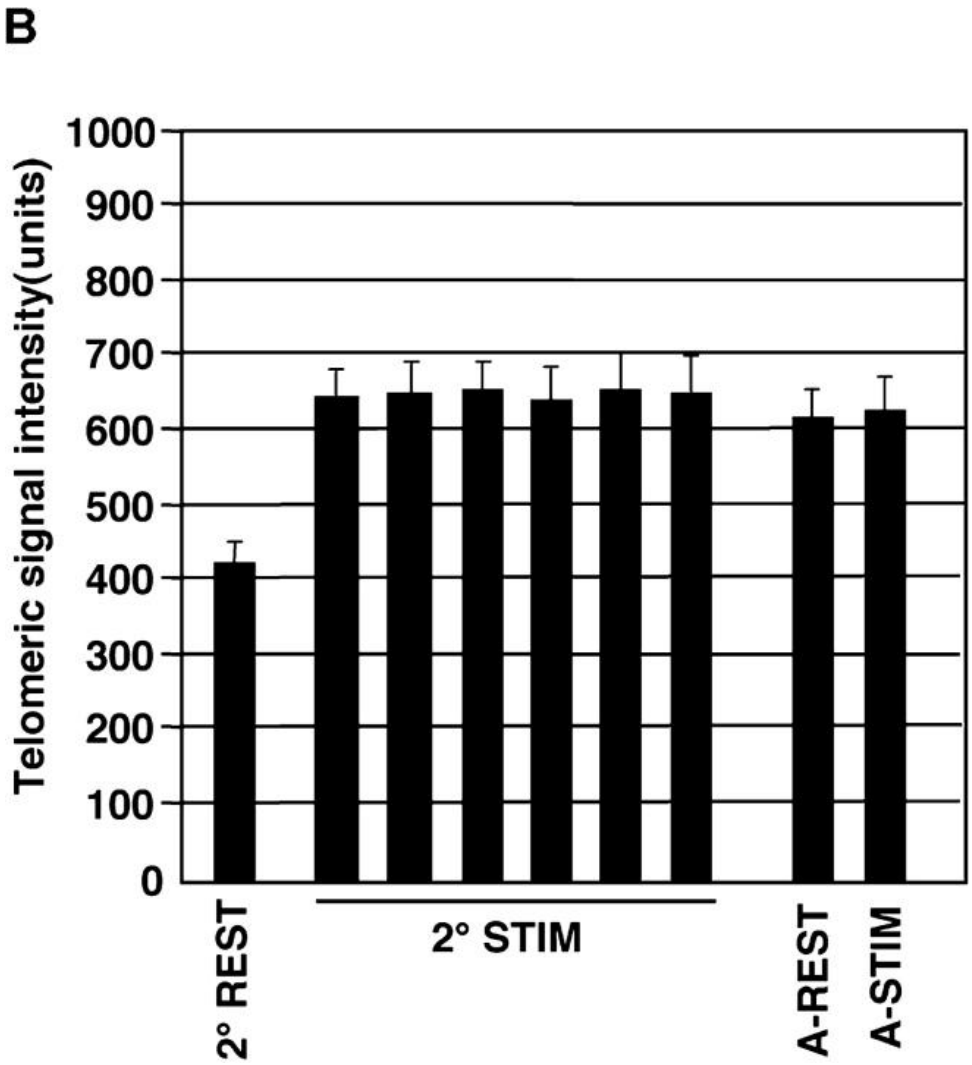

FISH analysis of telomere length after clonal stimulation of donor-derived T cells. (A) Splenic T cells were sorted into 10 pools of 10 cells, 9 cells from a H2K-GFP transgenic mouse, and 1 cell of donor type from a secondary HSC recipient, in growth media in a 96-well V-bottomed dish for stimulation. Resting splenic T cells were also collected via FACS, cyto-spun onto slides, and fixed at this time. 17 d after stimulation, T cells derived from the secondary recipient (i.e., non-GFP cells) were collected via FACS® from each stimulated pool in which they could be detected, and either cyto-spun onto glass slides, and fixed or used for confirmation of T cell functionality by TCR clonotype analysis (reference 48; unpublished data). The telomeres were detected by FISH using a FITC-conjugated peptide nucleic acid telomeric oligomer. Individual interphase nuclei are indicated by arrowheads. Sample images of stained nuclei collected from resting splenic T cells (top panel) and of one clonal pool of anti-CD3/CD28 stimulated splenic T cells from a secondary recipient (bottom panel) are shown. Original magnification: ×60. The size scale (μm) is indicated in the bottom left. (B) The fluorescent telomeric signal intensity was calculated and corrected for background for 20 well isolated individual resting or stimulated splenic T cell nuclei from a secondary recipient. Telomeric signal intensity was also measured for resting and

clonally stimulated splenic T cells (n = 20 for each) from a C57Bl6/Ka Thy1.1 mouse. The mean fluorescent signal intensity and standard deviation are shown. For all clonal expansions derived from T cells from the secondary HSC recipient, the telomere signal intensity increased significantly relative to resting T cells from the same mouse ($P \leq 0.005$; Student's t test).

Discussion

Results from a number of studies have indicated that extension of telomere length can occur in normal somatic cells. Lengthening of telomeres has been observed during development in the offspring of mice in which the set of telomeres inherited from one parent are longer than those inherited from the other (37). Compared with adult tissues, telomerase activity is relatively high in the germ line (15) and the developing embryo (38, 39) including embryonic stem cells (17) and therefore the increase in telomere length observed in this study is likely telomerase dependent. Previous studies have also provided strong evidence for telomere lengthening in B cells: germinal center (GC) B cells have longer telomeres than either precursor naive B cells or more mature memory B cells (40), and stimulation of murine splenocytes in vivo has been shown to be accompanied by an increase in telomere length in wild-type mice but not early generation (G1) $mTR^{-/-}$ mice (41). However, the selection of a rare subpopulation of B cells with an initial long telomere length, as opposed to true extension of telomeres, was not ruled out in these studies. Here we show that antigenic stimulation of T cells derived from serially transplanted HSCs with an initial short telomere length directly results in a telomerase-dependent extension of telomere length to a size roughly equal to that observed in T cells from young animals.

Although we believe our data favors a scenario in which telomere length is restored via a telomerase-dependent mechanism in most if not all resting T cells that have acquired shortened telomeres, other possible mechanisms warrant discussion. One alternative explanation for the restoration of telomere length that we observe in stimulated T cells from secondary HSC recipients is that HSCs and/or resting T cells with increased levels of telomerase activity are being selected for during transplantation or after stimulation, respectively. However, we have compared telomerase activity between HSCs isolated directly from donor animals and from primary and secondary recipients, and found no change in the level of activity with successive rounds of transplantation (unpublished data). Furthermore, we have previously shown that telomere length decreases in HSCs during serial transplantation, which would not be expected if cells with higher levels of telomerase were being selected for. Although we cannot rule out the possibility of selection of resting T cells with high initial levels of telomerase, a mechanism to explain the inability of telomerase to restore telomere length in these cells before stimulation would have to be presumed, as these cells almost certainly have a shortened telomere length before stimulation (Fig. 4; see Results). Furthermore, it would also have to be assumed that any T cells with higher levels of telomerase would either have to be a rare population or be able to further increase their levels of telomerase upon activation, as telomerase activity increases dramatically following antigenic stimulation of T cells (32–35; Fig. 2). It is also possible that the telomerase-independent ALT (alternative

lengthening of telomeres) mechanism (42) for extending telomeres may be contributing to the telomere elongation in activated donor-derived T cells. The rate of telomere length increase, ~7 kb over 16–17 d or ~8–12 population doublings, that we observe is relatively fast, akin to the rapid increase in telomere length observed in ALT-positive tumor cell lines (42). Also, after immunization, telomere length in splenocytes from late generation (G5) $mTR^{-/-}$ mice have been observed to increase by ~12 kb (41), which may very well be explained by the previous activation of ALT in these mice. However, we have not observed, in resting or activated T cells (Fig. 1 A), the large, heterogeneous distribution of TRFs that is characteristic of ALT-positive cells (42), nor have we observed an increase in telomere length after activation of T cells from telomerase-deficient mice (Fig. 3). Nevertheless, it will be of interest to further assess the possible contribution of ALT to the restoration of telomere length following activation of donor-derived T cells.

The observations reported here suggest that one function of telomerase in some or all subsets of T cells may be to restore telomere length upon antigenic stimulation in cells that have acquired shortened telomeres. In agreement with this notion is the positive correlation previously observed between telomerase activity level and telomere length after antigen stimulation of human $CD4^+$ T cells (43). One consequence of the ability to replenish telomere length in T cells with short telomeres is a concomitant increase in replicative capacity. This could perhaps be important not only in any rare naive or memory T cells in young individuals which may have acquired one or more critically short telomeres, but also in the elderly in which hematopoietic cells, including T cells, have very short telomeres (25). Specifically, it may be possible for these cells, upon antigenic stimulation in vivo, to thwart a premature replicative senescence induced by further telomere shortening via the regeneration of telomere length to a size observed in young individuals. To confirm this, it will be necessary to assess changes in telomere length after stimulation of T cells from elderly individuals, or, if they can be identified, T cells with short telomeres from young individuals.

As previously noted by Liu et al. (36) we find that TERT, surprisingly, appears to be predominantly present in the cytoplasm in resting T cells and translocates to the nucleus after antigenic stimulation (Fig. 2 C). It is quite likely that TERT translocation, as well as other events, are essential for the activation of telomerase in stimulated T cells. Although full details of the signaling mechanism leading to the nuclear translocation TERT have yet to be worked out, it may involve association of TERT with 14–3-3 proteins (44). The 14–3-3 family of signaling proteins act as molecular chaperones and have been shown to associate with TERT (44). In addition, TERT contains a NES-like motif in close proximity to the 14–3-3 binding site, suggesting that the binding of 14–3-3 proteins to TERT may inhibit the interaction of the exportin CRM1 with the TERT NES-like motif (44). The signaling mechanism for TERT translocation may also involve phosphorylation of TERT (36). It will be of great interest to identify all of the factors involved in the activation of TERT in resting T cells, as these factors may perhaps provide a novel target in therapies to treat T cell leukemias. It will also be important to assess the physiologic significance of the localization of TERT in the cytoplasm of

resting T cells, and to assess whether TERT is also localized in the cytoplasm of other hematopoietic cells, including HSCs.

The data reported here suggests that telomerase can extend telomere length in T cells during the first few doublings after stimulation, but only to a size equal to that observed in resting T cells in young animals. The mechanism which limits the amount by which telomerase can extend telomere length, although not well understood, may involve the interaction of the newly assembled telomeric chromatin with telomerase in a negative feedback loop. One telomeric binding protein in particular that probably has an important role in this feedback loop is the Myb-related protein TRF1, which binds at numerous sites along the telomeric DNA tract (45). Overexpression of TRF1 or inhibition of its normal association with telomeric chromatin leads to a decrease or increase in telomere length, respectively (46). Furthermore, TRF1 induces bending in telomeric DNA upon binding (47) which may in turn affect the enzymatic activity of telomerase. Future in vivo studies as to the effect of TRF1 function and expression on telomere length maintenance in embryonic stem cells and germ line cells, and telomere length rejuvenation in lymphocytes, should help shed more light on this subject.

Acknowledgments

We thank Ron dePinho, Lea Harrington, and Maria Blasco for providing the mTR knockout mice, the mTERT knock-out mice, and the K-370 TERT antibody, respectively. Thanks to L. Jerabek for excellent technical assistance, T. Knaak for operation of the FACS® machines, and to L. Hidalgo for animal care. This work was supported by National Institutes of Health grants CA 42551 and DK 53074 (I.L. Weissman) and National Research and Science Association/National Institutes of Health post-doctoral fellowship (CA76708) and Irvington Institute of Immunology fellowship (R.C. Allsopp).

The Role of NAD+ in Regenerative Medicine

Summary:

The understanding of the molecular and cellular basis of aging has grown exponentially over recent years, and it is now accepted within the scientific community that aging is a malleable process; just as it can be accelerated, it can also be slowed and even reversed. This has far-reaching implications for our attitude and approach toward aging, presenting the opportunity to enter a new era of *cellular* regenerative medicine to not only manage the external signs of aging but also to develop therapies that support the body to repair and restore itself back to a state of internal well-being. A wealth of evidence now demonstrates that a decline in cellular nicotinamide adenine dinucleotide (NAD+) is a feature of aging and may play a role in the process. NAD+ plays a pivotal role in cellular metabolism and is a co-substrate for enzymes that play key roles in pathways that modify aging. Thus, interventions that increase NAD+ may slow aspects of the aging trajectory, and there is great interest in methods for cellular NAD+ restoration. Given these recent advancements in understanding the cellular aging process, it is important that there is an integration between the basic scientists who are investigating the underlying mechanisms of cellular aging and the surgeons and aesthetic practitioners who are providing antiaging therapies. This will allow the effective translation of this vastly complex area of biology into clinical practice so that people can continue to not only stay looking younger for longer but also experience improved health and wellness.

In general terms, aging is considered the organism-wide loss of homeostasis, innate repair, and regenerative capacity, resulting in an accumulation of damage and the development of multiple copathologies. Aging is a complex and multifactorial phenomenon that includes many effects at the systemic level which are ultimately driven by critical changes at the cellular level. It is recognized that there are nine key cellular changes that underpin the cascade of events that lead to systemic age-related decline. These cellular causes of aging have been well characterized and are collectively referred to within the aging research community as the “hallmarks of aging.”[1]

The identification of the hallmarks of aging has marked a shift toward understanding aging not as a single process, but instead as a combination of multiple cellular changes. This has allowed the molecular and cellular root causes of many common aging phenotypes to be identified. For example, skin aging—arguably the most recognizable sign of aging—has traditionally been described at the histological level, but it is now understood that these changes result from more specific failures at a cellular level, revealing new therapeutic targets with the potential to address aging at its root cause (Fig. 1).

Fig. 1.

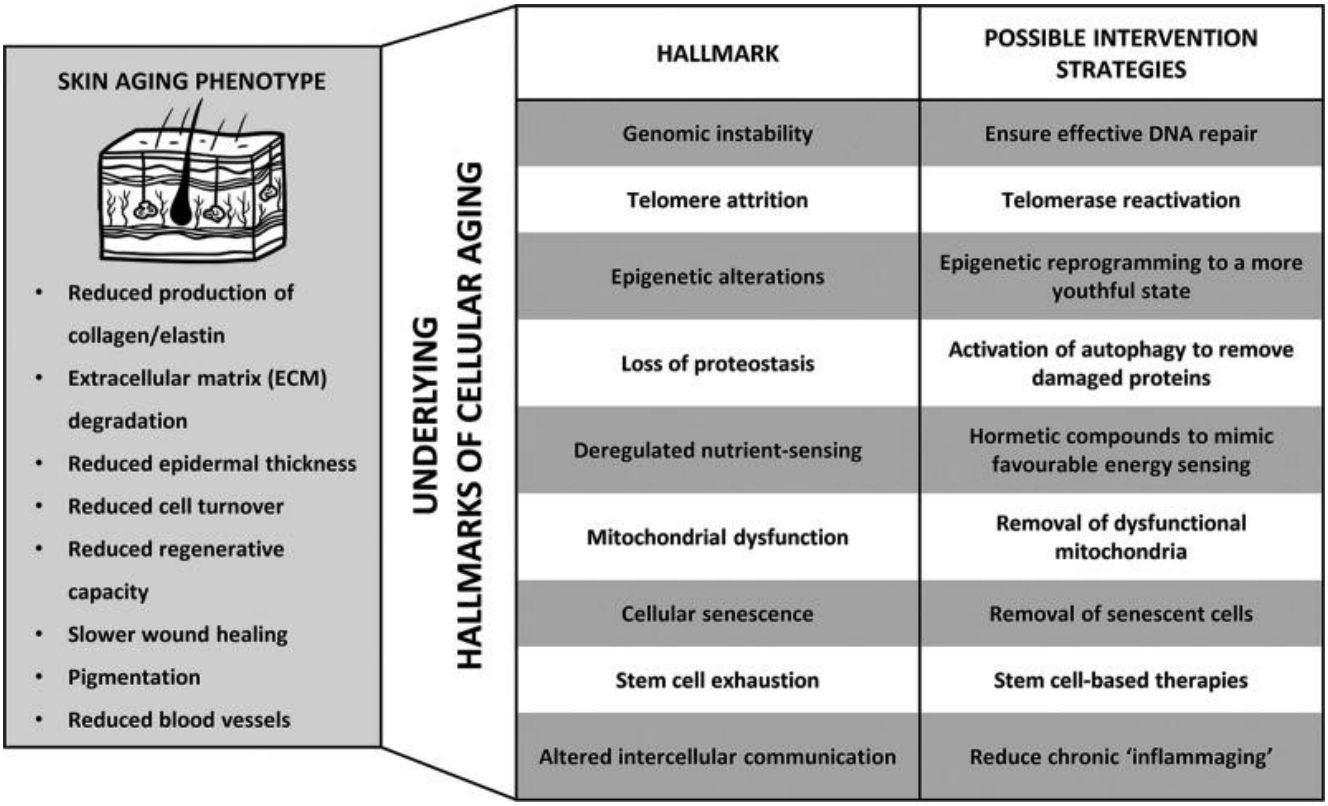

Traditionally, age-related dysfunction has been described at the histological level, but it is now known that these changes result from more specific failures at the cellular level. These key cellular changes are collectively known as the "hallmarks of aging" and designing interventions that target these hallmarks is currently an area of intense research.

NAD+ AS A TARGET FOR CELLULAR AGING

One area of intense research within the field of cellular aging surrounds the molecule nicotinamide adenine dinucleotide (NAD+). Metabolomics-based studies of aging have identified NAD+ as a central metabolic intermediate linked to many of the hallmarks of aging.[2] NAD+ is a cellular coenzyme that plays an essential role in both metabolic and signaling reactions. During its role in metabolism, NAD+ participates in redox reactions leading to the formation of ATP. Aside from this key role, NAD+ is also a critical regulator of a wide array of enzymes involved in making posttranslational modifications to proteins that change their activity.[3] This combination of metabolic and cell-signaling functions means that NAD+ acts as a metabolic messenger providing an important link between the energy status of the cell and downstream signaling for appropriate cellular adaptation to bioenergetic stress. Therefore, a proper maintenance of NAD+ levels is required to maintain tissue homeostasis and stress response.[4]

Despite its critical role, an age-dependent decrease of cellular NAD+ is observed across species. In humans, age-related NAD+ decline has been observed in the liver,[5] skin,[6] brain,[7,8] plasma,[9] skeletal muscle,[10] and monocyte-derived macrophages.[11] Chronically low NAD+ has been observed in accelerated aging disorders[12] and age-related disease states,[13–15] and has been linked to multiple hallmarks of aging.

Low NAD+ contributes to aging because NAD+ serves as an exclusive co-substrate for two key families of enzymes that affect cellular repair and longevity—the sirtuins (SIRTs) and the poly(ADP-ribose) polymerases (PARPs). These enzyme families regulate many signaling processes associated with cellular health and longevity and are directly dependent on NAD+ availability to perform their functions.

PRECLINICAL BENEFITS OF NAD+ RESTORATION

Restoration of NAD+ in vivo has been investigated extensively and has demonstrated whole-body benefits. This has been reviewed in detail recently.[16] Briefly, in mice, NAD+ levels have been found to decrease twofold by mid-age, correlating with the onset of multiple age-related issues.[5] Successful restoration of NAD+ to youthful levels resulted in cardiovascular improvements[17] and the reversal of multiple metabolic conditions.[18–21] Improvements to muscle function and endurance[20] were also observed together with increased mitochondrial function, ATP production[14] and an increased number and quality of muscle stem cells.[22] An increased capacity for organ protection and regeneration after injury was found in the liver, heart, and kidneys,[23–25] and NAD+ restoration was also found to rescue vision by reversing retinal degeneration.[26] Significant neurological benefits have also been demonstrated in Alzheimer disease animal models on NAD+ restoration, including improved cognition and nerve regeneration. NAD+ availability also appears to impact fertility, as strategies to boost NAD+ levels were found to improve oocyte quality and restore fertility in aged mice.[27]

CLINICAL BENEFITS OF NAD+ RESTORATION

These impressive preclinical results have now shifted the focus to human clinical trials with the hope of translating the benefits of NAD+ restoration to humans (**see Table, Supplemental Digital Content 1**, which shows human clinical trials that have measured NAD+ levels and clinical outcomes after NAD+ restoration, http://links.lww.com/PRS/F374). Notable observations so far include a trend towards an improvement in indicators of cardiovascular function including lower systolic blood pressure and aortic stiffness,[28] a promising reduction in the levels of circulating inflammatory cytokines in older males after only 3 weeks of NAD+ restoration[29] and an NAD+-associated increase in mitochondrial function and decreased proinflammatory factors in heart failure patients.[30] The diverse protective and regenerative capacity of NAD+ has been attributed to its involvement in the prevention of multiple hallmarks of cellular aging (Table 1).

Table 1.

Hallmark of Aging	Role of NAD+	References
Genomic instability	Adequate NAD+ availability is critical to drive DNA repair enzymes and pathways such as PARP1, SIRT1, and SIRT6	31–33
Cellular senescence	Low NAD+ promotes senescence in skin whilst restoration of NAD+ reduces the burden of senescent cells	40,41
Epigenetic alterations	NAD+-dependent sirtuins are critical for youthful epigenetic regulation. Reduced NAD+ means sirtuins cannot perform this critical role	43
Mitochondrial dysfunction	Adequate NAD+ is critical to healthy mitochondrial function and for the removal of damaged mitochondria	79
Telomere attrition	NAD+ restoration is found to alleviate telomere dysfunction	80
Altered intracellular communication	Low NAD+ promotes age-related inflammation	81
Loss of proteostasis	NAD+ is required for SIRT1-mediated activation of autophagy to clear damaged cellular proteins	60,61
Deregulated nutrient sensing	NAD+ levels are critical to sense the energetic status of the cell for adaptation to energy stress	4
Stem cell exhaustion	NAD+ restoration leads to stem cell rejuvenation	22

Hallmarks of Aging Are Key Cellular Changes That Underpin the Cascade of Events that Lead to Systemic Age-Related Decline*

NAD+ has been identified as a key metabolic intermediate linked to many of the hallmarks of aging.

THE ROLE OF NAD+ IN SKIN AGING

There is also growing evidence that NAD+ decline plays a critical role in the biology of skin aging. DNA damage and genomic instability are key features of skin aging due to the continued exposure of the skin to UV radiation and sophisticated DNA repair mechanisms exist to quickly repair damage before it becomes harmful to the cell. It has emerged that several of these repair mechanisms are directly dependent on NAD+ to perform their function, so its decline with age is problematic. For example, the DNA repair enzyme PARP1, and SIRTs 1 and 6, which are integral elements of the DNA repair response, are all critically dependent on NAD+ to function.[31–33] Decreasing NAD+ levels therefore contribute to reduced DNA repair and an accumulation of DNA damage. Accordingly, an age-associated decrease in both NAD+ and SIRT1 is observed in skin, whilst DNA damage is found to accumulate,[6] ultimately triggering other hallmarks of aging such as cellular senescence.

Cellular senescence is characterized by the cell entering a state of irreversible cell cycle arrest.[34] Both fibroblasts and keratinocytes have been found to become senescent with age[35] and, while they persist in the skin and remain metabolically active, they do not perform their normal function in contributing to skin health. For example, senescent fibroblasts no longer produce collagen and elastin resulting in a dysfunctional support matrix and skin that is not capable of efficient damage repair.[36] Senescent cells also have a distinct inflammatory secretory profile termed the “senescence associated secretory phenotype” (SASP), which has a profound detrimental effect on surrounding cells, leading to altered intercellular communication.[37] Senescent fibroblasts promote degradation of the extracellular matrix (ECM) by secreting matrix metalloproteinase-1 (MMP1) and other proinflammatory factors,[38] ultimately leading to thinning of the epidermis and decreased barrier function,[39] while the selective removal of senescent cells leads to normalization of the ECM and a reduction in inflammation.[37] Low NAD+ has also been found to promote senescence by reducing SIRT1 activity, which in turn reduces p63 expression, leading to a reduction in cell proliferation.[40] NAD+, SIRT1, and p63 are all found to decline in aged keratinocytes leading to senescence,[35] while the restoration of NAD+ reduces the senescent cell burden in dermal fibroblasts.[41]

As well as genomic instability, the aging process is characterized by changes to DNA methylation patterns known as “epigenetic drift,” which ultimately alters gene expression.[42] This has led to the development of “DNA methylation clocks” that predict the biological age of cells based on these measurable epigenetic changes. The NAD+-dependent SIRTs play a key role in epigenetic regulation, highlighting a major role for NAD+ in the cross talk between the metabolic state of the cell and epigenetic regulation of gene expression.[43] Indeed, many of the beneficial antiaging effects of healthy lifestyle practices such as fasting and exercise are coordinated by increasing NAD+ levels, which in turn activates SIRT1 to change the expression of beneficial genes. In skin, the SIRTs are linked to the preservation of collagen in the dermis and their activation is important in wound healing and regeneration of skin by promoting keratinocyte proliferation.[44] SIRT6 promotes genes associated with collagen production,[45] and both SIRT1 and SIRT6 mediate the inhibition of MMP-1 gene transcription, which degrades collagen.[46] Both SIRT1 and SIRT6 are found to be downregulated in older skin, and this correlates with a reduction in available NAD+.[47,48]

Aged skin also demonstrates mitochondrial dysfunction,[49] an aging hallmark that is directly linked to oxidative stress, increased MMP-1 expression, dermal atrophy, and epidermal hyperplasia.[50] Adequate cellular NAD+ is critical for normal mitochondrial function both directly through its role in oxidative phosphorylation and indirectly through activation of SIRT1 and SIRT3, which are involved in the biogenesis and degradation of damaged mitochondria.[51,52] Increasing cellular NAD+ has been found to improve mitochondrial function, activate mitophagy (the recycling of dysfunctional mitochondria), and improve keratinocyte regenerative capacity.[53,54]

An age-dependent dermal accumulation of oxidatively modified and damaged proteins has also been found to cause skin dysfunction.[55] ECM proteins such as collagen

become glycated to form Advanced Glycation End products (AGES) leading to dermal stiffness and decreased flexibility.[56] Autophagy mediates the recycling of AGES and other defective proteins and an age-related reduction in autophagic activity in dermal fibroblasts is found to reduce collagen, hyaluronan, and elastin, collectively leading to deterioration of dermal integrity and skin fragility.[57–59] Increasing data indicates that the maintenance of high NAD+ is critical to SIRT1-mediated activation of autophagy pathways and the clearance of damaged cellular proteins.[60,61]

CAUSES OF NAD+ DECLINE

The above discussion demonstrates clear evidence for the role of NAD+ decline in the development of the hallmarks of aging in the skin, and there has been great interest in understanding the root causes of NAD+ decline to determine strategies to successfully restore cellular NAD+ levels.

It is known that NAD+ metabolism comprises multiple precursors, production routes, recycling pathways, and a myriad of consuming enzymes. Evidence now suggests that a major cause of NAD+ decline is a disruption of this finely controlled network. Specifically, it has been found that NAD+ consumption starts to outpace NAD+ production and recycling with age[62] (Fig. 2).

Fig. 2.

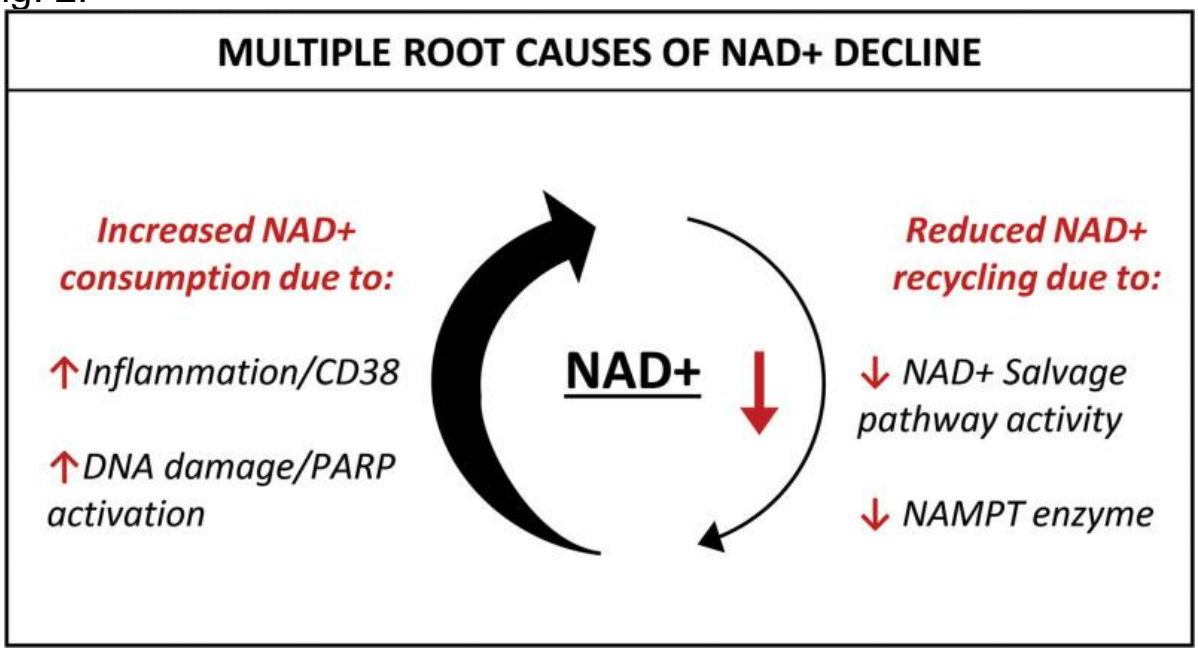

There are multiple root causes of NAD+ decline. Older cells exhibit excessive NAD+ consumption due to chronic inflammation and DNA damage which increases the activity of the NAD+ consumers CD38 and the PARPs. At the same time, reduced expression of the NAMPT enzyme means the salvage pathway is less efficient at recycling NAD+, resulting in cells that struggle to meet the demand for NAD+.

In its role as a coenzyme, NAD+ acts as a substrate that is irreversibly degraded by NAD+-consuming enzymes, including the SIRTs, PARPs, and CD38. The expression and activity of these NAD+-consuming enzymes have been found to increase with age meaning that the demand for NAD+ also increases. For example, age-associated increases in DNA damage activates NAD+-dependent PARP1,[63,64] and although PARP1 is a critical DNA repair enzyme, its persistent activation is harmful due to this contribution to NAD+ depletion. Indeed, overactivation of PARPs with resulting severe depletion of NAD+ has been highlighted recently by severe acute respiratory syndrome coronavirus 2 (SARS-CoV2), which is found to severely deplete cellular NAD+ due to overactivation of PARPs.[65]

The NAD+ glycohydrolase CD38 has also been recognized to consume large quantities of NAD+.[66] CD38 is found throughout the body and plays an important role in multiple aspects of the inflammatory response.[67] It is now clear that CD38 becomes overexpressed during aging due to chronic activation from persistent low-level "inflammaging," which in turn results in NAD+ depletion.[68,69]

This overactivation of NAD+-consuming pathways with age and disease can severely compromise NAD+ availability in cells, subsequently limiting utilization of NAD+ by other critical NAD+-dependent enzymes that promote good health, such as the SIRTs. Despite this increased demand for NAD+ throughout life, NAD+ levels should, in theory, be self-sustaining as cells have the ability to rapidly recycle the breakdown products of NAD+ consumption to replenish NAD+. This occurs via the salvage pathway, which plays a major role in restoring NAD+. Nicotinamide phosphoribosyltransferase (NAMPT) is the rate-limiting enzyme in this recycling process,[70] and it is now known that NAMPT levels decline with age in parallel with the decline of NAD+ in aged tissues.[5,71–77] This reduction in NAD+ biosynthesis via the salvage pathway is a significant factor in older cells because, as NAD+ consumption increases concurrently with age and demands for NAD+ replenishment and recycling increase, the resulting degraded NAD+ is no longer efficiently recycled, exacerbating a situation of declining NAD+ levels.[5]

METHODS TO RESTORE NAD+

The evidence demonstrates that the biology behind NAD+ decline is complex. NAD+ restoration using pure exogenous NAD+ is often not practical due to its unstable nature and poor bioavailability to most cell types, so efforts have focused on oral supplementation with the NAD+ precursor compounds nicotinamide (NAM), nicotinamide riboside (NR), and nicotinamide mononucleotide (NMN). These precursors are utilized by NAD+ biosynthesis pathways and converted to NAD+ within the cell. However, it is now clear that this popular approach ignores the root causes of NAD+ decline meaning supplementation with precursors alone such as NR or NMN do not offer a long-term efficacious solution for NAD+ restoration. Instead, strategies that simultaneously address the multiple root causes of NAD+ decline such as the combined administration of a NAD+ precursor, a CD38 inhibitor, and an NAMPT activator, hold potential for NAD+ restoration with greater measurable benefits (Fig. 3). Furthermore,

there is already a wealth of evidence to support these targets as interventions to successfully restore cellular NAD+ levels and multiple safe and well-tolerated active ingredients against these targets already exist.[62] This presents the opportunity for the development of oral, topical, and injectable formulations, allowing for both whole-body NAD+-restoring benefits alongside more targeted administration, resulting in the ultimate inside-outside approach to aging (Table 2).

Fig. 3.

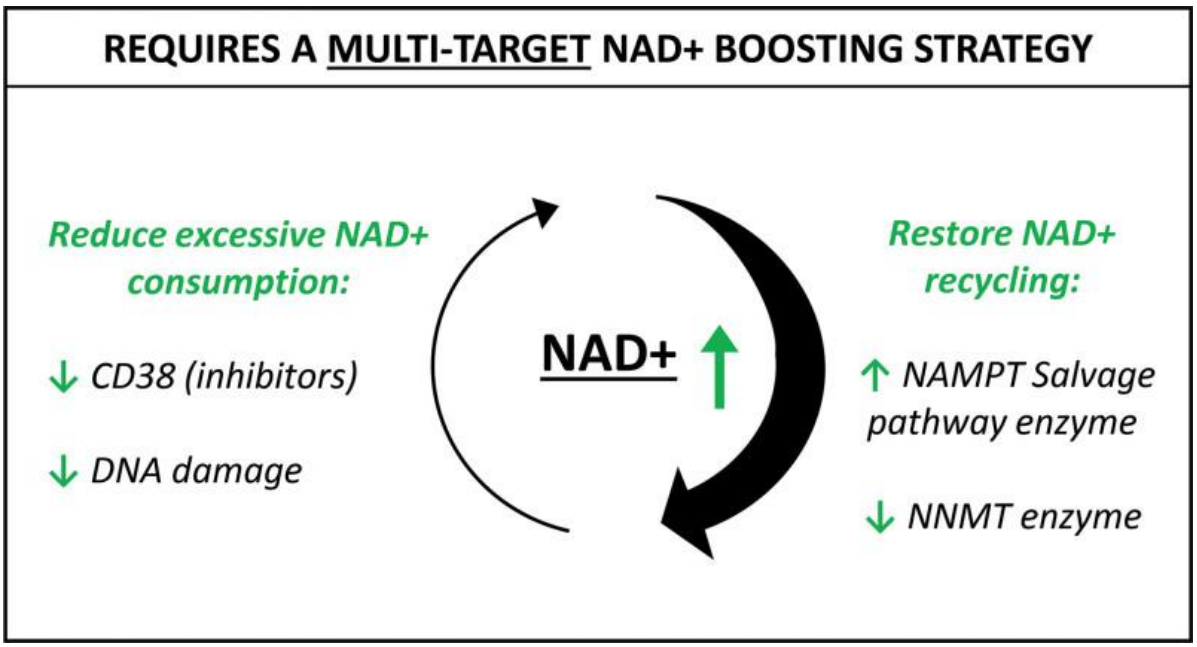

Successful NAD+ restoration requires a multitargeted strategy that simultaneously addresses the root causes of NAD+ decline. Therapies must reduce the excessive consumption of NAD+ with approaches such as CD38 inhibition and reduction of DNA damage, while improving the efficiency of NAD+ recycling by promoting upregulation of the rate-limiting salvage pathway enzyme NAMPT and inhibition of NNMT, an enzyme that promotes the removal of NAD+ breakdown products from the cell rather than recycling.

Table 2.

Potential Clinical Applications, Routes of Administration and Benefits of NAD+-Restoration Therapies

	Method of Administration	Potential Benefits
Systemic applications for NAD+-restoration	Oral supplementation	Whole-body improvements in cellular health contributing to improved healthspan Improved energy, cognitive function, and sense of well-being Improved sleep quality

	Method of Administration	Potential Benefits
Localized applications for NAD+-restoration	Intravenous	Pre-procedure administration to prime cells for optimal response to aesthetic treatments
		Improve healing/regenerative capacity pre/postsurgery
	Topical	Concentrated treatment for problematic areas
		Concentrated application to improve healing/regeneration postsurgery
	Injectable	Use in combination with aesthetic procedures such as microneedling

Open in a new tab

THE FUTURE OF NAD+ IN CLINICAL PRACTICE

Until recently, antiaging therapies were limited to repairing the consequences of aging, but now there is clear evidence that aging can be targeted from its root cellular cause giving the opportunity to slow and even reverse aspects of aging.[78]

NAD+ restoration has been identified as a key therapeutic target that can positively impact many of the hallmarks of cellular aging. Not only does it play a key role in skin aging but also demonstrates a great potential to improve multiple aspects of age-related decline across the whole body. This offers an unprecedented opportunity for practitioners to introduce NAD+-restoring therapies that not only impact the appearance of their patients but also their health and well-being (Table 2).

Given the rapidly aging population, addressing aging at the cellular level is now critically important. Many surgical procedures rely on the healing and regenerative capacity of the skin which is known to decline with age, leading to disappointing results or negative postsurgery outcomes. Improving health and resilience at the cellular level with NAD+ restoration could be harnessed as a way to ensure consistent results and recovery irrespective of patient age. It should also be noted that the efficacy of many nonsurgical aesthetic procedures such as microneedling and laser technologies ultimately rely on the activation of cellular stress pathways to trigger the clearance of damaged cells and stimulate the production of new collagen. Many of these pathways require adequate NAD+ levels for optimal function, meaning NAD+ restoration before treatment could be a strategy to ensure the underlying cells are in an optimal condition to respond to the treatment.

With this greater understanding of the benefits of NAD+ and how to design targeted strategies to maintain its availability, collaboration with clinical practitioners, who have

firsthand experience of the clinical manifestations of aging and access to patient groups for clinical trials, is now crucial to translate this exciting science into the clinic.

Near infrared low-level laser therapy and cell proliferation: The emerging role of redox sensitive signal transduction pathways

Mario Migliario [1], Maurizio Sabbatini [2], Carmen Mortellaro [1], Filippo Renò [3]

Abstract

Lasers devices are widely used in various medical fields (eg, surgery, dermatology, dentistry, rehabilitative medicine, etc.) for different applications, ranging from surgical ablation of tissues to biostimulation and pain relief. Laser is an electromagnetic radiation, which effects on biological tissues strongly depends on a number of physical parameters. Laser wavelength, energy output, irradiation time and modality, temperature and tissue penetration properties have to be set up according to the clinical target tissue and the desired effect. A less than optimal operational settings, in fact, could result in a null or even lethal effect. According to the first law of photobiology, light absorption requires the presence of a specific photoacceptor that after excitation could induce the activation of downstream signaling pathways. Low-level lasers operating in the red/near infrared portion of the light spectra are generally used for biostimulation purposes, a particular therapeutic application based on the radiant energy ability to induce nonthermal responses in living cells. Biostimulation process generally promotes cell survival and proliferation. Emerging evidences support a low-level laser stimulation mediated increase in "good" reactive oxygen species, able to activate redox sensitive signal transduction pathways such as Nrf-2, NF-kB, ERK which act as key redox checkpoints.

Keywords: ROS; biostimulation; cell proliferation; low-level laser therapy.

Similar articles

- Near-infrared laser increases MDPC-23 odontoblast-like cells proliferation by activating redox sensitive pathways.

  Rizzi M, Migliario M, Rocchetti V, Tonello S, Renò F.J Photochem Photobiol B. 2016 Nov;164:283-288. doi: 10.1016/j.jphotobiol.2016.08.049. Epub 2016 Sep 30.PMID: 27718420

- Pre-odontoblast proliferation induced by near-infrared laser stimulation.

  Rizzi M, Migliario M, Rocchetti V, Tonello S, Renò F.Eur Rev Med Pharmacol Sci. 2016 Mar;20(5):794-800.PMID: 27010131

- Effect of low-intensity (3.75-25 J/cm2) near-infrared (810 nm) laser radiation on red blood cell ATPase activities and membrane structure.

  Kujawa J, Zavodnik L, Zavodnik I, Buko V, Lapshyna A, Bryszewska M.J Clin Laser Med Surg. 2004 Apr;22(2):111-7. doi: 10.1089/104454704774076163.PMID: 15165385

- Molecular mechanisms of cell proliferation induced by low power laser irradiation.

  Gao X, Xing D.J Biomed Sci. 2009 Jan 12;16(1):4. doi: 10.1186/1423-0127-16-4.PMID: 19272168 **Free PMC article.** Review.

- Biological Responses of Stem Cells to Photobiomodulation Therapy.
  Khorsandi K, Hosseinzadeh R, Abrahamse H, Fekrazad R.Curr Stem Cell Res Ther. 2020;15(5):400-413. doi: 10.2174/1574888X15666200204123722.PMID: 32013851 Review.

Cited by

- Effect of photobiomodulation and corticopuncture methods on tooth displacement and gene expression: animal study.

  Vanderlei BMC, Torres MC, Paredes N, Garcez AS, Pavini PTM, Suzuki SS, Moon W.Lasers Med Sci. 2024 Nov 16;39(1):283. doi: 10.1007/s10103-024-04136-6.PMID: 39547960

- Efficacy of Photobiomodulation in the Management of Pain and Inflammation after Dental Implants: A Randomized Clinical Trial.

  Collado-Murcia Y, Parra-Perez F, López-Jornet P.J Clin Med. 2024 Sep 25;13(19):5709. doi: 10.3390/jcm13195709.PMID: 39407769 **Free PMC article.**

- A randomized sham-controlled trial of transcranial and intranasal photobiomodulation in Japanese patients with mild cognitive impairment and mild dementia due to Alzheimer's disease: a protocol.

  Yokoi Y, Inagawa T, Yamada Y, Matsui M, Tomizawa A, Noda T.Front Neurol. 2024 Jul 5;15:1371284. doi: 10.3389/fneur.2024.1371284. eCollection 2024.PMID: 39036627 **Free PMC article.**

- Immunoactivation by Cutaneous Blue Light Irradiation Inhibits Remote Tumor Growth and Metastasis.

  Yang Y, Yang R, Deng F, Yang L, Yang G, Liu Y, Tian Q, Wang Z, Li A, Shang L, Cheng G, Zhang L.ACS Pharmacol Transl Sci. 2024 Mar 16;7(4):1055-1068. doi: 10.1021/acsptsci.3c00355. eCollection 2024 Apr 12.PMID: 38633599

- Photo biomodulation of dental derived stem cells to ameliorate regenerative capacity: In vitro study.
  Medhat A, El-Zainy MA, Fathy I.Saudi Dent J. 2024 Feb;36(2):347-352. doi: 10.1016/j.sdentj.2023.11.018. Epub 2023 Nov 17.PMID: 38419992 **Free PMC article.**

Reprogramming: Emerging Strategies to Rejuvenate Aging Cells and Tissues

Quentin Alle [1,†], Enora Le Borgne [1,†], Ollivier Milhavet [2,*], Jean-Marc Lemaitre [1,*]

Abstract

Aging is associated with a progressive and functional decline of all tissues and a striking increase in many “age-related diseases”. Although aging has long been considered an inevitable process, strategies to delay and potentially even reverse the aging process have recently been developed. Here, we review emerging rejuvenation strategies that are based on reprogramming toward pluripotency. Some of these approaches may eventually lead to medical applications to improve healthspan and longevity.
Keywords: aging, senescence, epigenetics, stem cells, reprogramming, iPSC

1. Introduction

As we age, we become increasingly vulnerable to age-related diseases. The progressive aging of the population makes this issue one of, if not the, major current scientific concern in the field of medicine. Aging is an intricate process that increases the likelihood of cancer, cardiovascular disorders, diabetes, atherosclerosis, neurodegeneration and age-related macular degeneration. The regenerative capacity of cells and tissues diminishes over time and they thus become vulnerable to age-related malfunctions that can precipitate death. Developing prophylactic strategies to increase the duration of healthy life and promote healthy aging is challenging, as the mechanisms causing aging are poorly understood, even if great progress has been made from studying naturally occurring or accelerated-aging phenomena. We now know that aging inculcates many changes, or ‘hallmarks’: genomic instability, telomere shortening, epigenetic alterations, loss of proteostasis, cellular senescence, mitochondrial dysfunction, deregulated nutrient sensing, altered intercellular communication, and stem cell compromise and exhaustion [1].

These various hallmarks of aging are all active fields of molecular mechanistic study with much promise but relatively few tangible results have been translated into therapy.

Perhaps the most effective strategies so far have been those that focus on the removal of senescent cells with ‘senolytic’ drugs [2,3]. In some ways, however, we feel this is too focused on the symptoms of aging whereas perhaps the most promising strategy for the future would be to focus on the causes of aging and its corollary, the rejuvenative capacity of stem cells.

Simply expressing four transcription factors, OCT4, SOX2, KLF4 and c-MYC (OSKM), converts somatic cells into induced pluripotent stem cells (iPSCs) [4]. Reprogramming occurs through a global remodeling of the epigenetic landscape that ultimately reverts

the cell to a pluripotent embryonic-like state, with properties similar to embryonic stem cells (ESCs). This cellular reprogramming allows us to imagine cell therapies that restore organ and tissue function. Indeed, by reprogramming a somatic cell, from a donor into iPSCs, these cells can then be modified or corrected before redifferentiation, to produce ‘rejuvenated’ cells, tissues or organs, for replacement in the same donor or an immune-compatible person. In recent years, emerging results have led to new ideas demonstrating that the mechanics of cellular reprogramming can be used to reduce the deleterious effects of aging and to delay these effects by increasing regenerative capacity, either at the cellular or the whole-organism level.

In this review, then, we focus on emerging strategies that aim to rejuvenate cells or tissues based on stem cells, with an emphasis on cell reprogramming approaches that promise new routes for everyone to enjoy prolonged healthspan and lifespan.

2. Understanding the Aging Process

Aging brings increasing frailty. There are two major phases during aging. The first phase is healthy aging, where minor alterations accumulate. Then there is a second phase, so-called pathological aging, in which chronic clinical diseases and disabilities predominate and impair physiological functions [5].

The problems facing our aging population can be studied with a new demographic metric, the Healthy Life Years (HLY) or ‘disability-free life expectancy’ [6], which is defined by the European Statistical Office as the average number of years one can expect to live in the absence of these disorders, within the life expectancy and for a given age.

2.1. Age-Associated Pathologies

Deterioration of body functions with age is the main risk factor for major human pathologies and therefore the main factor limiting HLY. Moreover, since advanced age is the common causal influence, these chronic disorders often occur concurrently, as comorbidities, in the elderly [1,5]. Among these major pathologies are cancer, most commonly lung, breast, prostate, and colorectal cancers, and cardiovascular disorders including chronic ischemic heart disease, congestive heart failure, and arrhythmia. The latter two heart diseases are now the two leading causes of death [7,8]. Age-related diseases affecting the skeletal system are also common, particularly osteoarthritis and osteoporosis. Another disease that increases greatly with age is the muscular degeneration known as sarcopenia. Metabolic disorders such as diabetes and non-alcoholic hepatic steatosis also become more common with age [9]. Organ and tissue fibrosis, a pathological process characterized by inflammatory injury and excessive fibrous connective tissue production [10], also increases during aging and acts as one of the primary causes for age-related deterioration of human organs, including the lungs [11], kidneys [12], liver [13] and heart [14]. Lymphoid organs, such as the spleen, also undergo a structural loss of integrity in the elderly. Global deterioration of the immune

system increases susceptibility to infectious diseases and reduces the response to vaccination [15]. This has been widely illustrated lately by age-related mortality from COVID-19. Finally, there are neurodegenerative diseases, such as Alzheimer's disease, Parkinson's, and Huntington's disease and sensorial failures such as auditory and macular degeneration that all increase significantly in the aged [16,17,18].

The progressive functional and physiological decline of any living organism, leading inevitably to death, is the progressive accumulation of molecular and cellular damage occurring throughout its life.

Thus, aging is not a disease in itself but rather a biological process whose multiple causes and consequences add up and overlap.

2.2. Cellular Damage at the Heart of Aging

For decades, a large number of studies aimed at understanding the adverse effects of aging were carried out on a wide range of model organisms. In 2013, López-Otín et al. compiled much of this knowledge and referenced nine general hallmarks of aging in living organisms [1]. These hallmarks of aging affect the organism at different scales. Some occur at the molecular level within cells, while others impact tissues and even beyond, at the level of an organ or the entire organism. These elements were classified according to three important criteria. First, each hallmark must occur naturally during physiological aging. In addition, the experimental deterioration of each mark must accelerate aging, while, conversely, the experimental improvement of each mark must slow aging. Moreover, as aging occurs, all these hallmarks are gradually implemented and interact with each other and an integrative model of these events was proposed [1] that supports a multifactorial origin of age-related pathologies (Figure 1).

Figure 1.

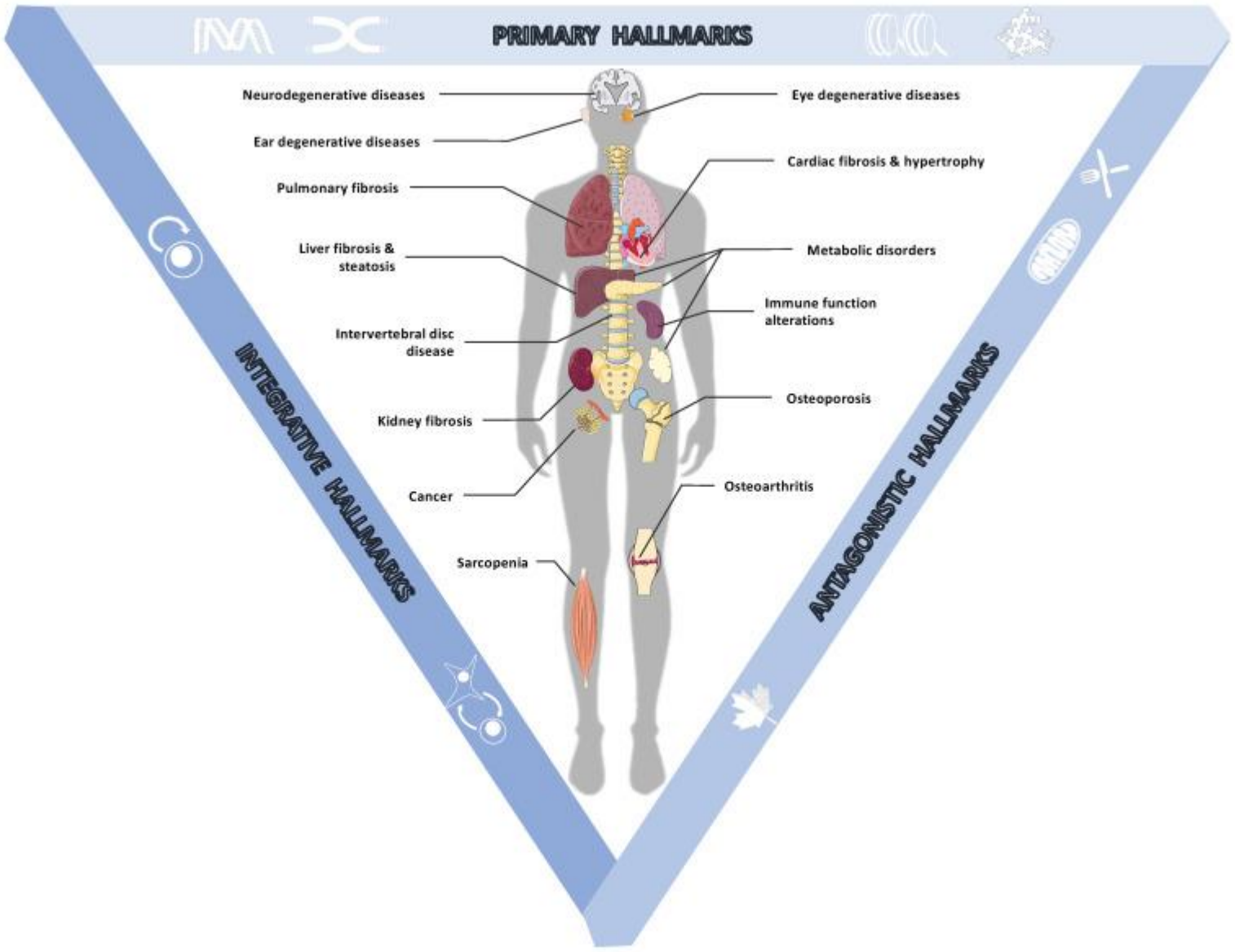

Hallmarks of aging at the origin of age-related diseases. Aging is characterized by a progressive loss of biological functions linked to the appearance and accumulation of molecular and cellular damage over entire lives. This damage has been classified into three categories by López-Otín [1]. (i) Primary hallmarks corresponding to molecular disorders occurring in cells: genomic instability, telomere attrition, epigenetic alterations, and loss of proteostasis. (ii) Antagonistic hallmarks, corresponding to alterations of damage response mechanisms: deregulated nutrient sensing, mitochondrial dysfunction, and cellular senescence. Finally, (iii) integrative hallmarks corresponding to tissue homeostasis failures: stem cell exhaustion and altered intercellular communication. Altogether, these interconnected hallmarks of aging act as cause and catalyst engendering a large set of age-related pathologies affecting the whole body.

2.2.1. The Primary Hallmarks of Aging Are the Triggering Events Whose Harmful Consequences Progressively Accumulate over Time

The hallmarks are structural changes to biological molecules that alter their functions. These changes increase molecular disorder, or decrease molecular fidelity, within cells. Molecular disorder can be blocked, or at least slowed, by repair and replacement processes. However, these mechanisms are also achieved by biomolecules, which are themselves subject to this increasing disorder [19]. The paradigms of aging-linked disorders are in the macromolecules, DNA, and protein, including genomic instability [20,21,22,23], telomere shortening [24,25,26], epigenetic alterations in DNA [27,28,29], and loss of proteostasis [30,31,32,33,34,35].

2.2.2. The Antagonistic Hallmarks Are Damage Response Mechanisms That Become Overwhelmed

In principle, antagonistic hallmarks of aging are activated to counter the primary hallmarks, but they progressively become negative in a process that is partly favored or accelerated by the primary damage.

Cells suffer many impairments, affecting all their molecules and compartments. Fortunately, they usually have the necessary weapons to deal with these problems. However, as we age, molecular chaos overwhelms our cells' declining capacity for control and repair. To temporarily stabilize and then eliminate overly damaged cells, we have cellular processes such as senescence. However, senescent cells accumulate within tissues during aging, in particular due to a decrease in their elimination by the immune system, and this accumulation incurs many age-related diseases [36]. Moreover, not only cells but also cell organelles can be damaged. Damaged mitochondria accumulate during aging, upregulating reactive oxygen species and decreasing energy levels and cellular respiratory capacity [37,38,39].

During aging, there is a general deregulation of the nutrient-sensing pathways that detect the intracellular and extracellular levels of nutrients and metabolites as well as the different hormones that regulate them, and several metabolic alterations thus accumulate over time, reducing functionality in metabolic disorders.

In addition, certain environmental factors act as catalysts of these deregulations such as hypercaloric nutrition and a sedentary lifestyle [40].

2.2.3. The Integrative Hallmarks Are Tissue Homeostasis Failures

Integrative hallmarks occur when the accumulated damage caused by the primary and antagonistic hallmarks cannot be compensated for by homeostatic mechanisms within

the aging tissues. Indeed, as we age, we witness the gradual accumulation of molecular damage that is no longer tolerated by cellular control mechanisms and thus the number of altered, dysfunctional senescent cells within tissues increases.

Reduced regenerative capacity and/or depletion of stem cells, resulting from accumulated cell damage, are among the major causes of the body aging process [41,42].

These important changes interfere with interactions and communication between cells, tissues, and organs, and result in the loss of tissue integrity. Senescent cells have a specific senescence-associated secretory phenotype (SASP) repertoire composed of pro-inflammatory cytokines (IL-1α, IL-6, IL-8), chemokines (CCL2, CXCL1), growth factors (VEGF), and metalloproteinases (MMP-1, MMP-3). SASP is a major source of circulating inflammatory factors [43,44]. The immune system itself also progressively declines in function over life. This decline, called immuno-senescence, reduces both humoral and cellular immune responses [45,46]. Immuno-senescence also favors a pro-inflammatory environment affecting endocrine, neurocrine, and neuronal intercellular communication.

Although the classification proposed by López-Otín is widely accepted, a few new hallmarks of aging have been identified since 2013, including stiffening of the extracellular matrix [47], tRNA-derived fragments [48], circRNA accumulation [49], and even microbiota dysbiosis [50].

3. The Promise of Pluripotent Stem Cells

Among the approaches to age-related pathological phenotypes, most are aimed at preventing or mitigating cell damage [1]. This involves activating cellular stress resistance mechanisms, either with antioxidant molecules or by suppressing senescent cells to reduce their impact on tissues.

An exception is heterochronic parabiosis, which aims at restoring the regenerative ability of older tissues through exposure to circulating juvenile factors [51,52,53,54,55,56,57].

This objective of restoring functions of a tissue or an organ, when the regenerative ability of older tissues is reduced, is a foundation of regenerative medicine.

Thus, new strategies are currently being developed around stem cells and the use of their regenerative potential to prevent the detrimental effects of aging. In particular, human pluripotent stem cells (hPSCs) including ESCs and, more recently, iPSCs, are an indefatigable source of cells for clinical use [58]. ESCs and iPSCs are pluripotent

and therefore have the ability to differentiate into any cell type of the body (with the exception of embryonic appendices). This characteristic, in addition to self-renewal, gives hPSCs a central role in a growing number of new cell therapies aimed at restoring functions of many tissues during aging.

3.1. Human Embryonic Stem Cells

ESCs were first obtained in mice [59,60] and in rhesus monkeys [61]. The work in primates paved the way for the first successful human embryonic stem cells (hESCs) to be derived a few years later [62]. Characterization of hESCs revealed specific surface markers expressed by these cells, and their ability to differentiate into the three embryonic layers: endoderm, ectoderm, and mesoderm. Following this breakthrough, a large number of studies demonstrated the possibility of differentiating ESCs into different specialized cell types, including mature neurons, cardiomyocytes, or insulin-producing cells [63], thus paving the way for future therapeutic applications.

3.2. Cell Reprogramming

Other methods aim to revert to the pluripotent state using somatic cells as starting material. Cellular reprogramming has revolutionized the understanding of many fields of biology and medicine, notably following the discovery of iPSCs in 2006. Two of the main contributors to cell reprogramming were awarded the Nobel Prize in Medicine in 2012, namely, Sir John Gurdon and Shinya Yamanaka [64].

Following the discoveries made in the field of somatic cell reprogramming by nuclear transfer [65,66], which led to therapeutic cloning, trans-differentiation, and cell fusion [67], it has been hypothesized that somatic cells can be directly reprogrammed into pluripotent cells through the action of appropriate transcription factors [68,69,70].

In 2006, Shinya Yamanaka's team validated this hypothesis with mouse and human cells [4,71]. They determined the minimum cocktail of factors necessary to generate cell colonies similar to those observed in ESC cultures. A final combination of four protein factors, since named Yamanaka factors or OSKM, reprograms somatic cells into induced pluripotent stem cells (iPSCs). OSKM is OCT4 and SOX2, which are stabilizers of pluripotency in ESCs and the early embryo [72,73,74], and KLF4 and C-MYC, which are important in the self-renewal and proliferation of ESCs in culture [75,76]. This discovery revolutionized stem cell research for two main reasons. The first is that this method is completely free of the ethical problems associated with the manipulation of human embryos for research purposes. The second, resulting directly from the first, is that it opens the door to autologous transplant strategies into a much larger space than was possible through classical somatic cell reprogramming by nuclear transfer. With iPSCs, autologous transplants of "reconstructed or repaired" cells, tissues, or organs can be derived from the patient's own cells, which avoids any risk of rejection down the line. Induced reprogramming represents the third and most recent source of hPSCs

developed for therapeutic applications, after therapeutic cloning and deriving ESCs from embryos.

3.3. Human Pluripotent Cells as an Experimental Modelling Tool

Reprogramming has revealed that cellular fate is highly plastic. Another parameter of prime importance for medical research is that, after having ascended the slope from one cell type to a pluripotent state, the cell can be brought back down along various different pathways from the original one. Thus, hPSCs create the possibility of in vitro differentiation into various cell types. In vitro differentiation can be used experimentally, to model different diseases, and therapeutically, to manipulate diseased states. In the following sections, we will discuss concrete examples, in the context of aging, of in vitro modelling of differentiation and pathologies, and the challenges of developing them into therapeutic solutions.

3.3.1. Organoids and Complex Tissues

Pluripotent stem cells (PSCs) spontaneously differentiate when culture conditions no longer stabilize their pluripotency. Equally, PSCs can be guided towards desired cell identities if specific stimuli are added, such as those present during embryonic differentiation. Examples of iPSC differentiation are now numerous and varied. The differentiation of iPSCs into renal podocytes [77,78], hematopoietic progenitors [77], neurons [79], endothelial cells [80], cardiomyocytes [81], retinal progenitors [82], pancreatic β islet cells [83], or ciliated epithelial cells [84], implies no limits to human tissue modeling in vitro. The recent development of organoids also illustrates the progress of knowledge in the manipulation of cell fate. Three-dimensional suspension cultures of pluripotent cells allow them to organize and differentiate into spheroid structures, in which several cell types cohabit. The cells thus form “mini-organs” in which cellular interactions mimic those that exist within tissues in vivo. Organoids have become very popular in recent years [85,86,87] and many teams model tissues and characterize the cell populations in these structures with increasing precision, particularly through high-throughput single-cell transcriptomics [88]. The most advanced organoids currently model the brain [89,90,91], intestine [92,93], kidney [94], heart [91,95,96,97], or retina [98].

More recently, the emergence of cell-printing technologies, using PSCs or differentiated cells as “inks”, has also led to advances in the formation of heterogeneous tissues and has even allowed the development of supports for ear cartilage regeneration [99,100,101].

Despite the rapid advances in this field, the level of complexity attained in cellular and organoid models still falls short of the real complexity of living organisms, in which large systems interact with each other and constantly adapt to changes brought about by the environment. These modeling strategies are thus complementary approaches to animal experimentation.

3.3.2. Modelling Age-Related Pathologies In Vitro

Technologies reprogramming human somatic cells into iPSCs [71,102], have also paved the way for the generation of patient-derived iPSCs, allowing the various pathological phenotypes to be recreated in vitro, e.g., for genetic disorders, including Duchenne muscular dystrophy, Becker muscular dystrophy, Parkinson's disease, Hungtington's disease, trisomy 21, and polymorphic catecholaminergic ventricular tachycardia [103,104,105].

Accelerated aging pathologies can also be modeled through reprogramming. Our group has modeled several of these syndromes. Indeed, we have demonstrated that cells from Werner syndrome patients can be reprogrammed while maintaining their shortened telomeres phenotype [106]. We also reprogrammed cells from a patient with Bloom syndrome, while maintaining the characteristic sister chromatid exchange phenotype [107]. Other teams have obtained similar results on several premature aging syndromes [108,109,110,111,112,113].

3.3.3. New Models for the Screening of Therapeutic Molecules

In addition to providing new knowledge about the molecular characteristics of pathologies and their development, pathology models derived from hPSCs can also provide key lead molecules in high-throughput screens [114,115]. Furthermore, these screens can test potential therapeutic agents on organoids in specific pathological contexts to assess toxicity and optimize treatment.

For example, evaluating therapeutic candidates for cardiotoxicity is a major phase in drug development, and thus a particularly important application in hPSC-based models [116,117,118,119,120].

Thus, hiPSCs can be broadly used as a modelling tool. Moreover, an important parameter, brought by the use of patient-derived iPSCs, is the personalized nature of this approach, allowing hypotheses to be tested in the patient's genetic background [121,122,123]. Furthermore, the intersection of stem cell research and genome editing research, and in particular, the recent advances in the use of CRISPR-Cas technology, promises to open up new possibilities in the correction of genetic mutations associated with pathological phenotypes [124,125,126,127]. These developments pave the way for future therapies based on cell or tissue replacement by their genetically corrected ex vivo equivalent derived from iPSCs.

4. New Strategies in Regenerative Medicine to Rejuvenate Cells and Tissues

Taking advantage of cell reprogramming, several strategies can be envisioned to rejuvenate cells and tissues. Two major types of treatment are of note. A classical therapeutic approach is the direct consequence of clinical applications based on the production of differentiated cells from iPSCs to regenerate or replace cells inside a damaged tissue or even replace the entire injured organ (Figure 2). Another more innovative and disruptive process is to act directly on the cells, inside the damaged tissue, to rejuvenate them, without modifying their identity. In the same vein, we can also imagine intervening prophylactically before the appearance of the damage induced by aging.

Figure 2.

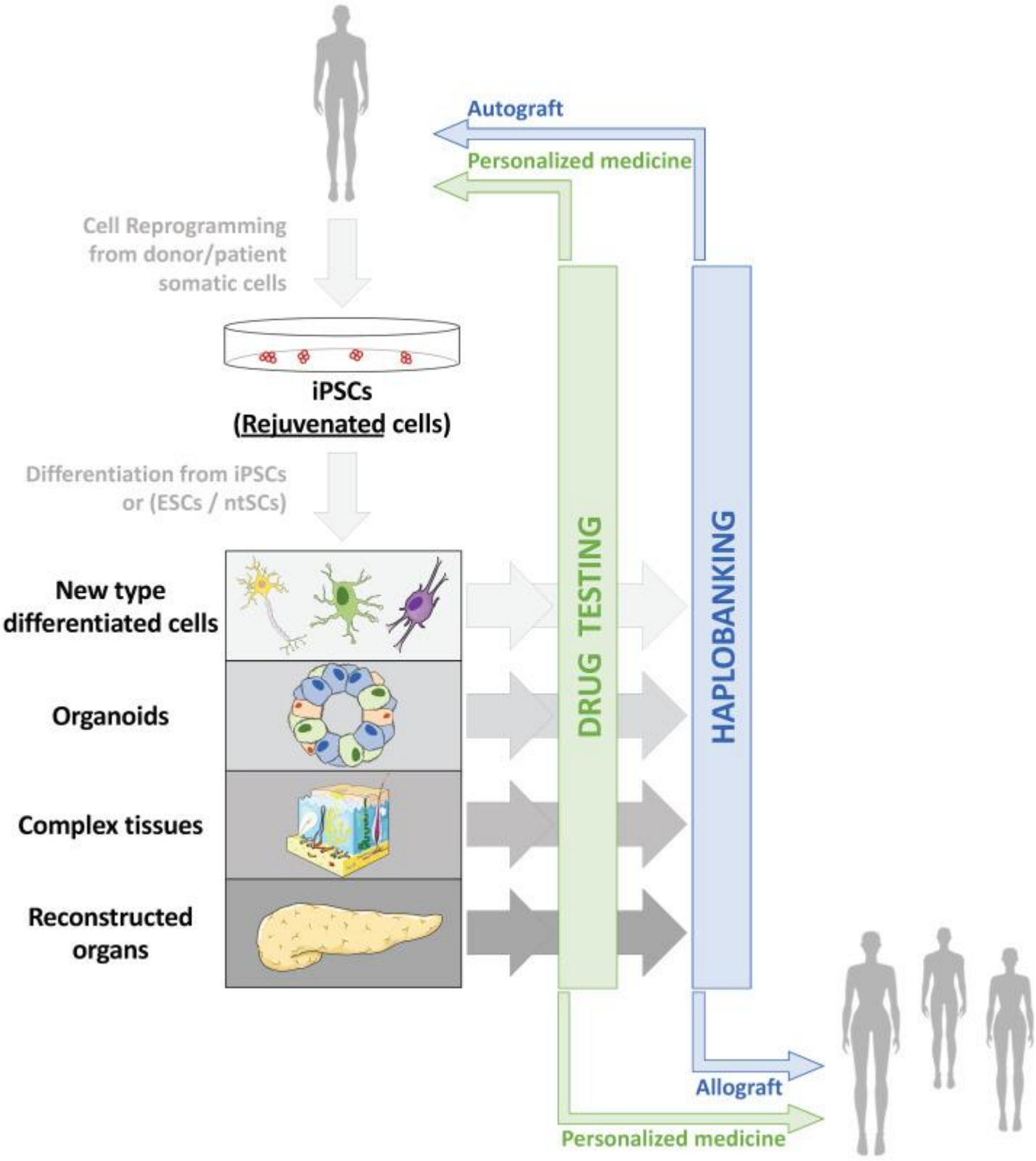

Applications of cell reprogramming and hPSCs to restore altered or aged tissues. Due to increased life expectancy and global population aging, two major health issues are

arising: increased prevalence of age-associated pathologies whose mechanisms remain only partially explored and understood, and increased age-associated tissue deterioration and loss of function. Therefore, human pluripotent stem cells (hPSCs), including embryonic stem cells (ESCs), nuclear transfer stem cells (ntSCs) and induced pluripotent stem cells (iPSCs) emerged as tools to model both age-associated pathologies and tissue deterioration: from 2D cell culture to 3D complex reconstructed tissues, through organoids, and cells or tissue replacement strategies. Thanks to cell reprogramming [4,71], iPSCs made it possible to envisage autografts, especially in aged patients, as reprogramming erases aging marks in iPSCs and allows production of “rejuvenated” cells after differentiation [128].

4.1. Clinical Applications of Human Pluripotent Stem Cells

All developments in the ex vivo reproduction of tissue for analytical purposes also benefit clinical applications that aimed at “repairing” humans. In contexts such as the shortage of organs to meet the demand for transplants, the inexistence of therapeutic solutions in certain cases of traumatic injuries or the problem of immune rejection of transplants after transplantation, therapies based on hPSCs and particularly iPSCs are extremely innovative and promising.

4.1.1. Production of hPSCs for Clinical Use

The therapeutic use of hPSCs requires safety standards, and it is therefore highly pertinent to develop reprogramming factors that minimize the risk of alterations. For example, Okita et al. demonstrated that the transgene encoding C-MYC could be reactivated and cause tumors in chimeric mice derived from retroviral-vector-reprogrammed iPSCs [129]. Other studies have also revealed that genetic and epigenetic alterations occur during very long-term maintenance of cells in culture and that culture techniques also have an impact at this level [130,131]. Quality control of the genomic integrity of clones used for therapeutic applications should therefore be applied, even when reprogramming has been carried out using non-integrative factors [132]. There have also been refinements to the composition of hPSC culture media and matrices that ensure the absence of xenogenic elements for clinical use [132,133].

The reprogramming of patient cells, although relatively cumbersome and expensive, has tremendous advantages for autologous therapies. Cells can easily be collected by blood sampling and thus very low surgical risk is associated with very little inconvenience to the patient. Recently, culture techniques in microfluidic systems have shown an increase in the efficiency of reprogramming when mRNA-like factors are used rather than conventional culture techniques. Moreover, this approach allows a drastic reduction in the amount of components needed for reprogramming [134,135].

iPSCs can also be used for allogeneic transplants. One approach is to build haplobanks in which cells would be characterized and selected for their compatibility with the recipient, in particular for human leukocyte antigen (HLA) [136,137,138]. Another

interesting possibility is to decrease cell immunogenicity, as demonstrated in mice by Deuse et al. [139]. In their experiments, they found that murine and human iPSCs lost their immunogenicity from the dual effects of CD47 overexpression and CRISPR-Cas9 ablation of major class I and II histocompatibility complexes [139]. This proof of principle suggests it will be possible to design several clones of “universal” iPSCs characterized and modified to be compatible with the general population, which would greatly reduce the cost compared to patient-specific strategies. However, such a strategy should be used with caution as it increases the risk of cancer development due to a reduction of cell immunogenicity. Therefore, in order to ensure maximum security, control of the system using suicide genes could be added [140,141].

4.1.2. Cell and Tissue Replacement Therapies

Therapies based on the transplantation of cells and tissues, differentiated from hPSCs, aim to replace or repair age-related injured, damaged, or non-functional tissues [142]. We will discuss a few illustrative examples. Many cell and tissue replacement trials have focused on the nervous system and traumas, such as spinal cord injuries, that often occur in accidents. These frequently lead to reduced motor functions, even paralysis, or loss of sensory functions. Unfortunately, there are no real classical therapeutic solutions yet for these situations. Demonstrating the potential of hPSCs, it was showed, in 2005, that the transplantation of human neural stem cells of fetal origin into the spinal cord of a primate—a marmoset—can promote functional recovery after injury. In particular, it was shown that the transplanted cells differentiate into neurons, astrocytes, and oligodendrocytes [143]. The same group went on to demonstrate in mice and marmosets that human neural stem cells derived from iPSC differentiation could improve motor functions, form synaptic connections with host neurons and reduce demyelination from injury [144,145]. This cell replacement strategy was also applied for deafness using hESCs differentiated into otic progenitors and then into ciliated cells and auditory neurons. After transplantation, these cells significantly improved auditory response thresholds in a model of lesion-generated auditory neuropathy [146].

Degenerative pathologies can also benefit from this type of therapeutic approach. Neurodegenerative diseases such as Alzheimer’s and Parkinson’s are among the interesting targets for cell therapy given their frequency in the population [147,148,149]. In monkeys, autologous transplantation of dopaminergic neurons, derived from iPSCs, avoided immunosuppression and significantly re-innervated the putamen, improved motor function and enhanced survival by over two years [150]. Retinopathies, such as age-related macular degeneration or retinitis pigmentosa, have also been targeted in several clinical trials using differentiated cells derived from hESCs or iPSCs [151,152]. In 2017, Mandai et al. performed an autologous retinal cell transplant of retinal cells derived from iPSCs from a patient with neovascular (or wet) AMD [153]. Another development by Ben M’Barek et al. focusing on the treatment of retinitis pigmentosa associated with mutations in the LRAT, RPE65 and MERTK genes, used a sheet of retinal pigmentary epithelium grown on a human biological matrix of amniotic origin. This leaflet, derived from hESCs using a GMP process, has been tested in mice and primates and is currently in clinical trials [152].

4.1.3. Organ Production in In Vivo Models

All the therapeutic strategies we have addressed consist of developing therapeutic cells or tissues ex vivo, under defined conditions, and then reimplanting them in the patient. Another approach consists of developing complete human organs directly in animal hosts. By creating in vivo models closer to human beings, it should be possible to generate functional and directly transplantable organs and circumvent the lack of organs [154,155].

By injecting iPSCs from one species into a blastocyst stage embryo of a second species, it is possible to generate interspecific chimeric individuals composed of cells from both species. Interspecific organogenesis then takes a specific organ of one species grown in a second species host that has a defect in the development of the organ in question. This was first performed in 2010 by Kobayashi et al., who injected rat iPSCs into a mouse blastocyst for which the genesis of the pancreas was genetically disabled by deletion of the PDX1 gene. This 'blastocyst complementation' resulted in a mouse with a functional mouse-sized rat pancreas [156]. The reverse experiment was performed a few years later by Yamaguchi et al., using the same genetic deletion in rats, with mouse iPSCs. Again, the host organism, the rat, had a normal rat-size functional pancreas, derived from the donor mouse cells [157]. Usui et al. showed in 2012 that it was possible to extend this process to other organs by performing intraspecific blastocyst complementation with wild-type mouse iPSCs and a mouse blastocyst, deleted for the SALL1 gene, i.e., in which kidney genesis is inactivated. The chimera resulting from the complementation also showed functional kidneys from the donor cells [158]. All these studies make it possible to envisage blastocyst complementation from hPSCs in blastocysts from animals such as pigs or sheep, whose organ size, anatomy, and physiology are close to those of human organs. However, Wu et al. have found that the frequency of human cells in chimeric pig embryos is currently very marginal [159].

Many improvements and discoveries still need to be made to make this type of strategy fully operational. Recently, it was demonstrated that the contribution of donor cells to host tissues is greatly improved by the artificial creation of a permissive niche that could even allow the formation of complete organs [160]. However, the main limitation to achieve interspecific chimerism is indisputably the pluripotent state of hPSCs. Indeed, two distinct states of pluripotency have been characterized—the naïve state corresponding to mouse ESCs and the primed state corresponding to hPSCs or to mouse epiblast stem cells (epiESCs) originating from the early post-implantation epiblast [161,162]. These different naïve and primed states have important archetypal differences, particularly in terms of cellular metabolism, the level of chromatin methylation, and gene expression. They also display important functional differences, notably in their ability to integrate into other species embryos [163]. Numerous research projects aim at developing and optimizing cell culture processes to increase the 'naivety'

of hPSCs to approach that of murine naive cells and to increase their capacity to integrate into blastocysts [164,165,166].

4.2. Organismal Rejuvenation through Cellular Reprogramming

As we have just seen, the new therapeutic solutions provided by regenerative medicine benefit, or will benefit, the fight against many age-related diseases. Many age-damaged tissues and organs can already be replaced, or may be considered for replacement in the near future, thanks to ongoing innovations in stem cell research. This would be possible thanks to organs grown ex vivo or produced in animals from iPSCs derived from patient cells. However, there are obstacles to realizing this vision.

4.2.1. Aging and Senescence, Two Obstacles to Reprogramming

One of these important limitations is the aging itself, of the individual, since, as we previously discussed, there are important changes that negatively and permanently affect cells as they age. Thus, developing autologous replacement strategies based on cells already altered by age would lead to the creation of new organs that are already old and therefore, by definition, damaged. Cell senescence, which is always increasing in the body during aging, is a major obstacle to cell reprogramming, reducing the effectiveness of autologous approaches in an aging context. It is notably via epigenetic remodeling of the CDKN2A locus and overexpression of the proteins p53, p16INK4A and p21CIP1 that senescence is thought to act as a barrier to reprogramming in older and damaged cells [167,168,169]. Consequently, inhibition of the p16INK4A pathway [170] or inactivation of the p53 gene [171,172] can increase reprogramming efficiency and have even enabled reprogramming in cells that failed to be reprogrammed under normal conditions, although these changes increased the susceptibility to genetic instability. The inactivation of p53 not only promoted reprogramming but also allowed reprogramming of cells via only two transcription factors: OCT4 and SOX2 [173]. One of the obstacles for reprogramming is thus falling.

Recently, Mahmoudi et al. demonstrated high variability in reprogramming in elderly fibroblast populations, due in part to the pro-inflammatory secretory profile of certain so-called “activated” fibroblasts. These fibroblasts are characterized by the secretion of inflammatory cytokines, notably TNF, and are also believed to be involved in the variability of in vivo wound healing rates in elderly mice [174].

4.2.2. Cellular Reprogramming to Erase Cell Aging

In many ways, iPSCs are considered equivalent to ESCs, if not indistinguishable. Although this is still under discussion, it is clear that these cells have much in common and that iPSCs have embryonic genetic and epigenetic characteristics. Among these characteristics, some are known to be altered by age, such as telomeric shortening. Thus, by restoring an embryonic state, reprogramming has demonstrated a very interesting ability to erase certain cellular marks of aging. Marion et al. have thus shown

that reprogramming fibroblasts with short telomeres resulted in an extension of the telomeres in the same way as reprogramming young fibroblasts with longer telomeres [175]. From a metabolic point of view, Surh et al. demonstrated that after reprogramming, iPSCs exhibit mitochondria similar to those of ESCs. Moreover, after redifferentiation, neo-fibroblasts significantly improved functionally, compared to their parent fibroblasts [176].

It is intuitive that re-programming promotes cell rejuvenation in certain ways, as an embryonic cell (or iPSC) has more juvenile feature than an adult cell. Furthermore, we demonstrated for the first time that cell reprogramming can even rejuvenate cells from centenarians, and that it can also overcome the barrier of cell senescence without directly inactivating senescence inducers such as p53, p16INK4A, and p21CIP1, as discussed in the previous paragraph [128]. The reprogramming protocol used has been optimized and is based on the use of a cocktail of the combined six reprogramming factors from pooling the overlapping four factor cocktails of Yamanaka [71] and Thomson [102], i.e., OCT4, SOX2, KLF4, C-MYC, NANOG, and LIN28 (OSKMNL). Following this protocol, we discovered that iPSCs reprogrammed from replicative senescing or centennial cells had restored telomere and mitochondrial functions, with a gene expression profile and a level of oxidative stress similar to hESCs. In addition, after their redifferentiation, the fibroblasts obtained had reset their proliferation capacity and had a similar transcriptomic profile to fibroblasts derived from hESCs, as well as a restored metabolism. This demonstrated conclusively that “cellular aging” is reversible. Overall, then, iPSC technology is now among the major regenerative medicine approaches for elderly patients and the one that promises the most perspectives for new therapeutic avenues.

4.2.3. Complete Cellular Reprogramming Causes Teratomas

As a result of all these observations, several teams around the world, including ours, have wondered whether cell rejuvenation by reprogramming could also be applied in vivo, directly within tissues, to prevent aging deteriorations. Thus, various distinct mouse models for in vivo reprogramming have been developed to explore this hypothesis.

Abad et al. were the first to address this question [177]. They developed two different functional transgenic murine lines, named i4F-A and i4F-B, both allowing the inducible expression of the four reprogramming factors in the presence of doxycycline. A polycistronic expression cassette encoding OSKM was inserted using a lentivirus-like vector into two different genome loci: an intron of the *Neto2* gene for the i4F-A lineage and into an intron of the *PPARγ* gene for the i4F-B lineage. The expression of the OSKM cassette is controlled by a doxycycline-inducible transcriptional activator (rtTA) in the Rosa26 locus. Firstly, mice were treated with a high dose, 1mg/mL, of doxycycline in drinking water to induce OSKM, which revealed a very rapid deterioration in the health of the animals after just one week, including significant weight loss and damage to the intestine and pancreas. Other protocols were then designed to minimize these

effects and maximize survival, which led to the generation of pluripotent cells in vivo, circulating in the blood, and thus validated the feasibility of direct reprogramming in animals. Unfortunately, these treatments also produced teratomas in many organs, especially the pancreas, kidneys, intestine, and adipose tissue, with an incidence of over 40%. Using another in vivo reprogramming model, Ohnishi et al. achieved results similar to Abad et al. [178], with a rapid degradation of health status due to the proliferation of undifferentiated dysplastic cells within the tissues. The authors also observed the appearance of teratomas in the kidneys, pancreas, and liver, even one week after stopping a seven-day treatment on their animals. Thus, although in vivo reprogramming has deleterious effects on health status and lifespan when carried out to completion, it is nevertheless possible to convert adult cells into embryonic cells in vivo just as in cell culture.

Based on the previously described mouse transgenic models [177], several studies have revealed a strong association between reprogramming and tissue senescence. In vivo, complete reprogramming requires senescence-associated secretory phenotype (SASP) factors, in particular IL-6 [179]. Indeed, Mosteiro et al. demonstrated the role of senescence in cell plasticity by generating teratomas in the lungs, only in the context of injury. In addition to the teratomas, this organ had high expression levels of senescence markers such as IL-6 and PAI-1. Inactivation of senescence in this tissue inhibits teratoma formation. Similar results obtained in injured muscle by Chiche et al., using the same model, highlighted the central role of $Pax7^{+}$ muscle stem cells in the reprogramming of this tissue [180].

Overall, these examples fully illustrate the importance, for any reprogramming strategy aiming at rejuvenating organisms, of first overcoming the conditions leading to deleterious total dedifferentiation of the cells.

4.2.4. Partial Cellular Reprogramming Rejuvenates Cells In Vitro and In Vivo

To overcome this ultra-dedifferentiation problem, Ocampo et al. have developed a protocol to induce partial reprogramming. Their work was the first proof that reprogramming can counteract aging, demonstrating in particular that cyclic expression of OSKM in vivo can prolong the life expectancy of mice recapitulating the human Hutchinson–Gilford Progeria Syndrome, while improving the age-related phenotype [181]. For the purposes of their experiments, the authors used reprogrammable homozygous progeria mice of genotype $Lmna^{G609G/G609G}$ $R26^{rtTA/+}$ $Col1A1^{4F2A/+}$ obtained by crossing a reprogramming model developed by Carey et al. [182] with the accelerated aging model developed by Osorio et al. [183]. The authors chronically induced OSKM with a dose of 1mg/mL of doxycycline in bottle water two days per week. It was observed that by following this induction protocol, the life expectancy of homozygous progeria animals was increased by almost a third, with a median life expectancy of 24 weeks for treated animals compared to 18 weeks for controls. This

improvement in longevity was also accompanied by an overall improvement in health, as well as maintenance of tissue integrity in organs such as the kidneys, spleen, stomach, and heart. These results were, however, obtained on animals with a homozygous *Lmna* gene mutation, i.e., that were highly abnormal [183]. It would be interesting to confirm these results in the context of normal physiological aging or in models closer to it, such as heterozygous progeria animals for this same mutation.

Interestingly, it was shown in the same study that induction of OSKM improves (i) the regenerative capacities of non-progeria animals of genotype $Lmna^{+/+}$ $R26^{rtTA/+}$ $Col1A1^{4F2A/+}$ [181], (ii) regeneration in a model of diabetes induced by streptozocin toxin administration, and (iii) in a model of muscle degeneration induced by intramuscular cardiotoxin injection. The improvements occur through an increase in the number of $Pax7^{+}$ satellite stem cells that are involved in muscle fiber regeneration [181]. In the same mouse model, Doeser et al. showed that local induction of reprogramming factors temporarily slowed skin wound healing by reducing the activity of fibroblasts and their transdifferentiation into myofibroblasts, illustrated by the down-regulation of the markers TGFβ1, COL1a1, and αSMA. The consequence of this phenomenon is a significant reduction in the formation of scar tissue during regeneration [184]. Recently, Rodríguez-Matellán et al. demonstrated, with the i4F-B model, that a cyclic induction three days per week by 2mg/mL of doxycycline improved cognitive functions in mice, with a positive correlation between an increase scored in object recognition memory test and the level of OSKM expression [185].

In addition, Ocampo et al. demonstrated that inducing OSKM for four days induces epigenetic rearrangement in the histone markers H3K9me3 and H4K20me3, which are known to be deregulated during aging, in vitro and in vivo in the tissues of treated animals. However, these short induction effects were reversible, suggesting that chronic induction is necessary to obtain impact on longevity [181].

To further investigate the impact of partial reprogramming in humans, Sarkar et al. recently developed an in vitro strategy based on the use of mRNA to allow the expression of the 6 OSKMNL reprogramming factors in young and old human cells [186], whose effectiveness in erasing aging hallmarks leading to a rejuvenated phenotype had previously been established by the work of our team [128]. They demonstrated, in fibroblasts and endothelial cells, that transient reprogramming could restore certain cellular characteristics altered in physiological aging, including two epigenetic clocks, namely a pan-tissue epigenetic clock based on 353 CpGs and a skin- and blood-focused second clock based on 391 CpGs, described to be highly correlated to chronological age. In addition, the authors demonstrated that reprogramming changed the level of H3K9me3, improved proteosomal activity and autophagosome formation, and decreased ROS. To analyze whether transient OSKMNL expression could also reverse age-related phenotypes such as increased levels of inflammation and decreased regenerative capacity of adult stem cells, the authors first analyzed the transcriptional consequences of reprogramming to chondrocytes in elderly osteoarthritic patients. They observed a significant reduction in intracellular mRNA levels of RANKL

and iNOS2, as well as in the levels of inflammatory factors secreted by the cells, such as MIP1A, IL-6, IFNA and MCP3. In a second step, they analyzed the power and regenerative capacity of transiently reprogrammed human muscle stem cells of different ages by transplanting them into a mouse muscle injury model. Reprogrammed aged stem cells became stronger and regenerated better muscle fibers [186]. These results are promising as they open the way to new in vivo reprogramming strategies for cell therapy interventions and validate the non-integrative approach to achieve the expression of reprogramming factors.

Another type of in vivo reprogramming strategy has been illustrated recently. Senís et al. demonstrated that in vivo reprogramming was achievable by delivering OSK factors with viral vectors [187]. This kind of approach has very recently been illustrated as a strategy for regeneration of the central nervous system in mice, and more precisely, for restoring vision [188]. In this study, the authors used AAV2 vectors for the controlled expression of a polycistronic cassette encoding OSK factors that they injected into the vitreous body of the mouse eye to reach the retina. To test the safety of this strategy, the authors maintained an induction for over 15 months to validate the absence of tumors or deformations of the retina. The authors then demonstrated that the induction of OSK in retinal ganglion cells increased their survival, the regeneration of their axonal extension and forming of the optic nerve, during different stress situations. These included a model of optic nerve injury by nerve compression, a model of glaucoma induced by ocular overpressure, and their final demonstration was in the context of age-related vision impairment. DNA methylation and transcriptomic profiles were also restored in these retinal ganglion cells. Furthermore, epigenetics seems to play an important role in the regeneration phenomenon, as the inhibition of TET1 and TET2 DNA demethylase acts as a barrier and prevents any restoration. Epigenetic reorganizations involved in transient reprogramming are the widely considered to be the driving force behind the global rejuvenation phenomenon observed both in vitro and in vivo [181,185,186,188,189].

In summary, then, the various modes of cellular reprogramming detailed above confirm it as an important avenue toward innovative therapies to combat the harmful effects of aging and age-related pathologies due to decreased regenerative capacities of stem cells altered by aging.

5. Conclusions

The above paragraphs address the many approaches based on the properties of cell pluripotency and reprogramming that can be used to counter the multifactorial damages of aging. “Classical” approaches using iPSCs and derived cells obtained after differentiation are now being intensively studied and developed, and clinical applications, although still in their infancy, are progressing very rapidly. Beyond this, methods based on a direct intervention through partial reprogramming as a strategy against aging have laid the foundations for more disruptive approaches (Figure 3). All these procedures can be used to rejuvenate cells or tissues. Depending on the timing,

the intervention can either be preventive or therapeutic. Moreover, these strategies, or a combination of them, might either delay or slow aging, or both. It is obvious that purely genetic techniques to induce reprogramming in humans are not feasible, and lifelong chronic induction is far from being translated to the clinic. However, the studies we summarize and many others that we have not had the space to cover establish a proof-of-concept for further investigations to define an optimal regimen suitable for clinical applications. Indeed, the identification of molecular and cellular pathways for tissue improvement or repair during aging opens the door for strategies for ectopic expression of reprogramming factors using non-integrative vectors or using mimetic molecules to activate endogenous reprogramming factors. In addition, these investigations could lead to the discovery of secondary and/or complementary pathways to intervene during aging and improve the healthspan. Thus, a wide range of therapeutic solutions based on induced pluripotent stem cells, but also on cell reprogramming strategies, is now available to improve healthy aging for the benefit of individuals and society.

Figure 3.

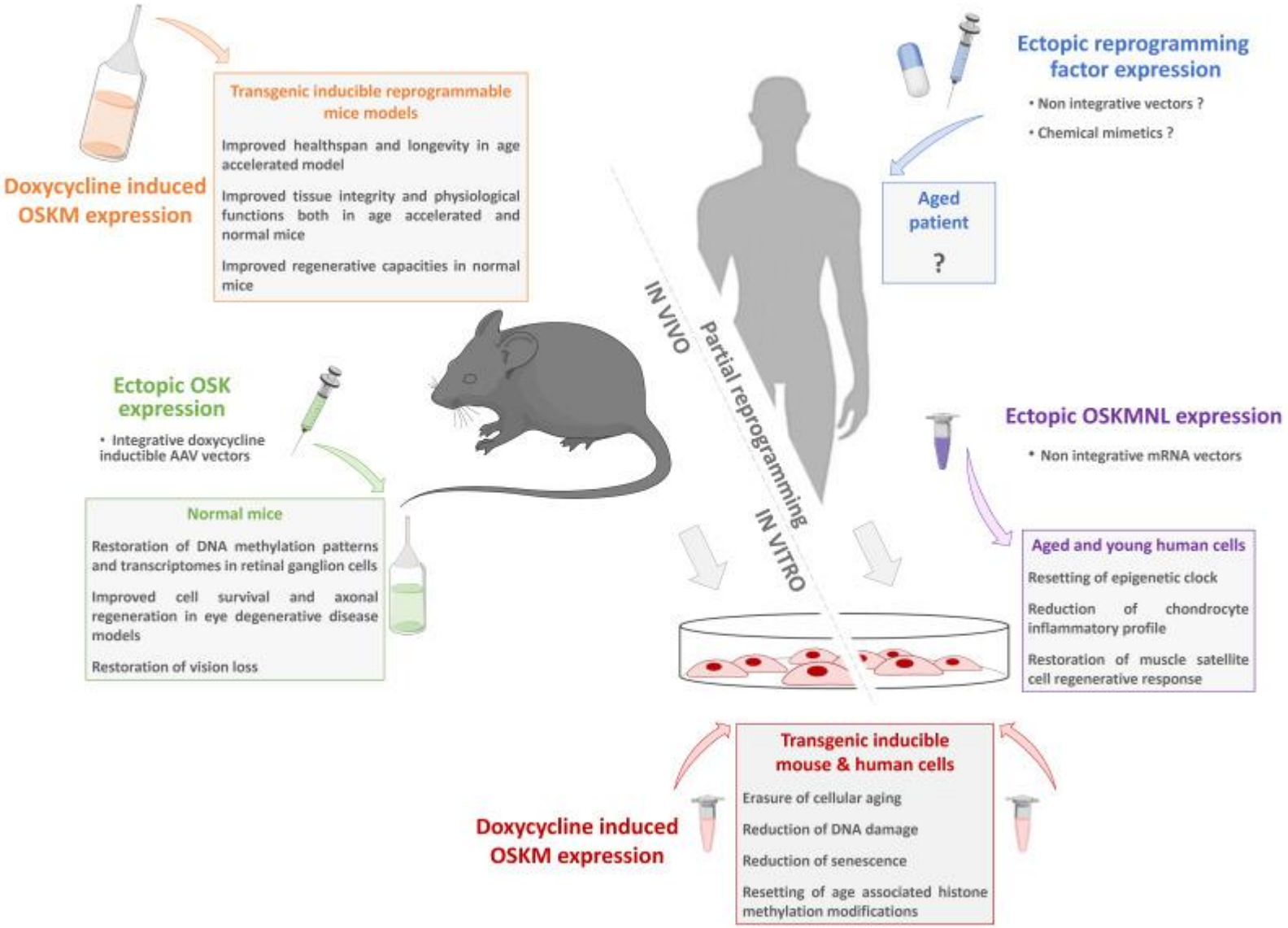

Partial reprogramming toward pluripotency as a new anti-aging strategy. For decades, complete cell reprogramming has been demonstrated to reset somatic cell physiology to a juvenile state equivalent to ESCs. Starting from transgenic models allowing inducible reprogramming factor expression to non-integrative vectors; numerous studies have recently demonstrated that a partial reprogramming is sufficient to restore the general characteristics of cellular aging without changing the identity of the cells. These innovative approaches pave the way for new strategies based on a safe transient reprogramming that can be directly transposed to humans.

Author Contributions

Q.A., E.L.B., O.M. and J.-M.L. drafted, wrote, and edited this review. All authors have read and agreed to the published version of the manuscript.

Review of light parameters and photobiomodulation efficacy: dive into complexity

Randa Zein [a], Wayne Selting [a,*], Michael R Hamblin [b,c,d]
PMCID: PMC8355782 PMID: 30550048

Abstract.

Photobiomodulation (PBM) therapy, previously known as low-level laser therapy, was discovered more than 50 years ago, yet there is still no agreement on the parameters and protocols for its clinical application. Some groups have recommended the use of a power density less than 100 mW/cm2 and an energy density of 4 to 10 J/cm2 at the level of the target tissue. Others recommend as much as 50 J/cm2 at the tissue surface. The wide range of parameters that can be applied (wavelength, energy, fluence, power, irradiance, pulse mode, treatment duration, and repetition) in some cases has led to contradictory results. In our review, we attempt to evaluate the range of effective and ineffective parameters in PBM. Studies *in vitro* with cultured cells or *in vivo* with different tissues were divided into those with higher numbers of mitochondria (muscle, brain, heart, nerve) or lower numbers of mitochondria (skin, tendon, cartilage). Graphs were plotted of energy density against power density. Although the results showed a high degree of variability, cells/tissues with high numbers of mitochondria tended to respond to lower doses of light than those with lower number of mitochondria. Ineffective studies in cells with high mitochondrial activity appeared to be more often due to over-dosing than to under-dosing.
Keywords: photobiomodulation, low-level laser therapy, parameters, mitochondrial numbers, effective and ineffective studies

1. Introduction

Since Mester,[1,2] in 1968, accidently discovered the positive effect of a ruby laser beam on hair growth and wound healing in mice, researchers have attempted to uncover the scientific basis for this phenomenon as well to establish the range of optical exposure parameters that lead to successful clinical outcomes. The possibility of stimulating a wide range of cells to improve wound healing and cellular growth has created a science referred to as low-level laser therapy (LLLT) or photobiomodulation therapy (PBMT). As an understanding of basic concepts has emerged, the very wide range of factors contributing to positive outcomes in some cases and negative outcomes in others has stymied the development of definitive protocols.

The multitude of variables to be considered is formidable. More than 1000 research articles have reported that a range of factors can apparently affect the chances of success including wavelength, energy density, power density, total energy, total power, pulse structure, spot size, tissue absorption characteristics, and treatment repetition regimen. Further parameters of lesser importance requiring both control and study are use of combination wavelengths, delivery method (contact, punctual, broad beam),

duration of treatment, inadvertent heating of tissue and even whether the source of photons is a laser, light-emitting diode (LED), or broad-spectrum light from a lamp.[3,4]

It has become apparent that, in order to achieve positive results with PBM, each of these dosimetric parameters must be controlled within a limited range of values. Of the many studies that have been conducted over the past 50 years, a number have attempted to determine the relative contribution of individual parameters to successful outcomes.

Consensus has (almost) been reached on one of the most important concepts in PBM. The so-called Arndt–Schultz law was originally proposed near the end of the 19th century. It states in original form that “For every substance, small doses stimulate, moderate doses inhibit, and large doses kill.”[5] This concept[6] also forms the basis of the science of “hormesis,” as reviewed by Calabrese and Mattson[7]

Pharmacological agents used at a therapeutic dose can be very beneficial while the same drug administered at a higher dose may be catastrophic. For many years, this Arndt–Schultz law has been used as a convenient concept to explain the cellular and tissue interactions with light.

Briefly, this law, when applied to PBM, states that, at very low levels of irradiation, photons are absorbed by subcellular chromophores present inside intracellular organelles, most notably, mitochondria. Absorption of energy by cytochrome C oxidase (CCO) in the mitochondrial respiratory chain is the primary initiating interaction triggering PBM effects.[8] Both adenosine triphosphate (ATP) production and oxygen consumption by the cells increase. This may lead to changes in nitric oxide (NO) levels, activation of secondary messenger pathways, activation of transcription factors, and growth factor production.[9] At this very low level, energy is absorbed by the cell but at such low amounts of energy that there are no observable gross changes (temperature or photochemical damage).

As the number of absorbed photons increases, stimulation of cellular metabolism, as noted above, begins to affect cellular activity, producing positive PBM effects. Both the number of photons and rate at which they are delivered has a significant influence on the response.[10,11]

As the number of photons increases beyond a particular level, the cellular stimulation disappears, and if the number of photons is even further increased, inhibition and cellular damage occurs. Current theories suggest that the mitochondrial membrane potential having reached a maximum at the optimum dose declines back to baseline and can be lowered below baseline by excessive doses of light.[12] ATP reserves within the cell begin to be depleted by excessive doses of light compromising the positive cellular function. Production of excessive reactive oxygen species (ROS), which can be

toxic, release of excessive free NO, which can damage cells, and activation of a cytotoxic mitochondrial-signaling pathway leading to apoptosis are also possible theories. At still higher levels of irradiation, depletion of cellular energy reserves or excess levels of the factors noted above become so significant that cellular metabolism falls below normal intrinsic levels and function is actually inhibited eventually leading to cell death.

This concept, represented by the Arndt–Schultz law of biphasic dose response, has become the foundational concept of PBM. However, the appropriate range of values of fluence and irradiance at which these significant transitions occur are not widely agreed upon. Numerous studies suggest that fluences ranging from 3 to 10 J/cm2, at the cellular level, will produce the desired stimulation of metabolic activity.[13,14]

While this protocol has become widely accepted, some studies suggest that biostimulation will occur in the range of 0.5 to 1 J/cm2 on an open wound and in the range of 2 to 4 J/cm2 to a target through overlaying skin.[15] Another respected source suggests that doses used for superficial targets tend to be in the region of 4 J/cm2 with a range of 1 to 10 J/cm2.[16–18] Doses for deeper-seated targets should be in the 10 to 50 J/cm2 range.[19–21]

While many studies have shown a positive effect of PBM,[17,18,21] a number have failed to show a benefit[22,23] and, in fact, some reports have shown negative outcomes at what are reported to be the same parameters of irradiation as other positive studies. Unfortunately, in many of the historical studies, important laser parameters were omitted or incorrectly presented.

Often, laser output total power is reported without consideration of the spot diameter at the surface of the target tissue. Therefore, power density, the most relevant parameter, is not reported and results are, predictably, inconsistent.

Sometimes the distribution of energy across the tissue surface is not noted in published studies introducing profound errors. As an example, most lasers are designed to emit in the TEM00 mode, which produces a Gaussian distribution of beam profile. By mathematical definition, cells in the exact center of the beam will be irradiated at precisely twice the indicated average output power while cells at the periphery of the irradiation spot will only receive about 13% of that power. If irradiation were to be delivered for 30 s, cells at the beam center would receive an energy dose of 6 J/cm2 while those at the periphery would receive 0.39 J/cm2. Obviously, the cellular response, taking into account the Arndt–Schultz law, will be different in each of these tissues. This could result in a conclusion of no-effect, positive effect, or negative effect, depending on which cells were observed in the analysis phase of the study.

Another basic concept that has been suggested to be relevant to the successful application of PBM is the Roscoe–Bunsen law of reciprocity.[24] This concept states that the most important parameter in PBM is the total quantity of photons absorbed by the target cells, and it is not important how quickly or how slowly these photons are delivered. This means that 100 mW/cm2 applied for 60 s for a dose of 6 J/cm2 will have the same effect as applying 1 W/cm2 for 6 s (6 J/cm2) or 6 W/cm2 for 1 s (6 J/cm2) using the same spot size.

Numerous studies have shown that, while this law is valuable for many parts of the parameter range, it does not hold true for the entire range.[18,25,26] The previously discussed theories of the biphasic dose response, supported by other studies, are the likely reason for this inaccuracy. Within a certain range of parameters, perhaps between 1 and 100 J/cm2, and at power densities from 1 to 100 mW/cm2, this linear reciprocity applies. However, beyond this range, reciprocity does not appear to apply. For instance, there exists a lower threshold (perhaps 0.5 mW/cm2) below which the illumination time could be infinite and would be no different from daylight. Similarly, the upper threshold is fixed by the possible photothermal effect if the power density is too large. The irradiance values, that produce unacceptable heating of the tissue, are governed by the wavelength and are ~750 mW/cm2 at 800 to 900 nm, about 300 mW/cm2 at 600 to 700 nm, and as low as 100 mW/cm2 at 400 to 500 nm. Furthermore, the illumination time is also important.[17] There exists a certain minimum length of time (few minutes) that the light needs to be on the tissue for the best effects to occur.[17]

The parameters of most importance in PBM are the power density (irradiance) measured in mW/cm2 and the energy density (fluence) measured in J/cm2. Many of the studies discussed here and, indeed, in most of the research literature, are based on the inaccurate statement of the laser output in Watts. Depending on the area irradiated by this beam of photons, the power density and the cellular effects produced will be very different.

As an example, 1 W delivered through a 400 μm diameter optical fiber will produce a power density of 796 W/cm2 while the same 1 W delivered through an 8-mm diameter therapy hand-piece will produce a power density of only 2 W/cm2.

Energy density is frequently reported in research literature but the spot area at the tissue is often omitted. This error makes it impossible to verify their findings or to see how they calculated the vital energy density information. Inconsistency in reporting these parameters is a major source of contradictory research findings and has done much to hinder the acceptance of PBM effects.

Another important factor that must be taken into account is the optical properties of the tissue itself.[27] Since the light is generally delivered as a surface spot shone onto the skin, the number of photons that actually penetrate into the tissue to arrive at the

pathological lesion is highly variable.[28] The first issue to be addressed is light reflection from the surface of the skin,[29] which can be minimized if the optical probe is held in firm contact with the skin.[30] The second issue is scattering of light within tissue. Scattering is wavelength dependent with shorter wavelengths undergoing more intense Mie scattering than longer wavelengths.[31] The third issue is absorption of the light by chromophores that are not biologically active. These nonactive chromophores are chiefly hemoglobin (both oxyhemoglobin and deoxyhemoglobin), myoglobin, and melanin.[27] However, it should be noted that some authors have suggested that photodissociation of oxygen from hemoglobin[32] or NO from myoglobin[33] could be a relevant mechanism in PBM. There is a growing trend for researchers in PBM to undertake modeling of tissue optical properties either by Monte-Carlo methods[34] or by use of tissue phantoms.[35]

1.1. Mitochondria and Cells

Mitochondria are highly important intracellular organelles whose main function is to act as “power plant” of the cell, generating ATP which is the main source energy for cellular activity and metabolism. Moreover, mitochondria play important roles in regulation of oxidative stress, calcium metabolism, apoptosis, and a host of signaling pathways.[36] It is believed that mitochondria originated when a primitive eukaryotic cell “captured” a primitive prokaryotic bacterium around the time the “great oxygenation event” occurred on the Earth.[37]

Mitochondria contain the electron transport chain responsible for transferring electrons from NADH through complexes I, II, III, and IV.[38]

When applying light to cells, mitochondria are the initial sites of light absorption and CCO (particularly, the CuA and CuB metal centers) are believed to be the photoacceptors.[39] Photon absorption results in setting in motion a cascade of reactions known as cellular signaling pathways leading to NO dissociation, ROS production, and increased ATP synthesis.[9]

The number of mitochondria in cells varies widely and it is strongly correlated with the metabolic requirements of the cell (how many chemical reactions the cell has to carry out) and may range from a few to thousands of individual organelles. Cells such as osteoblasts, keratinocytes, and fibroblasts have a lower number of mitochondria, whereas muscle cells, neural cells, cells composing internal organs (liver, kidneys, spleen, etc.), and myocardial cells contain a higher number of mitochondria. Broadly speaking, the proportion of mitochondria in a tissue type can be gauged by observing the color of the tissue (without containing any blood). For instance, dark colored tissues (liver, heart, kidney, gray brain matter) have a high concentration of mitochondria since CCO and other cytochromes are the most important cellular pigments, while light colored tissues (skin, bones, tendons) have few mitochondria. The following reports

discuss how mitochondrial numbers and mitochondrial activity have been determined in different cells and tissues.[40–43]

Furthermore, mitochondria in stem cells and induced pluripotent stem cells are poorly developed and low in number; mitochondrial function and structure have even been suggested as indicators of stem cell competence.[44]

The hypothesis of the present review is that the effects of PBM on different tissues can be explained by taking into account two main factors. First, what is the content of mitochondria in the cells comprising the bulk of the tissue? Second, what is the depth? Cells *in vitro* are very superficial, skin and some connective tissues are moderately superficial, while other tissues are deeper, bones, joints, brain, organs, etc. Moreover, tissues with high mitochondrial numbers tend to be deeper than those with low mitochondrial numbers.

Therefore, studies were divided into two groups based on the number of mitochondria at the cellular level and the depth of the tissue level.

Cells of tissues with higher numbers of mitochondria were assembled in one group (brain cells, muscle cells, neural cells, macrophages, monocytes) and cells with fewer mitochondria were assembled in another group (keratinocytes, osteoblasts, chondrocytes, fibroblasts, stem cells). Tissues with abundant mitochondria exist in organs, such as muscle, heart, liver, kidney, cells.

The purpose of this review paper was to compare effective and ineffective studies on cells and tissues in each group. Every effort was made to find or calculate relevant parameters even if they were not explicitly stated in the paper.

2. Materials and Methods

This study was conducted following Preferred Reporting Items of Systematic reviews and Meta-analysis.

Research questions: Is it possible to propose a practical protocol of for PBM or LLLT? What are the best parameters that produce a positive result in different circumstances?

2.1. Research Strategy for Article Identification

Research was conducted using the following electronic databases: Springer, PubMed, Google Scholar, and Cochrane Database.

Keywords used: LLLT, PBM, LLLT and osseointegration, LLLT and bone graft, LLLT and cells, LLLT and bone regeneration.

After collecting the data, the titles, abstract, and conclusions were checked and unrelated, and obviously biased articles were excluded. Also, all case reports and literature reviews were excluded. Only studies dated from 2007 to 2016 were included.

Evaluations of articles were independently performed by two reviewers. The initial search yielded 250 articles. After exclusion of unrelated articles, only 190 remained. Using the exclusion criteria listed in Table 1 reduced this number to 34 articles.

Table 1.
Eligibility criteria adapted from Cericato et al.[45] for selection of the studies.

Reason for exclusion	PubMed	Springer	Google Scholar	Cochrane	Total
Literature and/or systematic review	8	8	11	6	33
Article in language other than English	—	—	15	—	15
Letter from the editor, opinion articles	—	—	8	—	8
Fluence not mentioned	3	2	30	8	43
Use of very high fluence: density greater than 500 J/cm2	4	2	8	8	22
Article did not mention power or fluence rate	5	2	16	6	29
Other (book chapter, appendix, bibliograghy, index	—	—	4	2	6
Total exclusion	20	14	92	30	156

2.2. Assessment of the Studies

After obtaining full texts of all 34 relevant articles, they were evaluated and scored following the checklist using eligibility criteria adapted from Cericato et al.[45] described in Table 1. Articles with scores from 0 to 8 points were considered low quality and were excluded. Article with scores from 13 to 15 points were considered high quality while scores from 9 to 12 were considered moderate quality. Table 2 presents the details of the 34 studies finally included in this review.

Table 2.
Final list of studies that were included together with Cericato score.

Authors	Score (Cericato et al.)[17]
Fernandes et al.[46]	12
Mendez et al.[21]	12

Authors	Score (Cericato et al.)[17]
Barbosa et al.[20]	11
Huang et al.[47]	11
Huang et al.[48]	12
Sharma et al.[49]	11
Oron et al.[50]	10
Chen et al.[26]	12
Souza et al.[51]	11
Ferraresi et al.[52]	12
Zhang et al.[53]	12
Wang et al.[54]	12
Amaroli[19]	10
Tschon et al.[55]	11
Pyo et al.[56]	12
Migliario et al.[57]	12
Khadra et al.[32]	11
Skopin et al.[58]	12
Salehpour et al.[59]	11
Wu et al.[58]	12
Lopes-Martins et al.[18]	11
Bozkurt et al.[60]	12
Wang et al.[61]	11
Alves et al.[25]	11
Oron et al.[62,63]	11
Castano et al.[17]	12
Salehpour et al.[64]	11
Leal junior et al.[65,66]	12
Ando et al.[13]	11
Zhang et al.[67]	12
Baroni et al.[68]	11

Authors	Score (Cericato et al.)[17]
Leal Junior et al.[69]	11
Blanco et al.[70]	12
Disner et al.[71]	12

3. Effect of Varying a single parameter on PBM Efficacy

3.1. I-Effect of varying wavelength on PBM Efficacy

3.1.1. In vitro studies

It has been shown through many studies that CCO is the most important chromophore that absorbs light. Delpy and Cope[72] showed that over 50% of the light absorption between 800 and 850 nm was due to cytochrome c oxidase, with hemoglobin (oxy and deoxy) playing a minor role. CCO has two absorption bands, one in the red spectral region (~660 nm) and another in the NIR spectrum (~800 nm), which consequently are the wavelengths most often used in PBM[3].

In their study, Wang et al.[54] found that the mechanisms of action of 810 and 980 nm laser appeared to have significant differences. While the PBM effect occurred at both wavelengths, the chromophore was different between wavelengths. NIR wavelengths, such as 810 nm, stimulate mitochondrial activity and ATP production. At longer wavelengths, the mechanism of action of 980 nm relies on absorption by water leading to the activation of heat (or light)-gated ion channels and promotes cell proliferation via the TRPV1 calcium ion channel pathway.

The same study compared the effect on stem cell differentiation of these two different wavelengths, 810 and 980 nm. For each wavelength, different doses were used from 0.03 to 10 J/cm2, spot size 4 cm2, irradiance 16 mW/cm2, power 64 mW, and time of irradiance (3 J/cm2, 188 s) and (0.3 J/cm2, 18.8 s). The irradiance was adjusted by varying the distance between the laser and the target cells.

Both wavelengths showed a biphasic dose response. At 980 nm, a peak dose response was seen at 0.03 and 0.3 J/cm2 while 810 nm showed a peak response at 3 J/cm2. Moreover, the dose of 0.3 J/cm2 with the 980-nm laser had a better effect than any of the other groups.

A second study by Wang compared the effects of delivering four different wavelengths (420, 540, 660, and 810 nm) using the same parameters of 3 J/cm2 at 16 mW/cm2, on human adipose-derived stem cell differentiation into osteoblasts. They found that 420- and 540-nm wavelengths were more effective in stimulating osteoblast differentiation compared to 660 and 810 nm. Intracellular calcium was higher after 420 and 540 nm

and could be inhibited by the TRP channel inhibitors, capsazepine and SKF96365. They concluded that using blue and green wavelengths activated the light-gated calcium channels rather than CCO.[61,73]

3.1.2. In vivo studies

Mendez et al.[21] compared, histologically, the effect of using two different wavelengths (GaAlAs 830 nm and InGaAl 685 nm) on repair of cutaneous wounds in rats. The control group received no treatment; group II was irradiated with 685 nm, using a fluence of 20 J/cm2 with a spot diameter of 0.6 mm; group III was irradiated using 830 nm, 20 J/cm2; group IV was irradiated with both 830 and 685 nm using a total of 20 J/cm2; group V with 830 nm using 50 J/cm2; group VI with 685 nm, 50 J/cm2 and group VII using 830 and 685 nm, 50 J/cm2. Laser therapy was repeated four times over 7 days at 48 h intervals. They concluded that better results were observed when combining both wavelengths of 830 and 685 nm and attributed this advantage to different absorption and penetration. When comparing the two wavelengths used separately, 830 nm showed better results. While combining the wavelengths provides valuable information, it was not appropriate to include it in the tables of effectiveness.

Barbosa et al.[20] compared the effect of light application on bone healing in rats using red and infrared wavelengths. Forty-five rats were divided into three groups after femoral osteotomy: Gr I was used as control; Gr II was submitted to laser treatment using a red wavelength (660 to 690 nm); and Gr III were treated using an infrared laser (790 to 830 nm). Laser therapy was applied immediately after osteotomy and repeated every 48 h, three times a week, for a total of nine sessions over 21 days. The output power was set at 100 mW, energy 4 J, spot size 0.028 cm2, power density 3.5 W/cm2 for 40 s producing a fluence of 140 J/cm2. Animals were sacrificed, the femurs removed and subjected to optical densitometry analysis after 7, 14, and 21 days (five per group).[20] After 7 days, both laser-treated groups had significantly higher mean bone optical density compared with the control group but no significant difference between the two laser groups was seen. After 14 days, only Gr III treated with infrared energy showed significantly higher bone density than the control group. After 21 days, no significant difference of the mean bone density between the three groups was seen. They concluded that PBM accelerated bone repair in the initial phase and suggested that PBM in bone repair is both timing and wavelength dependent.

Al-Watban and Zhang[16] compared the efficacy of accelerating wound healing in diabetic rats using visible and NIR diode lasers at wavelengths of: 532, 633, 670, 810, and 980 nm. Each wavelength was delivered at doses of 5, 10, 20 and 30 J/cm2, using the same power density for all the wavelength of 22 mW/cm2 except for 633 nm (irradiance used: 15.5 mW/cm2) and 532 nm (10 mW/cm2). Results showed that there was a significant difference between the NIR and visible wavelengths with visible wavelengths being more effective than NIR. They also concluded that the optimum wavelength was 633 nm and the optimum dose was 10 J/cm2.

These studies suggest that the relationship between wavelength and fluence is crucial. If the target is CCO, it is well accepted that red light (630 to 670 nm) or near-infrared light (780 to 940 nm) will have positive effects, using fluences in the stimulatory range of 3 to 10 J/cm2.[16]

However, if the desired chromophore is ion channels within cells, the wavelengths that best affect the calcium channels are in the range of 420 to 540 nm.[54,61] Delivering just 3 J/cm2 when using 16 mW/cm2 will have the best effect. Using the higher wavelength of 980 nm may also have a beneficial effect for targeting water as a chromophore.[54]

Disner et al.[71] studied the effect of PBMT delivered to the head (over right prefrontal cortex) combined with attention bias modification (ABM) therapy on 51 human patients with elevated symptom of depression. PBMT was administered before and after blocks of ABM using 1064 nm, 3.4 W, irradiance of 250 mW/cm2 (3,400 mW/13.6 cm2=250 mW/cm2) for 4 min and a cumulative fluence of 60 J/cm2 (0.25 W/cm2×240 s=60 J/cm2). They found that PBMT led to greater symptom improvement especially among participants, whose attention span was responsive to ABM, and they concluded that the beneficial effect of ABM could be improved by adjunctive interventions, such as right prefrontal PBMT.

3.2. II-Effect of Varying Energy Density and Power Density on PBM Efficiency

3.2.1. In vitro studies with cells with high number of mitochondria

Fernandez et al.[46] stimulated the M1 profile (macrophages can have two different phenotypes called M1 and M2 depending on the type of cytokines they produce) of macrophages by using two different sets of laser parameters: 660 nm, 15 mW, 0.375 W/cm2, 20 s for 7.5 J/cm2 and 780 nm, 70 mW, 1.75 W/cm2, 1.5 s for 2.6 J/cm2 (the spot area calculated by current authors from available information was 0.04 cm2). Results showed that both lasers were able to decrease TNFα and iNOS expression but parameters used for 780 nm gave an additional decrease. Also, parameters used for 660 nm gave an up-regulation of IL-6 expression and production. They concluded that using 780 nm with high power and low energy density or 660 nm with low power and high energy density achieved similar results and the additional decrease by the parameters used with 780 nm suggest that this wavelength returned the cells to a nonstimulated state.

Authors	Wavelength (nm)	Fluence	Irradiance	Cell type
Fernandes et al.[46]	780	2.6 J/cm2	1.75 W/cm2; 70 mW, 0.04 cm2, 1.5 s	Macrophage
Huang et al.[47]	810	3 J/cm2	20 mW/cm2; 150 s, spot size 5 cm	Neural cells
Huang et al.[48]	810	3 J/cm2	25 mW/cm2, 2 min, spot size 5 cm	Neural cells
Sharma et al.[49]	810	0.03, 0.3, 3, 10, peak at 3 J/cm2	25 mW/cm2	Mouse cortical neuron
Oron et al.[50]	808	0.05 J/cm2	50 mW/cm2	Human neural cells
Chen et al.[26]	808	1 J/cm2	44.7 mW/cm2 170 mW, 3.8 cm2, 22.4 s	Monocyte
Souza et al.[51]	780	3 J/cm2	275 mW/cm2 [Power=70 mW, 1.5 s (2×) effective power 53.9 mW] Area=0.196 cm2 Beamspotarea=0.04 cm2	Macrophage
Ferraresi et al.[52]	Cluster 40 LEDs (20 infrared 850 nm and 20 red 630 nm)	2.5 J/cm2	28 mW/cm2 50 mW (IR) and 25 mW (red) Cluster: 1000 mW (IR) and 500 mW (red) 45 cm2, 90 s, distance: 156 mm	Myotube C2C12
Amaroli et al.[19]	808	3.0 J/cm2	100 mW/cm2 100 mW spotarea:1 cm2	Paramecium
Amaroli[19]	808	64 J/cm2	1000 mW/cm2 100 mW, spotarea=1 cm2	Paramecium
Chen et al.[26]	660	1 J/cm2	0.8 mW/cm2 6 mW, 7.5 cm2 1250 s	Monocyte
Chen et al.[26]	660	2 J/cm2	0.8 mW/cm2 6 mW, 7.5 cm2 2500 s	Monocyte

Authors	Wavelength (nm)	Fluence	Irradiance	Cell type
Souza et al.[51]	660	7.5 J/cm2 effective fluence 1.15 J/cm2	57.4 mW/cm2 Power=15 mW, 20 s Effectivepower 11.25 mW Irradiatedarea=0.196 cm2 Beamspotarea=0.04 cm2	Macrophage
Fernandez et al.[46]	660	7.5 J/cm2	0.375 W/cm2 15 mW, 0.04 cm2, 20 s	Macrophage

Lopes-Martins et al.[74] found a true biphasic response occurred in the neutrophils isolated from mice treated with different energy densities (1, 2.5, and 5 J/cm2) with a maximum effect at 2.5 J/cm2.

Huang et al.[47] irradiated cortical neuronal cells with a diode laser using 810 nm, 20 mW/cm2, 3 J/cm2, spot size of 5 cm, 150 s. They found that laser treatment reduced oxidative stress in primary cortical neurons *in vitro*.

Studies using PBM *in vitro* on cells with high numbers of mitochondria that reported positive results are summarized in Table 3. Ineffective parameters *in vitro* in cells with high numbers of mitochondria are reported in Table 7. In some cases, the same studies are included in both Tables 3 and 7 (effective and ineffective parameters) when the authors varied the parameters.

Table 3.

Effective treatment of PBM: *in vitro* studies in cells with higher number of mitochondria.

Table 7.

Authors	Wavelength (nm)	Fluence (J/cm2)	Irradiance	Cell type
Sharma et al.[49]	810	30	25 mW/cm2	Mouse cortical neurons
Chen et al.[26]	660	3	0.8 mW/cm2 6 mW, 7.5 cm2 3750 s	Monocyte
Chen et al.[26]	660	2	0.8 mW/cm2 6 mW, 7.5 cm2 2500 s	Monocyte
Amaroli et al.[19]	808	3.0	1000 mW/cm2, 1 W, 1 cm2 spot area	Paramecium

Authors	Wavelength (nm)	Fluence (J/cm2)	Irradiance	Cell type
Amaroli et al.[19]	808	64	100 mW/cm2, 1 W, 1 cm2 spot area	Paramecium

Ineffective treatment of PBM: *in vitro* studies in cells with higher number of mitochondria.

3.2.2. In vitro studies with cells with lower numbers of mitochondria

Tschon et al.[55] irradiated osteoblast–like cells using a 915-nm diode laser at the following parameters: 100 Hz pulsed mode, 50% duty cycle, and output power of 0.575 W. Laser energy was delivered in defocused mode using a concave lens to cover the growth area (1.91 cm2) at distance of 19 mm (power density calculated by current authors from available information was 150 mW/cm2). The laser was applied for 48, 96, and 144 s producing doses of 5, 10, and 15 J/cm2 (energy density calculated by current authors from available information was 7.2, 14.4, and 21.56 mJ/cm2), and specimens were examined after 4, 24, 48, and 72 h. *In vitro* scratch wounds treated with 5 and 10 J/cm2 were the first to reach complete coverage after 72 h, followed by 15 J/cm2, which reached complete healing after 96 h.

Pyo et al.[56] studied the effect of hypoxia and PBM on the expression of bone morphogenetic protein-2 (BMP-2); transforming growth factor-beta-1 (TGF-β1); type I collagen, osteocalcin; hypoxia inducible factor-1 (HIF-1) and AKT. Osteoblast cells were cultured under 1% oxygen tension and then exposed to hypoxia. These cells were then irradiated with an 808 nm diode laser; 1000 mW, continuous wave (CW) for 15 s for a stated energy density of 1.2 J/cm2 at each session (power density calculated by current authors from available information was 80 mW/cm2). Other cells were cultured 24 h more under hypoxia and irradiated a second and third time for a total energy density of 1.2, 2.4, and 3.6 J/cm2. Finally, further hypoxia was applied to the cells after irradiation. Cells were not exposed to laser energy in the control groups and were incubated under hypoxia at 1, 24, and 48 h. Results showed that hypoxia did not affect osteoblast viability (in the control group) and BMP-2, but it resulted in a decrease in osteocalcin, TGF-β, and expression of type I collagen. However, PBM applied to hypoxic osteoblasts stimulated osteoblast differentiation and proliferation through an increased expression of BMP-2, osteocalcin, and TGF-β. In addition, PBM inhibited HIF-1 expression and inhibited production of Akt.

Migliario et al.[57] irradiated murine preosteoblasts (MC-3 T3 –E1) in order to evaluate the effect of PBM on ROS in cells labeled with an ROS marker. They used a diode laser at 930 nm, 1 W, irradiation time of 1, 5, 10, 25, and 50 s, for a delivered fluence of 1.57, 7.87, 15.74, 39.37, and 78.75 J/cm2 (spot area calculated by current authors from available information was 0.63 cm2 and irradiance of 1.57 W/cm2). The laser application was delivered three times at 0, 24, and 48 h. They found that ROS generation was dose dependent and doubled at higher fluences (25 to 50 J/cm2). Also,

laser irradiation was able to increase preosteoblast proliferation starting from a fluence of 5 J/cm2. Increasing the fluence produced an increase in cell proliferation up to 25 J/cm2 and then a decrease at 50 J/cm2. The peak of cell proliferation occurred at 10 J/cm2. These results are partially in disagreement with other studies that suggest that 1 to 5 J/cm2 was optimal for cell proliferation. Contradictory results may be due to differences in irradiation parameters (wavelength, output power, energy density).

Zhang et al.[53] irradiated fibroblast cells with 628 nm. Power output was constant at 15 mW, irradiance 11.46 mW/cm2, and distance of 0.75 cm. Samples were irradiated for various time periods to yield final energy doses of 0.44, 0.88, 2.00, 4.40, and 9 J/cm2. They found a maximum increase in human fibroblast cell proliferation with a fluence of 0.88 J/cm2 and a reduction in the proliferation at 9 J/cm2.

Khadra et al.[75] investigated the effect of single and multiple doses on attachment and proliferation of human fibroblasts. Cells were cultured on titanium implants and divided into three groups: group I was used as a control, group II received GaAlAs 830 nm, output power 84 mW, 9 cm distance to the cells, a single dose of 3 J/cm2, 360 s (spot area calculated by current authors from available information was 10 cm2 and irradiance of 0.0084 W/cm2), group III was divided into three subgroups and exposed to multiple doses (one dose on each of three consecutive days) of 0.75, 1.5, and 3 J/cm2 corresponding to exposure times of 90, 180, and 360 s (spot area calculated by current authors from available information was 10 cm2). Results indicated that samples exposed to multiple doses of 1.5 and 3 J/cm2 showed a significantly proliferation. They concluded that the attachment of human fibroblasts to the titanium implant was enhanced by PBM. Both multiple and single doses significantly increased cellular attachment. Finally, 0.75 J/cm2 did not promote proliferation and cell attachment.

Skopin and Molitor[58] studied the effect of using different doses and different irradiances on wound healing in fibroblast cultures using 980-nm diode laser. They applied an irradiance of: 26, 49, 73, 97, and 120 mW/cm2 for a constant 2 min each, delivering 3.1, 5.9, 8.8, 11.6, and 14.4 J/cm2. They found a significant increase in cell division when using 26, 73, and 97 mW/cm2. This effect was negated at 120 mW/cm2.

Al-Watban and Andres[76] studied the effect of He–Ne laser on the proliferation of hamster ovary and human fibroblasts. Irradiance was held constant at 1.25 mW/cm2 using an accumulated dose over three consecutive days of 60 to 600 mJ/cm2. They found a peak response at 180 mJ/cm2. This study suggested that there is activation at a lower dose from 2 mJ/cm2 with a peak at 180 mJ/cm2. At higher doses, greater than 300 mJ/cm2, there was bioinhibition.

Authors	Wavelength (nm)	Fluence (J/cm2)	Irradiance	Cell type
Wang et al.[54]	420	3	16 mW/cm2 4 cm2, 188 s	Adipose stem cells
Wang et al.[54]	540	3	16 mW/cm2 4 cm2, 188 s	Adipose stem cells
Zhang et al.[53]	628	0.88	11.46 mW/cm2 Output power 15 mW, 0.76 cm distance to the surface, area=9.6 cm2	Fibroblast
Zhang et al.[53]	628	2.0	11.46 mW/cm2 Output power 15 mW, 0.76 cm distance to the surface, area=9.6 cm2	Fibroblast
Zhang et al.[53]	628	4.4	11.46 mW/cm2 Output power 15 mW, 0.76 cm distance to the surface, area=9.6 cm2	Fibroblast
Khadra et al.[32]	830	1.5	8.4 mW/cm2 84 mW, 10 cm2, 9 cm distance to cells	Fibroblast
Khadra et al.[32]	830	3.0	8.4 mW/cm2 84 mW, 10 cm2, 360 s, 9 cm distance to cells	Fibroblast
Tschon et al.[55]	915	7.2	150 mW/cm2, 100 Hz, 50% duty cycle, power 0.575 W, 48 s	Osteoblast
Tschon et al.[55]	915	14.4	150 mW/cm2 50% duty cycle, power 0.575 W, 96 s	Osteoblast
Migliario et al.[57]	930	7.8	1580 mW/cm2 1 W, 5 s, 0.63 cm2	Preosteoblast
Migliario et al.[57]	930	15	1580 mW/cm2 1 W, 10 s, 0.63 cm2	Preosteoblast
Migliario et al.[57]	930	39	1580 mW/cm2 1 W, 25 s, 0.63 cm2	Preosteoblast
Pyo et al.[56]	808	1.2	80 mW/cm2 15 s, 1 W	Osteoblast
Skopin et al.[58]	980	3.1	26.7 mW/cm2	Fibroblast
Skopin et al.[58]	980	8.8	73 mW/cm2	Fibroblast
Skopin et al.[58]	980	11.6	97 mW/cm2	Fibroblast

Authors	Wavelength (nm)	Fluence (J/cm2)	Irradiance	Cell type
Bozkurt et al.[60]	940	18	0.3 W/cm2 0.3 W, 60 s, distance: 0.5 to 1 mm	Cementoblast
Wang et al.[73]	810	3	16 mW/cm2 4 cm2, 188 s	Adipose stem cells
Wang et al.[61]	980	0.3	16 mW/cm2 4 cm2, 18.8 s	Adipose stem cells

Studies using PBM *in vitro* on cells with low numbers of mitochondria that reported positive results are summarized in Table 4. Ineffective parameters *in vitro* in cells with low numbers of mitochondria are reported in Table 8. In some cases, the same studies are included in both Tables 3 and 7 (effective and ineffective parameters) when the authors varied the parameters.

Table 4.

Effective treatment of PBM: *in vitro* studies in cells with lower number of mitochondria.

Table 8.

Ineffective treatment of PBM *in vitro* studies in cells with lower number of mitochondria.

Authors	Wavelength (nm)	Fluence (J/cm2)	Irradiance	Cell type
Tschon et al.[55]	915	20.56	150 mW/cm2 100 Hz, 50% duty cycle, power 0.575 W 144 s	Osteoblast
Migliario et al.[57]	930	1.57	1580 mW/cm2 1 W,1 s, 0.63 cm2	Preosteoblast
Migliario et al.[57]	930	78.7	1580 mW/cm2 1 W, 50 s, 0.63 cm2	Preosteoblast
Skopin et al.[58]	980	5.9	49 mW/cm2	Fibroblast
Skopin et al.[58]	980	14.4	120 mW/cm2	Fibroblast
Zhang et al.[53]	628	9.0	11.4 mW/cm2 15 mW, distance of 0.75 cm	Fibroblast
Khadra et al.[75]	830	0.75	8.4 mW/cm2 84 mW, 10 cm2, 360 s, 9 cm distance to cells	Fibroblast
Wang et al.[73]	980	20	16 mW/cm2 4 cm2, 1 W	Adipose stem cells

3.2.3. In vivo studies in tissues with high number of mitochondria: heart, brain, muscle, inflammation

Oron et al.[62] treated myocardial infarction with LLLT using an 810-nm laser. Fluence was held constant at 0.9 J/cm2 while irradiance was varied to deliver 2.5, 5, and 25 mW/cm2. A peak response was found at 5 mW/cm2, while treatment was less effective when using 2.5 and 25 mW/cm2.

Castano et al.[17] studied inflammatory arthritis in rats, comparing the effect of using high and low fluences (3 to 30 J/cm2) delivered at high and low irradiance (5 to 50 mW/cm2). Effective treatment was observed when using: 30 J/cm2 at 50 mW/cm2 for 10 min and 30 J/cm2 at 5 mW/cm2 for 100 min. Low fluence of 3 J/cm2 at 5 mW/cm2 for 10 min was also effective. Only the dose of 3 J/cm2 at 50 mW/cm2 for 1 min was ineffective. They concluded that at higher fluence (30 J/cm2), the PBM effect on arthritis did not depend on irradiance as both high and low irradiance were effective, while at a lower fluence of 3 J/cm2, only the lower irradiance was effective. Therefore, they concluded that the duration of the light exposure was of great importance. While some studies found (3 J/cm2, 50 mW/cm2) beneficial, this study did not. They suggest that because the duration was only 1 min, the light did not have sufficient time to produce a sufficient activation of cellular metabolism.[17]

Salehpour et al.[77] compared the therapeutic effect of a 10-Hz pulsed wave of NIR (810 nm) and red (630 nm) lasers with citalopram in rats that had been subjected to a model of chronic mild stress that causes depression. After inducing stress in rats, they were divided into: group I receiving PBM using NIR 810 nm and group II receiving 630-nm coherent light using identical parameters of: 10-Hz gated wave (50% duty cycle), fluence of 1.2 J/cm2 per session, output power 35 and 240 mW, respectively, 2 ms duration for both type of lasers, beam diameter of 3 mm, contact mode, and spot size of 0.07 cm2. Laser power was set at 6.2 W in the red wavelength and 39.3 W in the infrared wavelength for an irradiance of 89 and 562 mW/cm2, respectively. The average fluence for each session was 1.2 J/cm2 and totaling 14.4 J/cm2 for the entire 12 session treatment. Finally, group III was treated with the antidepressant drug citalopram that works by decreasing cortisol levels. Results showed that PBM using 10-Hz pulsed NIR laser had a better effect than red laser and the same effect as citalopram.

Salehpour et al.[59] studied brain mitochondrial function in mice after inducing mitochondrial dysfunction by administration of D-galactose. This model is considered to be a model of age-related cognitive dysfunction. Animals were treated with wavelengths of 660 and 810 nm at two different fluences: 4 and 8 J/cm2, 10 Hz, 4.75 W/cm2, 88% duty cycle, 200 mW, in contact, three times a week, 48 h between sessions, and 7-mm diameter power meter sensor. They found poor results with both wavelengths

Authors	Wavelength (nm)	Fluence	Irradiance	Tissue type
Alves et al.[25]	808	142.4 J/cm2	1.78 W/cm2 4 J, 50 mW, 0.028 cm2, 80 s per point	Arthritis
Oron et al.[62,63]	810	0.3 J/cm2	5 mW/cm2 5 mW, area 1.1 cm2, 60 s	Heart
Oron et al.[62,63]	810	0.9 J/cm2	5 mW/cm2	Myocardium tissue
Castano et al.[17]	810	30 J/cm2	50 mW/cm2	Arthritis
Castano et al.[17]	810	30 J/cm2	5 mW/cm2	Arthritis
Castano et al.[17]	810	3 J/cm2	5 mW/cm2	Arthritis
Salehpour et al.[59]	810	1.2 J/cm2	560 mW/cm2 39.3 W, spot size 0.07 cm2	Brain
Salehpour et al.[64]	810	8 J/cm2	89 mW/cm2 6.2 W, spot size 0.07 cm2	Brain
Wu et al.[78]	810	36 J/cm2	15 mW/cm2	Brain
Blanco et al.[70]	1064	250 mW/cm2	60 J/cm2	Brain (human)
Disner et al.[71]	1064	250 mW/cm2	60 J/cm2	Brain (human)
Ando et al.[13]	810	36 J/cm2	50 mW/cm2	TBI
Zhang et al.[67]	810	Fluence reaching the cortex 1.8 to 2.5 J/cm2 Average irradiance 36 J/cm2	150 mW/cm2 Pulse freq 10 Hz, pulse duration 50 ms, 4 min	TBI
Salehpour et al.[68]	810	1.2 J/cm2	89 and 562 mW/cm2 35 and 240 mW 10 Hz, 50% duty cycle; 0.07 cm2	Brain
Baroni et al.[68]	Cluster with 69 LEDs 660/850 nm	206.89 J/cm2	6.89 W/cm2 200 mW; 6 J per diode (30 s); 0.02 cm2 30 J per application point (5×6 J)×6 application points: total energy 180 J	Femoral quadriceps
Zhang et al.[80]	635	0.96 J/cm2	6.37 mW/cm2 5 mW, laser beam width 10 mm, 150 s	Preconditioning myocardium

Authors	Wavelength (nm)	Fluence	Irradiance	Tissue type
Salehpour et al.[59]	660	8 J/cm2	4.75 W/cm2 88% duty cycle, 200 mW, in contact three times a week, 7 mm diameter	Brain
Wu et al.[78]	660	36 J/cm2	15 mW/cm2	Brain
Lopes-Martins et al.[18]	655	0.5 J/cm2	31.25 mW/cm2 2.5 mW, spot area 0.08 cm2, 25 mW, 32 s	Muscle
Lopes-Martins et al.[18]	655	1 J/cm2	31.25 mW/cm2 2.5 mW, spot area 0.08 cm2, 25 mW, 80 s, 2.5 mW	Muscle

at 4 J/cm2 and an amelioration of the aging-induced mitochondrial dysfunction with 8 J/cm2

Wu et al.[78] induced traumatic brain injury (TBI) in mice and treated the animals using 660, 730, 810, or 980 nm, single dose treatment of 36 J/cm2 using an irradiance of 15 mW/cm2, 4-min duration, 4 h after injury. They found a significant improvement for mice having moderate to severe injury only when using 660 nm and 810 nm. The most desirable effect was seen at 810 nm, and both 730 and 980 nm did not produce any benefit.

Lopes-Martins et al.[18] investigated the effect of PBM on muscular fatigue in rats during tetanic contractions. Four groups of 32 rats received different doses of PBMT (0.5, 1.0, and 2.5 J/cm2), using parameters of 655 nm, spot area 0.08 cm2, 25 mW, 2.5 mW; 31.25 mW/cm2. Groups: 0.5 J/cm2 (32 s), 1 J/cm2 (80 s), 2.5 J/cm2 (160 s). Only the groups of 0.5 and 1 J/cm2 prevented the development of muscular fatigue in rats during repeated tetanic contractions.

Lopes-Martins et al.[74] in another study used 650-nm wavelength on acute inflammatory pleurisy in mice. Using the same power of 2.5 mW but different fluences of 3, 7.5, and 15 J/cm2. They found that under these conditions, 7.5 J/cm2 were more effective than either 3 or 15 J/cm2.

De Almeida et al.[79] studied muscle performance after inducing muscle contraction in 30 rats. Using 904 nm, 15-mW average power and different energies (0.1, 0.3, 1.0, and 3.0 J) they found that the 1.0 and 3.0 J groups showed significant enhancement (P<0.01) in total work. They conclude that 1.0 J decreased postexercise muscle damage and enhanced muscle performance.

Studies using PBM *in vivo* in tissues with high numbers of mitochondria that reported positive results are summarized in Table 5. Ineffective parameters PBM *in vivo* in tissues with high numbers of mitochondria are reported in Table 9. In some cases, the same studies are included in both Tables 5 and 9 (effective and ineffective parameters) when the authors varied the parameters.

Table 5.
Effective PBM treatment: *in vivo* on tissues with higher number of mitochondria.

Table 9.

Authors	Wavelength (nm)	Fluence (J/cm2)	Irradiance	Tissue type
Oron et al.[62,63]	810	0.3	2.5 mW/cm2 5 mW, area of irradiation of 1.1 cm2	Heart
Oron et al.[62,63]	810	0.3	25 mW/cm2 5 mW, area of irradiation of 1.1 cm2	Heart
Salehpour et al.[59]	660	4	4.75 W/cm2 10 Hz, 4.75 W/cm2, 88% duty cycle, 200 mW	Brain
Salehpour et al.[59]	810	4	4.75 W/cm2 10 Hz, 4.75 W/cm2, 88% duty cycle, 200 mW	Brain
Wu et al.[78]	980	36	15 mW/cm2	Brain
Alves et al.[25]	808	142.4	3.57 W/cm2 4 J, 50 mW, 0.028 cm2, 80 s per point	Arthritis
Lopes-Martins et al.[18]	655	2.5	31.25 mW/cm2 2.5 mW, spot area 0.08 cm2, 25 mW, 160 s, 2.5 mW	Muscle

Ineffective PBM treatment *in vivo* on tissues with higher number of mitochondria.

Open in a new tab

3.2.4. In vivo studies in tissues with a lower number of mitochondria: skin, bone, cartilage

Lanzafame et al.[15] treated pressure ulcers in mice with a 670-nm diode laser. Maintaining a constant fluence of 5 J/cm2 and using different irradiances (0.7, 2, 8, 40 mW/cm2), they found a significant improvement at 8 mW/cm2.

Prabhu et al.[81] found a biphasic dose response on excisional wound healing in mice when using a He–Ne laser (632 nm, 7 mW, 4 mW/cm2 at different fluences (1, 2, 3, 4,

6, 8, and 10 J/cm2). A clear biphasic dose response occurred with a peak benefit at a fluence of 2 J/cm2 and an inhibitory effect at the higher dose of 10 J/cm2.

Gal et al.[82] compared the wound tensile strength in rats at different power densities using 670 nm. A positive effect was seen when using 4 mW/cm2 delivered for 20 min, 50 s, (5 J/cm2), but this effect was not seen when using 15 mW/cm2 delivered for 5 min, 33 s, (5 J/cm2) at the same wavelength. This suggests that delivering the same fluence at a lower irradiance over more time was more effective.

Al-Watban and Delgado[83] studied, *in vivo*, the effect of laser irradiation on burn wound healing in rats. They created a superficial burn with an area of 1.534 cm2 and irradiated the wound with a diode laser at 670 nm, 200 mW, three times per week for 12 weeks at different doses of 1, 5, 9, and 19 J/cm2. Only the groups receiving the lower doses of 1 and 5 J/cm2 showed significantly better wound healing compared to the control, with the greatest effect obtained at 1 J/cm2.

Studies using PBM *in vivo* in tissues with low numbers of mitochondria that reported positive results are summarized in Table 6. Ineffective parameters PBM *in vivo* in tissues with low numbers of mitochondria are reported in Table 10. In some cases, the same studies are included in both Tables 6 and 10 (effective and ineffective parameters) when the authors varied the parameters.

Table 6.

Authors	Wavelength (nm)	Fluence (J/cm2)	Irradiance	Tissue type
Mendez et al.[21]	830	50	125 mW/cm2 35 mW 0.6 cm diameter	Wound healing
Lanzarfane et al.[15]	670	5	8 mw/cm2	Ulcer
Prabhu et al.[21]	632	2	4.0 mW/cm2 7 mw, 1.75 cm2	Wound healing
Gal et al.[21]	670	5	15 mw/cm2	Wound tensile strength
Al-Watban et al.[21]	670	1 and 5	130 mW/cm2 200 mW, 1.534 cm2	Wound healing
Mendez et al.[21]	830	20	125 mW/cm2 35 mW, 0.6 cm diameter	Wound healing
Barbosa et al.[20]	790	140	3500 mW/cm2 100 mW, 4 J, spot size 0.028 cm2	Bone

Authors	Wavelength (nm)	Fluence (J/cm2)	Irradiance	Tissue type
Barbosa et al.[20]	830	140	3500 mW/cm2 100 mW, 4 J, spot size 0.028 cm2	Bone

Effective PBM treatment: *in vivo* on tissues with lower number of mitochondria.

Open in a new tab

Table 10.

Authors	Wavelength (nm)	Fluence (J/cm2)	Irradiance	Tissue type
Lanzafame et al.[15]	670	5.0	0.7 mW/cm2	Ulcers (wound healing)
Lanzafame et al.[15]	670	5.0	2.0 mW/cm2	Ulcers (wound healing)
Gal et al.[82]	670	5.0	15 mW/cm2	Wound healing
Lanzafame et al.[15]	670	5.0	40 mW/cm2	Wound healing
Prabhu et al.[81]	632	10	4.0 mW/cm2 7 mw, 1.75 cm2	Wound healing
Al-Watban et al.[83]	670	9.0	130 mW/cm2 200 mW, 1.534 cm2	Wound healing
Al-Watban et al.[83]	670	19	130 mW/cm2 200 mW, 1.534 cm2	Wound healing
Kilik et al.[88]	636	5	1 mW/cm2 Probe to wound 10 cm	Wound healing

Ineffective PBM treatment *in vivo* on tissues with lower number of mitochondria.

3.3. III-Effect of Varying the Mode of Delivery on PBM Efficiency: CW or Pulsed

In a comprehensive literature review,[84] Hamblin included 33 studies, nine of them directly comparing pulsed wave and CW. Six of these studies found that pulsed wave offered better results than CW; one study found that both modes were equally effective and only two studies reported better result using CW. Hamblin et al. concluded from this review that pulsed light may be superior to CW light, particularly for wound healing and poststroke management, whereas CW may be more beneficial in patients requiring nerve regeneration. In addition, they concluded that it is impossible to draw any correlation between pulse frequency and pathological condition. They found that no particular frequency appears to be more or less effective than others. Finally, this review reported that the following frequencies were beneficial: 2, 10, 25, 50 Hz when using (670 nm, 20 mW, energy density, 2 J/cm2), 100 Hz when using (808 nm, 37.5 mW/cm2, 0.9 J/cm2) 292 Hz when using (800 mW/cm2; 21.6 J/cm2),

600 Hz when using (670 nm, 10 mW, 5 J/cm2), 1000 Hz when using (808 nm, 7.5 mW/cm2, 0.9–1.2 J, duty cycle, 30%), 1500 Hz when using (5 mW/cm2); 3000 Hz when using (10 mW/cm2) and 8000 Hz (N/A).

Gigo-Benato et al.[14] compared the effect of combined CW and pulsed laser (CW+PW) using 808 nm (CW) and 905 nm (PW) to either the CW (808 nm) or PW (905 nm) laser used separately. CW was applied at 29 J/cm2 while the pulsed wave laser was applied at 40 J/cm2. Results suggested that the combined laser was more effective in nerve regeneration than the CW alone or the PW alone.

Al-Watban and Zhang[16] evaluated the effects of using both pulsed and CW PBM in rats wound healing. After creation of elliptical wounds, animals were treated with a 635-nm diode laser, average power of 3.4 mW, spot size of 3.8 cm2, wound size of 1.04 cm2, irradiance of 0.89 mW/cm2, treatment duration 18.7 min and fluence of 1 J/cm2, three times per week. The dose was delivered using either CW or pulsed mode at: 100, 200, 300, 400, or 500 Hz. They found that the effect of using CW was more efficient than using pulsed laser and, when comparing different frequencies, 100 Hz had better effect on wound healing than the other frequencies.

This article contradicts Hamblin, who concluded that pulsed mode was more effective than CW in wound healing. Perhaps, Al-Watban found that CW was more efficient because he did not use the same fluence in CW that he used in pulsed mode. Moreover, he used gated CW rather than true pulsed wave.[16]

Ando et al.[13] treated TBI in mice comparing pulsed and CW 810-nm laser irradiation. The parameters used were: 810-nm diode laser, irradiance of 50 mW/cm2, spot diameter of 1 cm onto the injured head with a 12-min exposure giving a fluence of 36 J/cm2. They found that 10 Hz produced better results than 100 Hz or continuous mode.

el Sayed and Dyson[85] compared the effect of four different frequencies (2.5, 20, 292 and 20,000 Hz) and found that only 20 and 292 Hz were beneficial.

Sushko et al.[86] investigated pain induced in mice by hypodermic injection of 20 ml of 5% formalin solution into the footpad. They irradiated the mice using 640 and 880 nm LED in continuous or pulsed mode for 10 min. They found that pulsed mode was more effective than CW and frequencies of 10 and 8000 Hz were most effective, whereas pulse repetition rates of 200 and 600 Hz were less effective.

Ueda and Shimizu[87] studied the effect of three different pulse repetition rates on osteoblast-like cells from rats using these parameters (830 nm, 500 mW, 0.48 to 3.84 J/cm2) in CW mode and (1, 2, and 8 Hz) in pulsed mode. They found that 1 and

2 Hz markedly stimulated cellular proliferation, ALP activity, ALP gene expression, and bone nodule formation, and that 2 Hz was the best pulse repetition rate to stimulate bone nodule formation.

4. Review of Which Parameters Lead to Effective and Ineffective PBMT

It is difficult to compare studies done with different parameters, protocols, treatment objectives, and biological target tissues. Often, parameters are not completely presented or are of questionable accuracy. In this part of the review analysis, an attempt is made to draw at least some general inferences from the data presented in Tables 3–10.

4.1. Wavelength

Wavelength affects tissue penetration. Shorter wavelengths (600 to 700 nm) are considered best to treat superficial tissue, whereas longer wavelengths (780 to 950 nm) are preferred to treat deeper tissues. Red wavelengths penetrate 0.5 to 1 mm and near-infrared energy penetrates 2 mm before losing 37% of its intensity.[89–91]

The infrared wavelengths show better effects on bone repair compared to red wavelengths because red light has less capacity to penetrate compared to the infrared laser.

According to Karu,[8] wavelengths between 700 and 770 nm do not have any significant activity. Wu et al.[78] used a 730-nm laser on TBI in mice and found it to be ineffective while 660 and 810 nm lasers were effective. Gupta et al.[92] carried out a similar comparison on wound healing in mice and again found that 660- and 810-nm lasers were effective, while a 730-nm laser was not effective.

Barbosa et al.[20] concluded that the PBM effects of NIR were effective for more than 14 days, whereas the effects of red wavelength are lost after 14 days.

The combination of two wavelengths gives an additional effect of PBM. When comparing 830 and 685 nm, Mendez et al.[21] found that 830 nm offered better results. Much work still remains to define the optimal wavelengths. Nevertheless, NIR wavelengths are preferable for deep tissues and targets within the body, which require substantial doses of light.

4.2. Laser Versus Noncoherent Light

Both coherent lasers and noncoherent LEDs are used in PBMT. Laser beams are collimated and the light is more likely to be forward scattered within the tissue than noncollimated LED light.[5] This means that the penetration depth is likely to be deeper with lasers provided all the other characteristics are identical. Moreover, lasers emit coherent light, while LED light is noncoherent. The coherence length is higher for smaller bandwidths. For instance, gas lasers such as He–Ne laser have very long coherence lengths. Diode lasers have somewhat greater bandwidths and consequently shorter coherence lengths. When coherent laser light interacts with tissue, small imperfections in the tissue structure lead to different phases occurring in the individual wavefronts leading to mutual interference patterns. These interference patterns are called “laser speckles” and the size of the speckles is related to the light wavelength. In the visible range, the sizes are less than 1 μm. Subcellular organelles (such as mitochondria) have dimensions of this order and a theory proposes that the laser speckles are better to stimulate mitochondria than noncoherent LED light.[93–95] A recent review concluded that there were no substantial differences between lasers and LEDs for PBM applications provided all the other light parameters were equal.[96]

4.3. Fluence and Irradiance

The photon intensity i.e., irradiance (W/cm2 or spectral irradiance), must be adequate. Using higher intensity, the photon energy will be transformed to excessive heat in the target tissue and, using lower intensity, photons absorption will be insufficient to achieve the goal.

The dose also must be adequate (J/cm2). Using low irradiance and prolonging the irradiation time to achieve the ideal fluence or dose will not give an adequate final result. The Bunsen–Roscoe law of reciprocity, termed the second law of photobiology,[97] does not hold true for low incident power densities.

There is no fixed value of dose or fluence that always produces a positive PBM effect. Even within different studies on the same animal models, there can be contradictory findings. For instance, three papers looked at peri-implant bone regeneration after PBM. Menezes et al.[98] found that 20 J/cm2 was the best dose to deliver, whereas Massotti et al.[22] and Mayer et al.[23] found that 20 J/cm2 was the worst dose to deliver.

The optimal doses are directly related to different factors:

- •

  Wavelength

- •

Type of treatment being delivered: pain relief, wound healing, or tissue regeneration

- •

  Power density or irradiance

- •

  Energy density or fluence

- •

  Depth of the target tissue being treated

- •

  Spot size of the beam reaching the tissue surface and the actual target tissue.

In an attempt to determine whether the delivered fluence (J/cm2) was more or less important than the irradiance (mW/cm2), we constructed scatter plots (Figs. 1–4) of both the effective and ineffective studies arranged according to our categorization of the studies in Tables 2–9.

Fig. 1.

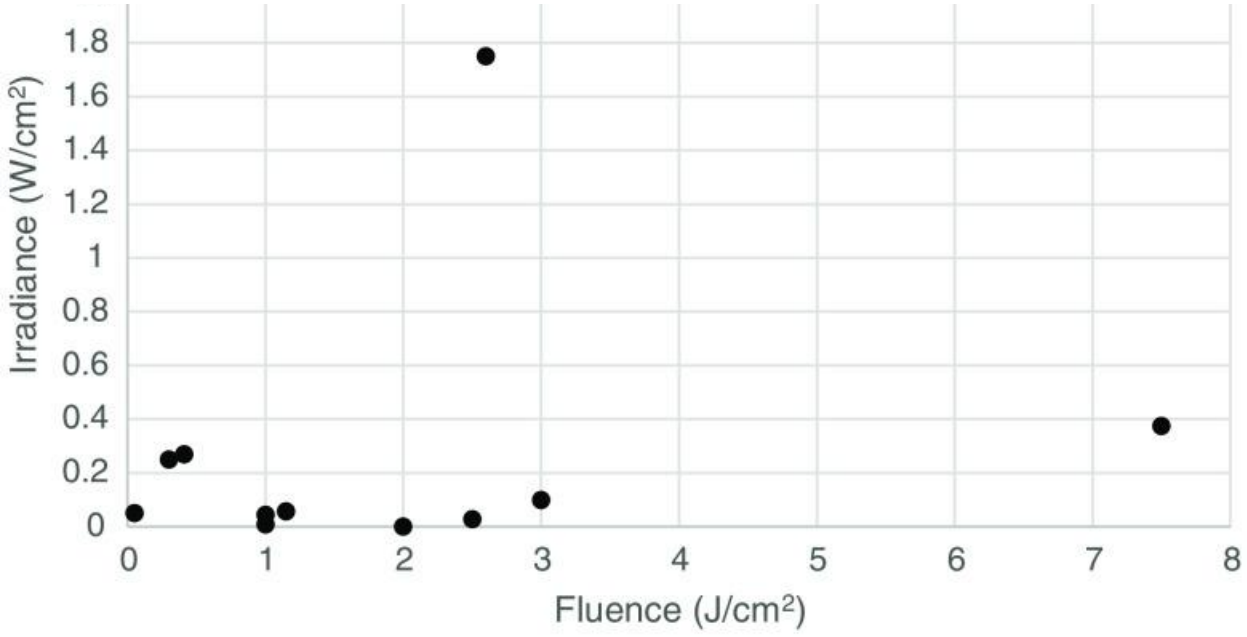
Irradiance (W/cm²)
1.8
1.6
1.4
1.2
1
0.8
0.6
0.4
0.2
0
0
1
2
3
4
5
6
7
8
Fluence (J/cm²)

(a)

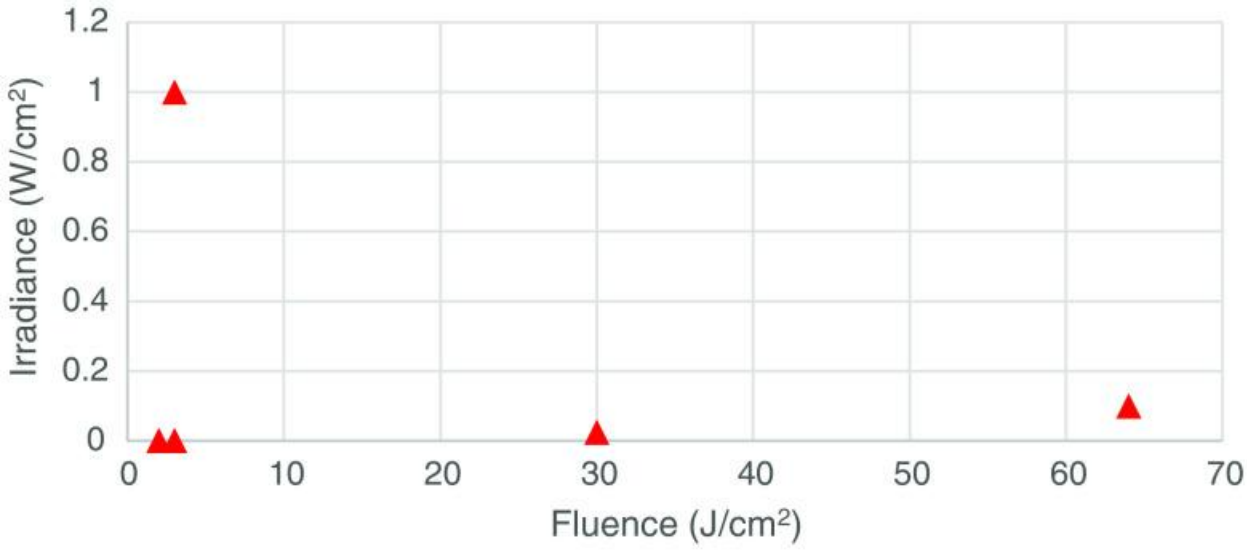
Irradiance (W/cm²)
1.2
1
0.8
0.6
0.4
0.2
0
0
10
20
30
40
50
60
70
Fluence (J/cm²)

(b)


Irradiance (W/cm²)
2
1.8
1.6
1.4
1.2
1
0.8
0.6
0.4
0.2
0

Studies on PBM of cells *in vitro* with higher numbers of mitochondria. (a) Effective (positive studies), (b) ineffective (negative studies), and (c) combination of effective (positive studies), and ineffective (negative studies).

Fig. 2.

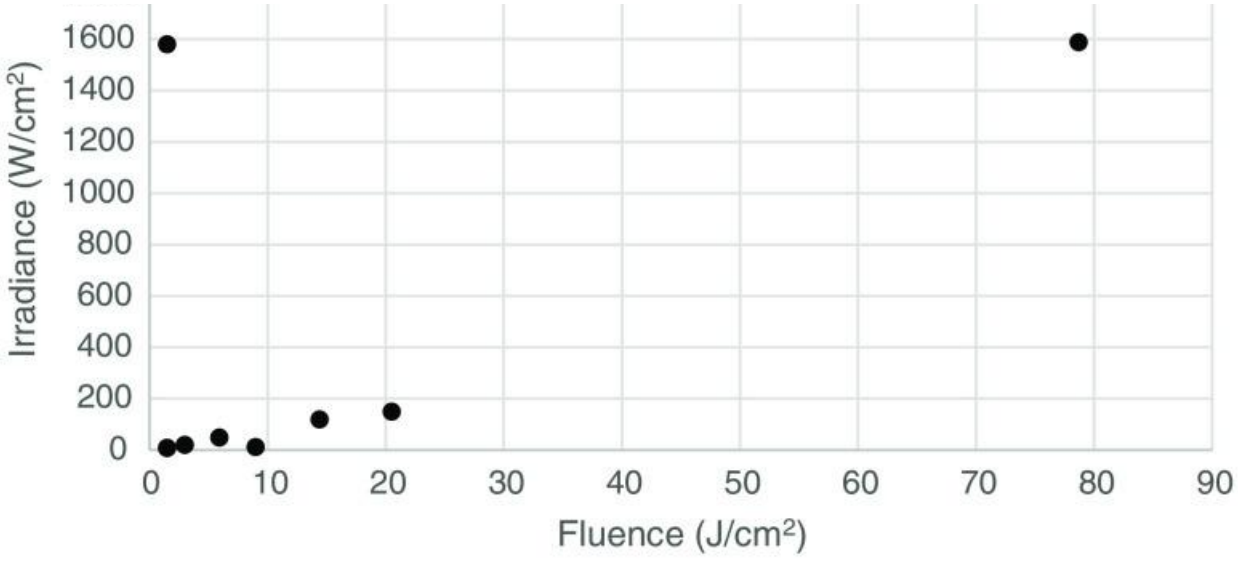
Irradiance (W/cm²)
1600
1400
1200
1000
800
600
400
200
0
0
10
20
30
40
50
60
70
80
90
Fluence (J/cm²)

(a)

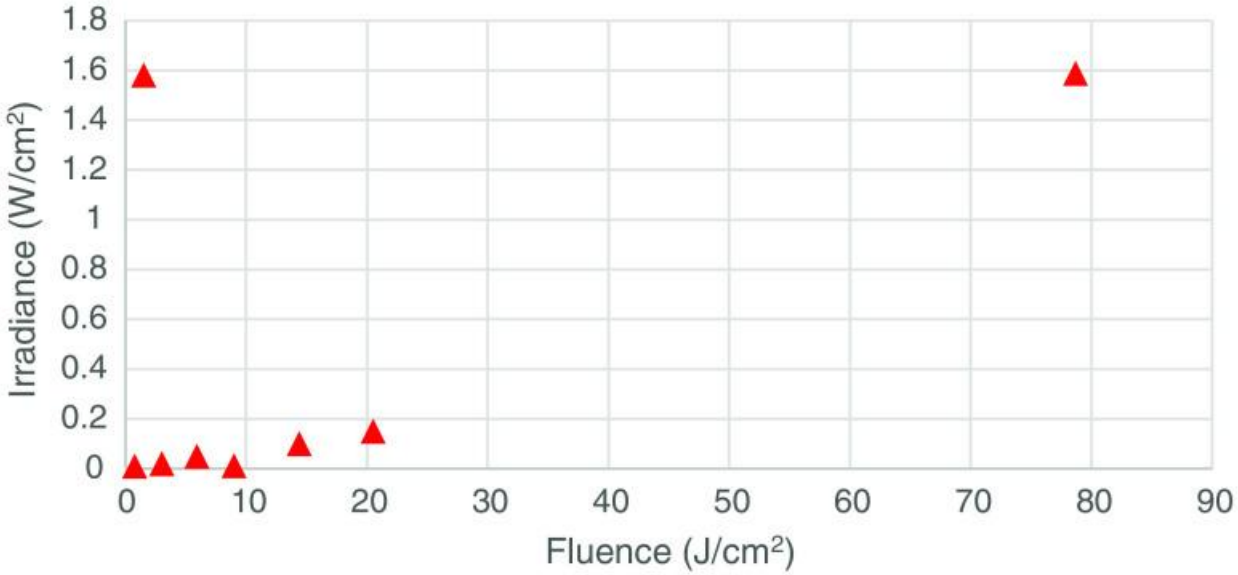
Irradiance (W/cm²)
1.8
1.6
1.4
1.2
1
0.8
0.6
0.4
0.2
0
0
10
20
30
40
50
60
70
80
90
Fluence (J/cm²)

(b)

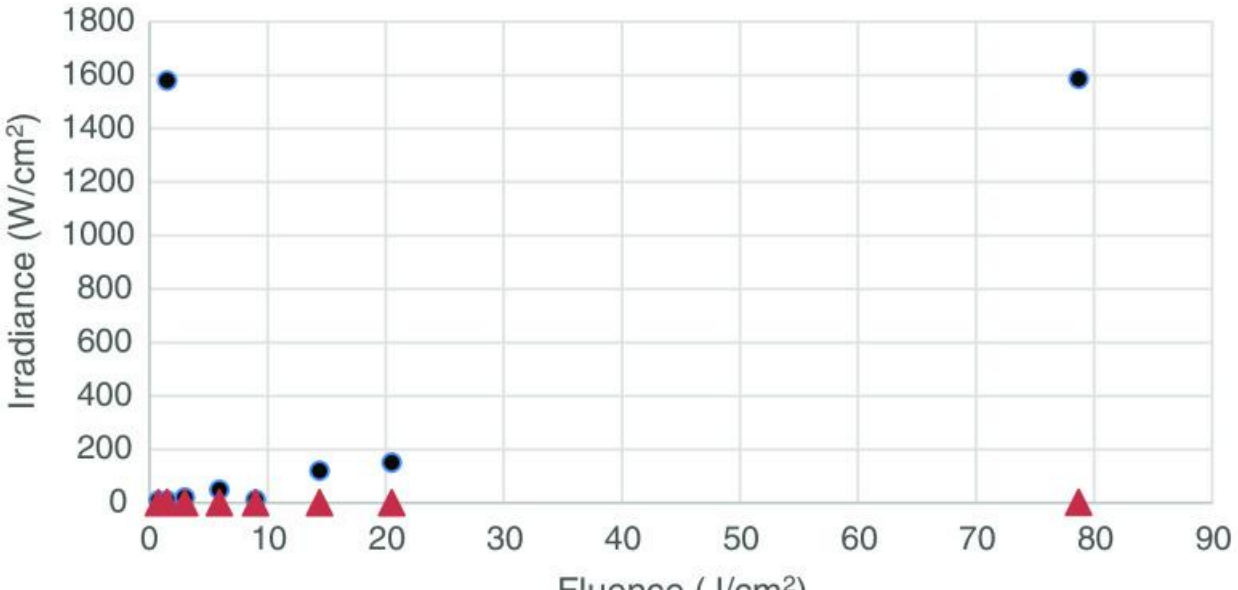
Irradiance (W/cm²)
1800
1600
1400
1200
1000
800
600
400
200
0
0
10
20
30
40
50
60
70
80
90

Open in a new tab

Studies on PBM of cells *in vitro* with lower numbers of mitochondria. (a) Effective (positive studies), (b) ineffective (negative studies), and (c) combination of effective (positive studies) and ineffective (negative studies).

Fig. 3.

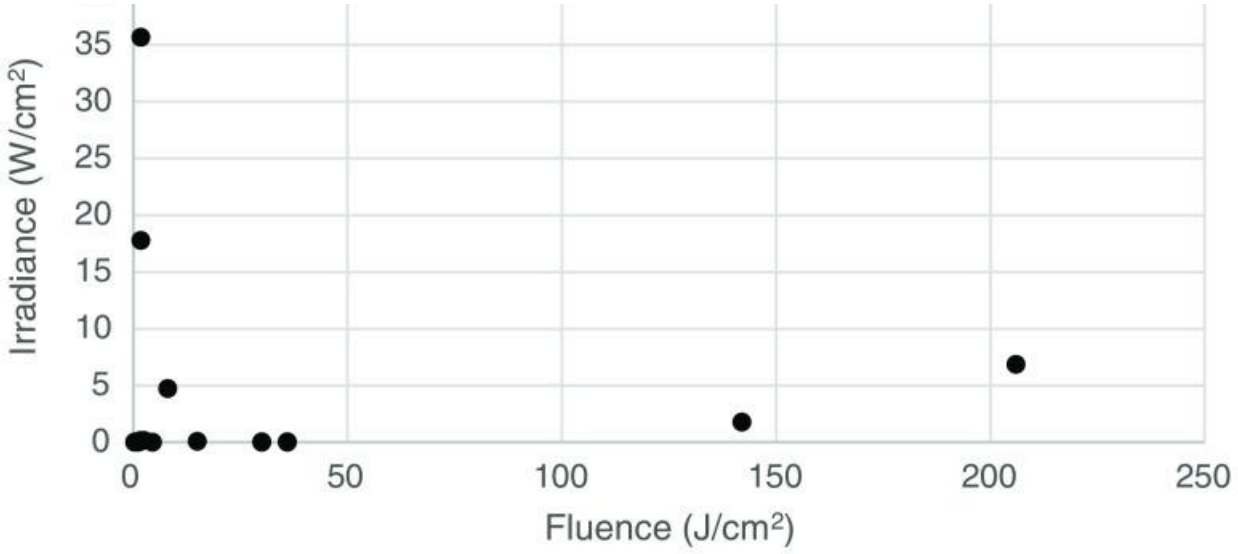
Irradiance (W/cm²)
35
30
25
20
15
10
5
0
0
50
100
150
200
250
Fluence (J/cm²)

(a)

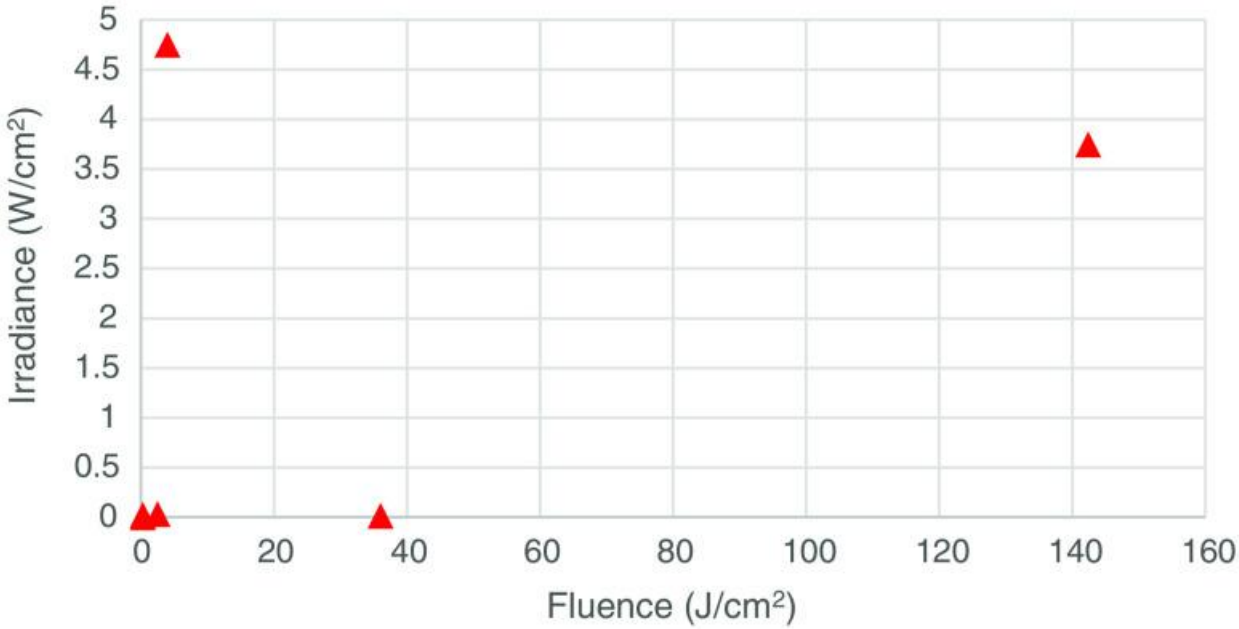
Irradiance (W/cm²)
5
4.5
4
3.5
3
2.5
2
1.5
1
0.5
0
0
20
40
60
80
100
120
140
160
Fluence (J/cm²)

(b)

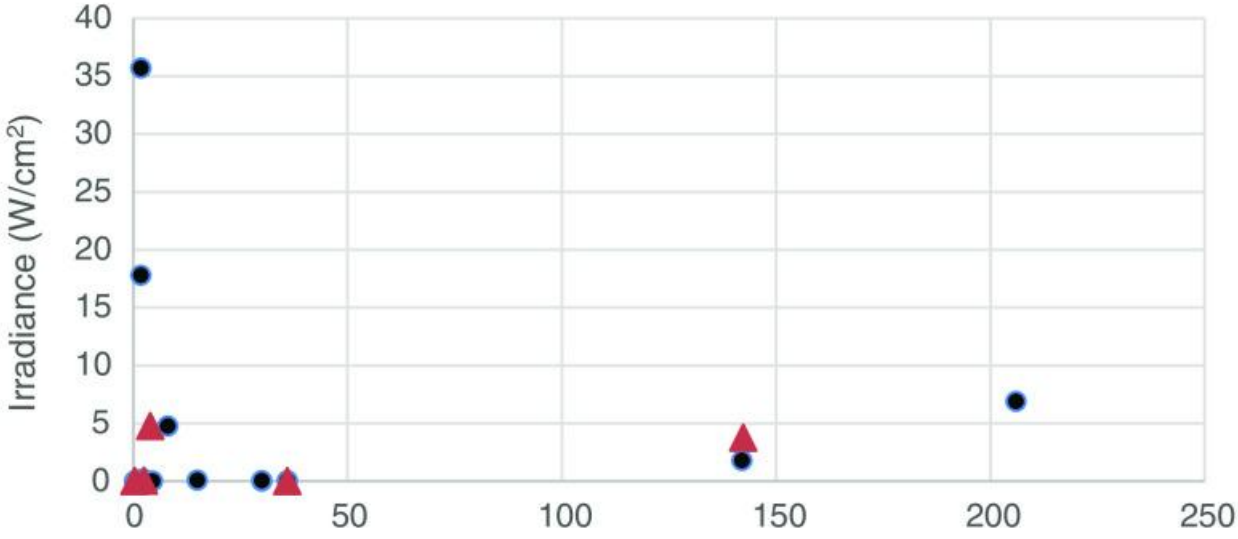
Irradiance (W/cm²)
40
35
30
25
20
15
10
5
0
0
50
100
150
200
250

Open in a new tab

Studies on PBM of tissues *in vivo* with higher numbers of mitochondria. (a) Effective (positive studies), (b) ineffective (negative studies), and (c) combination of effective (positive studies) and ineffective (negative studies).

Fig. 4.

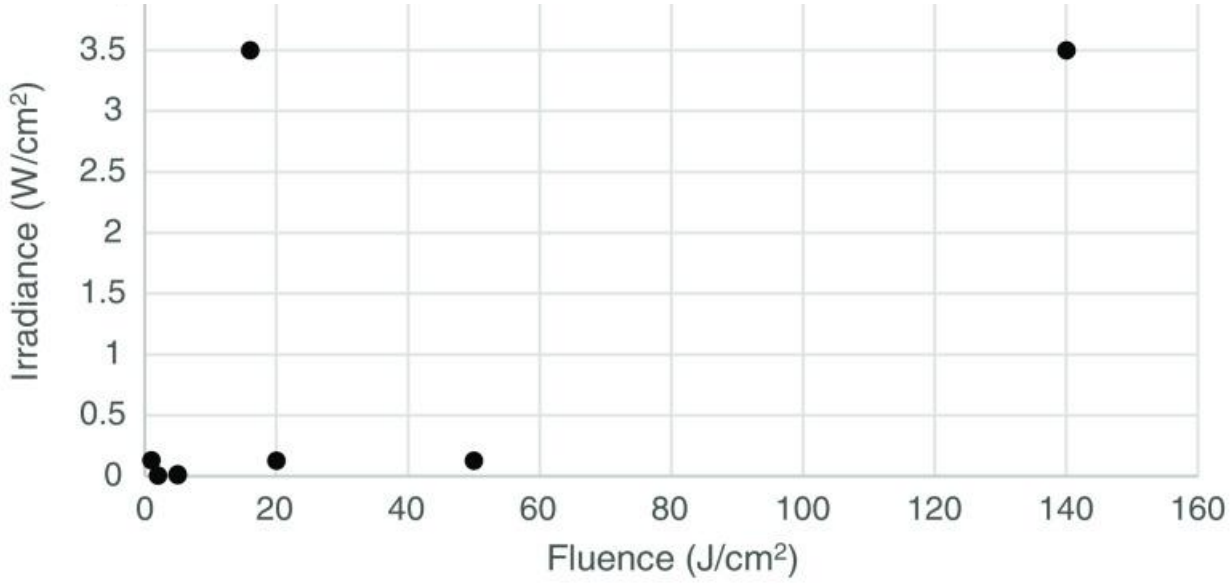
Irradiance (W/cm²)
3.5
3
2.5
2
1.5
1
0.5
0
0
20
40
60
80
100
120
140
160
Fluence (J/cm²)

(a)

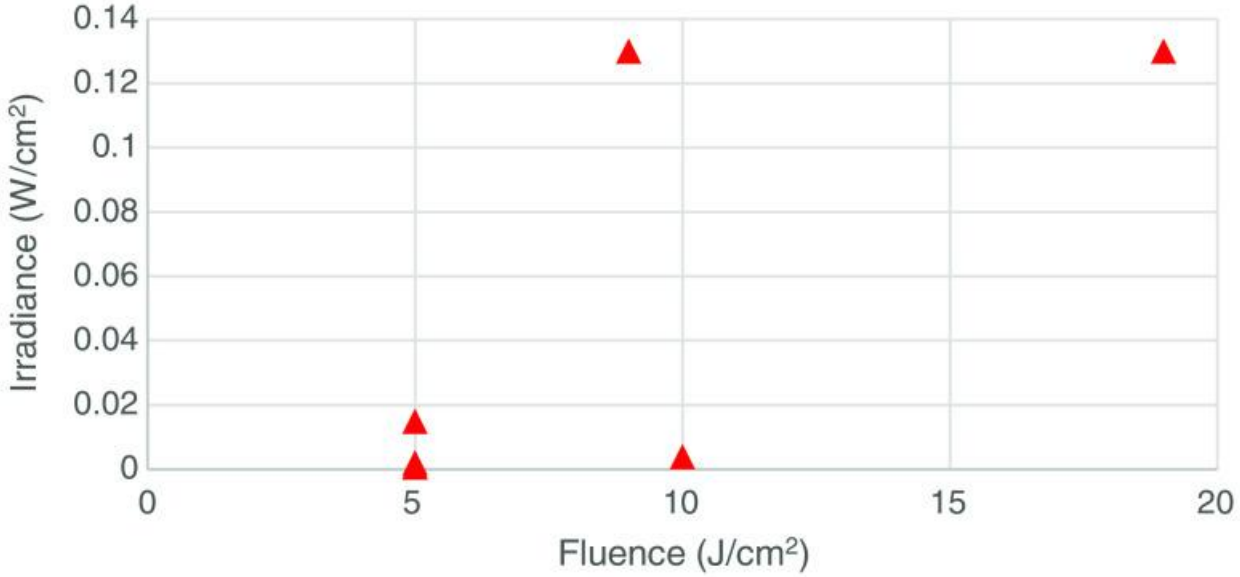
Irradiance (W/cm²)
0.14
0.12
0.1
0.08
0.06
0.04
0.02
0
0
5
10
15
20
Fluence (J/cm²)

(b)

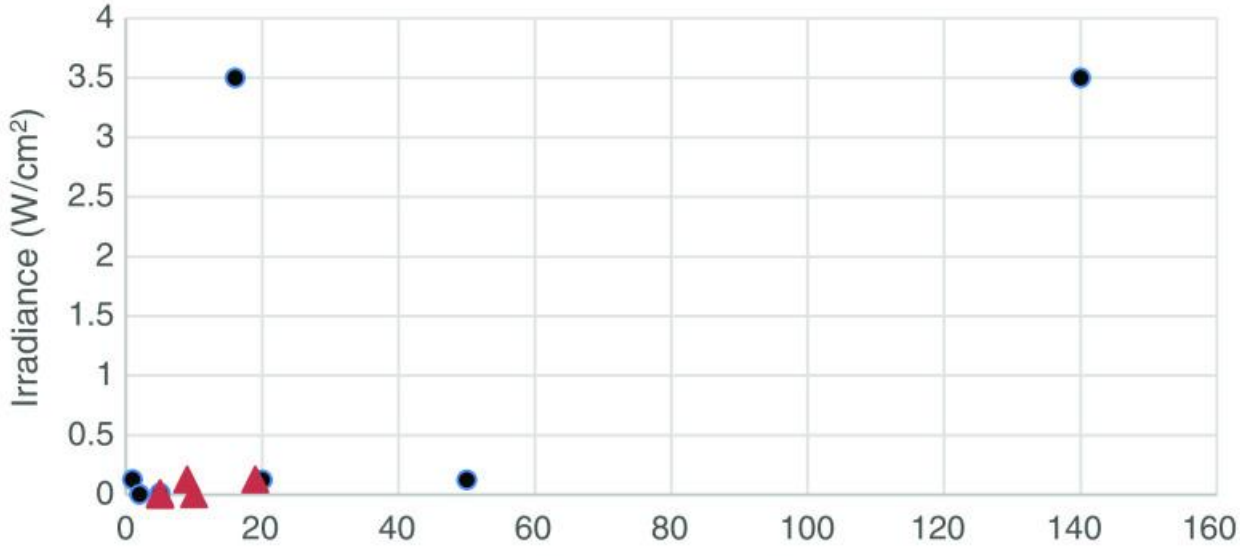
Irradiance (W/cm²)
4
3.5
3
2.5
2
1.5
1
0.5
0
0
20
40
60
80
100
120
140
160

Studies on PBM of tissues *in vivo* with lower numbers of mitochondria. (a) Effective (positive studies), (b) ineffective (negative studies), and (c) combination of effective (positive studies) and ineffective (negative studies).

4.3.1. In vitro studies

Figure 1(a) shows the plot of *in vitro* studies in cells with higher numbers of mitochondria, whereas Fig. 1(b) shows the corresponding plot for cells with lower numbers of mitochondria. The following observations can be made. In all the effective studies, the fluence was relatively low (<7.5 J/cm2) and in several cases, less than 1 J/cm2. However, in the ineffective studies, the fluence values were larger (all >3 J/cm2), and in two cases, very large values (30 and 65 J/cm2). There were more studies in the effective group (11) than in the ineffective group (5). This suggests that high-mitochondrial cells respond well to PBM and that ineffective studies are more likely to be due to over-dosing than to under-dosing.

Figure 2(a) shows the effective *in vitro* studies in cells with lower mitochondrial numbers. Again, the positive studies outweigh the negative studies [Fig. 2(b)] (15 to 8). The fluence values in the positive studies in the lower mitochondrial number subgroup appeared to be overall higher than the fluences used in the positive studies in the higher mitochondrial number subgroup. The fluences used in the negative studies in the lower mitochondrial number subgroup were only a little higher than those in the positive studies, suggesting that over-dosing was not such a big problem as it was in the higher mitochondrial number subgroup [Fig. 1(b)]. There were three positive studies that used relatively high irradiances (>1.5 W/cm2), as opposed to only one study in the positive high-mitochondrial subgroup.

4.3.2. In vivo studies

Figure 3(a) shows the plot of effective or positive studies *in vivo* on tissues composed of cells with higher numbers of mitochondria, whereas Fig. 3(b) shows the corresponding plot for ineffective or negative studies on tissues composed of higher mitochondrial number cells. Here, a difference is seen when comparing the two plots and with the analogous two plots from the *in vitro* studies. In the *in vivo* case, the fluence values in the effective studies subgroup [Fig. 3(a)] are higher than those in the ineffective studies subgroup [Fig. 3(b)]. This is the opposite of what was found in the *in vitro* case with cultured cells [compare Figs. 1(a) with 1(b)]. Hence, these observations tend to suggest that failure, *in vivo*, could be due to under-dosing while failure, *in vitro*, could equally well be due to over-dosing. *In vivo*, the depth of the tissue is important, while cells, *in vitro* culture, are generally a single monolayer. It is a fact that tissues with higher numbers of mitochondria (brain, heart, muscles, inflammatory cells) tend to be deeper within the body than tissues with lower numbers of mitochondria (skin, tendons, cartilage). There are, of course, some exceptions (bones and bone marrow), which have lower numbers of mitochondria but are still deep within the body.

Figure 4(a) shows the plot of effective treatment in tissue with a lower number of mitochondria, whereas Fig. 4(b) shows the plot of ineffective treatment on tissue with a lower number of mitochondria.

The following observation can be made:

The fluence values used in the positive studies are much higher than those in the negative studies, particularly when the tissue is deeper (such as bone). In addition, some studies used very low fluences of less than 1 J/cm2 to treat superficial tissue (wound healing) and had positive results.

Fluences used in the negative studies are generally less than 10 J/cm2, most of them used low irradiance. There are three studies that use lower fluence in combination with higher irradiance and produced positive results.

This would suggest that ineffective studies for tissue with lower mitochondria are more likely to be due to under-dosing rather than over-dosing. Fluence and irradiance are both important in determining the success of *in vivo* studies.

5. Conclusions

The limitation of this analysis was the relatively small number of studies that passed our inclusion and exclusion criteria. Nevertheless, some tentative conclusions can be drawn from the analysis that we can at least propose for other researchers to confirm or refute, as more well-documented studies continue to be published in the coming years.

- 1.

  Cells with higher numbers of mitochondria respond better to PBM than cells with lower numbers of mitochondria.

- 2.

  Ineffective studies on cells with higher numbers of mitochondria are as likely to be due to over-dosing as they are to under-dosing.

- 3.

  It is less likely that ineffective studies in cells with lower numbers of mitochondria will be due to over-dosing.

- 4.

The fluence delivered is more important in determining the success or failure of an *in vitro* study than the irradiance employed.

- 5.

  Tissues with higher numbers of mitochondria tend to be deeper within the body than tissues with lower numbers of mitochondria, therefore, over-dosing is less likely.

- 6.

  Ineffective studies *in vivo* are more likely to be due to under-dosing regardless of the number of mitochondria.

Acknowledgments

M.R.H. was supported by US NIH Grant Nos. R01AI050875 and R21AI121700.

Biographies

Randa Zein graduated as a dental surgeon from Lebanese University and became a restorative and aesthetic specialist in Toulouse, France. She holds her master's degree of laser dentistry in Genoa, Italy, and currently, she is enrolled in the PhD program of tissue engineering at Cardiff University, United Kingdom. Her field of interest is the use of technology to find new technical ways to treat Parkinson disease and tumor metastases.

Wayne Selting holds a BSc degree in electrical engineering and a MSc degree in biomedical engineering as well as a DDS. He is a former codirector of a postdoctoral master's degree in laser dentistry at Ospedale San Martino, University of Genoa, Italy. His research interests are in tissue penetration of laser and LED treatment modalities as well as optimizing parameters for both laser surgical intervention and photobiomodulation.

Michael R. Hamblin is a principal investigator at the Wellman Center for Photomedicine at Massachusetts General Hospital and an associate professor at Harvard Medical School since 1994. His research interests are in photodynamic therapy for antimicrobial applications and the treatment of localized infections, and for the stimulation of antitumor immunity. In photobiomodulation, he works on cellular and molecular mechanisms, applications to Alzheimer's and other brain diseases, pain, inflammation, and wound healing.

Disclosures

M.R.H. is on the Scientific Advisory Boards of the following companies: Transdermal Cap Inc., Cleveland, Ohio; Photothera Inc., Carlsbad, California; BeWell Global Inc., Wan Chai, Hong Kong; Hologenix Inc., Santa Monica, California; LumiThera Inc., Poulsbo, Washington; Vielight, Toronto, Canada; Bright Photomedicine, Sao Paulo, Brazil; Quantum Dynamics LLC, Cambridge, Massachusetts; Global Photon Inc., Bee

Cave, Texas, Medical Coherence, Boston, Massachusetts; NeuroThera, Newark DE JOOVV Inc., Minneapolis-St. Paul, Minnesota; Illumiheal & Petthera, Shoreline, Washington; MB Lasertherapy, Houston, Texas and has consulted for: USHIO Corp,. Japan; Merck KGaA, Darmstadt, Germany; Philips Electronics Nederland B.V.; Johnson & Johnson Inc., Philadelphia, Pennsylvania; UVLRx Therapeutics, Oldsmar, Florida; Ultralux UV Inc., Lansing MI; AIRx Medical, Pleasanton, California; FIR Industries, Inc., Ramsey, New Jersey.

Which wavelength is optimal for transcranial low-level laser stimulation?

Pengbo Wang [1,2], Ting Li [1,2]
Affiliations Expand

- PMID: 30043500
- DOI: 10.1002/jbio.201800173

Abstract

One of the challenges in transcranial low-level laser therapy (LLLT) is to optimally choose illumination parameters, such as wavelength. However, there is sparse study on the wavelengths comparison especially on human transcranial LLLT. Here, we employed Monte Carlo modeling and visible human phantom to compute the penetrated photon fluence distribution within cerebral cortex. By comparing the fluence distribution, penetration depth and the intensity of laser-tissue-interaction within brain among all candidate wavelengths, we found that 660, 810 nm performed much better than 980, 1064 nm with much stronger, deeper and wider photon penetration into cerebral tissue; 660 nm was shown to be the best and slightly better than 810 nm. Our computational finding was in a surprising accordance with previous LLLT-neurobehavioral studies on mice. This study not only offered quantitative comparison among wavelengths in the effect of LLLT light penetration effectiveness but also anticipated a delightful possibility of online, precise and visible optimization of LLLT illumination parameters.

Keywords: Monte Carlo modeling; low-level laser therapy (LLLT); photon fluence distribution; transcranial low-level laser stimulation; visible human.

PubMed Disclaimer

Similar articles

- Quantitative analysis of transcranial and intraparenchymal light penetration in human cadaver brain tissue.

  Tedford CE, DeLapp S, Jacques S, Anders J.Lasers Surg Med. 2015 Apr;47(4):312-22. doi: 10.1002/lsm.22343. Epub 2015 Mar 13.PMID: 25772014

- Penetration Profiles of Visible and Near-Infrared Lasers and Light-Emitting Diode Light Through the Head Tissues in Animal and Human Species: A Review of Literature.

  Salehpour F, Cassano P, Rouhi N, Hamblin MR, De Taboada L, Farajdokht F, Mahmoudi J.Photobiomodul Photomed Laser Surg. 2019 Oct;37(10):581-595. doi: 10.1089/photob.2019.4676. Epub 2019 Sep 25.PMID: 31553265 Review.

- Transcranial low level laser (light) therapy for traumatic brain injury.

  Huang YY, Gupta A, Vecchio D, de Arce VJ, Huang SF, Xuan W, Hamblin MR.J Biophotonics. 2012 Nov;5(11-12):827-37. doi: 10.1002/jbio.201200077. Epub 2012 Jul 17.PMID: 22807422 **Free PMC article.** Review.

- Optical Properties and Fluence Distribution in Rabbit Head Tissues at Selected Laser Wavelengths.

  Shanshool AS, Lazareva EN, Hamdy O, Tuchin VV.Materials (Basel). 2022 Aug 18;15(16):5696. doi: 10.3390/ma15165696.PMID: 36013828 **Free PMC article.**

- Effect of wavelength and beam width on penetration in light-tissue interaction using computational methods.
  Ash C, Dubec M, Donne K, Bashford T.Lasers Med Sci. 2017 Nov;32(8):1909-1918. doi: 10.1007/s10103-017-2317-4. Epub 2017 Sep 12.PMID: 28900751 **Free PMC article.**

Cited by

- Modifying Alzheimer's disease pathophysiology with photobiomodulation: model, evidence, and future with EEG-guided intervention.

Lim L.Front Neurol. 2024 Aug 23;15:1407785. doi: 10.3389/fneur.2024.1407785. eCollection 2024.PMID: 39246604 **Free PMC article.** Review.

- Devices used for photobiomodulation of the brain-a comprehensive and systematic review.

  Fernandes F, Oliveira S, Monteiro F, Gasik M, Silva FS, Sousa N, Carvalho Ó, Catarino SO.J Neuroeng Rehabil. 2024 Apr 10;21(1):53. doi: 10.1186/s12984-024-01351-8.PMID: 38600582 **Free PMC article.** Review.

- Phototherapy of Alzheimer's Disease: Photostimulation of Brain Lymphatics during Sleep: A Systematic Review.

  Semyachkina-Glushkovskaya O, Penzel T, Poluektov M, Fedosov I, Tzoy M, Terskov A, Blokhina I, Sidorov V, Kurths J.Int J Mol Sci. 2023 Jun 30;24(13):10946. doi: 10.3390/ijms241310946.PMID: 37446135 **Free PMC article.** Review.

- Photobiomodulation for knee osteoarthritis: a model-based dosimetry study.

  Feng Z, Wang P, Song Y, Wang H, Jin Z, Xiong D.Biomed Opt Express. 2023 Mar 30;14(4):1800-1817. doi: 10.1364/BOE.484865. eCollection 2023 Apr 1.PMID: 37078045 **Free PMC article.**

- Effects of 660-nm LED photobiomodulation on drebrin expression pattern and astrocyte migration.
  Yoon SR, Chang SY, Lee MY, Ahn JC.Sci Rep. 2023 Apr 17;13(1):6220. doi: 10.1038/s41598-023-33469-5.PMID: 37069238 **Free PMC article.**

Published: 02 March 2024

The long and winding road of reprogramming-induced rejuvenation

- Ali Doğa Yücel &
- Vadim N. Gladyshev

Nature Communications **volume 15**, Article number: 1941 (2024) Cite this article

Abstract

Organismal aging is inherently connected to the aging of its constituent cells and systems. Reducing the biological age of the organism may be assisted by reducing the age of its cells - an approach exemplified by partial cell reprogramming through the expression of Yamanaka factors or exposure to chemical cocktails. It is crucial to protect cell type identity during partial reprogramming, as cells need to retain or rapidly regain their functions following the treatment. Another critical issue is the ability to quantify biological age as reprogrammed older cells acquire younger states. We discuss recent advances in reprogramming-induced rejuvenation and offer a critical review of this procedure and its relationship to the fundamental nature of aging. We further comparatively analyze partial reprogramming, full reprogramming and transdifferentiation approaches, assess safety concerns and emphasize the importance of distinguishing rejuvenation from dedifferentiation. Finally, we highlight translational opportunities that the reprogramming-induced rejuvenation approach offers.

Article 07 March 2022

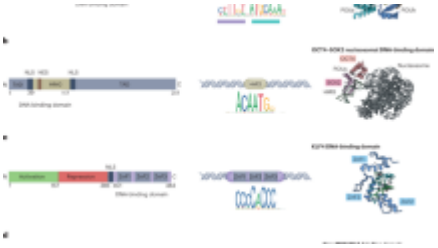

[Mechanisms, pathways and strategies for rejuvenation through epigenetic reprogramming]

Article 15 December 2023

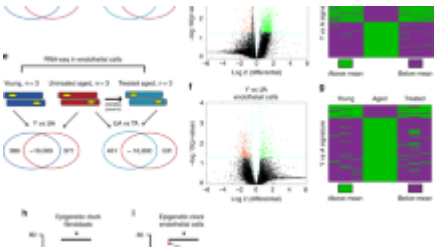

[Transient non-integrative expression of nuclear reprogramming factors promotes multifaceted amelioration of aging in human cells]

Article Open access24 March 2020

Introduction

Over the last century, remarkable strides in medicine and public health have contributed significantly to a substantial increase in average human lifespan. Diseases associated with aging are now the leading causes of mortality worldwide in humans[1]. However, disease-focused treatments have limitations, as incidence increases in parallel for many chronic diseases, and treating one disease often makes little difference on total disease burden. As such, aging-related illnesses are more and more challenging to manage with patients' advancing age. We now face the situation when geriatric medicine becomes progressively more impractical.

Preventive treatments targeting aging present a considerable potential as an alternative approach to combating aging-related diseases. However, to control the aging process—by either slowing it down or reversing it—one must understand the fundamental mechanisms of aging. For example, it is now well appreciated that epigenetic information is progressively lost over the lifetime of an organism[2], disrupting cellular homeostasis. Epigenetic biomarkers of

aging (aging clocks) can predict biological age through a variety of training approaches, even when based only on the variance of DNA methylation during aging[3]. Interestingly, reacquisition of the lost epigenetic information may be observed during the natural rejuvenation process that occurs during early embryogenesis as well as during cell reprogramming[4,5,6]. These strategies are in line with the notion of reprogramming-induced rejuvenation (RIR)[7], a recent discovery wherein old cells can revert to a younger state upon transcription factor or chemical treatments[8,9]. RIR is commonly accomplished through partial cell reprogramming, a method in which cells transiently undergo an induced pluripotent stem cell (iPSC) reprogramming[10,11,12,13,14,15,16]. In this perspective, we discuss recent advances in this area, offer insights how they are related to the nature of aging and rejuvenation, and highlight potential advantages and drawbacks of this RIR and its translational potential.

It was shown that partial cell reprogramming can enhance the physiological function of human muscle stem cells[10], ameliorate the aging mouse transcriptome and metabolome in vivo[11], rejuvenate human dermal fibroblasts on a multi-omics level[12], and reverse the epigenetic clock in vitro[10,12,13]. Furthermore, partial reprogramming can restore visual function in mice[14], prevent age-related physiological changes[8,15], and extend the remaining lifespan in wild-type mice[16]. The clinical potential of partial cell reprogramming is undeniable, but the technology has its pitfalls. We discuss potential future directions of partial cell reprogramming for therapeutic applications and biological mechanisms that support RIR. Lastly, we discuss the safety concerns of partial reprogramming and the significance of isolating RIR from dedifferentiation.

Therapeutic potential of partial reprogramming

Partial reprogramming holds significant therapeutic potential due to its capacity for cellular rejuvenation. There are two primary approaches that may help realize the therapeutic applications of this procedure. Organismal rejuvenation is the most challenging but also the most direct approach, due to its potential to reverse aging in a manner that is independent of the identity of the cells to which it is applied. Methods for reversing aging carry the potential to generate therapies that are more efficient and effective than those aiming

merely to slow down the aging processes. Organismal rejuvenation can be achieved in two ways. First, direct editing of the germline could equip each cell in the adult body with 4 F (OSKM, four Yamanaka factors), but it is currently prohibited to edit the genome of humans due to safety and ethical concerns. Another method involves delivering Yamanaka factors in the form of DNA or mRNA with the systems utilized in gene therapy. The effectiveness of this approach is currently limited by the low efficiency of existing delivery systems in certain tissues and their insufficient organ specificity[17]. However, with further advances in these methods, more precise and efficient partial cell reprogramming therapies may become feasible. Thus far, most partial cell reprogramming studies at the in vivo, full organismal level have been conducted in chimeric OSKM-inducible mice[8,11,15,18], with an exception where the AAV9 delivery system was used to deliver the OSK factors[16]. Tissue or system-specific partial cell reprogramming is more likely to lead to positive outcomes as a therapeutic measure in the near future because partial reprogramming is expected to yield different outcomes across various tissues.

In vivo rejuvenation of the whole organism or tissue with partial reprogramming

Administering doxycycline (dox) cyclically (2-day pulse, 5-day chase) to progeric LAKI mice carrying a Tet-inducible polycistronic OSKM cassette led to a median lifespan increase of 33% compared to control mice that received no treatment. Even after 35 cycles of dox administration, partial cell reprogramming caused neither weight loss nor mortality effects. In addition, partially reprogrammed mice apparently exhibited rejuvenation of certain cellular phenotypes, including the reduction of mitochondrial ROS and restoration of H3K9me levels[8].

The same group applied the partial cell reprogramming procedure used in a previous study to wild-type mice, based on a long-term (7 and 10 months) and short-term (1 month) induction of OSKM factors via dox administration. Histological analyses revealed no teratoma formation resulting from the process. While this study does not provide lifespan extension data, it offers valuable insights into in vivo cell rejuvenation. Cyclic cell partial reprogramming was shown to return the transcriptome, lipidome, and

metabolome of multiple tissues to a younger state. Moreover, this treatment increased skin regeneration capacity in mice[15].

Another study demonstrated that partial reprogramming with dox-inducible OSK factors can extend the remaining lifespan of 124-week-old wild-type mice by 109% compared to untreated mice. Interestingly, this study adopted a gene therapy approach instead of using transgenic mice. OSK vectors and rtTA vectors were delivered with the AAV9 capsid to ensure maximum vector distribution in all tissues. OSK expression was achieved with the cyclic administration of dox (1-day pulse, 6-day chase). c-Myc was excluded from the cocktail to reduce the risk of teratoma formation. The frailty index score of untreated wild-type mice was 7.5 points, while partially reprogrammed TRE-OSK mice exhibited the frailty index score of 6, suggesting that the therapy may be beneficial for both healthspan and lifespan[16].

Partial reprogramming has commonly been achieved by Yamanaka factor expression, but alternative partial reprogramming methods also exist. In particular, chemical reprogramming is an attractive method as it is a non-genetic approach, and it supports an easy delivery of small molecules throughout the body[19]. A two-chemical reprogramming procedure has shown to increase the *C. elegans* lifespan by 42.1%, and also to reduce DNA damage, ameliorate epigenetic age-related marks such as H3K9me3 and H3K27me3, partially prevent senescence and decrease oxidative stress[20]. Another study has shown the capacity to reprogram human somatic cells to pluripotent stem cells using chemicals[21,22]. Unlike OSKM-mediated reprogramming, chemical reprogramming has several steps and requires an intermediate plastic state. This could be useful for partial reprogramming studies as this approach is not as potent as the OSKM-mediated procedure, it requires several stages that could be targeted for rejuvenation, and the delivery of small molecules is advantageous, at least in the near-term, to the current gene delivery methods for therapeutic applications.

Partial chemical reprogramming of mouse fibroblasts using a 7c cocktail from Stage 1 small molecules has recently been shown to rejuvenate fibroblasts at a multi-omics scale[23]. Amelioration of mitochondrial oxidative phosphorylation, reduction in the level of aging associated metabolites, and both transcriptomic

and epigenomic clocks are all indicative of rejuvenation upon partial chemical reprogramming. Interestingly, OSKM-mediated partial reprogramming downregulated the p53 pathway, whereas this pathway was upregulated upon 7c-mediated partial reprogramming, similar to its changes during the normal aging process. p53 knockout is known to significantly increase the OSKM-mediated reprogramming efficiency, meanwhile shortening the reprogramming time to a week[24]. The p53 pathway is one of key inhibitors of OSKM-mediated reprogramming[25], and upregulation of this pathway during 7c-mediated partial reprogramming suggests that the two reprogramming types proceed through separate pathways during early reprogramming. Augmentation of the p53 pathway in mice causes stem cells to enter senescence at an earlier time point, which could potentially represent a safety issue for the in vivo 7c treatment[26].

It was hypothesized that a set of rapid cell divisions is essential for epigenetic remodeling during OSKM-mediated cell reprogramming[27], yet how the rate of division contributes to RIR is unknown. 7c-mediated partial reprogramming resulted in a decrease in cell proliferation, which suggests that increased proliferation is not strictly essential for cellular rejuvenation, as the opposite effect is observed during OSKM-mediated cell reprogramming[23]. Epigenetic clock reversal via 7c-mediated partial reprogramming suggests that even though the rate of cell proliferation decreases, epigenetic reprogramming can still occur efficiently. An alternative mechanism might exist for achieving epigenetic rejuvenation that doesn't solely rely on passive demethylation of the epigenome. Further research is required to establish the role of cell proliferation and efficacy and safety of partial chemical reprogramming, determine molecular mechanisms and pathways involved, and ultimately test it at the whole-organism level.

The age and gender of an organism also impact the ability of its tissues to undergo iPSC reprogramming. For example, young female mice are less likely to undergo reprogramming than young male mice, and older mice are more susceptible to reprogramming than younger ones[28,29]. Therefore, these factors must be taken into account when considering in vivo partial reprogramming therapies. Lifespan studies can require extensive resources and time. Hence, precise biomarkers of aging and rejuvenation at organismal and cellular levels

should be established. These biomarkers may include advanced multi-omic aging clocks, gene signatures, and integrated functional measures. Additionally, organismal biomarkers such as frailty index and functional tests need refinement. At the cellular level, in addition to omics-based aging biomarkers, it would be beneficial to develop aging biosensors and surface markers for profiling and imaging live cells. This integrated approach to biomarkers will not only deepen our understanding of the aging process but also potentially replace the need for extensive lifespan studies, thereby accelerating advances in the field.

Tissue-specific partial reprogramming and its applications

Apart from whole organism rejuvenation, partial cell reprogramming can be applied to specific tissues to achieve targeted rejuvenation. A promising application of partial cell reprogramming is restoration of function, e.g. visual function. When inducible OSK-containing AAV9 was delivered to the retinal ganglion cells of old mice and mice with glaucoma via intravenous delivery, continuous expression of OSK factors led to a partially restored vision. Unlike full-organism rejuvenation experiments, continuous expression of these factors did not cause teratomas even after 10-18 months[14]. This is particularly promising for potential applications in the nervous system due to the neurons' incomplete differentiation. Another study showed that six days of ectopic OSKM expression in the hearts of adult mice with myocardial infarction led to heart regeneration, and the infarct scar size decreased compared to that in control mice[30]. Unlike the previous study, twelve days of ectopic OSKM expression in the heart proved to be lethal for mice, suggesting that even post-mitotic tissues respond differently to partial cell reprogramming. One reason for this effect could be the c-Myc expression in the heart tissue. Although further research is needed in this field, it appears that post-mitotic tissue specific RIR may hold promise for therapeutic applications.

Scope of partial reprogramming-mediated rejuvenation

Aging is often discussed in the context of twelve hallmarks[31], and aging biomarkers, such as epigenetic clocks, are shown to capture some, but not all, of these hallmarks of aging. Epigenetic clock (Skin&Blood clock[32]) is associated with nutrient sensing, stem cell composition, and mitochondrial activity (Fig. 1)[33]. Partial cell reprogramming may partially reverse the

biological age as reported by epigenetic clocks. This is consistent with the findings that partial cell reprogramming can restore aged muscle cell potency and revert mitochondrial aging marks by reducing ROS levels[10]. Additionally, partial reprogramming has been shown to reduce inflammation, increase autophagosome formation, increase H3K9me3 levels, and improve proteostasis, all of which are additional hallmarks of aging. Interestingly, senescence levels were lower in old endothelial cells, but not in fibroblasts[9]. On the other hand, telomere attrition was not resolved with partial reprogramming (Fig. 1), as telomerase is only activated during late cell reprogramming[34]. The impact of partial cell reprogramming on other cellular hallmarks of aging, such as altered intercellular communication and genomic instability, is currently unknown in the case of in vitro models. Although it is well-characterized that iPSC lines tend to accumulate high numbers of small-scale mutations[35,36], the process of reprogramming is not inherently mutagenic[37,38]. However, if parental cells possess advantageous mutations prior to reprogramming, these mutations confer a competitive advantage during the reprogramming process, thereby favoring survival and dominance of such cells. This results in dominant colonies enriched with single nucleotide variants and small insertions and deletions. A significant portion of these mutations are observed in the regions associated with cell death, cell cycle, and pluripotency[37]. These observations suggest that while partial reprogramming does not increase genomic instability at the single-cell level, it might contribute to an overall increase in genomic instability within a population.

Fig. 1: Partial cell reprogramming ameliorates the hallmarks of aging.

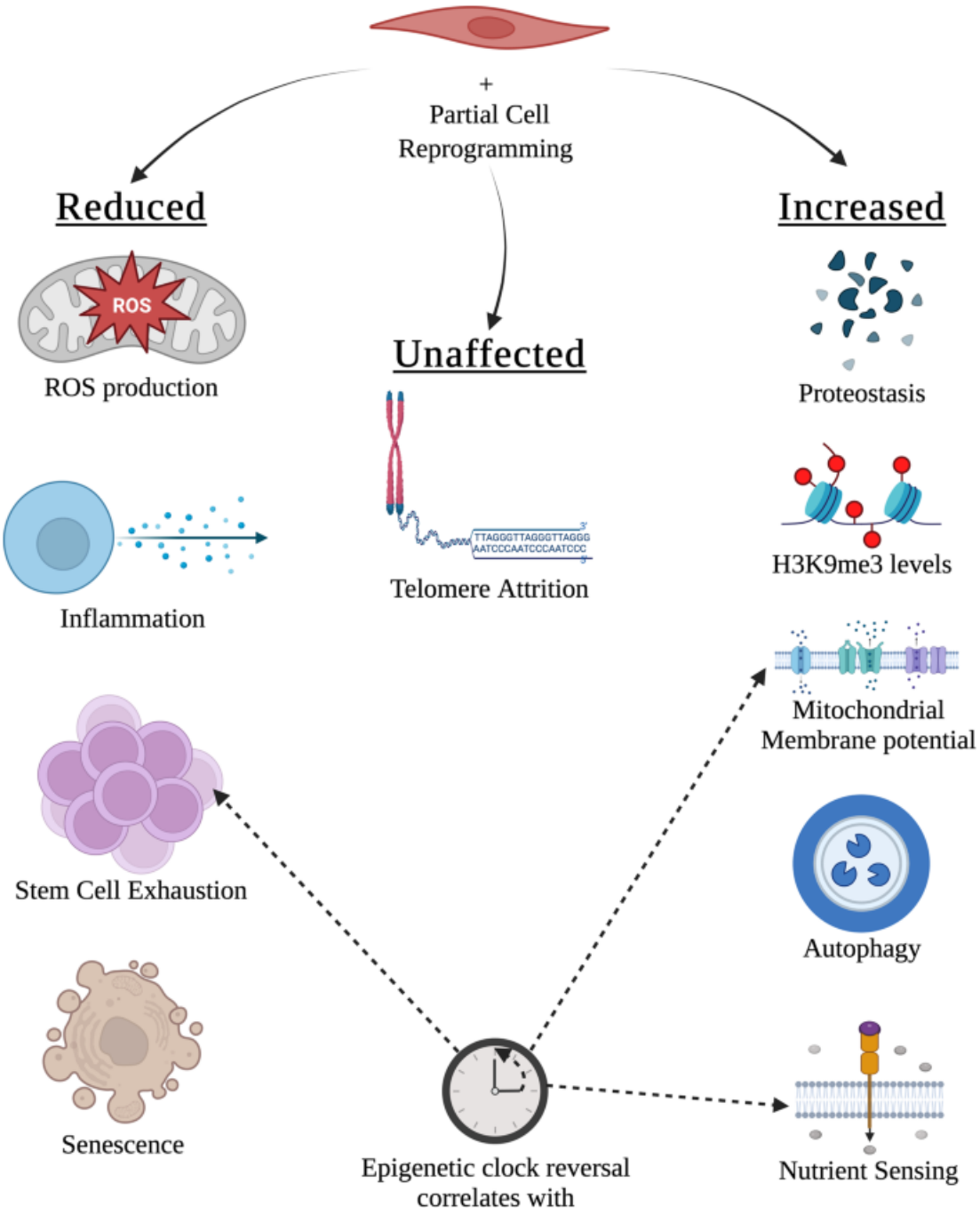

ROS production, inflammation, stem cell exhaustion and senescence levels show a decrease, and proteostasis, H3K9me3 levels, mitochondrial membrane potential, autophagy and nutrient sensing levels show an increase in partially reprogrammed somatic cells. Increased mitochondrial membrane potential and nutrient sensing, and stem cell exhaustion strongly correlate with age reversal as measured by an epigenetic (Skin&Blood) clock. Telomere attrition

is unaffected by partial cell reprogramming. Figure was created with BioRender.com.

While the reversal of biological age as measured by epigenetic clocks suggests rejuvenation, these two terms should not be used interchangeably[39]. Rejuvenation can be defined as the reversal of cellular or organismal state to a state that would be found in a younger version of the organism, even though the trajectories of aging and rejuvenation may not necessarily be the same. Epigenetic, transcriptomic, and chromatin accessibility clocks may be capable of capturing certain aspects of these overall states. However, the most striking difference between epigenetic clock reversal and rejuvenation lies in their relation to causality. The first developed clocks show high correlation with age[6,40], but their causal relationship with rejuvenation is yet to be determined, which is crucial for ascertaining their value as aging biomarkers for this type of treatment. In recent years, clocks claiming to measure biological age based on phenotypic aging and future mortality, as opposed to chronological age, have emerged[41,42]. Yet, their full applicability to rejuvenation has not been firmly established. One reason is that many clocks capture all age-related changes, whereas only some of them represent the accumulation of deleterious changes characterizing the aging process.

In this regard, the identification of CpG sites causal to aging through a Mendelian randomization approach coupled with age-related changes in DNA methylation, and the subsequent use of these sites for the development of epigenetic clocks is a new promising approach[43]. This strategy permits the construction of epigenetic clocks that may better predict longevity or a shortened lifespan. Interestingly, it was shown that commonly used epigenetic clocks are not enriched for CpG sites causally related to aging. Importantly, CpG sites that have a causal relationship with aging could be used to examine potential therapies. For example, DamAge, a clock specifically trained to capture age-related damaging changes in the DNA methylome, showed reversal of biological age, whereas AdaptAge, a clock trained to capture age-related adaptive changes, does not show this effect upon full iPSC reprogramming[43]. Further studies in this area may result in the next generation causality-informed clocks that are tuned for testing longevity interventions.

Clearly, more research is needed to understand the limits of applicability of existing biomarkers of aging for testing rejuvenation elicited by full and partial cell reprogramming. It must also be noted that even though both full reprogramming and partial cell reprogramming ameliorate cellular aging marks, there could be other factors that contribute to the observed beneficial effects in vivo. For instance, it has been shown that within a specific cell type or tissue, cells can exist in heterogeneous states with regard to biological age[44]. The overall epigenetic age of a tissue is determined by the combined contributions from various cell types, wherein certain stem cells may exhibit a younger epigenetic age than non-stem cells[33]. Tissue composition and individual aging states of cells might shift their response to partial cell reprogramming. Additionally, partially reprogrammed, biologically younger cells in an organism could proliferate more compared to biologically older cells, resulting in an overpopulation of younger cells through cell selection. Likewise, some damaged cells may be eliminated due to cell death. It has been suggested that during full reprogramming, cells harboring DNA damage are selectively eliminated through p53-mediated apoptosis[45]. This elimination of older and damaged cells could serve as a crucial selection mechanism, influencing the composition of cell population post-reprogramming. As previously discussed, parental cells with mutations conferring a survival or reprogramming advantage in genes associated with cell death, cell cycle, and pluripotency become dominant during iPSC reprogramming[37]. Although it is known which genotypic traits are favorable for iPSC reprogramming, it remains unclear if partial reprogramming selects for the same genotypic traits. Investigating this could provide insights into cell populations and their clonal selective advantage following partial reprogramming. RIR does not address the issues caused by DNA-damaged cells. On the contrary, it might amplify the tumorigenic behavior of individual cells due to clonal selection advantage. Thus, the population-level changes caused by partial reprogramming need to be thoroughly investigated to assess the benefits and risks on a larger scale.

Partial reprogramming and rejuvenation

As mentioned above, partial cell reprogramming may rejuvenate cells and improve their physiological conditions both in vivo and in vitro. However, the underlying mechanisms of this process are not yet understood. OSKM factors activate the pluripotency gene regulatory networks (GRNs) and change the

cells' chromatin landscape during reprogramming[46,47]. It's currently unknown whether pluripotency GRN is coupled with the rejuvenation process. During the transdifferentiation of fibroblasts to neurons and oligodendrocytes, cells preserve their aging features as well as their transcriptomic age[48]. When blood cells are directly reprogrammed into neural stem cells using non-integrating Sox2 and c-Myc, their DNA methylation age decreases compared to the donor peripheral blood cells[49]. Interestingly, their epigenetic age does not decrease close to ground zero (lowest biological age of the organism) achieving full rejuvenation, unlike the epigenetic age of pluripotent stem cells after full iPSC reprogramming. Oct4 and Sall4 expression levels do not increase at any point during this direct conversion, and the pluripotency GRN is at least partially inactive[49]. This suggests that the pluripotency GRN might be necessary for the reduction of epigenetic age of cells to the ground level, but it's not required to partially rejuvenate the cells. Additionally, Oct4 is a master regulator of pluripotency[50], but it is not essential for rejuvenation. Interestingly, neural stem cells after direct conversion preserve between 5.5% and 39.4% of the donor blood cells' chronological age[49].

These results may be interpreted in several ways:

1. 1.

   The pluripotency network is not active throughout the conversion process, whereas this network is essential for epigenetic rejuvenation of cells (Fig. 2a).

   Fig. 2: Direct conversion of old peripheral blood mononuclear cells to neural stem cells results in epigenetic clock reversal.

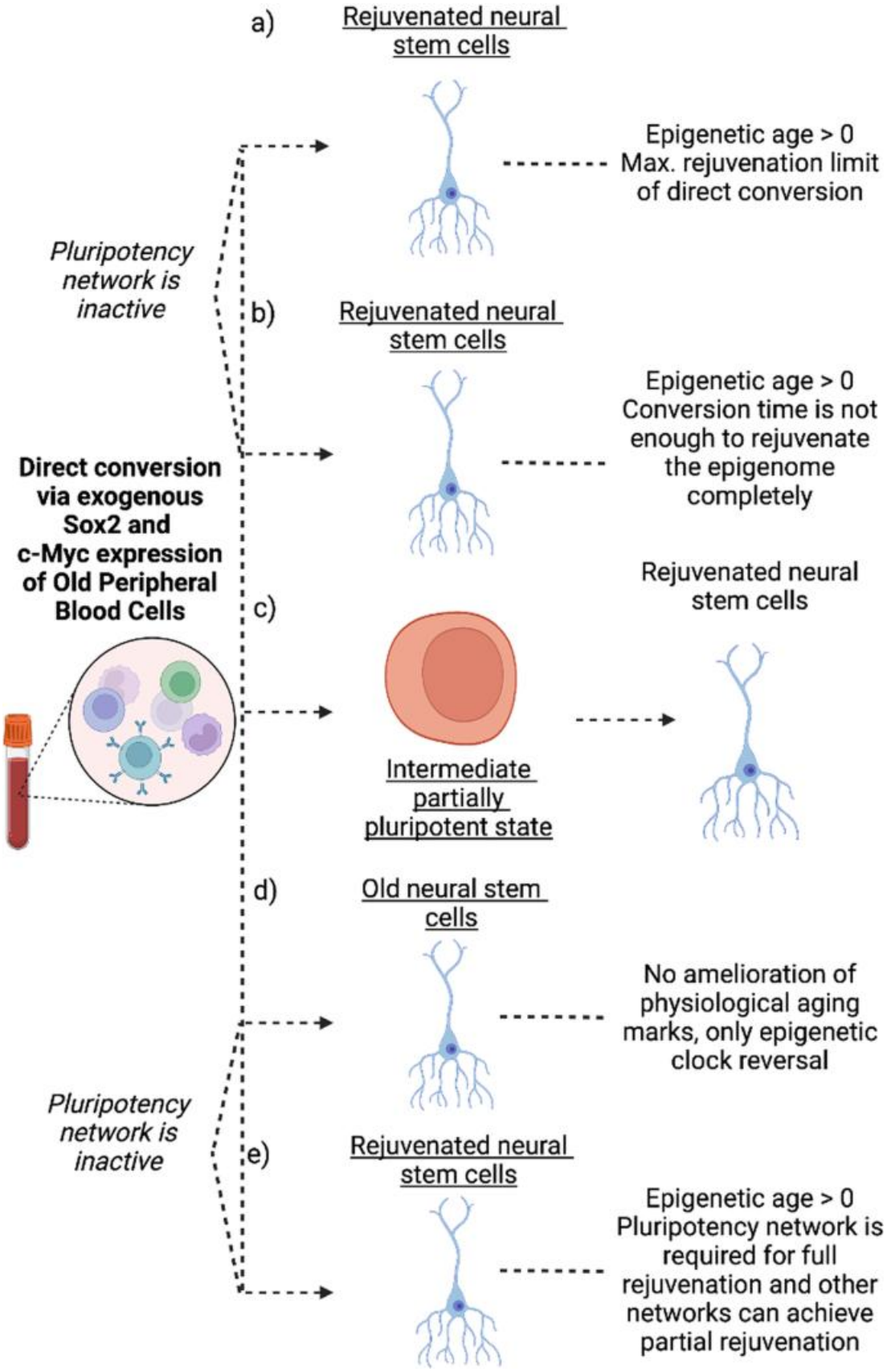
a)
Rejuvenated neural stem cells
Epigenetic age > 0
Max. rejuvenation limit of direct conversion
Pluripotency network is inactive
b)
Rejuvenated neural stem cells
Epigenetic age > 0
Conversion time is not enough to rejuvenate the epigenome completely
Direct conversion via exogenous Sox2 and c-Myc expression of Old Peripheral Blood Cells
c)
Rejuvenated neural stem cells
Intermediate partially pluripotent state
d)
Old neural stem cells
No amelioration of physiological aging marks, only epigenetic clock reversal
Pluripotency network is inactive
e)
Rejuvenated neural stem cells
Epigenetic age > 0
Pluripotency network is required for full rejuvenation and other networks can achieve partial rejuvenation

Several explanations of the observed rejuvenation effect are possible as discussed in the text. **a** Direct conversion cannot achieve full rejuvenation. **b** Direct conversion can achieve full rejuvenation in an extended conversion period. **c** An intermediate state is required for rejuvenation where the pluripotent network is active. **d** Even though epigenetic clock reversal is observed, no age-related functional changes in the cells is observed. **e** Pluripotency network is required for full rejuvenation whereas other networks responsible during direct conversion can only partially rejuvenate. Figure was created with BioRender.com.

2. 2.
   The pluripotency network is not reactivated, and rejuvenation without the pluripotency network requires a longer time. Therefore, the time length of the direct conversion procedure is not sufficient to epigenetically rejuvenate the cells (Fig. 2b).

3. 3.

   The pluripotency network is partially active, and this partial activation is key for epigenetic rejuvenation (Fig. 2c).

4. 4.

   There is no functional rejuvenation, and epigenetic clocks measure something other than rejuvenation, although this is unlikely due to the high correlation of the Horvath clock with functional assays in previous reports (Fig. 2d).

5. 5.

   The pluripotency network is required for full rejuvenation, whereas other networks may be required for partial rejuvenation (Fig. 2e).

Another study further supports the notion that rejuvenation can be partially separated from the pluripotency GRN. This conclusion can be drawn from

observations showing only a 35% average reduction in transcriptomic clock rejuvenation when genes associated with pluripotency are removed from the analysis of RIR[51]. The removal of epithelial-to-mesenchymal transition (EMT)-related genes causes a 37% average reduction in transcriptomic clock measures, potentially making them more significant to rejuvenation than the pluripotency GRN[51]. It is important to note that mesenchymal-to-epithelial transition (MET) during human fibroblast iPSC reprogramming is activated during late reprogramming whereas it is activated during early reprogramming in mouse fibroblasts[52]. This suggests that the impact of EMT genes in humans and mice could be partially different. In addition, EMT-related genes might not contribute to the human RIR. In the same study, when analyzed with the transcriptomic clock, iPSC colonies obtained with alternative 7 F reprogramming[53] (Jdp2-Jhdm1b-Mkk6-Glis1-Nanog-Essrb-Sall4) were not rejuvenated when the Sall4 factor was removed from the reprogramming cocktail. 7F-Sall4 cocktail decreased the reprogramming efficiency significantly. Interestingly, Esrrb removal resulted in a decreased reprogramming efficiency, but Esrrb removal did not intervene with the transcriptomic rejuvenation, suggesting a potential decoupling of rejuvenation and reprogramming. Esrrb is known to be required for the completion of iPSC reprogramming by opening hypermethylated DNA regions during late Yamanaka-factor-mediated iPSC reprogramming[54].

Recent research has also shown that Esrrb is essential for the establishment of naive pluripotency by making the epigenome available to Oct4 and Sox2[55]. The exact role of Esrrb during 7 F reprogramming is unknown since 7F-mediated iPSC reprogramming follows a different reprogramming path than Yamanaka-factor-mediated reprogramming. Given its importance in the establishment of naive pluripotency, the link between cellular rejuvenation and the naive state should be further investigated. Although rejuvenation is primarily achieved through reprogramming cells to a pluripotent or multipotent state, direct conversion could be a potential rejuvenation mechanism. By analyzing chromatin modifications, transcription factors, and DNA modifications during multiple types of reprogramming, rejuvenation pathways can be more specifically targeted. Partial reprogramming, iPSC reprogramming, and direct reprogramming provide diverse approaches for studying rejuvenation. A comparative analysis of these reprogramming

techniques can offer further insights into the mechanisms and pathways of rejuvenation.

iPSC reprogramming and partial cell reprogramming

Partial reprogramming aims to maintain cellular identity while achieving cellular rejuvenation, whereas full iPSC reprogramming aims to facilitate cellular dedifferentiation. This is the primary distinction between partial cell reprogramming and full iPSC reprogramming. Partial cell reprogramming is a relatively new field with few studies reporting on it. In contrast, iPSC reprogramming, discovered in 2006[34], is one of the most studied concepts in stem cell biology, with a wealth of supporting literature. Given similarities in their biological mechanisms, the field of partial cell reprogramming should not disregard the existing literature on full iPSC reprogramming. This is particularly critical as it remains unknown which Yamanaka factors are essential drivers of cellular rejuvenation. Although the c-Myc proto-oncogene is one of the original Yamanaka factors[56], its exogenous expression is not necessary for RIR and can be omitted in in vivo partial cell reprogramming studies[14,16]. Exogenous expression of Klf4, despite its role in activating key pluripotency factors, is also not necessary for full iPSC reprogramming[57]. While Sox2 is endogenously active in adult neural progenitor cells[58], neural progenitor cells do epigenetically continue to age[33], suggesting that Sox2 is not directly linked to rejuvenation, but a downstream pathway of Sox2 might be. As mentioned earlier, epigenetic rejuvenation can be achieved without the transcriptional activation of Oct4[49]. These results suggest that rejuvenation is not attained from overexpression of a single key factor but rather from a synergistic effect of these factors with other transcriptional networks. This also applies to full iPSC reprogramming, as Sox2-Oct4 and Sox2-Oct4-Klf4 multimeric complexes are master regulators of pluripotency and play important roles for full iPSC reprogramming[59]. Sox2, Oct4 and Klf4 have overlapping target genes and cooperate to form a functional enhancosome to create a pluripotent specific transcriptome[60]. In contrast, c-Myc is known to regulate a distinct set of gene targets and it binds to 22.4% of all promoters in the genome, regulating a wide variety of genes such as cell cycle and metabolism genes[61]. Exclusion of c-Myc from the reprogramming cocktail does not harm the rejuvenation process and suggests that target genes of c-Myc are not directly involved with the pathways of rejuvenation[14,16].

The notion that these four factors are not directly causing rejuvenation of cells and none of them are essential for it suggests the possibility of other transcription factors primarily involved in epigenetic rejuvenation. These four factors are involved in reprogramming of the entire epigenome during naive iPSC reprogramming, which makes it challenging to pinpoint activation of which downstream pathway is primarily responsible for rejuvenation. Transcriptomic clock rejuvenation achieved by 7 F reprogramming and cellular rejuvenation achieved by multipotent reprogramming[62] further shows that exogenous overexpression of Yamanaka factors is separable from the rejuvenation process. Therefore, the question is whether dedifferentiation is key to rejuvenation or not. Even though the current literature shows that rejuvenation is observed together with dedifferentiation, there is no established causal relation between the two concepts. If the pathways responsible for rejuvenation are also responsible for the suppression of cellular identity genes, high-throughput mutation screening for the transcription factors responsible for rejuvenation can be performed to separate cell identity suppression from epigenetic rejuvenation.

Safety concerns of partial cell reprogramming

Although partial reprogramming is a promising and exciting technique, there are issues that hinder its therapeutic applications. The primary concern stems from the technique's intense potency. Yamanaka factors used for partial reprogramming activate pluripotency and differentiation genes, increase proliferation, and suppress somatic cell identity[62,63]. These changes can lead to teratoma formation when these factors are continuously expressed in vivo[29,64,65]. Strictly speaking, even one fully reprogrammed cell is already too many cells at risk of teratoma, so this is a serious challenge for the intended translational potential. During epigenetic reprogramming caused by OSKM expression, suppressive epigenetic marks can be removed, which may lead to activation of oncogenes and an increase in the cancer rate. Furthermore, the coding point mutation rate is known to be elevated during iPSC reprogramming[66] caused by clonal selection[37], which may lead to genomic instability, also increasing the risk of cancer and heterogeneity in tissues. Moreover, continuous expression of Yamanaka factors may result in liver and intestinal failure in mice[67]. When intestinal and hepatic continuous expression of OSKM is absent during therapy, there's a significant decrease in mortality,

with 60% of mice surviving a month of continuous OSKM expression. Whole-body OSKM expression increases proliferation in tissues that are already proliferative, leading to a loss of function[67,68]. Although the contribution of hepatic and intestinal OSKM expression to these detrimental effects is not complete, it is substantial. This underscores the critical need for targeted tissue or organ-specific partial reprogramming therapies. The currently optimized method of partial reprogramming is the maturation phase partial reprogramming, which necessitates 13 days of continuous expression of Yamanaka factors in vitro. The maturation phase is proposed as the last exit prior to the point of no return for iPSC reprogramming, and significant epigenetic rejuvenation is observed on this day[12]. However, this optimized in vitro method may be highly damaging in in vivo models, as a continuous expression of Yamanaka factors for more than 2 days may have lethal effects in mice[8,67]. In vivo studies now focus on cyclic partial reprogramming, whereas in vitro studies on continuous single-cycle reprogramming, which hampers the establishment of a clear connection between these two model systems. To safely transform this method into a therapy, the impact of partial reprogramming on each tissue and system must be carefully investigated. Ethical concerns surrounding lifespan and healthspan extension therapies, particularly in the context of partial cell reprogramming, also warrant careful consideration and necessitate the creation of appropriate regulation and legislation.

Future directions and open questions

During the aging process, certain loci increasingly come under regulation to decrease methylation variance, whereas other loci show an increase in variance due to the lack of regulation[3]. This suggests that various genes contribute to aging differently. Partial reprogramming does not provide selective rejuvenation; rather, it reprograms a wide portion of the epigenome, including parts that regulate genes not critical to aging. This lack of specificity may become evident during whole-organism partial cell reprogramming because each tissue takes a different path. Selective and targeted rejuvenation in various tissues would provide comprehensive, safe, and synergistic rejuvenation throughout the whole body. To achieve this, RIR mechanisms must be better understood in order to rejuvenate certain loci in various cell types.

Present evidence suggests that pluripotency is not inherently linked to the rejuvenation process. However, it remains unclear whether pluripotency or certain transitionary cell states can be completely uncoupled from rejuvenation. A key question to be investigated is whether certain components contributing to biological age reversal can rejuvenate the entire epigenome or only certain loci. EMT and pluripotency associated genes seem to play significant roles during rejuvenation, contributing to 37% and 35% of the transcriptomic clock rejuvenation, respectively. Both gene clusters lead to a loss in cellular identity[51]. The same analysis suggests that integrin cell interactions, collagen formation, and ECM organization gene clusters contribute to transcriptomic age rejuvenation[51]. If certain transcription factors regulating these clusters contribute to rejuvenation, they could potentially rejuvenate cells without any signs of lost cellular identity. However, it should be noted that the expression of these potential transcription factors for a prolonged period does not guarantee the rejuvenation of the entire epigenome. A similar problem arises in the case of the direct conversion of peripheral blood cells to neural stem cells[49]. If there is a limit to rejuvenation when the pluripotency network is not present, the impact of the loci that remain epigenetically old must be understood.

The low efficiency of partial cell reprogramming remains a problem, with only about 25% of cells in culture being partially reprogrammed[12]. Research in the iPSC reprogramming field is now performed to understand the factors that reduce reprogramming efficiency, such as chromatin remodelers and regulatory transcription factors. Applying the same logic to partial cell reprogramming is essential to increase the overall efficiency of the technique. It is also important to note that some key factors that decrease reprogramming efficiency are associated with cellular identity preservation[47,57]. Preservation of cellular identity must be considered while increasing the fraction of rejuvenated cells.

Additionally, persistence of rejuvenation mediated by partial cell reprogramming is an aspect that necessitates further investigation. A transcriptional analysis of adipogenic cells, reprogrammed for three days and then followed for an additional ten days, suggests that broad gene programs continue to exhibit rejuvenation[62]. However, it is crucial to note that cellular

identity states of these cells post-partial reprogramming are not identical to those of their parental cells. It is essential to investigate in detail whether these cells maintain their rejuvenated states after the reprogramming period, lose all rejuvenation signs upon reverting to their initial cellular state, or experience an accelerated loss of their youthful states compared to regular cells. Therefore, the longevity of rejuvenation effects mediated by partial reprogramming continues to be a relevant and unresolved question.

There are legitimate concerns about the safety of OSK(M)-mediated partial reprogramming. To translate research in the field into clinical therapies, more research on the roadmap of partial reprogramming needs to be conducted. Furthermore, to better evaluate the results of in vivo cyclic reprogramming studies, in vitro cyclic reprogramming must be performed, and the difference between cyclic and continuous partial reprogramming must be identified.

In conclusion, while partial reprogramming holds great therapeutic potential, the real focus should be on rejuvenation research, defining its nature and ways to quantify it. Understanding rejuvenation is also key to translational success, as benefits of age reversal must be considered against risks. More research into safety and tissue-specific responses of this technique are required.

Mitochondria & Anti-Aging: Boosting Cellular Energy for Regenerating.

Who doesn't desire a long, healthy, and vibrant life? But when your age number increases, your hope for a refreshing and energetic life fades away. And the logic? Mitochondrial functions decline with age – the primary source of cellular energy. [1]

Recent research has revealed exciting insights into how mitochondria impact health and aging. [2] It turns out that mitochondria – tiny powerhouses of energy – play a significant role in regulating your life span and are closely linked to the aging process. By improving mitochondrial function, you can potentially slow down the effects of aging and enjoy a healthier, more vibrant life.

And the best natural way to boost your mitochondria levels and ultimately enhance cellular function? Red light therapy (RLT) might be just what you need! By improving blood flow, reducing inflammation, and enhancing the energy-making powerhouses in your cells (aka mitochondria), this therapy can help you feel and look your best. [3]

What are Mitochondria?

Mitochondria are essential structures in your cells that play various roles, including cell signaling, steroid synthesis, and cell death. But their most important job is generating cellular energy. Mitochondria act like a powerhouse of the cells, transforming the food you eat, water you drink, and oxygen you breathe into ATP – a form of energy – that your cells and body can use. It's like an "energy currency of life" vital to everything you do.

What makes mitochondria so unique is that they have their own ribosomes and DNA. Although they're too small to see with the naked eye, mitochondria influence nearly every aspect of your life. A single cell can have anywhere from one to thousands of mitochondria. Interestingly, the number of mitochondria can vary depending on factors like exercise, nutrient intake, and aging.

Better Mitochondria, Better Aging: The Link Between Cellular Health and Longevity

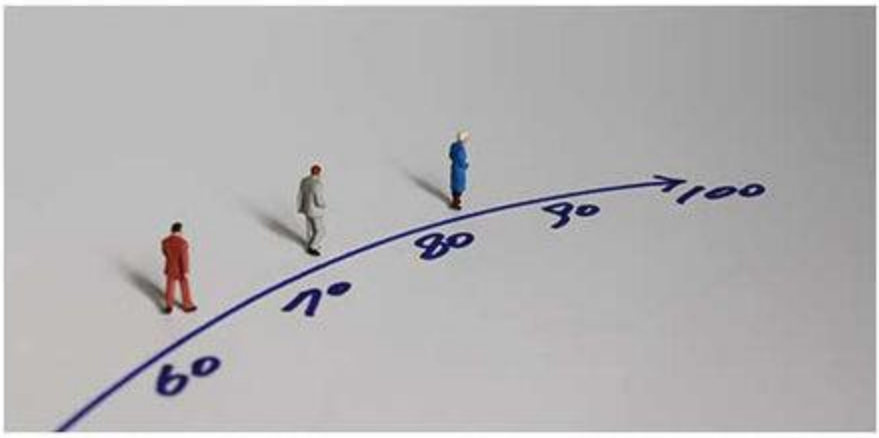

Mitochondria are essential for cellular health and skin rejuvenation, and their role in skin aging has become an area of intense research in recent years. Their dysfunction is linked to pigmentation, stress-induced wrinkle formation, and hair greying and loss. As the largest organ in your body with a high turnover rate, your skin relies on mitochondrial function for optimal performance.

Research shows that addressing mitochondrial function can improve skin health and fight signs of aging. So, understanding the role of mitochondria in skin aging is crucial for developing effective prevention strategies and improving anti-aging formulas for mature skin. [4] Targeting mitochondrial

signaling can increase cellular health, slow aging, and help rejuvenate the skin.

Red Light Therapy: Natural Way to Stimulate Mitochondria and Boost Cellular Energy

Red light therapy has emerged as a safe and natural therapeutic approach to enhance cellular function, reduce inflammation, and improve blood flow, among other things. Red light therapy stimulates adenosine triphosphate (ATP) production, a molecule that plays a crucial role in cellular energy production and many other biological processes.

Working Mechanism of Red Light Therapy

By stimulating the mitochondria, red light therapy helps promote the production of ATP, thereby improving the overall cellular function. [5] This therapy increases the number and boosts the function of mitochondria, resulting in enhanced cellular energy production and performance.

The electron transport chain mediated by cytochrome C oxidase (Cox) is one of the primary mechanisms through which red light therapy improves mitochondrial function. By dissociating nitric oxide (NO) and Cox, red light can prevent and reverse the harmful roadblock to ATP production caused by NO-Cox, thus promoting optimal cellular function.

Revitalize Your Cells with Full-Body Red Light Therapy

Full-Body Red Light Therapy simultaneously stimulates trillions of cells in your body, promoting faster healing time and increasing cellular energy production, providing natural healing benefits to your entire body.

Unlike supplements that claim to boost "mitochondria" levels, full-body red light therapy is a much better answer. It works by directly targeting your cells through a light panel, bypassing your digestive system, allowing for more efficient absorption and utilization of the therapy's benefits.

So, don't let age slow you down – try full-body red light therapy and revitalize your entire skin cells!

Reference

1. Bratic, A., & Larsson, N.-G. (2013, March). *The role of mitochondria in aging*. The Journal of clinical investigation. https://www.ncbi.nlm.nih.gov/pmc/articles/PMC3582127/#:~:text=According%20to%20the%20MFRTA%2C%20mitochondria,that%20drives%20the%20aging%20process.
2. Bratic, A., & Larsson, N.-G. (2013b, March 1). *The role of mitochondria in aging*. The Journal of Clinical Investigation. https://www.jci.org/articles/view/64125
3. Ferraresi, Dr. C. (2022). *Red light therapy for cellular health and ATP Energy*. Joovv. https://joovv.com/blogs/joovv-blog/how-red-near-infrared-light-stimulates-cellular-respiration-boosts-energy-production
4. Stout, R., & Birch-Machin, M. (2019, May 11). *Mitochondria's role in skin ageing*. Biology. https://www.ncbi.nlm.nih.gov/pmc/articles/PMC6627661/
5. Natick, N. (2020). *Health benefits of Red Light Therapy*. PatriotDirect Family Medicine | Natick, MA. https://patriotdirectfm.com/2020/02/health-benefits-of-red-light-therapy/#:~:text=The%20primary%20function%20of%20red,procedure%20also%20improves%20thyroid%20function.

Unlocking Tissue Regenerative Potential by Epigenetic Reprogramming

panelPradeep Reddy [1], Sebastian Memczak [1], Juan Carlos Izpisua Belmonte [1]
https://doi.org/10.1016/j.stem.2020.12.006Get rights and content

Summary

The regeneration potential of axons projecting from retinal ganglion cells (RGCs) is lost shortly after birth. In *Nature*, Lu et al. (2020) demonstrate that epigenetic reprogramming of RGCs by overexpression of *Oct4*, *Sox2*, and *Klf4* leads to axon regeneration and restoration of vision in a glaucoma model and aged mice.

Main Text

As we age, maladies increase. The role of genetics in aging has been amply demonstrated by the characterization of many loci that influence aging traits. Several studies are also pointing to the epigenome as a key regulator of health and lifespan. A case in point was the cellular reprogramming to pluripotency by the forced expression of the four Yamanaka factors *Oct4*, *Sox2*, *Klf4*, and *c-Myc* (Takahashi and Yamanaka, 2006). Followup studies showed that reprogramming of old cells resulted in the transformation of multiple aging phenotypes to a younger state, including the restoration of telomere length, mitochondrial function, and gene expression profiles (Zhang et al., 2020). This cellular rejuvenation was maintained during the differentiation of induced pluripotent stem cells (iPSCs) and led to the generation of biologically younger somatic cells.

One caveat of this approach is that systemic and continuous expression of the Yamanaka factors *in vivo* leads to broad cellular changes, including loss of cell identity, abnormal proliferation, and tumorigenesis (Abad et al., 2013; Ohnishi et al., 2014). In contrast, when these factors are expressed for short and repeated intervals, they improved age-related phenotypes and extended lifespan of a premature aging mouse model. Moreover, regeneration capacity of muscle and pancreas in aged wild-type mice was increased (Ocampo et al., 2016). Importantly, this partial reprogramming protocol did not induce any tumor formation or cell identity change. Along the same line, partial reprogramming reduces fibrosis and scar formation in skin (Doeser et al., 2018), improves memory, and reduces aging phenotypes in dentate gyrus cells (Rodríguez-Matellán et al., 2020) (Figure 1). The transient expression of Yamanaka factors together with LIN28 and NANOG can also ameliorate aging in old human cells *in vitro* (Sarkar et al., 2020).

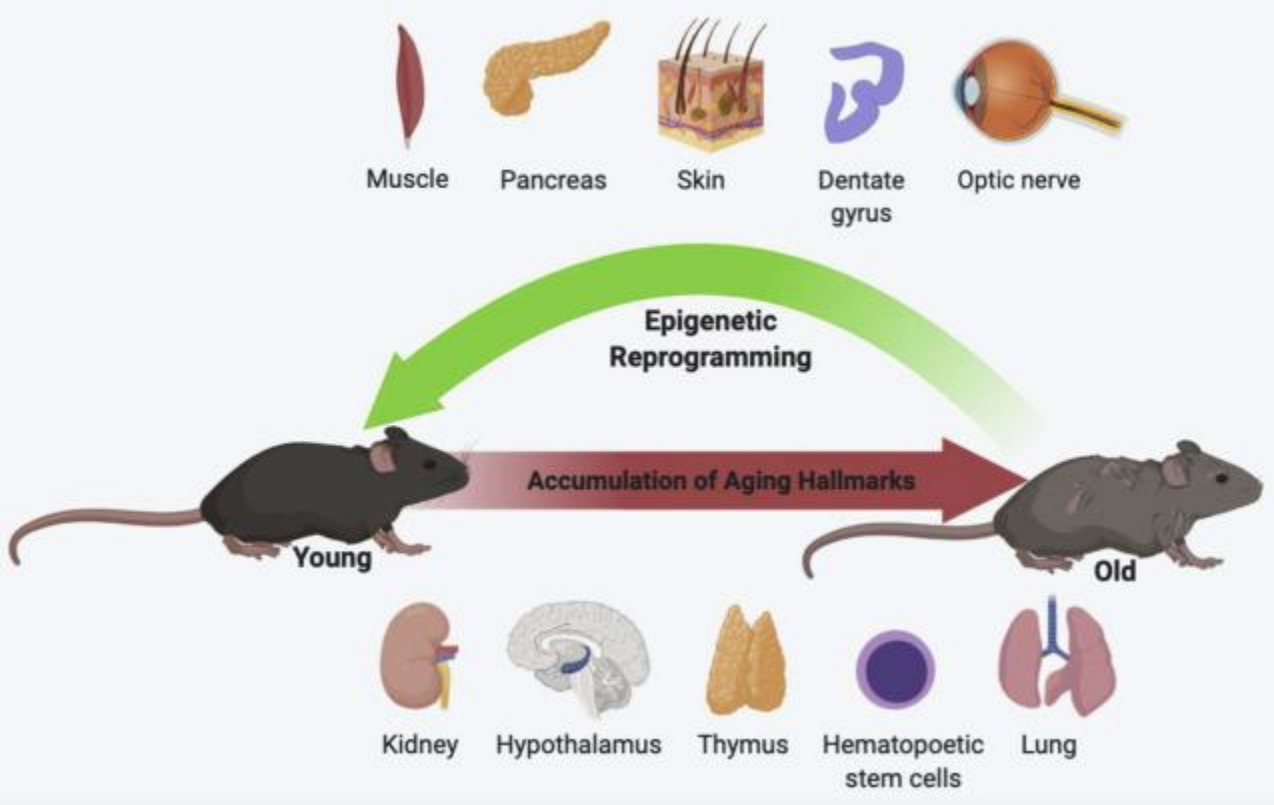

Figure 1. Epigenetic Reprogramming of Organs to Reverse the Hallmarks of Aging
Epigenetic reprogramming is currently performed in many different cells, tissues, and organs to ameliorate or reverse age-associated phenotypes, with optical nerves as the latest example (Lu et al., 2020). The goal of this approach is to extend the regenerative potential and healthspan of an organism. Created with BioRender.com.

A therapeutically relevant target of these interventions (reviewed in Zhang et al., 2020) is the regenerative potential of cells and tissues: during mammalian embryogenesis and early stages of life, many tissues can faithfully and quickly regenerate after an injury; however, aged tissues repair incompletely and oftentimes accompanied by scar formation and functional loss. This is the case for instance in axons projecting from retinal ganglion cells (RGCs) that lose their regenerative potential within days after birth. Now, Lu et al. (2020) demonstrate that epigenetic reprogramming of RGCs by overexpression of *Oct4*, *Sox2*, and *Klf4* (OSK) can induce partial rejuvenation, axon regeneration, and, strikingly, restoration of vision in a model of glaucoma as well as in aged mice (Lu et al., 2020). The authors used adeno-associated virus (AAV) to express the OSK proteins in RGCs under the control of the inducible tetracycline response element promoter. In an optic nerve injury model, an increase of regenerative capacity of RGCs upon OSK expression was detected in adult mice. Notably, no change in the number of RGCs was observed and long-term OSK expression did not lead to negative consequences such as structural changes or tumorigenesis. An increased eye pressure damages the optic nerve, resulting in glaucoma, a progressive and permanent loss of vision, that affects many millions of people worldwide. Eye injection of OSK-AAVs in a glaucoma mouse model restored axon density to that of control levels. The authors also

examined potentially beneficial effects of their treatment during physiological aging where impaired vision is rampant. 12-month-old healthy mice displayed an increase in visual acuity and electrical activity of RGCs upon treatment. Notably, RNA sequencing of RGCs after 4 weeks of OSK induction revealed that mRNA levels were restored to a state similar to that of youthful 5-month-old cells. In addition, after mechanical RGC injury, the authors observed global DNA methylation changes similar to the ones observed during aging, and OSK induction partially reversed these changes. Loss-of-function experiments revealed that the DNA demethylases TET1 and TET2 are required for axon regeneration while global reduction of DNA methylation by overexpression of the TET1 catalytic domain alone, without OSK induction, could not regenerate axons. Lastly, OSK expression ameliorated the DNA methylation changes and axon loss in differentiated human neurons after drug-induced injury. Together these experiments indicate evolutionary conservation of the rejuvenation effects caused by epigenetic reprogramming.

The current study is an important step forward in trying to identify commonalities and differences between epigenetic reprogramming and regeneration. By leaving out c-Myc from the original OSKM cocktail, the authors induced strong regeneration in RGCs while detrimental effects were avoided. The OSK combination, however, can generate fully reprogrammed iPSCs. Here, Lu et al. did not observe induction of pluripotency or tumor formation, even after continuous expression of OSK for longer periods. Further investigation is needed to determine whether this phenomenon is specific to the neuronal lineage. This study also raises other interesting mechanistic questions, such as what effects OSK can have on other non-neuronal somatic cells and on stem cells. Which other hallmarks of aging are affected? How long do the rejuvenation effects last? How are changes in epigenetic clocks related to changes in cellular phenotypes? Is there a hierarchy of changed loci, i.e., a pathway to rejuvenation and/or regeneration?

Within the different strategies that aim at reversing cellular aging, epigenetic reprogramming gained attention following studies where several different intra-cellular age-associated phenotypes could be ameliorated simultaneously. Further experiments will be required to determine which treatments derived from the original reprogramming protocol have the biggest potential to prevent age-associated loss-of-function and diseases (Figure 1). One focus will be the identification of downstream druggable targets of epigenetic reprogramming to develop novel and more specific approaches. These may include screens for small molecules or other non-protein factors to modulate activities of specific genetic loci. One example of such a novel technology is *in vivo* targeted gene activation based on histone modifications, which allows for the targeted activation of endogenous genes that are silenced during aging or that can help to restore the homeostasis and function of different tissues or organs (Liao et al., 2017). Moreover, exciting advances in the field of single-cell technologies will allow us to answer questions such as, “Are there common, amenable hallmarks of aging across tissues and cell types, and how many and which cells need to be reprogrammed to achieve tissue and organismal rejuvenation?” The study of Lu et al. is an important contribution to the continuously increasing data demonstrating how extending regeneration potential can contribute to rejuvenation by promoting physiological tissue homeostasis. The ability to restore the epigenetic landscape of old tissues has the potential to dramatically expand organ and organismal healthspan.

Low-level laser (light) therapy increases mitochondrial membrane potential and ATP synthesis in C2C12 myotubes with a peak response at 3-6 hours

Cleber Ferraresi [1,2,3,4], Beatriz Kaippert [4,5], Pinar Avci [4,6], Ying-Ying Huang [4,6], Marcelo Victor Pires de Sousa [4,7], Vanderlei Salvador Bagnato [3], Nivaldo Antonio Parizotto [1,2], Michael R Hamblin [4,6,8,*]

PMCID: PMC4355185 NIHMSID: NIHMS646190 PMID: 25443662

Abstract

Low level laser (light) therapy has been used before exercise to increase muscle performance in both experimental animals and in humans. However uncertainty exists concerning the optimum time to apply the light before exercise. The mechanism of action is thought to be stimulation of mitochondrial respiration in muscles, and to increase adenosine triphosphate (ATP) needed to perform exercise. The goal of this study was to investigate the time course of the increases in mitochondrial membrane potential (MMP) and ATP in myotubes formed from C2C12 mouse muscle cells and exposed to light-emitting diode therapy (LEDT). LEDT employed a cluster of LEDs with 20 red (630 ± 10 nm, 25 mW) and 20 near-infrared (850 ± 10 nm, 50 mW) delivering 28 mW/cm^2 for 90 sec (2.5 J/cm^2) with analysis at 5 min, 3 h, 6 h and 24 h post-LEDT. LEDT-6h had the highest MMP, followed by LEDT-3h, LEDT-24h, LEDT-5min and Control with significant differences. The same order (6h>3h>24h>5min>Control) was found for ATP with significant differences. A good correlation was found (r=0.89) between MMP and ATP. These data suggest an optimum time window of 3-6 h for LEDT stimulate muscle cells.

INTRODUCTION

Mitochondria are the organelles responsible for energy production in cells and for this reason have a very important role in cellular function and maintenance of homeostasis. This organelle has an intriguing and well designed architecture to generate adenosine triphosphate (ATP) that is the basic energy supply for all cellular activity (1, 2).

Mitochondria contain a respiratory electron transport chain (ETC) able to transfer electrons through complexes I, II, III and IV by carrying out various redox reactions in conjunction with pumping hydrogen ions (H^+) from the mitochondrial matrix to the intermembrane space. These processes generate water as the metabolic end-product, as oxygen is the final acceptor of electrons from the ETC, that is coupled with synthesis of ATP when H^+ ions return back into mitochondrial matrix through complex V (ATP synthase), thus completing the ETC. Changes in the flow of electrons through the ETC and consequently in H^+ pumping produce significant modulations in the total proton motive force and ATP synthesis. These changes can be measured by mitochondrial membrane potential (MMP) and content of ATP (1).

Since the earliest evidence that low-level laser (light) therapy (LLLT) can increase ATP synthesis (3, 4), several mechanisms of action have been proposed to explain LLLT effects on mitochondria. One of the first studies reported increased MMP and ATP synthesis measured at an interval of 3 minutes after LLLT (3). Years later, other authors extended the measurement of this “extra” ATP-induced by LLLT in HeLa (human cervical cancer) cells (4). With intervals of 5 to 45 minutes, these authors found no change in ATP synthesis during the first 15 minutes after LLLT, but after 20-25 minutes ATP levels increased sharply and then came back to control levels at 45 minutes (4).

More recent studies have reported LLLT effects on mitochondria in different types of cells (5-9). In neural cells LLLT seems to also increase MMP, protect against oxidative stress (5) and increase ATP synthesis in intact cells (without stressor agents)(6). In mitochondria from fibroblast cells without stressor agents, LLLT also increased ATP synthesis and mitochondrial complex IV activity in a dose-dependent manner (7). In myotubes from C2C12 cells, LLLT could modulate the production of reactive oxygen species (ROS) and mitochondrial function in a dose-dependent manner in intact cells or in cells stressed by electrical stimulation (9).

Increases in mitochondrial metabolism and ATP synthesis have been proposed by several authors as a hypothesis to explain LLLT effects on muscle performance when used for muscular pre-conditioning or muscle recovery post-exercise (10-12). However, there is a lack in the literature to identify immediate and long-term effects of LLLT on mitochondrial metabolism and ATP synthesis in skeletal muscle cells that in turn could confirm these hypotheses.

This current study aimed to identify the time-response for LLLT by light-emitting diode therapy (LEDT) in modulation of MMP and ATP content in myotubes from C2C12 intact cells (mouse muscle cells) only under the stress of the culture. Moreover, the second objective was to correlate MMP with ATP content within a time range of 5 minutes to 24 hours after LLLT. Our goal was to find the best time-response for LLLT which could be useful in future experimental and clinical studies investigating muscular pre-conditioning, muscle recovery post-exercise or any other photobiomodulation in muscle tissue.

MATERIALS AND METHODS

Cell culture

C2C12 cells were kindly provided by the Cardiovascular Division of the Beth Israel Deaconess Medical Center, Harvard Medical School, USA. Cells were grown in culture medium (DMEM, Dulbecco's Modified Eagle's Medium - Sigma-Aldrich) with fetal bovine serum (20% FBS - Sigma-Aldrich) and 1% antibiotic (penicillin and streptomycin) in humidified incubator at 37 °C and 5% CO_2.

C2C12 cells were cultured and a total of 1.71×10^5 cells approximately were counted in a Neubauer chamber. Next, these cells were distributed equally into 30 wells (approximately 5.7×10^3 cells per well) into two different plates:

- 15 wells in black plate (Costar® 96-Well Black Clear-Bottom Plates) for analysis of MMP.
- 15 wells in white plate (Costar® 96-Well White Clear-Bottom Plates) for analysis of ATP synthesis.

Moreover, both plates were subdivided into five columns with 3 wells per column (triplicate):

- LEDT-Control: no LEDT applied to the cells.
- LEDT-5min: LEDT applied to the cells and assessments of ATP and MMP after 5 minutes.
- LEDT-3h: LEDT applied to the cells and assessments of ATP and MMP after 3 hours.
- LEDT-6h: LEDT applied to the cells and assessments of ATP and MMP after 6 hours.
- LEDT-24h: LEDT applied to the cells and assessments of ATP and MMP after 24 hours.

After plating C2C12 cells were cultured for nine days in culture medium (DMEM) containing 2% heat-inactivated horse serum (Sigma-Aldrich) in a humidified incubator at 37 °C and 5% CO_2 to induce cell differentiation into myotubes, as described in a previous study (9). At the 10^{th} day, LEDT-24h group received LEDT. At 11^{th} day all remaining groups received LEDT and were assessed for ATP and MMP at specific times in accordance with each group.

Light-emitting diode therapy (LEDT)

A cluster of 40 LEDs (20 red – 630 ± 10 nm; 20 infrared – 850 ± 20 nm) with a diameter of 76 mm was used in this study. The cluster was positioned at a distance of 156 mm from the top of each plate and irradiation lasted 90 s with fixed parameters as described in table 1. Each group of wells received LEDT individually, and all others wells of each

plate (groups) were covered with aluminum foil to avoid light irradiation [Figure 1]. LEDT parameters were measured and calibrated using an optical energy meter PM100D Thorlabs® and sensor S142C (area of 1.13 cm^2). In addition, we chose use red and near-infrared light therapy at the same time in order to promote a double band of absorption by cytochrome c oxidase (COX) based on specific bands of absorption reported previously (2, 13-16). The room temperature was controlled (22-23 °C) during LEDT irradiation, which did not increase temperature on the top of plates more than 0.5° C. This increase of 0.5 °C was dissipated to room within 2 minutes after LEDT.

Table 1.

All parameters of light-emitting diode therapy (LEDT). Control did not receive LEDT.

Number of LEDs (cluster): 40 (20 infrared-IR and 20 red-RED)
Wavelength: 850 ± 20 nm (IR) and 630 ± 10 nm (RED)
LED spot size: 0.2 cm^2
Pulse frequency: continuous
Optical output of each LED: 50 mW (IR) and 25 mW (RED)
Optical output (cluster): 1,000 mW (IR) and 500 mW (RED)
LED cluster size: 45 cm^2
Power density (at the top of plate): 28 mW/cm^2
Treatment time: 90 s
Cluster energy density applied on the top plate: 2.5 J/cm^2
Application mode: without contact
Distance from plate or power meter: 156 mm

Figure 1. Myotubes from C2C12 cells.

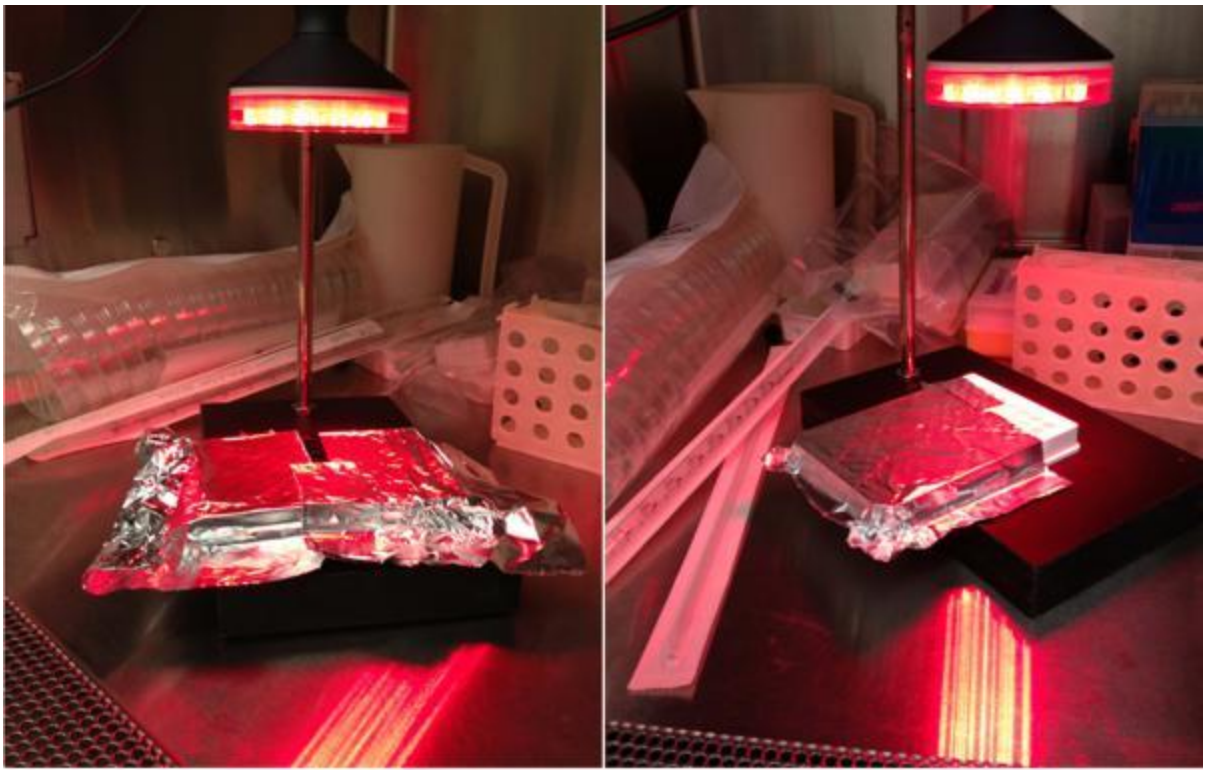

Experimental setup for irradiation of the white and black plates containing myotubes from C2C12 cells using light-emitting diode therapy (LEDT) without contact.

Mitochondrial membrane potential (TMRM) assay

This analysis was performed using cells placed into black plate. MMP was assessed using tetramethyl rhodamine methyl ester (TMRM – Invitrogen/ Molecular Probes) at a final concentration of 25 nM. Nuclei of myotubes from C2C12 cells were labeled using Hoechst (Sigma-Aldrich) at a concentration of 1mg/ ml. Each well was incubated for 30 min, 37 °C and 5% CO_2 with 100 µl of solution containing TMRM and Hoechst. Next, this solution was carefully removed from each well and added 100 µl of buffer solution containing HBSS (Hank's Balanced Salt Solution – Life Technologies Corporation) and 15 mM HEPES (4-(2-hydroxyethyl)-1-piperazineethanesulfonic acid – Life Technologies Corporation). The myotubes were imaged in a confocal microscope (Olympus America Inc. Center Valley, PA, USA) using an excitation at 559 nm and emission at 610 nm. Three random fields per well were imaged with a magnification of 40x water immersion lens. Images were exported and TMRM fluorescence incorporation into mitochondrial matrix was measured using software Image J (NIH, Bethesda, MD).

Adenosine triphosphate (ATP) assay

This analysis was performed using cells placed into white plate. Firstly, the medium was carefully removed from each well followed by addition of 50 µl/well of CellTiter Glo Luminescent Cell Viability Assay reagent (Promega). After 10 min of incubation at room temperature (25 °C), luminescence signals were measured in a SpectraMax M5 Multi-

Mode Microplate Reader (Molecular Devices, Sunnyvale, CA) with integration time of 5 s to increase low signals (17). A standard curve was prepared using ATP standard (Sigma) according to manufacturer's guideline and then ATP concentration was calculated in nanomol (nmol) per well.

Pearson product-moment correlation coefficient (Pearson's r)

The correlation between TMRM and ATP content in myotubes from C2C12 cells was calculated using Pearson's r. The *r* values were interpreted as recommended previously (18): 0.00–0.19 = none to slight; 0.20–0.39 = low; 0.40–0.69 = modest; 0.70–0.89 = high; and 0.90–1.00 = very high.

Sample size calculation

The sample size was calculated based on that necessary to obtain significant differences among all groups with ATP content. The statistical power of 80% and the effect size (greater than 0.75) were found to be satisfactory.

Statistical analysis

Shapiro-Wilk's W test verified the normality of the data distribution. ATP and TMRM were compared among all groups using one-way analysis of variance (ANOVA) with Tukey HSD post hoc test. Pearson product-moment correlation coefficient (Pearson's r) was conducted between TMRM and ATP. Significance was set at $P < 0.05$.

RESULTS

Mitochondrial membrane potential (TMRM)

LEDT-6h group increased MMP (10.77 AU, SEM 0.88) compared to: Control (3.79 AU, SEM 0.46): $P < 0.001$; LEDT-5min (4.11 AU, SEM 0.52): $P < 0.001$; LEDT-24h (4.91 AU, SEM 0.47): $P = 0.001$. LEDT-3h (7.87 AU, SEM 0.59) increased MMP compared to Control ($P = 0.019$) and LEDT-5min ($P = 0.031$). These results are graphically presented in figure 2. All non-significant results were Control *versus* LEDT-5min ($P = 0.997$) and *versus* LEDT-24h ($P = 0.816$); LEDT-5min *versus* LEDT-24h ($P = 0.935$); LEDT-3h *versus* LEDT-6h ($P = 0.113$) and *versus* LEDT-24h ($P = 0.103$).

Figure 2. TMRM.

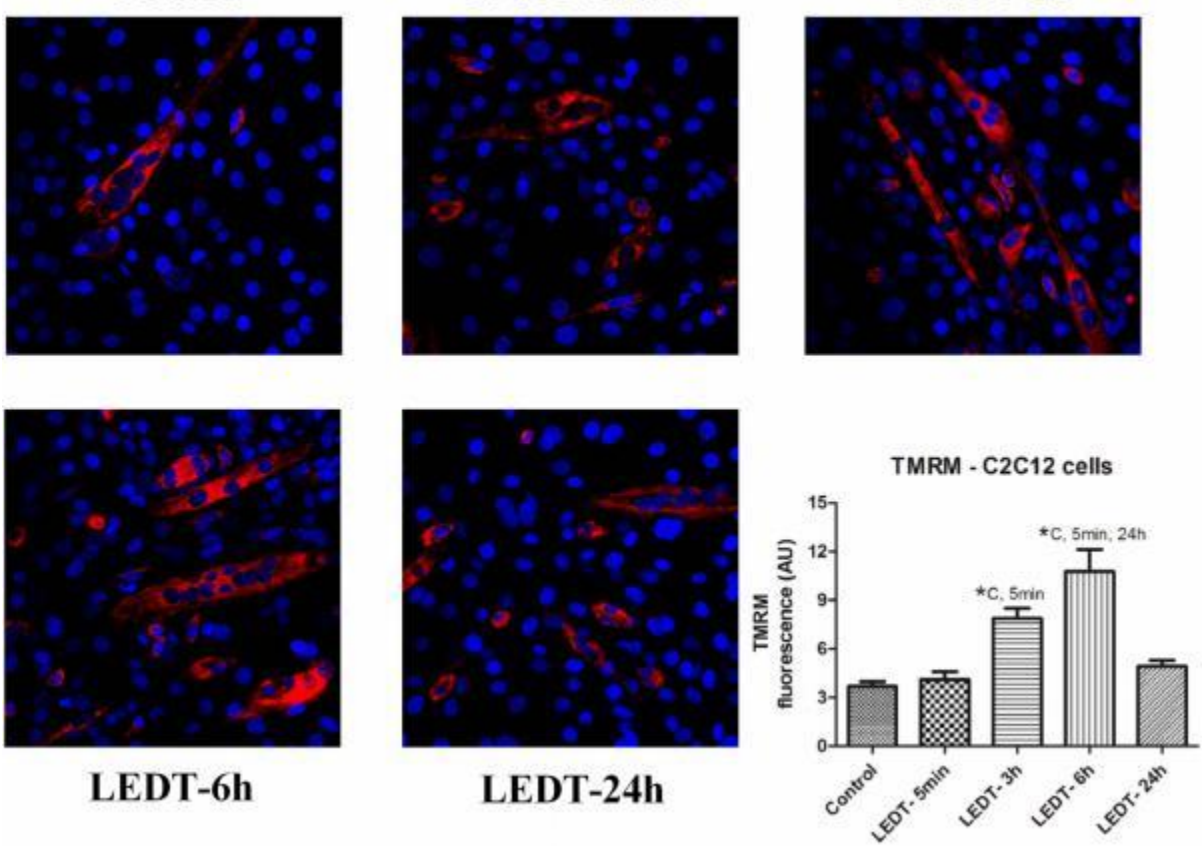

Analysis of mitochondrial membrane potential using tetramethyl rhodamine methyl ester (TMRM) stained in red. Images with a magnification of 40x. Abbreviations: LEDT= light-emitting diode therapy; AU= arbitrary units; C= control group; 5min= LEDT-5min group; 24h= LEDT-24h group; *= statistical significance ($P < 0.05$) using one-way analysis of variance (ANOVA).

ATP assay

LEDT-6h increased ATP contents (4.53 nmol/ well, SEM 0.19) compared to: Control (1.28 nmol/ well, SEM 0.05): $P < 0.001$; LEDT-5min (2.01 nmol/ well, SEM 0.16): $P < 0.001$; LEDT-24h (2.77 nmol/ well, SEM 0.16): $P = 0.007$. LEDT-3h increased ATP contents (3.73 nmol/ well, SEM 0.17) compared to Control ($P < 0.001$) and LEDT-5min ($P = 0.008$). LEDT-24h increased ATP contents compared to Control ($P = 0.020$). These results are graphically presented in figure 3A. All non-significant results were Control *versus* LEDT-5min ($P = 0.385$); LEDT-3h versus LEDT-6h ($P = 0.299$) and versus LEDT-24h ($P = 0.169$); LEDT-24h versus LEDT-5min ($P = 0.338$).

Figure 3. ATP and Pearson's r.

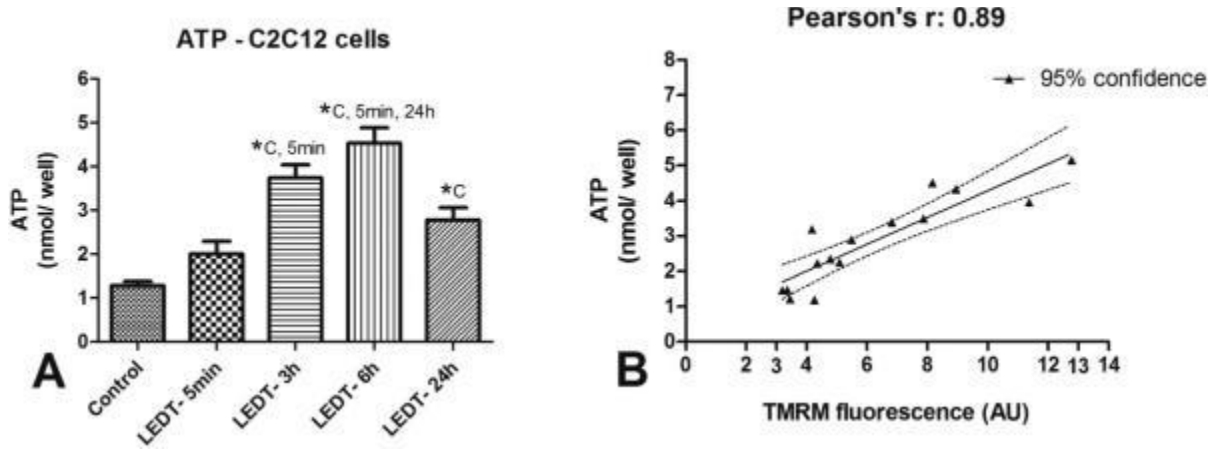

A) Analysis of adenosine triphosphate (ATP) content between groups. **B)** Pearson product-moment correlation coefficient (Pearson's r)between ATP and mitochondrial membrane potential using TMRM. Abbreviations: LEDT= light-emitting diode therapy; TMRM= tetramethyl rhodamine methyl ester; nmol= nanomol; AU= arbitrary units; C= control group; 5min= LEDT-5min group; 24h= LEDT-24h group; *= statistical significance ($P < 0.05$) using one-way analysis of variance (ANOVA).

Sample size

The statistical power and the effect size regarding ATP content in all groups were calculated in order to ensure the minimal power of 80% and large effect size (> 0.75). We used the mean ATP content of each group and the highest value of standard deviation among all groups, which was observed in LEDT-6h. Our results demonstrate a difference between groups with a statistical power of 99%, effect size of 3.42 (very large effect) and total sample size of 10, i.e., 2 wells per group (5 groups). These calculations demonstrate that our sample size was small, but adequate (3 wells per group).

Pearson product-moment correlation coefficient (Pearson's r)

TMRM incorporation into mitochondrial matrix of myotubes from C2C12 cells showed a high correlation (r=0.89) with ATP content ($P < 0.001$).

DISCUSSION

This current study identified a well-defined time-response for the LEDT-mediated increase in MMP and ATP synthesis in myotubes from C2C12 cells under the stress of the cell culture. The light dose used was based on previous study that already reported benefits of LLLT on mitochondria of myotubes (9). In addition, we found a strong correlation between MMP and ATP content measured during a wide range from 5 minutes (immediate effect) to 24h (prolonged effect). To our knowledge this is the first study investigating the time-response for light therapy modulation of mitochondrial metabolism in conjunction with ATP synthesis in muscle cells.

C2C12 is a cell line originally isolated from dystrophic muscles of C3H mice by Yaffe and Saxel (19). In culture it rapidly differentiates into contractile myotubes (muscle fibers) especially when treated with horse serum instead of fetal bovine serum. These myotubes contain multi-nucleated cells that express proteins characteristic of skeletal muscle such as myosin heavy chain and creatine kinase (20).

One of first effects of LLLT reported in literature was a modulation on MMP and ATP synthesis in mitochondria isolated from rat liver (3) and in HeLa cells (4). Our results are in accordance with these previous studies, showing an increased MMP and ATP synthesis in myotubes from C2C12 cells. However, light therapy seems to produce a different time-response of MMP and ATP synthesis among different cell types. While HeLa cells showed a peak of ATP synthesis around 20 minutes after light therapy (4), mitochondria from liver showed an immediate increase in MMP and ATP synthesis (3). In the present study we found that muscle cells need a longer time in the range of 3h to 6h to show the maximum effect of light therapy and convert it into a significant increase in MMP and ATP synthesis, comprising an increase around 200% to 350% over the control values. In addition, we found that 24h after irradiation, myotubes could still produce significantly more ATP compared to LEDT-Control while LEDT-5min showed no significant difference.

Cytochrome c oxidase (COX) has been reported to be the main chromophore in cells exposed to red and near infrared light (2, 21, 16, 15). However, although COX activity is important in the immediate effects of photon absorption, the measurement of its activity may be insufficient to confirm whether light therapy can induce “extra” ATP synthesis. For this reason the measurement of MMP in conjunction with ATP synthesis can provide information on how fast changes occur in the electron transport chain (ETC), and H^+ pumping from the mitochondrial matrix to the intermembrane space, as well as how much H^+ ions are returning to the mitochondrial matrix (1). In this perspective, our results are consistent with Xu et al. (9) who reported no immediate effects of light therapy on MMP. Moreover, although Xu et al. (9) did not assess ATP content, our results showed no significant responses for ATP increment immediately after light therapy compared to control group.

Our results for MMP in conjunction with ATP content had a high correlation (Pearson's r = 0.89) during the time range of 5min to 24h, suggesting a linear and positive dependence of ATP synthesis on the value of MMP (ETC and H^+ pumping) in muscle cells, suggesting a new and more efficient time-response or time-window for LEDT stimulate muscle cells (see figure 4A and 4B). These results are very important for muscle recovery post-exercise (10, 11) because they suggest a prolonged effect of light therapy on ATP synthesis necessary to repair muscle damage. In addition, muscular preconditioning using light therapy for improvement of performance before a bout of exercise (12) could possibly be optimized by application at the appropriate time. However more studies *in vivo* and clinical trials are needed to confirm our hypotheses.

Figure 4. Mechanism of action of LEDT on mitochondria.

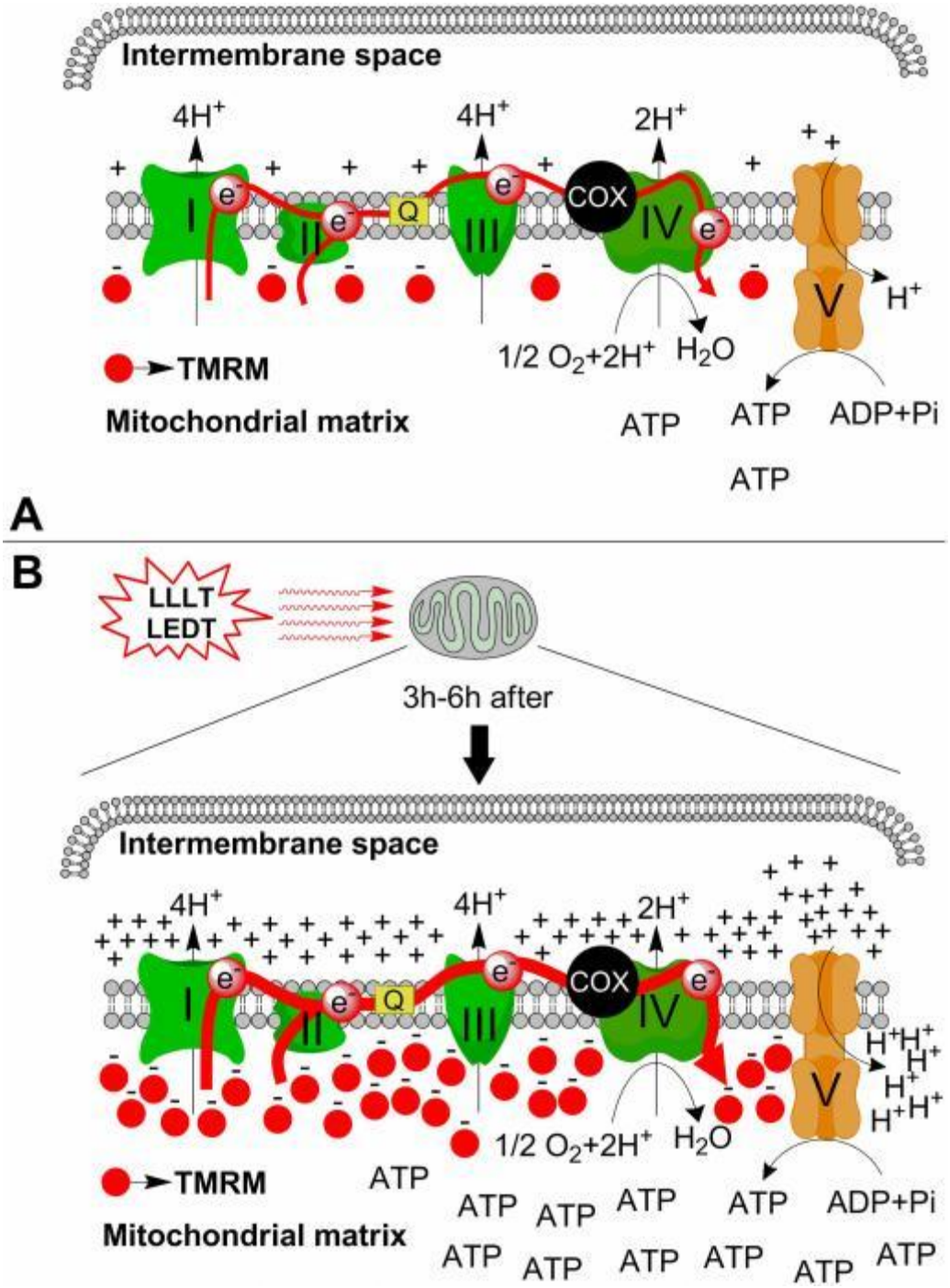

A) Mitochondria of myotubes from C2C12 cells without low-level laser therapy (LLLT) or light-emitting diode therapy (LEDT). There is a normal flux of electrons (red arrow) through all complexes of electron transport chain, normal pumping of H^+, normal synthesis of ATP and modest take up of TMRM by the mitochondrial matrix. **B)** Mitochondria of myotubes from C2C12 cells 3 to 6 hours after LEDT. There is an increased flux of electrons (ticker red arrow), increased pumping of H^+, increased

synthesis of ATP and increased take up of TMRM by the mitochondrial matrix. Abbreviations: I, II, III, IV and V= complexes of the mitochondrial electron transport chain; H^+= proton of hydrogen; - = electron of hydrogen; O_2= oxygen; H_2O= metabolic water; Q= quinone; COX= cytochrome c oxidase; ATP= adenosine triphosphate;TMRM= tetramethyl rhodamine methyl ester.

Muscular pre-conditioning using LLLT or LEDT have been reported as therapeutic approaches to improve muscle performance in both experimental models (22-24) and in clinical trials (12). However, although this improvement reported in the literature has been significant, some studies have not found positive results (25). Furthermore, differences between groups treated with light therapy or placebo seem to be not so large. These differences reported in experimental models varied between 80% to 150% of the values found for control groups for fatigue test induced by electrical stimulation (22-24). In clinical trials these differences varied between 5% to 57% increases in number of repetitions and maximal voluntary contraction (12). Possibly these relatively modest increases could be due to allowing insufficient time necessary for the muscle cells to convert light therapy into biological responses as identified in our study for MMP and ATP synthesis. Consequently, protocols for muscular pre-conditioning that have been done up to now (22-24, 12), i.e., generally applying light 5 minutes before the exercise, may not possibly achieve the best result. Based on our results, we suggest to wait 3h to 6h after light therapy irradiation to obtain the best increase in muscle performance in muscular pre-conditioning regimen, since MMP and ATP availability are important for muscle performance (26, 27). Once more time, we would like to remark the needed of more studies *in vivo* and clinical trials to confirm our hypotheses. At this point, it is valuable to reference two previous studies that had a similar initiative (28, 29). Hayworth et al. (28) found increments in COX activity 24h after apply LEDT over rats muscles; Albuquerque-Pontes et al. (29) found a time-window, wavelength-dependence and dose-response for COX activity increase also after LLLT in rats muscles. Both studies used animals without any kind of stress, such as this present study used cells only under the stress of the cell culture. We believe that these previous studies combined with our results are extremely valuable for the discovery and understanding of mechanisms of action of LLLT on muscle tissue, and may offer guidance on the future use of LLLT in clinical practice.

Our study was designed to test one dose of light during a time-response to show that there is time-dependency for LLLT to produce secondary responses in muscle cells. For this reason, the current study used a constant dose (fluence) of light as reported in a previous study (9) as well as a constant power density. Since there is a possible biphasic dose response (30, 31), use of different parameters such as fluence, wavelengths or irradiance could produce different responses. In addition, red and near-infrared light therapy was delivered at the same time in order to take advantage of the double bands in COX to absorb the light (2, 13-16).

CONCLUSION

This is the first study reporting the benefits of mixed red and near-infrared light therapy on MMP in conjunction with ATP synthesis in myotubes from C2C12 cells (muscle cells from mice). Moreover, a well defined time-response was found for the increase in ATP synthesis mediated by MMP increased by light therapy in myotubes.

Our data suggest that 3h to 6h could be the best time-response for light therapy to improve muscle metabolism. In addition, our results lead us to think there may be possible cumulative effects if light therapy is applied at intervals less than 24h that may have clinical relevance when LLLT is used for muscle post-exercise recovery. Finally, we believe that use of light therapy for muscular pre-conditioning could be optimized in future studies whether the time-response for increases in ATP and MMP found in this study are taken account.

ACKNOWLEDGMENTS

We would like to thank Professor Zoltan Pierre Arany and his instructor Glenn C. Rowe for the C2C12 cells and Andrea Brissette for assistance with multiple roles including purchase of reagents. Cleber Ferraresi would like to thank FAPESP for his PhD scholarships (numbers 2010/07194-7 and 2012/05919-0). MR Hamblin was supported by US NIH grant R01AI050875.

Mechanisms, pathways and strategies for rejuvenation through epigenetic reprogramming

Andrea Cipriano [1,2,8], Mahdi Moqri [1,3,4,8], Sun Y Maybury-Lewis [5,8], Ryan Rogers-Hammond [5], Tineke Anna de Jong [1,2], Alexander Parker [1,2], Sajede Rasouli [1,2], Hans Robert Schöler [6], David A Sinclair [5,7,✉], Vittorio Sebastiano [1,2,✉]

PMCID: PMC11058000 NIHMSID: NIHMS1985135 PMID: 38102454

.

Abstract

Over the past decade, there has been a dramatic increase in efforts to ameliorate aging and the diseases it causes, with transient expression of nuclear reprogramming factors recently emerging as an intriguing approach. Expression of these factors, either systemically or in a tissue-specific manner, has been shown to combat age-related deterioration in mouse and human model systems at the cellular, tissue and organismal level. Here we discuss the current state of epigenetic rejuvenation strategies via partial reprogramming in both mouse and human models. For each classical reprogramming factor, we provide a brief description of its contribution to reprogramming and discuss additional factors or chemical strategies. We discuss what is known regarding chromatin remodeling and the molecular dynamics underlying rejuvenation, and, finally, we consider strategies to improve the practical uses of epigenetic reprogramming to treat aging and age-related diseases, focusing on the open questions and remaining challenges in this emerging field.

Aging is the primary driver of many leading causes of death, including type 2 diabetes, neurodegenerative disease and cardiovascular disease. The precise reason for why we age is not completely understood, but the progressive nature and influence of external factors suggest that the process probably stems from a failure of maintenance mechanisms that ultimately impact epigenetic regulation and gene expression[1,2]. Several studies highlight how the external environment and the genetic background of an organism have pivotal roles in the aging process by affecting events that maintain epigenetic information[2,3].

Identifying and measuring biological aging is challenging owing to its multifactorial nature. Progress in the field led to the identification of critical biological changes based on the following criteria: (1) manifestation during physiological aging, (2) accelerated aging upon aggravation and (3) improvement of the aging process and increased lifespan with intervention[1,4]. These changes, collectively referred to as the ‘hallmarks of aging’, include mitochondrial dysfunction, loss of proteostasis, loss of stem cell function, cellular senescence, DNA damage, telomere attrition and impaired nutrient sensing.

Among the hallmarks of aging, loss of epigenetic information has been proposed as a critical cause of aging that precedes many other aspects of age-related deterioration[2,5–8]. Perturbing these epigenetic networks leads to extensive changes in gene expression that directly impact proteostasis, nutrient sensing, senescence and several other hallmarks of aging, suggesting that epigenetic networks are delicate and that their disruption probably initiates other events that cause cells to lose their function over time[8,9].

In contrast to the view of aging as an irreversible and unidirectional process akin to an increase in cell entropy, recent studies have demonstrated that multiple interventions, acting at different levels, can delay or even reverse this process[10–17]. These approaches aim to mitigate or even prevent aging-associated decline through repair or replacement strategies. Such interventions have been successful in reducing cell damage and preserving tissue health, but the long-term impact on whole organisms is still poorly understood[11–14].

One emerging strategy to intervene in the progression of biological aging is epigenetic reprogramming (Box 1), a technique first used by Shinya Yamanaka[18] to revert differentiated cells in vitro back to a pluripotent state. The landmark paper used four transcription factors, namely OCT4, SOX2, KLF4 and MYC (OSKM), to erase cell identity and reset cell-type-specific epigenetic signatures. Subsequent studies showed induced pluripotent stem (iPS) cell induction in vivo, indicating the possibility of cell de-differentiation in living organisms[19–21]. Although this discovery holds great promise for regenerative medicine, the observed frequency of tissue dysplasia and tumorigenesis implies that full cell reprogramming is not a viable anti-aging approach. Conversely, other works have shown that aging-associated DNA methylation patterns and biomarkers persisted when cells were transdifferentiated (Box 1) to different cell types, emphasizing the necessity of partial de-differentiation for rejuvenation (Box 1) to occur[22–25]. All this evidence ultimately led to the question of whether a similar, but modified, approach could be refined to rejuvenate cells in the context of age reversal. Early reports using cells derived from old donors to generate iPS cells demonstrated beneficial effects on senescence phenotypes and telomere length[26–28].

BOX 1.

Key terms

Cellular reprogramming

Cellular reprogramming is the process that allows the conversion of differentiated cells back into a pluripotent state (generating iPS cells). This conversion was first achieved in 2006 by Takahashi and Yamanaka, who demonstrated that the introduction of a specific combination of transcription factors can reprogram somatic cells, such as fibroblasts, into a pluripotent state resembling embryonic stem cells[18,122,123]. This groundbreaking discovery has revolutionized the field of regenerative medicine and opened up possibilities for disease modeling, drug discovery and personalized therapies. Cellular

reprogramming can also be achieved by using small molecules able to reset the epigenome[71,124], laying the foundations for developing safer regenerative therapeutic strategies.

Transdifferentiation

Transdifferentiation, also known as direct epigenetic conversion or direct cell reprogramming, is a process in which one specialized cell type is directly converted into another specialized cell type without passing through an intermediate pluripotent state[125]. This cellular reprogramming approach involves the modification of the epigenetic landscape of the starting cell, leading to the activation of a distinct transcriptional program associated with the desired cell fate. Transcription factors or other regulatory molecules are introduced into the starting cell to initiate the epigenetic remodeling and redirect its identity toward the target cell lineage. This direct conversion strategy offers a promising avenue for generating specific cell types for regenerative medicine and disease modeling, bypassing the need for pluripotent stem cells as an intermediate step.

Rejuvenation

Rejuvenation, in the context of biological systems, refers to the restoration or enhancement of cellular or organismal functions to a more youthful or healthier state, retaining their differentiated state. It encompasses the reversal or the attenuation of age-related deterioration, aiming to promote longevity and vitality[126,127]. In the context of rejuvenation research, longitudinal studies enable the assessment of the sustained effects of interventions on various parameters, including lifespan, healthspan and functional outcomes. By following individuals or model organisms longitudinally, it is possible to gather valuable data on the long-term efficacy and safety of rejuvenation approaches, as well as potential side effects or limitations[1]. Rejuvenation can be achieved through different strategies, including genetic interventions, epigenetic modifications, cellular reprogramming, regenerative therapies or modulating the organism’s environmental exposure. These approaches aim to counteract the accumulation of damage, restore cellular homeostasis and enhance tissue repair and regeneration[1,128].

These findings raised the question of whether reprogramming strategies could be harnessed to target age-related damage by manipulating the epigenome without compromising cell identity or function.

In this Review, we describe the current state of transient reprogramming in the context of rejuvenation and discuss areas of future investigation, including fine-tuning reprogramming approaches for safety and for tailoring to specific tissues.

Reprogramming factors

OSKM, known collectively as the Yamanaka cocktail, were used in the first successful generation of mouse iPS cells[18]. Shortly after, the same factors were used to induce pluripotency in various mouse and human somatic cell types[29,30]. Until now, cocktails containing combinations of the 'canonical' Yamanaka cocktail are frequently used for inducing partial reprogramming. In addition, partial reprogramming has also been achieved using other proteins and/or molecules. Here, we will review the structure and function of these factors in epigenetic reprogramming (below).

OCT4

Multiple studies have suggested OCT4 (Fig. 1a) as the master regulator of epigenetic reprogramming[31–33], as OCT4 overexpression alone is sufficient to induce pluripotency when other canonical reprogramming factors are endogenously expressed or are in the presence of other chromatin remodeling chemical factors[32,34,35]. Supporting this notion, optimal reprogramming requires threefold excess of OCT4 relative to the other factors[36].

Fig. 1 |. Structural diagram of each reprogramming factor.

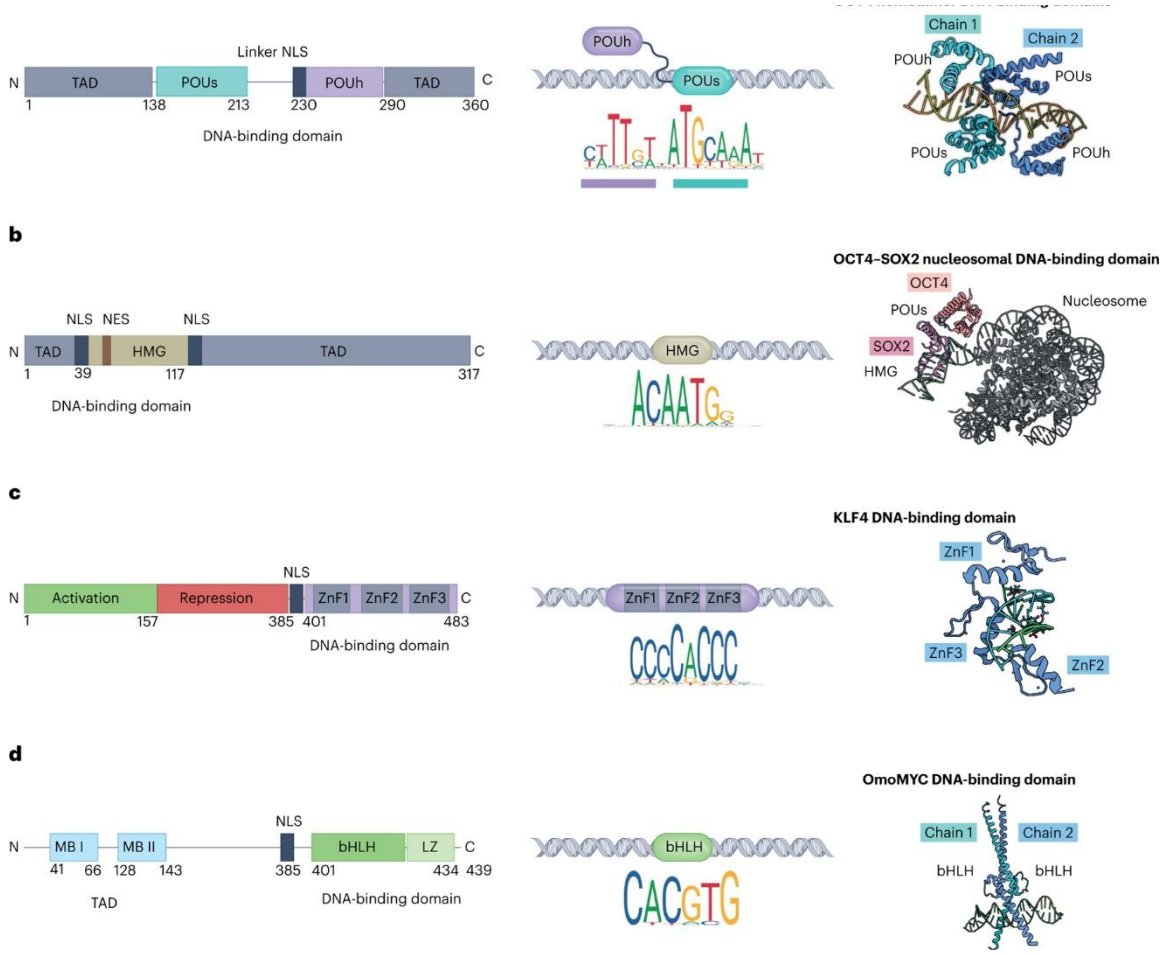

The linear domain structure (left), DNA-binding sequence (center) and DNA-binding domain structures (right) for OCT4, SOX2, KLF4 and MYC factors. **a**, OCT4 (PDB ID: 3L1P) refers to the isoform OCT4A encoded by the *POU5F1* gene, a DNA-binding transcription factor. The OCT4 DNA-binding (POU) domain consists of a POU-homeodomain (POUh) and a POU-specific (POUs) domain connected by a linker region. **b**, SOX2 (PDB ID: 6T90) contains a highly conserved, high mobility group (HMG) box DNA-binding domain comprising three α-helices, which bind the DNA minor groove and bend it by 90°. Early structural determination of the HMG POU-DNA revealed that the enhancers of target genes support the gene-specific configuration of the SOX2–OCT4 complex that binds DNA. The HMG includes two nuclear localization signals (NLS) and a nuclear export signal (NES). **c**, KLF4 (PDB ID: 5KE7) is a member of the cell-type specificity and Krüppel-like factor (SP/KLF) family, characterized by three zinc finger motifs (ZnF1, ZnF2 and ZnF3) with conserved ββα structure within the C terminus. The zinc fingers of KLF4, the second and third motifs, in particular, are responsible for contacting KLF4-specific sequences at the promoters of target genes, making them essential for KLF4-dependent reprogramming. **d**, MYC (PDB ID: 5I50) is a member of the basic helix–loop–helix zipper (bHLHZip) class of transcription factors, containing an N-terminal transactivation domain (TAD), two highly conserved sequences (known as MYC boxes), a central region containing a NLS and a C terminus containing the helix–loop–helix motif. The C terminus of MYC heterodimerizes with its obligatory partner MAX, which also contains a helix–loop–helix, and forms a stable four-

helix structure, capable of recognizing specific DNA sequences (such as CACGTG) at the promoters and enhancers of target genes[75]. The leucine zipper (LZ) domain is involved in protein dimerization and DNA binding. Created with BioRender.com.

During full reprogramming, OCT4 has been implicated in at least four distinct mechanisms. First, OCT4 directly recruits the BAF chromatin remodeling complex to promote a euchromatic chromatin state that enhances reprogramming factor binding[37–39]. Second, OCT4 directly binds enhancers of Polycomb group-repressed genes, which modify histones and silence target genes, to induce conversion of their associated promoters from monovalent to bivalent domains[40,41]. Third, OCT4 binds regulatory regions of pluripotency network genes to create an autoregulatory pluripotency network[42,43]. Finally, OCT4 directly binds and upregulates KDM3A and KDM4C, which demethylate H3K9Me2/3 at regulatory regions of pluripotency genes and promote their transcription by inducing a permissive epigenetic state[44].

SOX2

SOX2 is a transcription factor expressed during the emergence of the inner cell mass and is a developmentally essential gene, as its absence results in embryonic lethality[45]. Although SOX2 and its multifaceted roles in developmental as well as cancer biology have been well studied, most studies of SOX2 in the context of reprogramming focus on its heterodimerization and cooperative role with OCT4 (refs. 46–50) (Fig. 1b). Single-molecule imaging shows that SOX2 engages the chromatin first and primes the target site for subsequent OCT4 binding[47]. This is also supported by in vivo studies, suggesting that SOX2 alone can open the chromatin and bind target DNA sites before the arrival of OCT4 (ref. 51). Interestingly, OCT4/SOX2-shared sites have the most profound increase in accessibility during early reprogramming, and this partnership is critical for inducing pluripotency[51].

KLF4

KLF4 is a transcription factor containing both activator and repressor domains, conferring a dual function during cell differentiation[52] (Fig. 1c). OCT4 and SOX2 are mainly responsible for increasing chromatin accessibility during full iPS cell reprogramming, and KLF4 (as well as MYC, described in detail below) is believed to drive the first wave of transcriptional activation[42]. Co-immunoprecipitation and chromatin immunoprecipitation followed by sequencing studies reveal that OCT4–SOX2 binding increases KLF4 binding by several folds, mostly in chromatin regions that are closed in human fibroblasts[41,53,54]. We discuss the details of this process in the ‘Partial reprogramming events’ section.

MYC

In contrast with the OSK factors, which function synergistically as pioneer factors during reprogramming, MYC (Fig. 1d) does not exert this function[55]. Although recent studies

suggest that MYC is not required to initiate reprogramming[56,57], it is considered one of the most potent amplifiers of reprogramming[58]. The presence of MYC increases OSK binding by twofold[53], and MYC binding increases by 40-fold with OSK, supporting the notion that the modulatory activities of OSK and MYC on each other are bidirectional. The strongly pro-proliferative effects of MYC underlie its potential oncogenic ability, suggesting that in vivo or in therapeutic contexts it should be used with caution[57].

Additional factors

Next to OSKM, the reprogramming potential of additional factors is being studied and might give us alternatives for therapeutic or clinical implementation. One of the most studied factors besides OKSM is NANOG, a transcription factor belonging to the pluripotency network[59] and sharing 90% of the OCT4 and SOX2 binding regions[42]. It has been shown that NANOG and LIN28 in combination with SOX2 and OCT4 can reprogram human somatic cells into iPS cells[30] by increasing reprogramming efficiency by 76-fold[60]. Shahini et al. showed that NANOG alone has a pivotal role in ameliorating of senescence hallmarks and inducing rejuvenation in myogenic progenitor cells both in vitro and in vivo[61]. In addition to cell intrinsic transcription factors for cellular reprogramming, modulators such as vitamin C[62–65], IL-6[66–68], TGFβ[69] and bone morphogenetic proteins[70] have been shown to regulate cellular reprogramming by affecting DNA methylation levels, thereby adjusting the expression of certain microRNAs or facilitating the mesenchymal-to-epithelial transition (MET). Recent studies have demonstrated the potential of small molecule stimulation in facilitating chemical reprogramming by inducing an intermediate plastic state[71–73]. These small molecules effectively target key signaling pathways involved in cellular reprogramming, benefiting both human and mouse somatic cells[71–73]. Notably, specific small molecules such as 3-deazaneplanocin A, 5-azacytidine, sodium butyrate and RG108 have emerged as potential epigenetic modifiers[72]. As chemical reprogramming does not require integration into the genome, this approach holds the advantages of increased translational potential, preservation of genomic integrity and precise control of induction.

Partial reprogramming events

As epigenetic landscapes are reset, somatic cells undergo multiple intermediate stages during transcription factor-induced reprogramming. Here, we break down the early interactions between OSKM and chromatin that facilitate the cellular rejuvenation phase of reprogramming.

Somatic silencing and transcriptional remodeling

Cellular rejuvenation through partial reprogramming requires a careful balance of epigenetic remodeling and cell identity conservation, which can be achieved using a subset of reprogramming factors. Several studies have tried to define the molecular mechanisms underlying OSKM-driven reprogramming, but most have focused on pluripotency rather than cellular rejuvenation as the end goal. Despite these different contexts, ‘early transient events’ evoked by OSKM factors, such as somatic silencing

and chromatin remodeling while reprogramming is initiated, seem to be required for both cellular rejuvenation and full reprogramming[74–76].

Silencing the somatic gene-associated chromatin regions is the earliest event in reprogramming and is tightly regulated by OSK factors that canonically function in pluripotency[77]. As OSK factors are generally known as transcriptional activators[78,79], it may seem counterintuitive for chromatin closing to be the first step induced by these factors. There are currently two proposed models for how OSK influences somatic silencing: (1) displacement of somatic transcription factors away from their enhancers[80] and (2) downregulation of somatic factors with SAP30 through decreasing H3K27ac levels[77]. Interestingly, both models suggest that some somatic gene-associated chromatin loci that become inaccessible following OSK induction are not enriched with OSK binding motifs, supporting the notion that OSK induces somatic silencing through direct and indirect mechanisms.

OSK factors interact with the genome and each other differently in mice than in human cells[80–82], complicating the design and interpretation of studies. Specifically, in mouse embryonic fibroblasts (MEFs), OCT4 binds somatic enhancers during reprogramming and may initiate their inactivation, whereas in human fetal fibroblasts, OCT4 and SOX2 bind putative enhancers and remain bound in iPS cells. Ultimately, the ‘intermediate’ stages examined in these studies may reflect more of an incomplete, almost-pluripotent cell type, as opposed to the true epigenetic landscape during reprogramming. Given the differences in reprogramming duration and presumably dynamics, detangling the precise underpinnings of OSK-driven somatic silencing in different reprogramming contexts is challenging but critical.

As somatic programs are silenced, transcriptional remodeling events activate the pluripotency program. It was initially reported in MEFs that transcriptional remodeling occurs in two waves, the first driven by MYC and KLF4 in the first 3 days and the second by OSK (ref. 83). Genes associated with cell proliferation, metabolism and cytoskeleton organization were activated first, with developmental genes temporarily downregulated. Such changes were highly correlated with altered cell division, DNA replication, chromatin modification and the DNA damage response protein levels[84]. Clues on how these events relate to epigenomic rejuvenation may come from examining the mechanistic behaviors of OSKM, as discussed in the previous section. First, MYC primarily facilitates early gene induction for proliferation, whereas OCT4 and SOX2 induce chromatin opening while also binding readily open chromatin enriched with KLF4 motifs, supporting the notion that KLF4 recruits OCT4 and SOX2 to somatic chromatin that later becomes closed[83]. These findings are consistent with the proposed dual role of KLF4 in both transcriptional activation and repression.

The distinct mechanisms observed among combinations of OCT4 and SOX2 (without KLF4) versus OSK may explain the controversy regarding whether OSK mainly function as the pioneer factors or bind readily open chromatin in early reprogramming, or

both[80,82,83,85]. Importantly, we must note that all of the transcriptional remodeling studies utilizing OSKM occupancy data are limited to the events that occur in the beginning (fibroblasts) or end points (pluripotent stem cells), with everything in between still up for interpretation[80,83,85]. As the early events in reprogramming are largely transient[81], we are probably missing critical transitional OSKM–chromatin dynamics during such events, leaving mechanistic questions largely unanswered.

Resetting the epigenetic landscape

Along with transcriptional remodeling of somatic and pluripotency programs, OSKM transiently induces changes to histone tail post-translational modifications and DNA methylation. Changes in DNA methylation were initially thought to happen in the late stages of reprogramming[83], but a recent study revealed that loci near *Oct4*, *Klf4* and *Nanog* are demethylated earlier and de novo DNA methylation occurs in late reprogramming[85]. This reveals a cooperative relationship between DNA methylation and histone modifications that was not previously appreciated. On nucleosomes, levels of H3K4me2, a transcriptional activation mark, change rapidly at enhancers of pluripotency and development-related genes before gene expression changes are observed. At the same time, H3K4me3 levels at promoters remain largely stable and are correlated with transcriptional changes[86]. By contrast, repressive H3K27me3 is depleted only in enhancers that gain H3K4me2 toward a pluripotent state. Thus, alterations or additions of specific chromatin features are thought to 'prime' the transient epigenetic landscape for reprogramming before gene regulation[85]. Consistent with this notion, early loss of H3K27me3 is associated with acquiring a partially open or primed chromatin state[87].

A valuable tool to enhance reprogramming efficiency and gain mechanistic insights into epigenetic rejuvenation is the generation of pre-iPS cells. These cells, which have embryonic stem cell-like morphology[88] and SSEA-1 expression[85], may help to identify critical events occurring before cell identity programs are erased. Using this system, Chen and colleagues found that H3K9me3 inhibits full reprogramming of pre-iPS cells into stem cells, effectively functioning as a barrier to pluripotency[88]. Similarly, reducing H3K9me3 and H3K36me3 through inducible expression of a demethylase (KDM4B) improves iPS cell reprogramming efficiency[89]. How histone methylation at *cis*-regulatory elements affects transcriptional activation and repression is becoming more apparent, but the precise temporal order of epigenetic modifications and fluctuating dynamics over the course of cellular reprogramming remains elusive. Moreover, there are variations among cell-type-specific chromatin states during the early-to-intermediate phases of reprogramming that still need to be defined.

DNA methylation is another epigenetic feature that has a role in developmental programming and epigenetic reprogramming of aged cells. DNA methylation during iPS cell reprogramming facilitates chromatin remodeling while silencing differentiation-associated genes[90,91]. Despite the extensive changes in DNA methylation immediately before the final stages of MEF to iPS cell conversion, several sites in transiently

accessible chromatin lack DNA methylation before OSK binding. Moreover, enhancer chromatin opening generally follows OSK binding, which suggests that chromatin accessibility establishment occurs independently of DNA methylation. There is also evidence that changes to methylation occur in parallel with the observed alteration in chromatin contacts, and active DNA methylation via TET and TDG enzymes is required for rejuvenation[92].

Because the state of chromatin features and engagement with OSKM factors have primarily been defined in the context of iPS cell reprogramming, many aspects of partial reprogramming are poorly defined. It will be interesting to decipher when, where and how the interplay among chromatin features and OSKM factors change in the context of epigenetic reprogramming.

Proliferation, metabolic switch and MET

In addition to overhauling the epigenetic landscape via somatic silencing and chromatin remodeling, reprogramming to pluripotency appears to require cell division[93] so that cells can progress through the cell cycle-associated transcriptional dynamics[91]. With full reprogramming, the kinetics can be increased through both proliferation-dependent and independent ways, suggesting that multiple mechanisms coalesce to attain pluripotency. It is worth noting, however, that full reprogramming is relatively inefficient, with ~3% of cells reaching full reprogramming in the first round[83]. However, there is evidence that continued proliferation and OSKM expression eventually convert all cells to iPS cells, although such treatment can make cells vulnerable to apoptosis and cellular senescence[85,93].

Nonetheless, cell proliferation does not seem to be always required to reach pluripotency. For example, overexpression of LIN28 increases cell proliferation and accelerates iPS cell formation, but overexpression of NANOG achieves the same goal independent of cell proliferation. As such, proliferation and pluripotency may be complementary to promote survival during development, rather than acting sequentially. Hanna and colleagues[93] point out that increased cell proliferation may promote reprogramming by amplifying transiently reprogrammed daughter cells that ultimately become stem cells. Additionally, the group notes that nuclear changes during cell division may stabilize the dynamic epigenetic landscape governed by the pluripotency network. Whether the ‘transiently reprogrammed’ daughter cells in this context represent epigenetically rejuvenated youthful cells remains to be investigated, as well as the molecular mechanisms underlying heterogeneity of reprogramming latency.

The earliest phenotypic and transcriptional changes following OSKM expression begin with an immediate increase in cell proliferation induced by MYC[58]. At this point, cells also transition from the mesenchymal-to-epithelial state that is actively induced during this early phase and are required to progress through the reprogramming process[94–96]. Interestingly, cells switch from oxidative phosphorylation to glycolysis during this early

reprogramming phase[58]. Similar to gene expression changes, clustering analysis of proteins with temporal expression dynamics similar to gene expression changes reveals that electron transport chain proteins are downregulated in the first 3 days of reprogramming before a gradual metabolic switch to glycolysis, a characteristic that is typically seen in rapidly proliferating cells[84,97]. Moreover, multiple extracellular matrix proteins, including mesenchymal markers, are rapidly reduced, marking the initiation of MET. This process reverses the epithelial-to-mesenchymal transition in development and differentiation, characterized by downregulation of cell adhesion and motility. Interestingly, OSKM facilitates MET by suppressing the regulation of epithelial-to-mesenchymal transition through multiple mechanisms, such as OCT4 and MYC repression of TGFβ signaling[33,94], OCT4 and SOX2 activation of miR-200 family[33,98], and OCT4 and KLF4 chromatin opening and activation of epithelial genes[37].

Partial reprogramming as a strategy for epigenetic rejuvenation

Although developments in cellular reprogramming have proposed several new and promising medical avenues[19–21], continuous expression of OSKM factors in vivo is limited by substantial safety concerns including severe weight loss, the formation of circulating totipotent stem cells and teratomas in several organs[19]. Ohnishi et al.[21] provided evidence that the duration of OSKM overexpression has a pivotal role in the de-differentiation process. These initial findings identified the factors' expression levels and duration of treatment as sensitive components of the process and helped to establish parameters for in vivo rejuvenation applications. Through careful fine-tuning of in vivo reprogramming protocols, subsequent research from Ocampo and colleagues later established the potential for the technique to modulate phenotypes of aging. We will walk through the recent landmark findings targeting aging and age-related diseases by partial epigenetic reprogramming below (Fig. 2).

Fig. 2 |. Timeline highlighting publications on partial reprogramming in mouse and human models.

Important takeaways from in vitro and in vivo partial reprogramming experiments with the aim of relieving aging phenotypes. Brown and blue boxes indicate works performed in mice and humans, respectively.

Whole-organism partial reprogramming in mouse

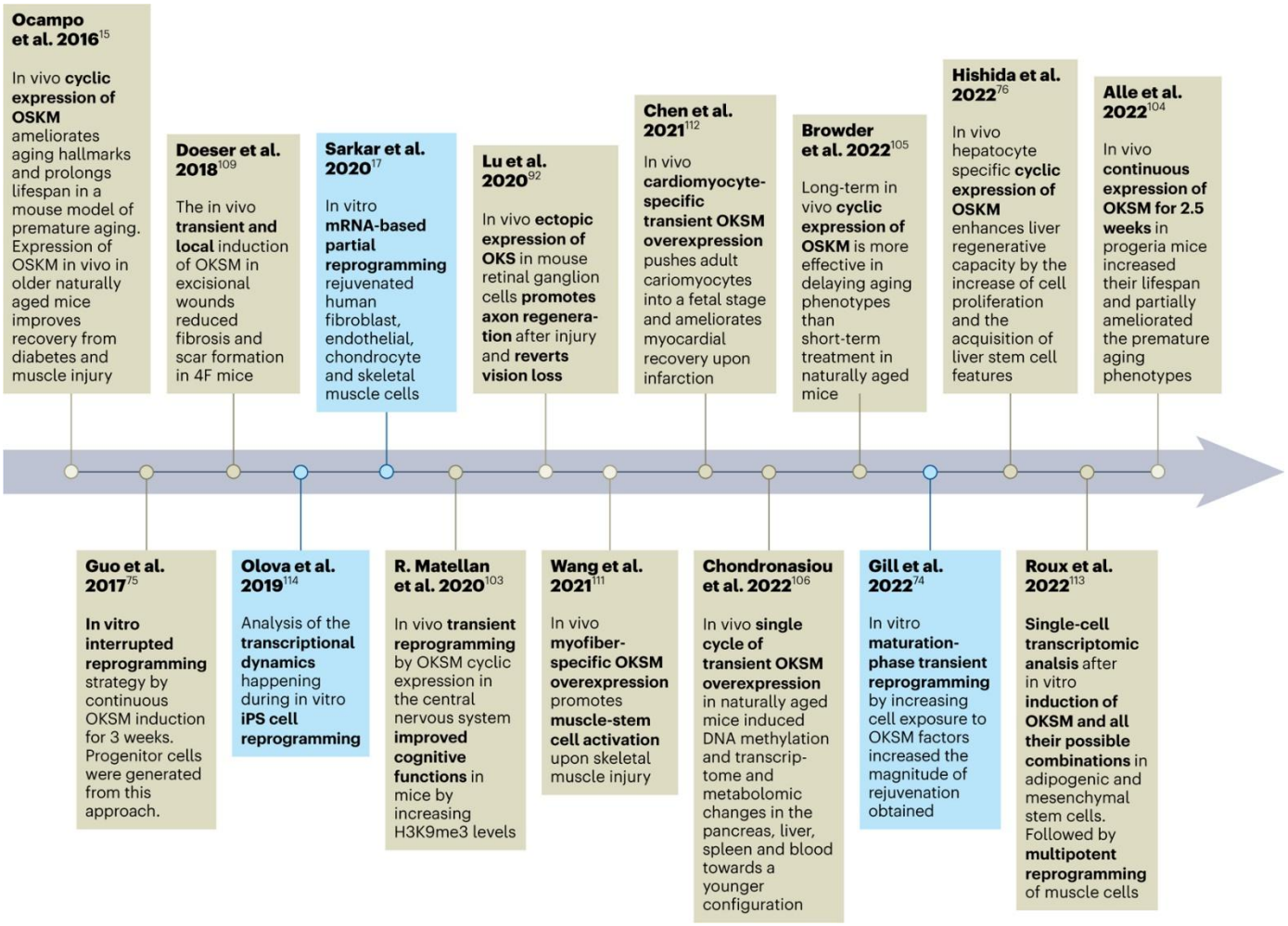

The idea of inducing epigenetic transition to a ‘youthful’ state without the loss of cell identity, defined as ‘epigenetic rejuvenation’, was proposed for the first time in 2010 (refs. 99–101). Leveraging these findings and other works[101,102], Ocampo et al. reached an unprecedented milestone: in vivo rejuvenation through OSKM by using the LAKI premature aging mouse model engineered to carry a doxycycline (DOX)-inducible OSKM polycistronic cassette (4F) (Fig. 3a). Excitingly, pulsing OSKM expression in heterozygous LAKI 4F mice ameliorated cellular and physiological aging markers without any sign of teratomas, which were seen if the same protocol was carried out on a homozygous 4F mouse. In addition, the Ocampo reprogramming protocol improved recovery from diabetes and muscle injury in old wild-type mice, confirming their results in the context of normal physiological aging. However, the observed rejuvenation effects were transient and diminished after stopping the DOX cycle in vitro[15]. The work from

Ocampo et al. opened a new chapter in the transient reprogramming field and set into motion experiments attempting to find a way to reprogram, prove age reversal and define optimal parameters.

Fig. 3 |. Summary of detailed in vivo whole-organism partial reprogramming protocols.

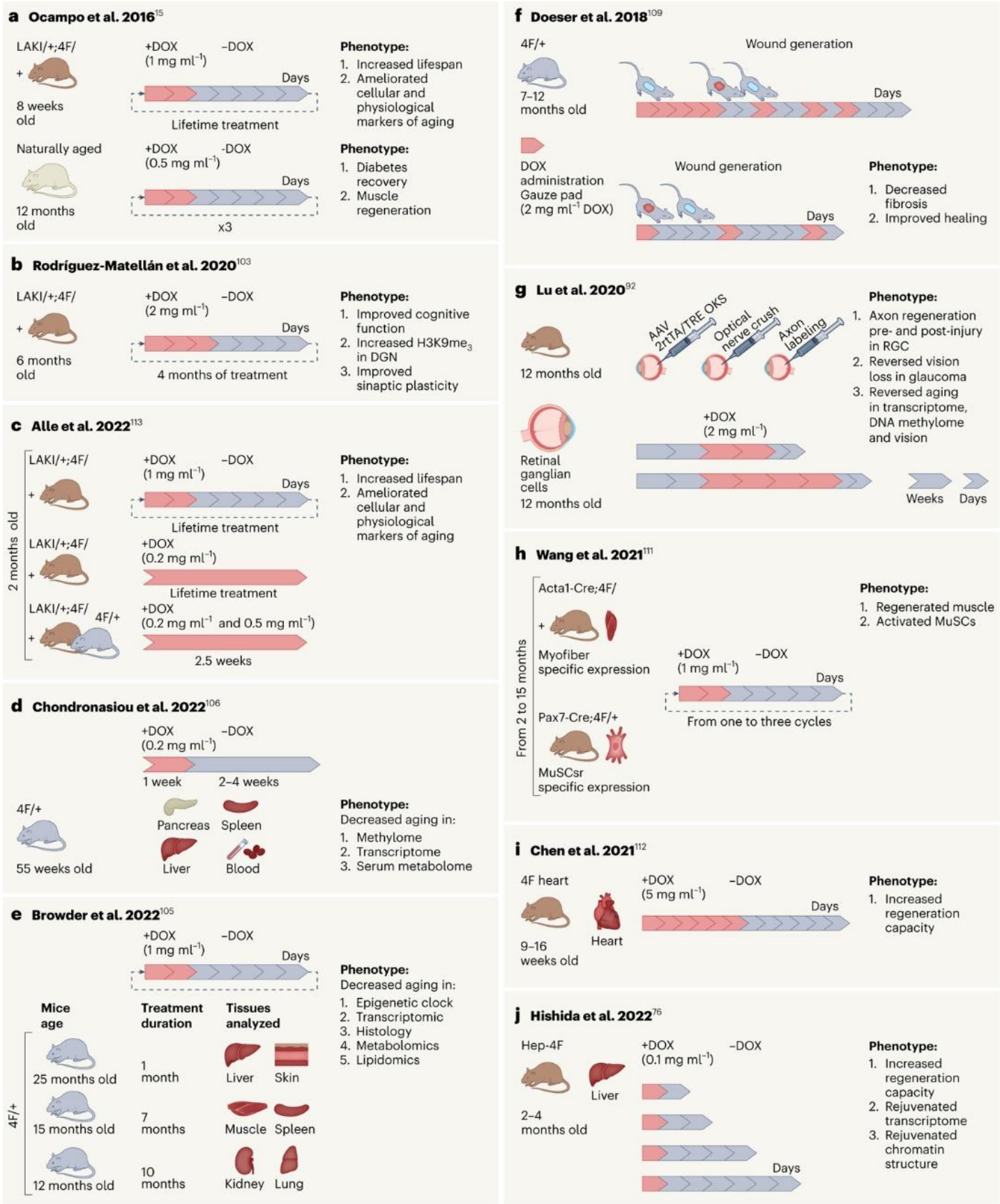
a Ocampo et al. 2016[15]
LAKI/+;4F/+
8 weeks old
+DOX (1 mg ml−1)
−DOX
Days
Lifetime treatment
Phenotype:
1. Increased lifespan
2. Ameliorated cellular and physiological markers of aging
Naturally aged
12 months old
+DOX (0.5 mg ml−1)
-DOX
Days
x3
Phenotype:
1. Diabetes recovery
2. Muscle regeneration
b Rodríguez-Matellán et al. 2020[103]
LAKI/+;4F/+
6 months old
+DOX (2 mg ml−1)
−DOX
Days
4 months of treatment
Phenotype:
1. Improved cognitive function
2. Increased H3K9me3 in DGN
3. Improved sinaptic plasticity
c Alle et al. 2022[113]
2 months old
LAKI/+;4F/+
+DOX (1 mg ml−1)
−DOX
Days
Lifetime treatment
LAKI/+;4F/+
+DOX (0.2 mg ml−1)
Lifetime treatment
LAKI/+;4F/+ 4F/+
+DOX (0.2 mg ml−1 and 0.5 mg ml−1)
2.5 weeks
Phenotype:
1. Increased lifespan
2. Ameliorated cellular and physiological markers of aging
d Chondronasiou et al. 2022[106]
+DOX (0.2 mg ml−1)
−DOX
1 week
2–4 weeks
4F/+
55 weeks old
Pancreas
Spleen
Liver
Blood
Phenotype:
Decreased aging in:
1. Methylome
2. Transcriptome
3. Serum metabolome
e Browder et al. 2022[105]
+DOX (1 mg ml−1)
−DOX
Days
Mice age
Treatment duration
Tissues analyzed
4F/+
25 months old
1 month
Liver
Skin
15 months old
7 months
Muscle
Spleen
12 months old
10 months
Kidney
Lung
Phenotype:
Decreased aging in:
1. Epigenetic clock
2. Transcriptomic
3. Histology
4. Metabolomics
5. Lipidomics
f Doeser et al. 2018[109]
4F/+
7–12 months old
Wound generation
Days
DOX administration Gauze pad (2 mg ml−1 DOX)
Wound generation
Days
Phenotype:
1. Decreased fibrosis
2. Improved healing
g Lu et al. 2020[92]
12 months old
AAV 2rtTA/TRE OKS
Optical nerve crush
Axon labeling
Retinal ganglian cells 12 months old
+DOX (2 mg ml−1)
Weeks
Days
Phenotype:
1. Axon regeneration pre- and post-injury in RGC
2. Reversed vision loss in glaucoma
3. Reversed aging in transcriptome, DNA methylome and vision
h Wang et al. 2021[111]
From 2 to 15 months
Acta1-Cre;4F/+
Myofiber specific expression
+DOX (1 mg ml−1)
−DOX
Days
From one to three cycles
Pax7-Cre;4F/+
MuSCsr specific expression
Phenotype:
1. Regenerated muscle
2. Activated MuSCs
i Chen et al. 2021[112]
4F heart
9–16 weeks old
Heart
+DOX (5 mg ml−1)
−DOX
Days
Phenotype:
1. Increased regeneration capacity
j Hishida et al. 2022[76]
Hep-4F
2–4 months old
Liver
+DOX (0.1 mg ml−1)
−DOX
Days
Phenotype:
1. Increased regeneration capacity
2. Rejuvenated transcriptome
3. Rejuvenated chromatin structure

a–**e**, Whole-organism partial reprogramming for Ocampo et al. 2016 (ref. 15) (**a**), Rodríguez-Matellán et al. 2020 (ref. 103) (**b**), Alle et al. 2022 (ref. 104) (**c**), Chondronasiou et al. 2022 (ref. 106) (**d**) and Browder et al. 2022 (ref. 105) (**e**). **f**–**j**, Tissue-specific partial reprogramming for Doeser et al. 2018 (ref. 109) (**f**), Lu et al. 2020 (ref. 92) (**g**), Wang et al. 2021 (ref. 111) (**h**), Chen et al. 2021 (ref. 112) (**i**) and Hishida et al. 2022 (ref. 76) (**j**). Each panel shows the strain of mice used and the respective ages (left), the tissues analyzed and the protocol of partial reprogramming (center) and the phenotype analyzed (right). Pink and grey arrows indicate days or weeks (specified below or above the arrow) of DOX administration and DOX removal, respectively. Created with BioRender.com.

Mechanistic studies were later complemented from Rodríguez-Matellán et al., who demonstrated that the cyclic expression of OKSM improved cognitive functions in mice by increasing H3K9me3 levels in dentate gyrus adult neurons. Migration, survival and, by consequence, synaptic plasticity (Fig. 3b) were all improved[103], suggesting that cell physiology could be enhanced through partial reprogramming without affecting cell replication.

As more insight was garnered regarding experimental approaches to achieve partial reprogramming, dynamics of four-factor expression were identified as a primary variable that needed to be addressed in reprogramming efficacy. A recent paper published by Alle and colleagues demonstrated that rejuvenation outcomes might be more consistent by modifying OSKM methods (Fig. 3c)[104]. Specifically, they compared continuous overexpression of OSKM with a lower dosage of DOX (0.2 mg ml^{-1}) in LAKI/+;4F/+ mice to the standard protocol of Ocampo and colleagues and observed a near-identical increase in the lifespan of mice treated with both protocols. It is noteworthy that, when the same continuous induction protocol was applied by Abad et al., it resulted in teratoma formation and mice death, indicating possible intrinsic genetic differences between the different strains (probably due to the different 4F insertion and the different genetic background of the mice R26rtTA/+;Col1a14F2A/+;LmnaG609G/+ versus R26rtTA/+;Col1a14F2A/+;) that could account for the divergent outcomes observed. Furthermore, a single 2.5-week period of continuous overexpression increased lifespan by 15% and partially ameliorated the premature signs of aging in mice, despite having no noticeable difference in the median age of death. Interestingly, when the same protocol was applied to nonprogerice mice, the effects were markedly less pronounced, with lifespan only being extended by 18 weeks. This finding led authors to speculate that healthy animals may be less sensitive to partial reprogramming early in life (Fig. 3c).

Additionally, work from the Serrano and Belmonte groups has further examined reprogramming in naturally aged mice, using single-shot and cyclic OSKM, respectively[105,106]. In particular, Chondronasiou and colleagues demonstrated that a single pulse of continuous OSKM induction for 7 days (using 0.2 mg ml^{-1} of DOX) in naturally aged mice can trigger epigenetic, transcriptomic and metabolomic rejuvenation

patterns (Fig. 3d) (interestingly, no effect on the number of senescent cells was detected). The study demonstrated that the rejuvenation effect was more prominent in the pancreas than the spleen, liver and blood[106]. In addition to this, the authors, in a related study, monitored the roadmap of reprogramming in the pancreas and identified intermediate reprogramming states by using a single-cell transcriptomic, which could be functionally relevant for tissue regeneration and rejuvenation[107]. This study also highlights how OSKM overexpression has drastically different effects on different cell types within the same organ. This is probably due to the different plasticity or susceptibility of the different cell types to reprogramming, further stressing the importance of studying these molecular dynamics in individual cell types to be able to design cell-type-specific rejuvenation protocols.

Browder and colleagues have instead increased the duration of partial reprogramming to up to 10 months using the 4F/+ mouse model at different ages with a cycling DOX regimen[105] (Fig. 3e). In this study, a short-term cycling partial reprogramming cohort was compared with two different cohorts of long-term partial reprogramming and subsequently examined for markers of rejuvenation (Fig. 3e). They did not observe teratoma formation during the long-term treatment. Most importantly, they found that an extended treatment regimen leads to more pronounced rejuvenation effects as compared with short term when examining epigenetic clocks, transcriptomics and metabolomics in several different organs and tissues (skin and kidney in particular). It is important to highlight that, whereas previous studies have predominantly focused on the premature aging LAKI model, these two studies both implemented wild-type, natural aging models, thus providing more physiologically relevant insights. In addition, it was demonstrated in these studies that cells can be effectively rejuvenated by employing different regimens of overexpression. These findings are consistent with Macip and colleagues who reported in 2023 that adeno-associated viruses encoding an inducible OSK system extended the median remaining lifespan of extremely old mice by 109% compared with untreated mice and improved several health parameters, including frailty[108].

Tissue-specific partial reprogramming in mouse

Despite making substantial progress and providing clear evidence that controlled induction of reprogramming factors could improve cell function and extend lifespan without forming iPS cells in mice, many questions remained. Why rejuvenation was temporary, how systemic induction prevented loss of cell identity and whether benefits were due to cell autonomous or nonautonomous events remained poorly understood and required further analysis. Doeser et al. took advantage of well-characterized wound healing protocols to fill in the gaps. Instead of adding DOX to drinking water, they applied DOX directly to wounds to induce local overexpression of OSKM and measured the effect on wound healing (Fig. 3f). Results from these experiments uncovered an essential element of OSKM rejuvenating potential, showing that local and transient factor exposure to cutaneous wounds significantly reduced fibrosis[109]. Analysis of treated tissues revealed that the observed effects were due to diminished fibroblast-to-myofiber differentiation, promoting healing and concomitantly reducing scar formation. It

is essential to note here that despite the induction being local, the cell types responsible for the rejuvenation cannot be uniquely identified because of the heterogeneous composition of the skin at the cellular level.

The demonstration that the DNA methylation clock can be reversed in vivo by reprogramming and that long-term reprogramming can be achieved using a specific subset of reprogramming factors came from Lu et al. in 2020 (ref. 92). The authors showed that the ectopic and constant expression of OSK in retinal ganglion cells in vivo is able to restore vision by promoting axon regeneration in aged and glaucomatous mice without increasing cell proliferation (Fig. 3g). Interestingly, induction of the factors both before and after the optical nerve injury led to increased regeneration capability of retinal ganglion cells. The authors demonstrated that the observed regenerative phenotype is mediated by the active contribution of TET1 and TET2 DNA demethylases and the TDG DNA glycosylase, indicating a critical role for dynamic DNA methylation during partial reprogramming. Similar results were also obtained in human neurons, suggesting an evolutionarily conserved mechanism[92]. Of note, when OSK were co-delivered as monocistronic vectors, no axon regeneration was observed, further supporting the idea that specific levels of OSK expressions of the elements in addition to cell identity are essential to exert optimal function. Importantly, this study is also the first to show that cellular damage accelerates epigenetic aging, a change that OSK counteracts to allow cells to regain youthful gene expression patterns and functions. Interestingly, whole-body overexpression of OSK for a year was found to have no observable negative effects, suggesting that MYC might be responsible for some of the toxicity. However, it is crucial to note that continuous ectopic overexpression of OCT4 also resulted in dysplastic growth in epithelial tissues[110], providing additional evidence for the tissue-specific nature of these effects.

Similarly, Wang and colleagues focused on muscle stem cells (MuSCs) and employed a MuSC-specific OSKM inducible mouse model to investigate OSKM's effects on muscle regeneration. They showed increased MuSC activation and proliferation only when the factors are overexpressed before the injury (both in old and young mice) without affecting their self-renewal capability. This increase in MuSC proliferation upon OKSM overexpression was induced via p53–p21 signaling, which inhibits Wnt4 and contributes to the activation of MyoD and YaP in MuSCs, suggesting that manipulation of specific pathways may be critical to achieving rejuvenation[111] (Fig. 3h). Interestingly, the specific overexpression of the factors in MuSCs did not improve muscle regeneration, arguing that the rejuvenation effect on MuSCs is cell nonautonomous and induced by myofibers[111]. Shortly after, similar work showing that partial reprogramming of a specific cell type can revert aging by promoting cell regeneration came from Chen and colleagues[112] (Fig. 3i). The authors were able to partially reprogram in vivo adult mouse cardiomyocytes, bringing them from an adult to a fetal stage where the cells could proliferate without losing their identity. Cardiomyocytes were then allowed to regenerate after myocardial infarction. Interestingly, similar to prior reports, the effects induced were almost wholly reversed after 6 days of DOX withdrawal[112], and partial de-differentiation results correlated with the cardiomyocyte developmental stage,

confirming the dependence of the phenotype observed on the epigenetic state of the cells.

Following this work, Hishida et al. showed other evidence of the importance of the level of expression of OSKM factors, depending on the targeted cell type. They examined the effects of partial reprogramming, specifically on liver regeneration capacity, using an Alb–Cre-transgene 4F mouse model (Hep-4F), and applied an optimized DOX treatment (0.1 mg ml^{-1})[76] (Fig. 3j). One day of DOX treatment resulted in increased cell proliferation in the liver and loss of mature hepatocyte markers, indicative of successful partial reprogramming to a progenitor state and enhanced liver regeneration capacity. In addition, the global transcriptomic analysis showed that chromatin accessibility was actively changed by 4F, suggesting that reprogramming is dependent on chromatin reshaping. Furthermore, they showed that expressing only MYC, known as a hepatocyte proliferation accelerator, could not induce the loss of hepatocyte markers. This suggests that cell proliferation is not the only driver of partial reprogramming[76].

In vitro partial reprogramming in mouse

The possibility of pushing partial reprogramming further to promote cell regeneration via partial de-differentiation by a temporal and partial loss of cell identity came from the work of Guo and colleagues[75]. The authors generated ‘induced progenitor-like cells’ in vitro by expressing OSKM for 3 weeks in fully differentiated bronchiole secretory cells from 4F mice (Fig. 4a). Proliferative capacity was restored and accompanied by a shift toward a transcriptionally intermediate state, characterized by a minimal expression of embryonic stem cell-related genes and the constitutive expression of tissue-specific profiles. Interestingly, 2 weeks after DOX withdrawal, cells returned to their fully differentiated stage by preserving their lineage commitment both in vitro and in vivo, as shown by their ability to repopulate injured airway epithelium in vivo[75].

Fig. 4 |. Summary of detailed in vitro partial reprogramming protocols in mouse and human.

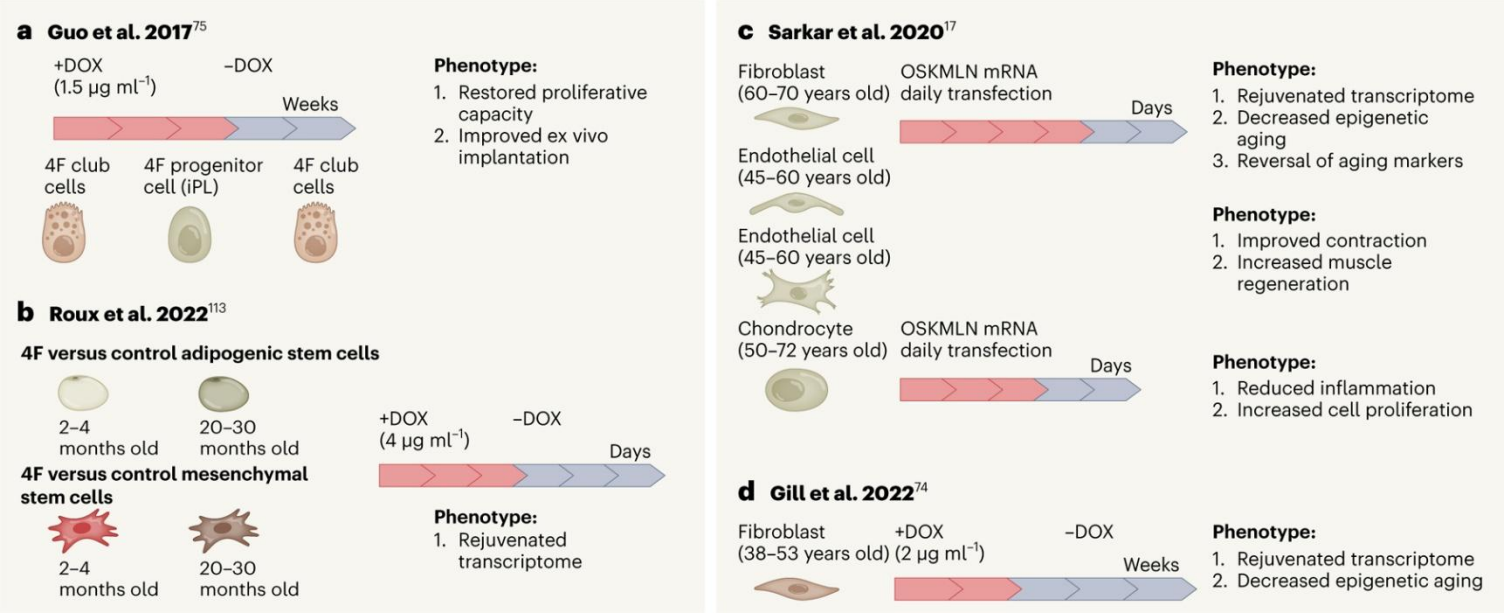

a,**b**, Mouse summary of reprogramming protocols for Guo et al. 2017 (ref. 75) (**a**) and Roux et al. 2021 (ref. 113) (**b**). **c**,**d**, Human summary of reprogramming protocols for Sarkar et al. 2020 (ref. 17) (**c**) and Gill et al. 2021 (ref. 74) (**d**). Each panel shows the cell type used with the respective donor or mice ages (left), the protocol of partial reprogramming (middle) and the phenotype analyzed (right). Pink arrows indicate days or weeks (specified above each induction protocol) of DOX administration (**a**,**b**,**d**) or mRNA transfections (**c**), and purple arrows indicate days or weeks upon DOX removal (**a**,**b**,**d**) or after mRNA transfections (**c**). Created with BioRender.com.

Roux and colleagues obtained a similar partial de-differentiation event in adipogenic and mesenchymal stem cells from old and young mice[113] (Fig. 4b). Using a single-cell approach to account for potential heterogeneity, the transcriptome of each cell population revealed suppression of somatic cell identity genes in both cell types while inducing hallmark pluripotency programs following 3 days of OKSM DOX exposure and 3 days of DOX withdrawal (Fig. 4b). These findings echoed previous observations using bulk approaches[75,114], but the resolution of single-cell RNA sequencing here showed that reprogramming events are consistently partial. Interestingly, based on RNA velocity analysis, they forecasted that partially reprogrammed cells tended to transition back toward their original gene expression states[113]. Further analysis will be required to fully understand the role of identity suppression and retrieval during partial reprogramming. Interestingly, Roux and colleagues used the same induction protocol to repeat their analysis and overexpressed all the possible combinations of the four factors in both cell types in a pooled screen. They found that all combinations of the Yamanaka factors at least partially suppressed the cell identity program and restore youthful gene expression at a magnitude that correlated with the number of factors used rather than their identities. This was a critical finding because it provided evidence of a synergistic function between the factors that directly impacted reprogramming potential. Finally, to prove that partial reprogramming can be achieved by also overexpressing cell-type-

specific regenerative factors, they tried a new partial reprogramming approach in skeletal MuSCs by overexpressing the *Msx1* gene (which is involved in digit and limb regeneration[115–117]). They found that this approach partially restores youthful gene expression in myogenic cells and promotes differentiation without inducing any partial loss in cell identity[113], further supporting the idea that other transcription factors might represent a safer alternative to induce epigenetic rejuvenation as also reported by other groups[61,118].

In vitro partial reprogramming in human cells

Although experiments in mice provided foundational evidence that epigenetic reprogramming can reverse aspects of aging, it is an open question of how these effects will translate into human biology. Early experiments in human cells were somewhat encouraging as they provide evidence that some of the biomarkers of aging (that is telomere lengths) were responding to the epigenetic reprogramming, but protocols relied upon rejuvenation through re-differentiation after iPS cell formation[20,26,28]. The first attempt to optimize the process in humans and eliminate the need to start from a blank slate was made by Manukyan and colleagues in 2014, nearly 2 years earlier than the landmark publication from Belmonte's group[15]. LIN28, an RNA-binding protein best known for its role in promoting pluripotency via regulation of the microRNA let-7, was added to the OSKM cocktail and used to treat senescent fibroblasts. After 9 days of reprogramming, HP1b mobility, an indicator of active cell cycling, was restored to the same levels found in young fibroblasts without sacrificing cell identity[100].

A detailed description of reprogramming kinetics in human cells was provided by Olova and colleagues in 2019 (ref. 114), who analyzed epigenetic and transcriptomic data to define the time course of human dermal fibroblast rejuvenation[119]. Using Horvath's clock[120], they found that epigenetic rejuvenation started between days 3 and 7, continuing until day 20 when the treated cells reached an epigenetic age of zero[114]. Transcriptomic analysis of fibroblast gene signatures showed an overall reduction in expression with comparatively stable levels until day 15. By contrast, pluripotency genes showed an inverse relationship that steadily increased over time until reaching an apparent threshold around the same time. These observations led to the conclusion that this time point represents an optimal point for achieving epigenetic rejuvenation without losing cell identity. The rationale for this conclusion lies in the fact that many aging-associated epigenetic marks are shed without the initiation of actual pluripotency programs. Maintenance of somatic profiles makes these cells more probable to revert toward the original and previously established cell fate when the expression of reprogramming factors is stopped.

Although this work established a benchmark for reprogramming human cells, it was not possible to consider transcriptional heterogeneity during reprogramming as bulk-based analyses were used, which (as previously discussed) were later shown to exert mosaic-like expression patterns in tissues[113]. Exploiting this caveat has led to single-cell-based

transcriptomic approaches and a better understanding of reprogramming potential in specific cells and tissues. Leveraging directives from foundational publications, Sarkar et al. obtained the first evidence of partial reprogramming-induced rejuvenation in old human cells in vitro[17]. A new, noninvasive messenger RNA-based delivery strategy was used for the transient expression of six reprogramming factors, OSKM, LIN28 and NANOG (OSKMLN), in human cells (Fig. 4c). Transcriptomic analysis of the three cohorts of cells showed that OSKMLN treatment induced a more youthful and cell-type-specific gene expression profile without affecting the expression of cell-specific genes. Importantly, the extent of OSKMLN reprogramming was multifaceted and far-reaching, as epigenetic hallmarks of aging (H3K9me3, HP1g, LAP2a and SIRT1), functional parameters (autophagosomal, mitochondrial and proteasomal activities) and epigenetic clocks were significantly impacted, with treated cells more closely resembling younger cells compared with their age-matched old counterparts. Interestingly, rejuvenation was retained 6 days after interrupting the treatment. Similar results were also obtained in chondrocytes and human MuSC cell types, confirming that this method works in different cell types. These findings validate a nonintegrative clinical method for reprogramming and open avenues for in vitro and in vivo rejuvenation strategies.

Although substantial progress was made concerning developing an efficacious reprogramming cocktail, the timing and duration of induction was still open for optimization. Fortunately, work in mice identified a window, known as the maturation phase, during reprogramming where cells were most probable to experience rejuvenation without crossing the threshold and become iPS cells[96]. Gill and colleagues took advantage of this window and induced extended overexpression of the reprogramming factor cocktail for 10–14 days before withdrawing for an additional 4 weeks to allow for fibroblast re-differentiation (Fig. 4d)[74]. With this protocol, defined as ‘maturation phase partial reprogramming’, they achieved more substantial rejuvenation than had been described before at levels comparable to Guo et al.’s work in mice[74,75]. Specifically, analysis of the epigenetic clock after in vitro partial reprogramming showed approximately 30 years of rejuvenation. Surprisingly, rejuvenation only occurred when the factors were overexpressed for 13 days, and no significant effects were observed at the other time points, suggesting that day 13 is a critical time point in the rejuvenation process, though, notably, later time points (days 15 and 17) failed to show an epigenetic rejuvenation effect. Moreover, rejuvenation effects were maintained for at least 4 weeks after treatment, representing the most extended retention of youthful status following reprogramming. A possible explanation for these interesting outcomes may be that fibroblast-specific enhancers remained demethylated during partial reprogramming[74], which may indicate retention of epigenetic memory required for reversion to the proper somatic state.

Concluding remarks and future perspectives

The ability to re-shape the chromatin into a more youthful state without inducing irreversible changes to cell identity has pioneered a new area of aging research. In this Review, we have focused on elucidating the biological mechanisms and pathways involved in reprogramming initiation, as well as the connection between reprogramming

and epigenetic rejuvenation. Collectively, the works described suggest that timing and the identity of each factor and their relative stoichiometry require fine-tuning in different cell types to achieve a rejuvenated phenotype. For these reasons, they may need to be tailored for each organ or tissue to promote rejuvenation without inducing a complete loss in cell identity.

In this direction, tissue-specific overexpression studies paired with single cell-based analyses will be invaluable to better consider the unique identity of the cells and of their initial chromatin state, as well as the co-existence in vivo of cell autonomous and nonautonomous functions.

An important aspect to consider is whether a partial ‘de-differentiation’ is necessary for effective rejuvenation. Although some studies suggest that rejuvenation of the epigenome can occur without a de-differentiation step and involve ‘re-differentiation’[121], others indicate that partial de-differentiation has a crucial role. These diverse perspectives underscore the complexity of cell-type-specific rejuvenation mechanisms and highlight the need for further investigation to determine the precise requirements in different cellular contexts. In addition to this, the use of a naturally aged system has important strengths over premature genetic models, as the latter may introduce confounding factors that can alter the outcome of the results.

Despite being useful to validate feasibility in human cells and perform molecular studies, partial reprogramming in vitro poses additional challenges as cultured cells often lose some aging-related features observed in vivo and might exhibit confounding environment-induced phenomena.

Another limiting factor in advancing the field is the lack of suitable and universal molecular biomarkers for measuring age reversal. Existing epigenetic clocks, originally developed for different purposes, have not been thoroughly demonstrated to provide accurate readouts for anti-aging interventions.

Lastly, safety remains a critical aspect of partial reprogramming. Although some studies have not seen any detriment to tissues after more than a year of overexpression[92], this issue remains unresolved. Although RNA-based approaches or the replacement of OKSM genes with potentially safer genes or small molecules acting as chromatin modulators hold promise, comprehensive evaluation and mechanistic investigation will be necessary to establish safety and efficacy in humans.

The convergence of these diverse sets of evidence underscores the necessity for additional strengthening and validation by the scientific community to establish acceptance and credibility regarding certain findings. The resulting perplexity serves as a stark reminder of the ongoing challenge in developing clinically applicable rejuvenation protocols. However, it also highlights the vital importance of

comprehending the intricate molecular dynamics that underlie this process. Such understanding is indispensable for paving the way toward the development of effective and safe strategies that hold the potential to be applied to humans in a clinical setting.

Supplementary Material

Supplementary File 1
NIHMS1985135-supplement-Supplementary_File_1.pdf (95.9KB, pdf)

Acknowledgements

This work has been supported by: MCHRI, Woods Family Endowed Scholarship in Pediatric Translational Medicine (Stanford Maternal & Child Health Research Institute), the Breakthrough in Gerontology Award (BIG Award, AFAR/Glenn Foundation) and the Milky Way Research Foundation to V.S. By Paul F. Glenn Foundation for Medical Research and NIA/NIH grants R01AG019719 and R01DK100263 to D.A.

Rejuvenating senescent and centenarian human cells by reprogramming through the pluripotent state

Laure Lapasset[1], Ollivier Milhavet, Alexandre Prieur, Emilie Besnard, Amelie Babled, Nafissa Aït-Hamou, Julia Leschik, Franck Pellestor, Jean-Marie Ramirez, John De Vos, Sylvain Lehmann, Jean-Marc Lemaitre

- PMID: 22056670
- PMCID: PMC3219229
- DOI: 10.1101/gad.173922.111

Abstract

Direct reprogramming of somatic cells into induced pluripotent stem cells (iPSCs) provides a unique opportunity to derive patient-specific stem cells with potential applications in tissue replacement therapies and without the ethical concerns of human embryonic stem cells (hESCs). However, cellular senescence, which contributes to aging and restricted longevity, has been described as a barrier to the derivation of iPSCs. Here we demonstrate, using an optimized protocol, that cellular senescence is not a limit to reprogramming and that age-related cellular physiology is reversible. Thus, we show

that our iPSCs generated from senescent and centenarian cells have reset telomere size, gene expression profiles, oxidative stress, and mitochondrial metabolism, and are indistinguishable from hESCs. Finally, we show that senescent and centenarian-derived pluripotent stem cells are able to redifferentiate into fully rejuvenated cells. These results provide new insights into iPSC technology and pave the way for regenerative medicine for aged patients.

Similar articles

- Reversibility of cellular aging by reprogramming through an embryonic-like state: a new paradigm for human cell rejuvenation.

  Lemaitre JM.Cent Asian J Glob Health. 2014 Jan 24;2(Suppl):88. doi: 10.5195/cajgh.2013.88. eCollection 2013.PMID: 29805851 **Free PMC article.**

- Rejuvenation of Cardiac Tissue Developed from Reprogrammed Aged Somatic Cells.

  Cheng Z, Peng HL, Zhang R, Fu XM, Zhang GS.Rejuvenation Res. 2017 Oct;20(5):389-400. doi: 10.1089/rej.2017.1930. Epub 2017 Jun 20.PMID: 28478705

- The aging signature: a hallmark of induced pluripotent stem cells?

  Rohani L, Johnson AA, Arnold A, Stolzing A.Aging Cell. 2014 Feb;13(1):2-7. doi: 10.1111/acel.12182. Epub 2013 Nov 21.PMID: 24256351 **Free PMC article.** Review.

- Molecular insights into the heterogeneity of telomere reprogramming in induced pluripotent stem cells.

  Wang F, Yin Y, Ye X, Liu K, Zhu H, Wang L, Chiourea M, Okuka M, Ji G, Dan J, Zuo B, Li M, Zhang Q, Liu N, Chen L, Pan X, Gagos S, Keefe DL, Liu L.Cell Res. 2012 Apr;22(4):757-68. doi: 10.1038/cr.2011.201. Epub 2011 Dec 20.PMID: 22184006 **Free PMC article.**

- mTOR-regulated senescence and autophagy during reprogramming of somatic cells to pluripotency: a roadmap from energy metabolism to stem cell renewal and aging.
  Menendez JA, Vellon L, Oliveras-Ferraros C, Cufí S, Vazquez-Martin A.Cell Cycle. 2011 Nov 1;10(21):3658-77. doi: 10.4161/cc.10.21.18128. Epub 2011 Nov 1.PMID: 22052357 Review.

Cited by

- Leveraging Cell Migration Dynamics to Discriminate Between Senescent and Presenescent Human Mesenchymal Stem Cells.

  Amiri F, Mistriotis P.Cell Mol Bioeng. 2024 Jul 20;17(5):385-399. doi: 10.1007/s12195-024-00807-0. eCollection 2024 Oct.PMID: 39513008 **Free PMC article.**

- Mapping the future of oxidative RNA damage in neurodegeneration: Rethinking the status quo with new tools.

  Wheeler HB, Madrigal AA, Chaim IA.Proc Natl Acad Sci U S A. 2024 Nov 12;121(46):e2317860121. doi: 10.1073/pnas.2317860121. Epub 2024 Nov 4.PMID: 39495912 **Free PMC article.**

- Human iPSCs from Aged Donors Retain Their Mitochondrial Aging Signature.

  Lejri I, Cader Z, Grimm A, Eckert A.Int J Mol Sci. 2024 Oct 18;25(20):11199. doi: 10.3390/ijms252011199.PMID: 39456998 **Free PMC article.**

- A cellular identity crisis? Plasticity changes during aging and rejuvenation.

  Gorelov R, Hochedlinger K.Genes Dev. 2024 Oct 16;38(17-20):823-842. doi: 10.1101/gad.351728.124.PMID: 39293862 Review.

- Age- and disease-related autophagy impairment in Huntington disease: New insights from direct neuronal reprogramming.
  Luo C, Yang J.Aging Cell. 2024 Aug;23(8):e14285. doi: 10.1111/acel.14285. Epub 2024 Jul 23.PMID: 39044402 **Free PMC article.** Review.

Mitochondria: A Potential Rejuvenation Tool against Aging

Qian Hua Phua [1,2], Shi Yan Ng [1,3,4], Boon-Seng Soh [1,2,*]
PMCID: PMC10917551 PMID: 37815912

Abstract

Aging is a complex physiological process encompassing both physical and cognitive decline over time. This intricate process is governed by a multitude of hallmarks and pathways, which collectively contribute to the emergence of numerous age-related diseases. In response to the remarkable increase in human life expectancy, there has been a substantial rise in research focusing on the development of anti-aging therapies and pharmacological interventions. Mitochondrial dysfunction, a critical factor in the aging process, significantly impacts overall cellular health. In this extensive review, we will explore the contemporary landscape of anti-aging strategies, placing particular emphasis on the promising potential of mitotherapy as a ground-breaking approach to counteract the aging process. Moreover, we will investigate the successful application of mitochondrial transplantation in both animal models and clinical trials, emphasizing its translational potential. Finally, we will discuss the inherent challenges and future possibilities of mitotherapy within the realm of aging research and intervention.
Keywords: aging, mitochondria, mitotherapy, lifespan, healthspan

Introduction

Aging is a complex phenomenon that involves multi-factorial degeneration at a cellular, organismal and molecular level. Biological aging correlates with an overall physiological decline of functional tissues and organs, which eventually results in a myriad of age-related pathologies. These include Alzheimer's disease (AD), Parkinson's disease (PD), cardiovascular diseases (CVD), cancer, hearing loss, and osteoarthritis, amongst many others [1]. At a cellular and molecular level, aging has been associated with increased oxidative stress, accumulations of DNA modifications, epigenetic alterations, and organelle damage [2, 3]. Amongst the array of hallmarks associated with aging, there has been a growing interest in the role of mitochondria and how its defects can influence aging phenotypes.

The mitochondrion is a multi-faceted organelle that contributes to diverse functions including cellular metabolism, intracellular signaling, and immune response [4]. With advanced age, there is an associated increase in mitochondria perturbations due to the gradual build-up of mitochondrial DNA (mtDNA) mutations, increased reactive oxygen species (ROS), impaired respiratory chain activities, and altered mitochondrial dynamics [5]. Disruption in mitochondrial dynamic affects mitophagy, hence contributing to the accumulation of defective mitochondria [6]. Altogether, given the tight interconnections among the numerous pathways, will accelerate the decline of tissue function and ultimately hasten the aging process.

The interplay between mitochondria and the aging process

The mitochondria free radical theory of aging proposes that as individual ages, there is a buildup of ROS that results from oxidative phosphorylation that drives further mitochondria deterioration and cellular damage, which accelerates the aging process [3, 7]. The overproduction of ROS causes oxidative damage to the mtDNA, mitochondrial proteins, respiratory complexes, and mitophagy [8, 9]. Supporting this, a study observed a significant increase in the activity of manganese-dependent superoxide dismutase (MnSOD) in human skeletal muscles with advancing age [10]. Another study by Ji et al. further suggested that heightened MnSOD activity serves as a potential defense mechanism against elevated ROS levels [11]. Over time, the interplay between aging, heightened ROS levels, and impaired mitochondrial function creates a vicious cycle that accelerates the aging process, thus affecting lifespan and healthspan.

However, it is also important to note that ROS also plays a crucial role in activating signalling pathways that are involved in proliferation and survival, in response to age-induced stress. For instance, studies have shown that activation of stress-resistance pathways by ROS can enhance the lifespan of organisms such as *C. elegans* and *S. cerevisiae* [12, 13]. Considering these findings, it is plausible that age-associated declines are observed only when ROS levels surpass a certain threshold. This indicates that ROS may have a dual role, acting as both damaging agents and important mediators of stress response pathways.

Mitochondria DNA mutations, accumulate with age and are particularly evident in energetically demanding organs including the brain, skeletal muscle, retina, ovaries, hepatocytes, and heart [14]. While these mutations are randomly distributed across the mitochondrial genome, aged tissues exhibit a higher occurrence of base-substitution, whereas post-mitotic tissues tend to show a greater prevalence of large-scale deletions [15]. Over time, a multitude of studies have collectively shown the presence of different mitochondrial deletions in a broad range of age-related diseases. Among them, the most extensively studied modification is the 4977-bp deletion in mtDNA (mtDNA4977) [16]. This deletion has been observed to accumulate as individuals age and is detected in various tissues of older individuals, with a higher frequency in tissues characterized by high oxygen consumption [17, 18] Similar to humans, a 3867-bp deletion analogous to the 4977-bp deletion was also observed to accumulate in aged mice [19].

In the context of neurodegeneration, patients with PD were found to express higher levels of mtDNA deletions in their striatum and substantia niagra as compared to normal aging individuals [20, 21]. Similarly, mtDNA deletions were found in AD mice models, resulting in disruptions in mitochondria function [22]. Besides neurodegenerative diseases, ragged red fibers (RRF) within skeletal muscles becomes increasingly prominent with advanced age. These RRF serve as a compensatory response to mitochondrial respiratory capacity impairments. Notably, in the later stages of aging, a

substantial portion of these RRF fibers exhibit a significant mtDNA deletion, which correlates with a deficiency in cytochrome c oxidase activity, an important component of the mitochondrial respiratory chain. These findings strongly indicate that mtDNA deletions play a pivotal role in the progression of aging-related sarcopenia [23]. In the context of aging-related heart failure, mutated mice models which encompass high levels of mtDNA deletions exhibit a range of cardiac aging phenotypes. These include cardiac hypertrophy and dilatation, mosaic pattern due to cytochrome *c* oxidase deficiency, perturbations in diastolic and systolic function, as well as cardiac fibrosis [24-26].

Around 1% of the mitochondrial proteome, including 13 vital proteins in respiratory chain complexes, is encoded by mtDNA [14]. Throughout an individual's lifetime, mtDNA mutations build up, resulting in complex defects, impaired oxidative phosphorylation, and cellular dysfunction [27]. The first evidence demonstrating the direct impact of mtDNA mutations on premature aging came from the creation of "mtDNA-mutator mice," which express a proof-reading-deficient version of the catalytic subunit of polymerase gamma (PolgA) [24]. These mutator mice contain a high level of mtDNA point mutations and deletions, which is thought to be closely associated with the expression of pre-mature aging phenotypes such as age-related hearing, hair and muscle loss [24, 26]. Interestingly, in the mutator mice's liver and heart mitochondria, complexes I, III, and IV were significantly downregulated, possibly due to accumulated mtDNA point mutations causing amino acid substitutions in mtDNA-encoded respiratory subunits, impairing protein structure. Consequently, these alterations disrupt complex assembly, leading to respiratory chain deficiency and promoting premature aging phenotypes [28].

In relation to this, heteroplasmy, which refers to the co-expression of mutant and wild type mtDNA copies within a cell, serves as an indicator for measuring the level of mtDNA mutations. When heteroplasmy exceeds a certain threshold, tissues become energetically compromised, resulting in an undesirable loss of function. A population study conducted on individuals over 70 years of age discovered an increase in a particular mitochondrial mutation, m3243A>G [29]. Elevated heteroplasmy at this site was found to be associated with an increased risk of dementia-related and stroke mortality [29]. A separate study conducted by the same group also reported that increased heteroplasmy level at 20 different disease-causing mtDNA sites was correlated with decreased cognitive function, hearing, vision and mobility function in elderly individuals [30]. These studies suggest that mtDNA heteroplasmy could serve as a valuable biomarker for age-related function.

Mitochondria are highly complex and dynamic organelles that are constantly undergoing fusion and fission events. The process is vital to facilitate essential cellular functions such as adaptation to nutrients availability, mitigate mitochondrial trafficking which aids in Adenosine 5'-triphosphate (ATP) production, and most importantly the maintenance of a well-interconnected mitochondrial network [3, 31]. Earlier studies conducted on animal models such as flies and nematodes reported the presence of enlarged and

fragmented mitochondria, effects of disrupted dynamics [32, 33]. In Drosophila, inclination toward fission was reported during aging. Increased fission activity causes fragmented mitochondria, which disrupt cellular homeostasis and signaling. This, in turn, results in germline stem cell loss and ultimately leads to tissue degeneration. [34]. Considering the significance of preserving mitochondrial architecture integrity in aging, attaining a well-balanced fusion and fission process is essential for increased longevity.

Mitophagy, a subset of autophagy, in which mitochondria are selectively degraded, is a highly vital process that regulates the quality of mitochondria through the elimination of poorly or non-functional mitochondria. The maintenance of mitochondria quality is essential as it affects multiple vital cellular functions such as metabolism, homeostasis and disease prevention [35]. Impaired mitophagy leads to pro-aging metabolic perturbations such as an increase in ROS and mtDNA mutation, as well as impaired ATP production [36]. Interestingly, studies reported the close association of mitophagy-related genes in longevity, as observed in model organisms. For instance, PTEN Induced Kinase 1 (PINK-1) overexpression with α-synuclein in dopaminergic neurons enhance lifespan in Drosophilia, whereas the loss of Parkin shorten lifespan [37, 38]. Similarly, in *C. elegans*, the loss of PINK1 and Parkin reduces the lifespan of mitochondria respiration mutants [39]. Apart from studying animal models, Fang et al. have observed a significant reduction in basal levels of mitophagy in the hippocampus of patients with AD. This decrease in mitophagy contributes to the accumulation of malfunctioning mitochondria and subsequently impairs cellular metabolism. In their study, Fang et al. also found that restoring mitophagy abolished tau hyper-phosphorylation in human neuronal cells associated with AD. Additionally, significant improvements were observed in cognitive decline and amyloid-beta (Aβ) pathology in both mice and *C. elegans* models of AD when mitophagy was reinstated [40]. Based on current studies and understanding, it appears that mitophagy is an essential cellular process that helps to promote lifespan.

Currently, the available evidence on mitophagy in humans is limited. To fully understand the implications of mitophagy in human cellular processes, further investigations are crucial. These additional studies will provide a deeper understanding of the significance and potential advantages associated with mitophagy in diverse human cellular processes. As researchers continue to uncover the role of mitophagy in aging, enhancing this process has emerged as a potential therapeutic target for promoting healthy aging and mitigating the effects of age-related diseases. Further studies are necessary to confirm the potential benefits and establish the most effective strategies to harness mitophagy for human health and longevity.

Mitotherapy

Mechanisms of mitochondrial transfer

Mitochondrial transfer is a natural phenomenon that takes place under both normal and pathogenic conditions. In 1969, Ruby et al. uncovered the concept of mitochondrial

transfer when they observed the presence of mitochondria within intercellular tunnels connecting adjacent developing mouse oocytes [41]. Among the various methods of mitochondrial trafficking, tunneling nanotubes (TNTs) represent a significant route, enabling the transfer of mitochondria between distinct cell lines through a coculture system [42, 43]. TNTs consist of actin or microtubule-based cytoplasmic extensions, creating intracellular transport networks that facilitate cargo transfer [44]. When TNTs were abolished, a considerable decrease in mitochondrial transfer within cocultures was observed [45]. To support long-range intercellular communication, extracellular vesicles act as carriers, encapsulating mitochondria and releasing them into blood vessels or tissues [46, 47]. Hayakawa et al. reported that the release of extracellular mitochondrial particles by astrocytes conferred neuroprotective effects and promote neuronal viability post-ischaemic stroke [48]. Lastly, mitochondria could also be transferred via cell fusion or gap junctions formed via connexins and cytoskeleton proteins [49]. In a study conducted by Acquistapace et al., live cell imaging revealed the presence of functional mitochondria in mouse cardiomyocytes directly co-cultured with human adipose-derived stem cells [50]. The successful transfer of mitochondria through cell fusion is essential for the reprogramming of post-mitotic murine cardiomyocytes into proliferating cardiac progenitors [50]. The topic on mitochondrial mechanism has been extensively reviewed by Liu et al. [51]. Understanding how mitochondria are transferred is important as it sets the foundation for mitotherapy translational application in clinical trials.

Current interventions targeting mitochondrial function enhancement in the context of disease and aging

Given the pivotal roles of mitochondria, several studies have reported the use of various approaches that could enhance mitochondria function. These approaches encompass pharmacological supplements as well as dietary interventions and exercise regimens. Caloric restriction (CR) is a widely recognized anti-aging approach that has been shown to markedly increase lifespan and delay age-related pathologies across various organisms, including non-human primates [52, 53]. Long-term caloric restriction has also been associated with a reduced incidence of chronic illnesses, including cancer, cardiovascular disease, and hypertension [54]. The effects of CR are complex and mitochondrial function is one of the key mechanisms by which CR extends lifespan (Fig. 1). Studies have shown that caloric restriction can modulate mitochondrial activity through several processes, including mitophagy, mitochondrial biogenesis, metabolic shifts as well as mitochondrial respiration [55, 56].

Figure 1.

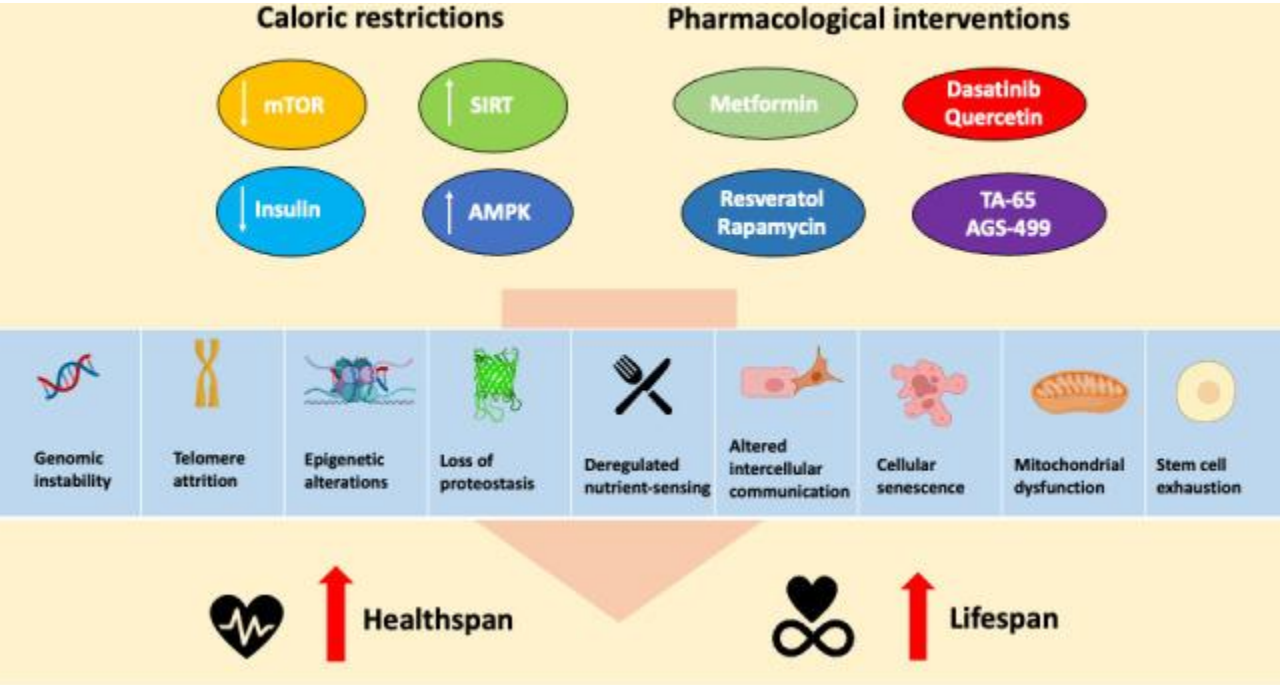

Open in a new tab

Nutritional and pharmacological interventions against the hallmarks of aging. This figure was created with BioRender.com.

Nisoli et al. documented a substantial increase in mitochondrial content in the brain, heart, liver, and adipose tissue, following a 30% caloric restriction. Furthermore, the amount of mtDNA and expression of various important players of mitochondrial biogenesis such as peroxisome proliferator-activated receptor-γ coactivator 1α (PGC-1α), nuclear respiratory factor-1 (NRF-1), and mitochondrial transcription factor A (TFAM) were significantly elevated in mice fed with CR diet. These findings collectively indicate a promotion of mitochondrial biogenesis due to CR. In conjunction with the up-regulation of these genes, an increase in ATP concentration was observed, serving as an indication of enhanced respiratory activity [57].

To better understand the association between CR and metabolism, extensive research has been conducted to explore the underlying mechanisms by which CR influences the metabolic network, resulting in an increased lifespan through the stimulation of mitochondrial biogenesis. However, the precise mechanisms involved are still not fully understood. Nevertheless, SIRT1 and AMP-activated protein kinase (AMPK) have emerged as crucial factors in mediating the longevity effects associated with CR [58, 59]. Supporting this, a number of studies suggest that SIRT1 activates PGC-1α through deacetylation, ultimately enhancing mitochondrial activity [60, 61]. Furthermore, Bergeron et al. reported long-term activation of AMPK was shown to lead to the activation of NRF-1 and, consequently, an enhancement in muscle mitochondrial density [62].

In addition, CR has been shown to modulate respiratory capacity in different tissues. This includes enhancing mitochondrial respiration rate in brown adipose tissue and reducing maximal respiratory rate while limiting hydrogen peroxide release. These findings highlight the multifaceted effects of CR on cellular respiration [57, 63, 64]. In the brain, CR was revealed to effectively reduce the age-related membrane rigidization and limited the production of oxy-radicals when mitochondria were stimulated with succinate, highlighting its potential in preserving mitochondrial function in the aging brain [65]. In another study, older mice subjected to caloric restriction (CR) exhibited heightened respiration rates, indicating that CR enhances the inherent function of the respiratory chain. Interestingly, skeletal muscles from these mice undergoing caloric restriction (CR) showed lower levels of 8-oxo-dG, indicating reduced oxidative DNA damage. This implies that caloric restriction (CR) has the potential to reduce oxidative stress by improving the capacity of internal antioxidant defenses in skeletal muscles, ultimately leading to enhanced mitochondrial integrity and optimal functional performance [66].

In addition to dietary interventions, numerous studies have provided evidence that regular exercise can significantly improve mitochondrial function by increasing the content of mitochondria, enhancing oxidative phosphorylation, and improving respiratory capacity [67-71]. Endurance training has been shown to elevate the levels of mitochondrial proteins involved in β-oxidation, the tricarboxylic acid (TCA) cycle, and the electron transport chain, thereby enhancing energy capacity [68]. Remarkably, long-term exercise has been found to increase mitochondrial volume by a substantial 40-50%, accompanied by improvements in oxidative capacity and a reduction in ROS [72]. Furthermore, several studies have reported that exercise training facilitates the elimination of abnormal mitochondria, promoting the turnover of healthy mitochondria [73, 74]. Taken together, these findings demonstrate how the incorporation of CR and consistent exercise into lifestyle practices can significantly enhance mitochondrial health and cellular bioenergetics.

Other means to enhance mitochondrial function includes nutritional supplements. This includes various options such as vitamins, antioxidants, enzyme inhibitors, and co-factors [75]. Enhancing mitochondrial biogenesis to address respiratory capacity deficiencies holds promise as a potential approach for treating mitochondrial diseases. One strategy with great potential involves targeting peroxisome proliferator-activated receptors (PPARs), which play a crucial role in governing mitochondrial bioenergetics and metabolic homeostasis [4]. For instance, pioglitazone, a FDA-approved drug belonging to the thiazolidinediones (TZDs), activates PPARs, have exhibited promising outcomes in promoting mitochondrial biogenesis in diabetic patients, thereby enhancing oxidative phosphorylation (OXPHOS) activity [76, 77]. Apart from targeting PPARs, other potential targets for restoring mitochondria function involve targeting the modulation of PGC-1-α through SIRT1 and AMPK [4]. For instance, dietary supplementation of NAD+ precursors, nicotinamide mononucleotide (NMN) increased NAD+, activating SIRT1 signalling. This elevation in SIRT1 activity leads to improved mitochondrial biogenesis, enhanced mitochondrial function and a boost in both

metabolic fitness and exercise endurance [78, 79]. Altogether, the exploration of pharmacological supplements targeting mitochondrial function through enhancing mitochondrial biogenesis and improving oxidative phosphorylation demonstrates promising avenues for therapeutic interventions in mitochondrial diseases.

In relation to longevity, certain compounds that mimic the effects of caloric restriction (CR), such as metformin and resveratrol, as well as rapamycin, an established mTOR signaling antagonist, have demonstrated the ability to extend both lifespan and healthspan in *C. elegans* and mouse models. These compounds target AMPK and complex 1 of the mitochondrial respiratory chain [80-82]. The effects of these interventions have been observed in mouse models that were fed a high-calorie diet and treated with resveratrol. Administration of resveratrol led to increased AMPK and PGC1-α activity, accompanied by a rise in mitochondrial abundance. Additionally, there was improvement in muscle function and enhanced insulin sensitivity, which are beneficial changes associated with longevity[83].

These findings suggest that caloric restriction and its pharmacological mimetics hold promise in positively influencing mitochondrial activity and biogenesis, which may ultimately contribute to an extended lifespan and improved health outcomes [80-82]. While CR and pharmacological interventions offer promising anti-aging benefits, CR demands considerable lifestyle changes, and pharmacological treatments may have side effects like metabolic imbalances, respiratory depression, and increased cancer risk with long-term use [84, 85]. These concerns must be thoroughly assessed for safety before implementing such interventions.

Mitochondrial transplantation

In recent years, mitochondrial transplantation has proven to exhibit vast therapeutic benefits in disease treatment particularly metabolic, neurological and cardiac pathology [86]. The translation of bench to bedside stemmed from McCully *et al.* in 2009, where they isolated fresh mitochondria from healthy cardiac tissue and injected them into the ischemic region of the rabbits' hearts during early reperfusion. Following the transplant, there was a notable reduction in myocardial necrosis and a significant improvement in post-ischemic function [87]. Following McCully *et al*, other studies also displayed the benefits of mitochondrial transplantation through cardiac ischemia models. In 2016, Cowan et al. displayed the ability of exogenous mitochondria to decrease myocardial infarct size and increase post-ischemia cardiac functionality through coronary vascular perfusion in a rabbit model [88]. Following, Guariento et al. demonstrated an interesting and novel concept of preischemic mitochondria transplantation which has proven to be a therapeutic strategy for prophylactic myocardial protection in porcine models of regional ischemic reperfusion injury (IRI). Through both single and serial delivery of autologous mitochondria, myocardial infarct size has been significantly reduced and cardiac function improved tremendously. Notably, the therapeutic outcomes of serial delivery and single delivery were similar in comparison [89]. Besides cardiac improvement, the therapeutic potential of mitochondrial transplantation has been

Targeted organs	Disease models	Methods	Types of transplant	Therapeutic outcomes	Ref.
Brain	Parkinson's disease in healthy C57BL/6J mice models	Intravenous injection	Xenogeneic	• Increased ETC activity • Reduction in ROS activity • Prevention of cell apoptosis and necrosis	[120]
Brain	Alzheimer's disease in AD mice models	Intravenous injection	Xenogeneic	• Enhanced cognitive performance • Significant decrease in neuronal loss • Reduced gliosis in the hippocampus	[121]
Brain	Cerebral ischemic injury in Sprague-dawley rat models	Intracerebroventricular injection	Autologous	• Reduction in cellular oxidative stress and apoptosis • Enhanced neurogenesis • Decreased brain infarct volume • Reversed neurological deficits	[122]
Brain	Sprague-dawley rats with spinal cord injury	Injection into the mediolateral gray matter	Allogenic	• Maintenance of bioenergetics	[123]
Heart	Ischemia-reperfusion heart in New Zealand white rabbits	Injection into the ischemic zone of the heart	Allogenic	• Significant reduction in apoptosis and necrosis • Enhanced cellular viability • Myocardial functional recovery	[87]
Heart	Ischemia-reperfusion heart in New Zealand white rabbits	Injection into the ischemic zone of the heart	Autologous	• Reduction in myocardial necrosis and inflammatory markers • Enhanced oxygen consumption rate and high energy synthesis • Enhanced ATP	[112]
Heart	Ischemia-reperfusion heart in Yorkshire pigs	Injection into the left coronary ostium	Autologous	• Enhanced regional and global myocardial function • Decreased myocardial infarct size	[124]
Liver	Fatty liver C57BL/6J mice models	Intravenous injection	Xenogeneic	• Decreased lipid content • Restored cellular	[90]

Targeted organs	Disease models	Methods	Types of transplant	Therapeutic outcomes	Ref.
				redox content • Reduction in oxidative stress	
Liver	Ischemia-reperfusion injury in the liver of Wistar rat models	Injection into spleen	Allogenic	• Reduction in oxidative stress • Reduction in mitochondrial damage and subsequent cell death	[125]
Lung	Ischemia-reperfusion injury in the lung of C57BL/6J mice models	Injection into pulmonary artery	Allogenic	• Improved lung mechanics and enhances tissue recovery	[91]

demonstrated in other organs. For example, exogenous mitochondria have been demonstrated to rescue hepatocyte function in high-fat diet-induced fatty liver mice, a model of non-alcoholic fatty liver disease [90]. Similarly, enhanced lung mechanics and improved tissue recovery were observed in ischemia-reperfusion injury mice models that received mitochondrial transplantation [91]. In the most recent study by Hayashida et al., performing mitochondrial transplantation immediately following resuscitation from cardiac arrest substantially improved both survival rates and neurological recovery for rats experiencing post-cardiac arrest [92]. Existing mitochondrial transplantation in different animal models is summarised in table 1.

Table 1.
Summary of existing mitochondria transplantation in animal models.

In addition to animal models, mitochondrial transplantation has proven its success in human clinical studies as well. The first clinical application occurred in 2017, where healthy autologous mitochondria were harvested and isolated from nonischemic skeletal muscle and injected into the damaged myocardium of 5 pediatric patients who required central extracorporeal membrane oxygenation (ECMO) support for ischemia-reperfusion-associated myocardial dysfunction [93]. Upon the surgical procedure, none of the patients suffered from arrhythmia, 4 out of 5 patients demonstrated improvement in ventricular functions and were successfully removed from ECMO support [93]. Thereafter in 2020, the same group reported the success of autologous mitochondria transplantation in a study conducted on a greater pool of pediatric patients. Similarly, no patients suffered from adverse short-term complications such as arrhythmia or scarring [94]. Patients who received the mitochondria transplantation were successful in detaching from ECMO support and exhibited improvement in the ventricular strain [94]. Currently, there are only two clinical trials, notably from the same group of researchers,

McCully et al., targeting pediatric patients suffering from ischemia-reperfusion-associated myocardial dysfunction. Further studies have to be conducted for optimal surgical process of mitochondria transplantation across different organs to better demonstrate the robustness of mitotherapy.

Revolutionizing mitotherapy's future with bioengineered mitochondria

To advance mitotherapy and maximize the potential of mitochondria as an innovative tool for disease treatment, multiple supplementary measures can be pursued to enhance its effectiveness in combating diverse pathologies. One promising approach involves the exploration of gene editing technology specifically targeted at correcting mtDNA genes, subsequently reducing mutant mtDNA, improved mitochondria function and ultimately eliminating mitochondrial diseases. Current tools for mitochondrial gene editing includes restriction endonucleases (RE) technology, zinc finger nuclease (ZFN) technology, transcription activator like effector nuclease (TALEN) technology and even CRISPR/Cas9 system [95]. In independent studies employing distinct mitochondrial gene editing technologies, RE and ZFN, the correction of m.8993T>G mutation has been successfully corrected. This correction resulted in a decrease in mutant mtDNA levels, restoration of ATP and wild type mtDNA levels, and the reestablishment of normal mitochondrial membrane potential (MMP) [96, 97]. In addition, another gene-editing tool, TALEN has also effectively eliminated m.3243A>G mutation in mitochondrial disease patient-specific induced pluripotent stem cells, which subsequently displayed restoration of mitochondrial respiration and bioenergetics [98]. Collectively, these gene editing tools alter the level of mtDNA heteroplasmy, eliminating the mutant fraction and ultimately resulting in enhanced mitochondrial bioenergetics. In the realm of genetic modification *in vivo*, it is also crucial to prioritize the careful design of delivery systems to prevent any unintended off-target effects. Despite the utilization of the CRISPR-Cas9 gene-editing tool, its implementation remains controversial due to numerous unresolved questions associated with off-target effects [99]. Methods to circumvent some of these off-target effects *in vivo* have been extensively discussed by Han et al. [100]. The potential to genetically correct mtDNA *in vivo* presents tremendous opportunities in enhancing the patient's cellular metabolism, leading to improved health outcomes and unparalleled efficiency in cellular energy utilization.

An alternative strategy to enhance mitotherapy involves implementing surface modifications to mitochondria, aiming to improve the uptake and specific targeting of exogenous mitochondria by desired tissue or cell types. A recent study by Nakano et al., showed that mitochondria coated with cationic and fusogenic lipids, DOTAP and DOPE exhibited elevated MMP, improved uptake and neuroprotection in neurons [101]. In addition, peptide-labelled mitochondria also enhanced delivery into dopaminergic neurons and improved locomotive activity in the PD rats [102]. Lastly, polymer functionalization of mitochondria using Dextran-triphenylphosphonium (TPP) has shown a three-fold increase in cellular internalization by cardiac cells compared to uncoated mitochondria. This uptake was accompanied by a metabolic shift from glycolytic to

oxidative state and an increase in the oxygen consumption rate [103]. Although the current body of research on mitochondria as a targeted drug delivery vehicle is limited, significant advances have been achieved in the field of exosomes. In the case of cerebral ischemia therapy, cyclo(Arg-Gly-Asp-DTyr-Lys) peptide [c(RGDyK)] conjugated exosomes which contained curcumin were found to accumulate in the region of ischemic brain lesions upon intravenous injection [104]. As a result, there was a significant suppression of inflammatory response and cellular apoptosis in the lesion area. The cumulative evidence from these examples highlights the immense potential of bioengineered surface modification on mitochondria, which could open up new avenues for targeted delivery and improved cellular uptake, making it a promising and novel strategy for efficient drug delivery in the treatment of diseases, particularly those related to metabolic impairments. Collectively, the convergence of these approaches pave the way for more effective and precise interventions in treating mitochondrial-related diseases.

Mitotherapy and aging

During aging, dysfunctional mitochondria compilation causes the deterioration of cellular and physiological health, resulting in age-related phenotypes. Hence, the replacement of aged mitochondria with healthy, mutation-free ones, presents an alternative avenue to investigate as a potential anti-aging treatment. Extrapolating from the technology of mitochondria transfer, Zhao et al. experimented with the concept of harvesting young, healthy mitochondria and injecting them into aging models. In this study, they performed intravenous injections of healthy, allogenic mitochondria isolated from young mice into aged mice and observed enhanced metabolic alterations [105]. Upon mitotherapy treatment, the level of ROS dropped, and ATP content increased significantly as compared to the aged mice. Besides metabolic improvement, there was also a functional enhancement in the cognitive and motor performance in learning and memory abilities [105]. Lastly, mitotherapy also improved mouse sports endurance, evident from longer swimming time in treated mice [105]. This study is the first to uncover new insights on mitotherapy and its huge potential in anti-aging context.

In an independent recent study by Javani et al., mitochondria obtained from young rat brain were transplanted into aged rats which resulted in the attenuation of aging-related stress induced anxiety and depressive-like behavior [106]. Studies have demonstrated a strong correlation between aging, chronic stress, and impaired mitochondria and bioenergetics. This association ultimately leads to a decrease in energy levels, which in turn contributes to the development of depression [107]. However, by introducing young mitochondria through transplantation, the levels of ATP and MMP were restored. This restoration significantly improved cellular bioenergetics and consequently led to an amelioration of age-related neurobehavioral changes [106]. While the current number of examples illustrating mitotherapy's translational application in addressing aging-related disorders is limited, with extensive research, mitotherapy holds great potential in managing and mitigating the effects of aging.

Limitations & future perspectives

As described above, there are multiple studies which demonstrated the success of mitochondrial transplantation. However, there are also some challenges faced in the process. Firstly, isolation and storage are major concerns for the therapy to succeed. Whilst freshly isolated mitochondria are often used in mitotherapy, the storage condition plays a huge role in the organelle's functionality. It has been reported that prolonged storage of mitochondria correlates with a decline in mitochondria respiratory capacity. Additionally, the preservation of the integrity of the membrane potential is important for mitochondria to function optimally. Even though several researchers have experimented on different storage buffers such as University of Wisconsin solution, Eurocollins solution and 4-(2-HydroxyEthyl)-1PiperazineEthaneSulfonic acid (HEPES)-sucrose-based buffer to preserve mitochondria, these are of limited effectiveness against mitochondria impairment [108, 109]. Improving mitochondria quality control is critical, therefore it would be best for a standardized protocol to be established for optimal harvest and storage conditions, whilst following the strict guidelines of safety and ethics.

Additionally, immunological response plays a vital role in the effectiveness of the therapy. Similar to other forms of surgical procedures, it is important to investigate the mechanism of immune reaction to mitochondria transplant. Significant inflammatory response was observed in a mouse heterotopic heart transplantation model, which led to eventual graft rejection [110]. When endothelial cells were exposed to extrinsic mitochondria, there was an up-regulation of adhesion molecules, and this promotes the secretion of inflammatory cytokines [110]. However, there were also studies that reported the absence of inflammatory markers elevation post-transplantation of autologous mitochondria [111-113]. While previous studies were mostly conducted using autologous mitochondria, Ramirez-Barbieri et al showed that immune response was not triggered despite the administration of syngeneic and allogenic mitochondria [113]. In addition, Acquistapace et al. also demonstrated the success of mitochondria transfer in a cross-species co-culture system between mouse and human [50]. The significance of these findings is extremely important, as they expand the potential sources of donor mitochondria for therapeutic purposes. This approach also creates a readily available supply of healthy mitochondria, thus offering a promising avenue for therapeutic translation.

To reduce the risk of an immune reaction, immunosuppressants are often co-administered with mitochondria during transfer, as has been done in previous studies. Another method to potentially reduce immune rejection could be through the encapsulation of mitochondria by microvesicles or liposomes. It has been proven that the membrane of extracellular vesicles aids in maintaining the functional integrity and lifespan of mitochondria in the bloodstream [114, 115]. To further improve the uptake and targeting efficacy, extra modifications could be made to the membranes of these transport vehicles, as discussed previously (Fig. 2).

Figure 2.

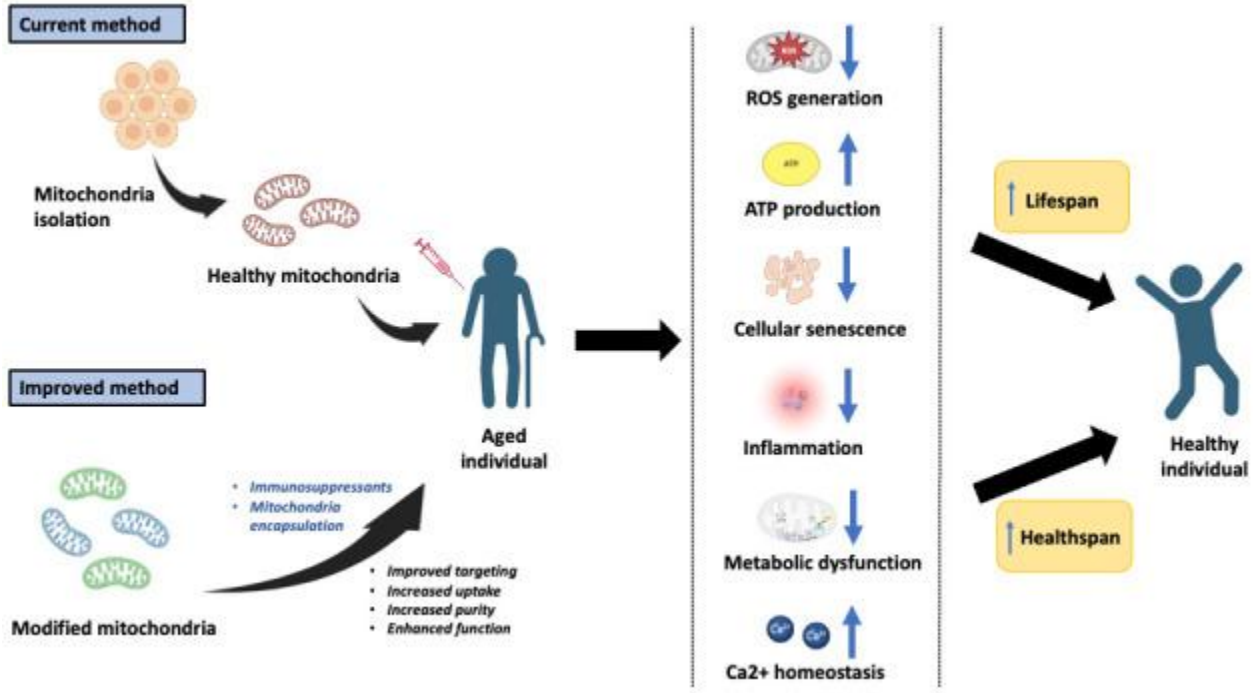

Open in a new tab

An overview of mitotherapy's current and future therapeutic translation. This figure was created with BioRender.com.

Ethical and safety considerations of mitotherapy

From an ethical perspective, mitotherapy generally aligns with established standards, as numerous studies have shown that personal traits are primarily determined by genes derived from nuclear DNA [116]. However, there are specific concerns related to the origin of donor mitochondria. In autologous transplantation, where mitochondria from tissue with a low risk of mtDNA mutation are used to treat the same individual, ethical concerns are rarely raised. In cases of mitochondrial allogenic transfer, preferential consideration is often given to close family members, and if not feasible, haplotype matching should be considered [117, 118]. Lastly, while xenogenic transfer has shown feasibility, it is still in its infancy stages and requires further investigation before its ethical implications can be fully understood. In-depth exploration of the ethical issues surrounding mitochondrial transplantation can be found in other review articles [116, 119].

Conclusion

Mitochondria play a crucial role in numerous cellular processes, including metabolism, intracellular signaling, apoptosis, and immune response, making them a vital target for therapeutic interventions. The decline in mitochondrial function is closely linked to

aging, as disruptions in their activity can lead to a cascade of impaired cellular pathways and quality control mechanisms, ultimately resulting in the accumulation of defective mitochondria and accelerated aging. To counteract this aging process, the transfer of healthy, functional mitochondria may serve as a potential treatment option. However, current clinical trials exploring mitotherapy for aging are scarce, highlighting the need for further research to unlock the full potential of mitochondrial therapies in aging-related applications. Addressing ethical and safety concerns will also be crucial moving forward. In summary, mitotherapy holds significant promise as an innovative approach to combat aging, paving the way for ground-breaking advancements in the improvement of healthspan and lifespan in the future.

Acknowledgements

We express our gratitude to Jeremy Kah Sheng Pang for proofreading and providing comments on the manuscript. This work is supported by the Agency for Science, Technology and Research (Singapore). Qian Hua Phua is supported by the A*STAR Graduate Scholarship.

Volume 59, December 2024, 102478

Mitochondria-targeting near-infrared (NIR) materials orchestrating the symphony of precision diagnosis and therapy

lShu Gao [a c], Chunrong Qu [a], Jun Wang [a c], Kun Qian [a], Zhen Cheng [a b c]

Highlights

- •
  This review outlines the physiological roles of mitochondria and their link to pathological processes.
- •
  This review elucidates the design and application effects of mitochondria-targeting near-infrared (NIR) materials.
- •
  This review explores the fascinating properties of mitochondria-targeting NIR materials in the imaging and therapy.
- •
  This review connects mitochondria-targeting NIR materials with advances in nanotechnology and drug delivery systems.

- •
  This review analyzes the current challenges of mitochondria-targeting NIR materials and proposes future research trends.

Abstract

Mitochondria are essential for maintaining cellular survival and function, and their dysfunction is implicated in cancer, cardiovascular abnormalities, neurodegenerative diseases, aging, and so on, carrying significant pathophysiological implications. Conducting research focused on mitochondria helps elucidate the mechanisms of disease development and offers new therapeutic perspectives for combating challenging conditions like malignant tumors, myocardial injury, Parkinson's disease, and other related ailment. In recent years, the flourishing development of near-infrared (NIR) technology has provided powerful tools for mitochondrial research. NIR light serves as both an information carrier for biological imaging and analysis, and as a non-invasive stimulus in drug delivery, phototherapy, and energy conversion applications. Currently, a large number of NIR materials have been applied to target mitochondria in disease diagnosis, treatment, and theranostics. These materials have garnered significant attention due to their unique properties and remarkable in vivo performance. This review aims to provide researchers developing mitochondria-targeted NIR materials for biomedical applications with an advanced and comprehensive guide. It not only offers valuable insights into design strategies, material properties, and applications in disease diagnosis and treatment, such as strategies to improve imaging sensitivity, specificity, and therapeutic efficacy, but also delves into the existing challenges in the field, issues that persist in clinical translation, and future prospects.

Graphical Abstract

Introduction

Biological processes such as protein synthesis, transmembrane signal transduction, proliferation, and differentiation require a sufficient supply of energy. For eukaryotic organisms, mitochondria primarily fulfill this role. Organs like the heart, muscles, liver, and brain, which have high energy demands, possess a high density of mitochondria. The importance of mitochondria has spurred extensive research into their molecular mechanisms, genetics, and functions to elucidate their biological significance [1]. The health of mitochondria is closely linked to disease, with approximately 50 % of deaths worldwide related to mitochondrial damage [2]. Abnormal mitochondrial manifestations discovered in diseases can serve as biomarkers, deepening our understanding of the diseases (reflecting pathological information). For instance, an increase in mitochondrial DNA (mtDNA) copy number may indicate kidney damage, brain injury and cancer, while a decrease may suggest the presence of neurodegenerative conditions or aging [3]. Pharmacological interventions aimed at enhancing mitochondrial biogenesis, oxidative phosphorylation (OXPHOS), and antioxidative capacity or modulating mitochondrial autophagy and supplementing essential mitochondrial components can treat or prevent a variety of diseases, including inflammation, liver disease, and aging [4], [5], [6]. Additionally, by elevating reactive oxygen species (ROS) to induce oxidative stress, lowering mitochondrial membrane potential ($\Delta\Psi_m$), altering membrane permeability, and triggering the release of cytochrome *c* (cyt *c*), heat shock proteins (HSPs), and Smac/Diablo into the cytoplasm, apoptosis can be induced, exerting an anti-cancer effect [7], [8]. Therefore, more and more strategies are being applied to target and regulate mitochondrial function to explore the relationship between mitochondria and diseases, hoping to bring new perspectives and more effective methods to the diagnosis and treatment of diseases.

The physiopathological characteristics of mitochondria made them ideal target for near-infrared (NIR) materials developed for the research or diagnosis of relative diseases. Physical environmental factors such as pH, temperature, polarity, hypoxia, viscosity, and biological active components like overexpressed enzymes, reactive oxygen, nitrogen, sulfur species, and ions, can all reflect pathological information and guide the design of mitochondria specific imaging probes [9]. Targeting these stimuli, responsive mitochondrial-targeting NIR imaging agents can also be developed using reporter groups or self-immolative strategies, achieving more precise and specific evaluation and diagnosis [10], [11].

Moreover, the critical importance of mitochondria to cells makes them an excellent therapeutic target. Involvement in numerous metabolic networks and signaling pathways, along with high sensitivity to heat and ROS, makes mitochondria critical sites for phototherapy and chemotherapy. Mitochondria also coordinate immune functions, intervening in T cell differentiation and macrophage polarization [12]. Mitochondria-derived damage-associated molecular patterns (DAMPs) released during injury can activate immune responses, used for tumor immunotherapy [13].

In many research fields, the development and application of NIR materials have flourished in recent years, becoming a prominent research hotspot. Optical imaging avoids ionizing radiation involved in widely practiced medical imaging modalities, such

as computed tomography (CT) and positron emission tomography (PET), and offers a safer, non-invasive functional imaging technique with rapid feedback and high sensitivity, with detection limits reaching 10^{-9}–10^{-12}M [14]. Longer wavelength NIR fluorescence provides deeper penetration depth, higher signal-to-background ratio, improving image quality and offering better imaging options [15].

Besides, NIR fluorophores can convert the energy of photons into other forms during biological imaging, simultaneously exerting therapeutic effects and achieving diagnosis along with treatment. This approach, called theranostic, greatly simplifies the treatment process, reduces patient discomfort, and can serve multiple purposes, such as monitoring drug release and accumulation at targeted sites [16]. With the development of nanotechnology and drug delivery strategies, as well as various imaging and treatment materials, multimodal imaging and treatment have gradually come into view, offering more comprehensive methods to reveal and combat diseases. By targeting mitochondria or focusing on mitochondria for treatment strategies, the specificity of disease theranostics can be significantly improved, reducing side effects on normal tissues, enhancing therapeutic index, and promoting precision and personalized medicine [17], [18], [19].

For the advantages listed above, mitochondria and NIR technology have become hotspots in biomedical research, with many mitochondria-targeting NIR materials emerging, displaying a variety of attractive properties, and shining in the field of disease treatment and diagnosis. However, no literature has yet provided an overview of this interdisciplinary field. Considering the increasingly prominent position of mitochondria-targeting NIR materials, it is necessary to comprehensively summarize the research achievements in this field in recent years. Currently, most mitochondria-targeting NIR materials are used to combat solid tumors, while a smaller portion is employed to address issues related to cardiovascular damage, inflammation, neurodegenerative diseases, and aging. This review, starting from the physiological role of mitochondria and their relationships with diseases, introduces mitochondria-targeting NIR materials, detailing their specific biological applications, and discussing their design, photophysical properties, and therapeutic methods and effects (Fig. 1). Furthermore, it explains the targeting strategies applied to various materials and highlights some interesting uses of NIR technology. Finally, it discusses the present challenges and future directions in this field to inspire researchers in related areas.

Why mitochondria?

Approximately 2–3 billion years ago, primordial eukaryotes established an endosymbiotic relationship with aerobic α-proteobacteria, which gradually evolved into modern mitochondria and eukaryotic organisms [20]. Mitochondria, functioning like engines, supply energy for cellular physiological activities, facilitating processes such as proliferation, differentiation, physiological metabolism, and signal transduction [21]. This chapter initially outlines the fundamental functions, physiological

NIR

Optical technology holds diverse and significant implications in imaging, diagnosis, and disease treatment. Its non-invasive, non-destructive, and real-time characteristics position it prominently in medical practices such as biochemical analysis, pathological toxicological examination, in vivo imaging, as well as disease diagnosis and treatment [109]. When light is directed towards biological tissues, such as the skin, a portion of it is reflected off the surface, while some light penetrates

Therapy

Diagnosing to ascertain the nature and severity of a disease is fundamental, with the ultimate goal in disease management being to adopt reasonable treatment methods to eradicate or alleviate the condition. This section presents common therapeutic strategies currently employed in both clinical and pre-clinical research domains and elaborates on the contributions of targeting mitochondria to these treatment methods, followed by a discussion on the significance of multimodal therapy. Finally,

NIR theranostic agents

NIR imaging can seamlessly integrate with the multiple therapeutic approaches mentioned earlier to facilitate theranostics. Mitochondria represent effective targets for such theranostic applications. Mitochondria-targeting NIR theranostic materials have shown superior capabilities in diagnosing diseases, monitoring progression, evaluating toxicity, and determining therapeutic efficacy. Currently, a wide variety of theranostic agents has been developed (Fig. 11), and their key properties are

Conclusion and prospect

The intersection of mitochondria-targeting and NIR technology has sparked considerable interest, illuminating the path to exploring the life sciences. In diagnostics, NIR serves as an excellent means of spatiotemporal control, allowing for drug release through photolytic groups, as well as alterations in light and energy through upconversion or resonance energy transfer, among others. Connecting NIR fluorophores with chemotherapy drugs via responsive groups enables precise drug release at

CRediT authorship contribution statement

Zhen Cheng: Writing – review & editing, Supervision, Funding acquisition, Conceptualization. **Kun Qian:** Writing – review & editing, Writing – original draft, Conceptualization, Supervision. **Jun Wang:** Validation, Writing – review & editing. **Chunrong Qu:** Writing – review & editing, Visualization. **Shu Gao:** Writing – review & editing, Writing – original draft, Visualization, Conceptualization.

Acknowledgements

This work was funded by the National Natural Science Foundation of China (U2267221 and 81901799), Shanghai Municipal Science and Technology Major Project (TM202301H003), Gansu Science and Technology Major Project (23ZDFA014), State Key Laboratory of Drug Research (No. SIMM0120231004), and the Shandong Laboratory Program (SYS202205).

Shu Gao received his Bachelor's degree in Pharmacy from Shandong University and is currently a Master's degree candidate under the supervision of Professor Zhen Cheng at the Shanghai Institute of Materia Medica, Chinese Academy of Sciences. His research focuses on developing novel mitochondria-targeting theranostic agents and near-infrared (NIR) biomedical materials.

Mitochondrial signal transduction

Martin Picard[1,2,3] ✉ · Orian S. Shirihai[4,5]

Summary

The analogy of mitochondria as powerhouses has expired. Mitochondria are living, dynamic, maternally inherited, energy-transforming, biosynthetic, and signaling organelles that actively transduce biological information. We argue that mitochondria are the processor of the cell, and together with the nucleus and other organelles they constitute the mitochondrial information processing system (MIPS). In a three-step process, mitochondria (1) sense and respond to both endogenous and environmental inputs through morphological and functional remodeling; (2) integrate information through dynamic, network-based physical interactions and diffusion mechanisms; and (3) produce output signals that tune the functions of other organelles and systemically regulate physiology. This input-to-output transformation allows mitochondria to transduce metabolic, biochemical, neuroendocrine, and other local or systemic signals that enhance organismal adaptation. An explicit focus on mitochondrial signal transduction emphasizes the role of communication in mitochondrial biology. This framework also opens new avenues to understand how mitochondria mediate inter-organ processes underlying human health.

1. health

Introduction

Our collective view of mitochondria evolved from that of dynamic cytoplasmic granules or “bioblasts”[1] to bean-shaped ATP-synthesizing chemiosmotic machines,[2,3] motivating the popular “powerhouse of the cell” analogy.[4] Subsequently, mitochondria became known as maternally inherited organelles[5] with their own genome, in which mutations can cause disease,[6,7] setting off the field of mitochondrial medicine. The imaging of living mitochondria dynamically exchanging proteins and DNA[8] and triggering death via propagating apoptotic waves[9,10] later

sparked an era of mitochondria as dynamic organelles undergoing constant fusion/fission events, enabling functional complementation[11,12] and mitochondrial quality control.[13] Most recently, the omics era and a new quantitative handle on intermediate metabolism have cast mitochondria as biosynthetic and signaling organelles[14,15] that produce signals influencing cell and organism behaviors via metabokine/mitokine signaling,[16,17,18] mito-nuclear crosstalk,[19,20,21,22] and remodeling of the epigenomic machinery across species.[23,24,25,26] Through these theoretical transitions, mitochondria have become the most studied organelle in the biomedical sciences (Figure 1).

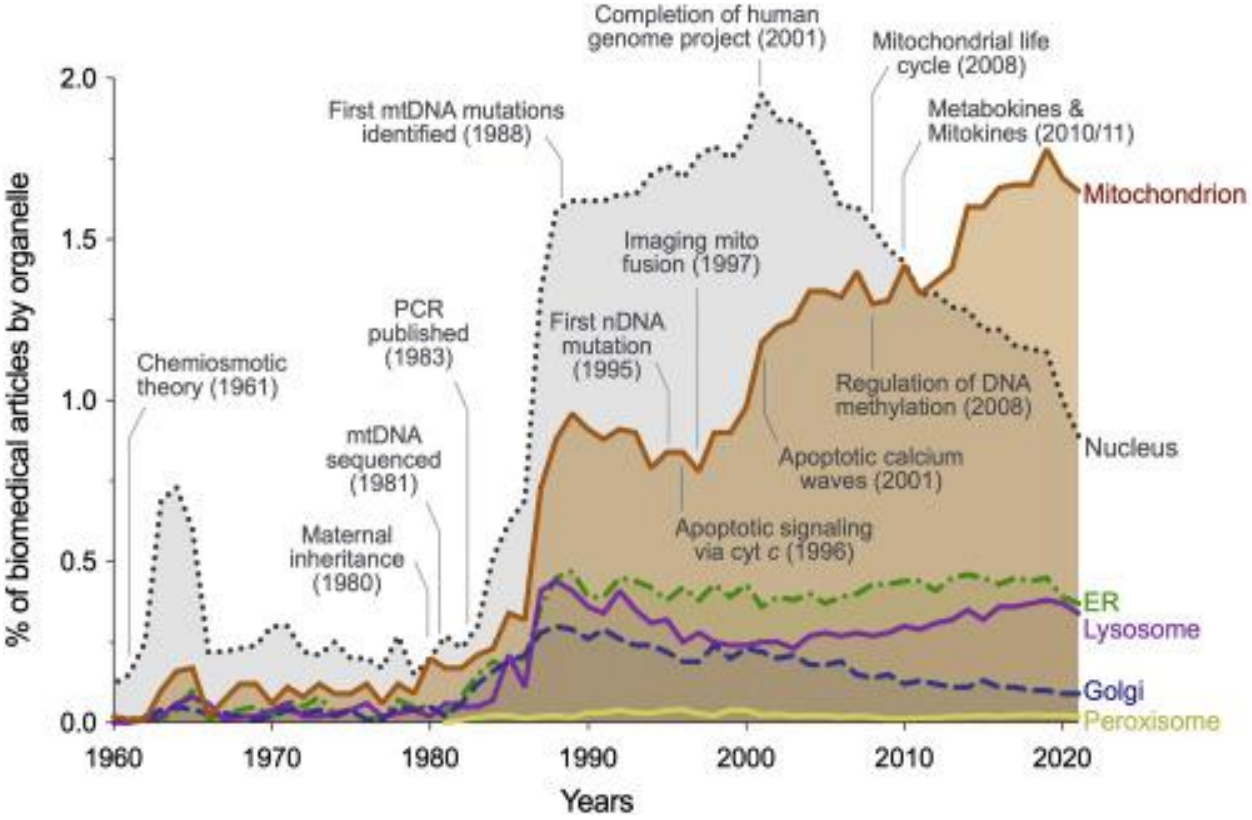

Figure 1 Modern historical landmarks in mitochondrial research illustrate the need for an integrative view of this multifaceted organelle

Show full captionFigure viewer

Outside of their intracellular roles as organelles, mitochondria also operate beyond the confines of the cell.[27] They undergo physical transfer from cell to cell,[28,29,30] influence neurotransmitter metabolism and inter-cellular communication at the neural synapse,[31,32] synthesize all circulating steroid hormones that ensure sexual reproduction and species survival in mammals,[33] and as discussed below, even contain receptors for systemic hormones.[34] These discoveries are not only blurring cellular boundaries, but also revealing mitochondria in a light that emphasizes communication—i.e., the bidirectional transfer of information from organelle to organism—as a natural aspect of their biology.

It is a particularly exciting time for mitochondrial biology. Community resources like MitoCarta[35] and MitoCoP,[36] together with spectacular theoretical advances in mitochondrial research, have brought insights to diverse fields across the biological sciences and medicine.[37] This includes, but is not limited to, immunometabolism, behavioral neuroscience, and psychobiology. As examples, energy metabolism in general and mitochondria in particular play

permissive and instructive roles in stem cell differentiation and in the acquisition of immunometabolic phenotypes,[38] influence whether animals are socially dominant or submissive,[39] and influence how multiple organ systems in mice respond to evoked stress.[40] In humans, mitochondrial energy production capacity also appears to dynamically respond to subjective psychosocial experiences,[41,42] providing a foundation to begin understanding the mind-mitochondria connection. These discoveries are contributing to mechanistically linking sub-cellular bioenergetic processes to physiological, health-related organismal phenotypes. Thus, scientific progress not only among mitochondrial biology but also more broadly in the biomedical sciences[43] has been and likely will continue to be catalyzed by increasingly accurate and integrative models of mitochondrial behavior.

In this perspective, we argue that as we move toward increasingly accurate mechanistic models of the role of mitochondria in human health, we need an understanding of mitochondrial behavior extending far beyond energetics. As echoed by others,[44,45] the "powerhouse" analogy promotes an overly simplistic picture of this beautifully complex organelle. The outdated mechanical analogy is too unidimensional to guide integrative scientific thinking. The challenge ahead is to integrate current prevailing perspectives of mitochondria as inherited, dynamic, energy-transforming, signaling organelles whose influence extends to all cellular compartments, and to the whole organism. Here we propose that our existing knowledge of mitochondrial biology can be integrated under the common framework of mitochondrial signal transduction. Consequently, a more integrative and accurate analogy portrays mitochondria as the processor of the cell—or more precisely as the mitochondrial information processing system (MIPS).

Why mitochondrial signal transduction?

Signal transduction involves input-to-output transformation. It is a generalizable process in biology, taking place across all living, complex adaptive systems. Signal transduction allows single cells to sense, migrate toward, and respond to stimuli,[46] and enables organelle networks to interact and accomplish complex cellular operations that isolated organelles could not accomplish.[47] At the organ level, signal transduction also allows the brain to receive, integrate, and process multiple streams of sensory information to generate a coherent internal representation of the outside world.[48] This process is analogous to the way in which an antenna or sensor coupled to information processing systems—as in a cell phone, for example—receives and converts simple signals (e.g., radio waves) into intelligible outputs of different kinds (e.g., sounds, images, etc.). In the same way, cellular signal transduction systems such as the MIPS convert complex combinations of ions, proteins, nutrients, and energetic states into goal-driven genetic programs, which guide the reorganization of metabolic pathways and drive adaptive behaviors (to grow and divide, contract, secrete, die, etc.). Signal transduction allows cells and organisms to respond and adapt to environmental demands.

Through evolution, the endosymbiotic incorporation of mitochondria marked the transition from a selfish unicellular world to a multicellular reality.[49] In multicellular organisms, a vital priority became the metabolic coordination and cell-to-cell cooperation toward a shared common goal—to sustain the organism. Cellular cooperation produced a sort of "social contract" among increasingly specialized cells.[50] Thus unified as an organism, cells make decisions not based solely on their individual states hardwired in the genome, but based on the collective state of the organism established through information exchange and communication between organs, cells,

and organelles.[51] This collective principle implies that to ensure survival, cellular and organismal decisions must be matched to the local and systemic energetic constraints, which are reflected in the bioenergetic state of mitochondria.[52,53] For an organism, achieving faster responses to changing bioenergetic conditions means faster transitions to new optimal states. This, in turn, maximizes energetic efficiency and minimizes the risk of damage.[54] Therefore, the role of mitochondria in optimizing cellular and organismal behavior toward health—defined as optimal responsiveness to challenges[55]—requires mechanisms that transduce information, from organelle to organism.

The pillars of mitochondrial signal transduction

Before reviewing the specific molecular components and mechanisms that support signal transduction within the MIPS, we describe some general features of signal transduction. Signal transduction within the MIPS is an extension of the traditional process of receptor-mediated detection of (extra)cellular signals, signal amplification, and transduction into downstream secondary messengers (Figure 2). Mitochondrial signal transduction consists of three main processes:

(1)
Sensing: The ability of mitochondria to detect metabolic and hormonal inputs, and to transform these inputs into morphological, biochemical, and functional mitochondrial states.

(2)
Integration: The pooling of multiple inputs into common effectors driven by the exchange of information among mitochondria and other organelles, and influenced by the current state of the mitochondrial network and of the cell.

(3)
Signaling: The production of mitochondrial outputs, or signals, that transmit information locally to direct metabolic pathway fluxes and influence other organelles, including nuclear gene expression, and systemically to regulate the physiology and organismal behavior.

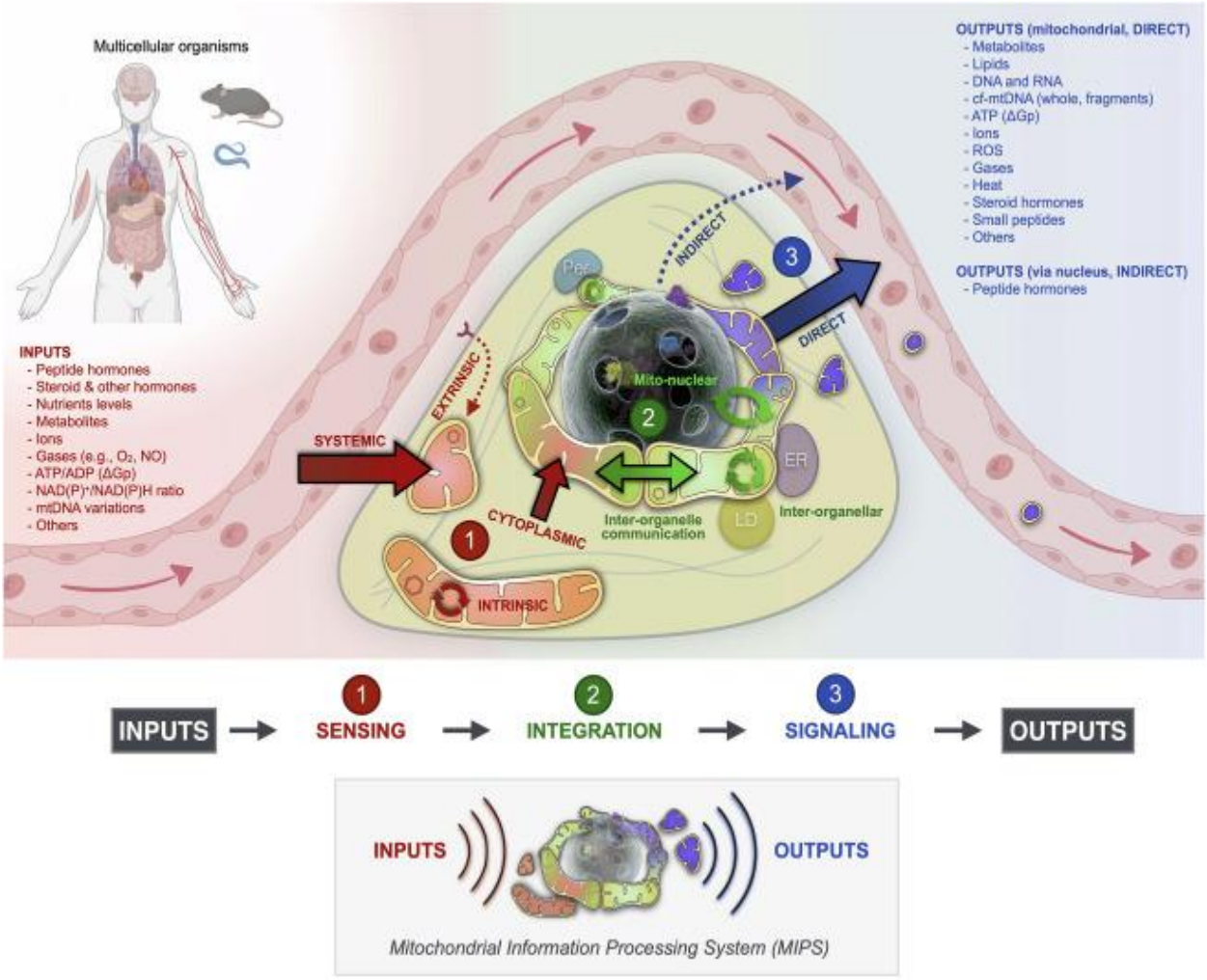

Figure 2 Three-step model of mitochondrial signal transduction

Show full captionFigure viewer

The flow of information through the MIPS proceeds sequentially as follows: incoming signals are sensed by molecular receptors and biological structures on/within mitochondria (sensing), which exchange with each other molecular signals and labile states such as membrane potential via fusion/fission processes and other (non)physical interactions (integration), and which simultaneously release signaling factors such as metabolites, cofactors, proteins, nucleic acids, and heat that propagate information beyond the mitochondrial membranes (signaling). Figure 3 illustrates the repertoire of known mitochondrial substrates and mechanisms available for signal transduction. This broad repertoire emphasizes communication at different levels of biological organization, including protein-protein interactions (molecular), inter-organelle communication (sub-cellular organelles), autocrine or inter-cellular paracrine transfer (cells), and endocrine information transfer (organs and systems).

Figure 3 The hallmarks of mitochondrial signal transduction

Show full captionFigure viewer

In the following three sections, we first review the known molecular machinery responsible for mitochondrial input sensing (step 1), the processes enabling information integration within mitochondrial networks (step 2), and the resulting signals that communicate mitochondrial states intracellularly and systemically (step 3). To avoid the natural tendency to emphasize only specific well-known examples that would naturally narrow the spectrum of physiological processes to which mitochondrial signal transduction may apply, we discuss the mechanisms involved in the sensing, integration, and signaling stages sequentially. Recognizing that mitochondria are not all created equal, we then discuss tissue-specific mitochondrial features relevant to signal transduction. We close by considering outstanding questions and opportunities that an integrated mitochondrial signal transduction perspective raises for cell biology and clinical/translational research.

Mitochondrial sensing

The main molecular features that enable mitochondrial sensing include traditional ligand-activated receptors, transporters, and biochemical reactions such as the oxidative phosphorylation (OxPhos) system within the outer and inner mitochondrial membranes (OMM

and IMM) and the mitochondrial genome (Figure 4). These components enable mitochondria to rapidly and selectively sense changes in specific biochemical inputs. In the same way that a capsaicin receptor allows a sensory cell on the taste bud to depolarize and convert the spicy molecule into an action potential (recognizable as information by the brain), the mitochondrial sensing machinery converts simple inputs into biochemical, functional, and/or morphological changes (eventually converted to outputs that cells recognize). Mitochondrial inputs range in their nature from atoms, gases, and ions to small molecules and metabolites, proteins, lipids, DNA, and temperature, as well as physical interactions with surrounding organelles (Figure 3). In this section, we cover the molecular machinery that allows the MIPS to selectively sense and respond to extrinsic and intrinsic inputs (MIPS step 1 of 3).

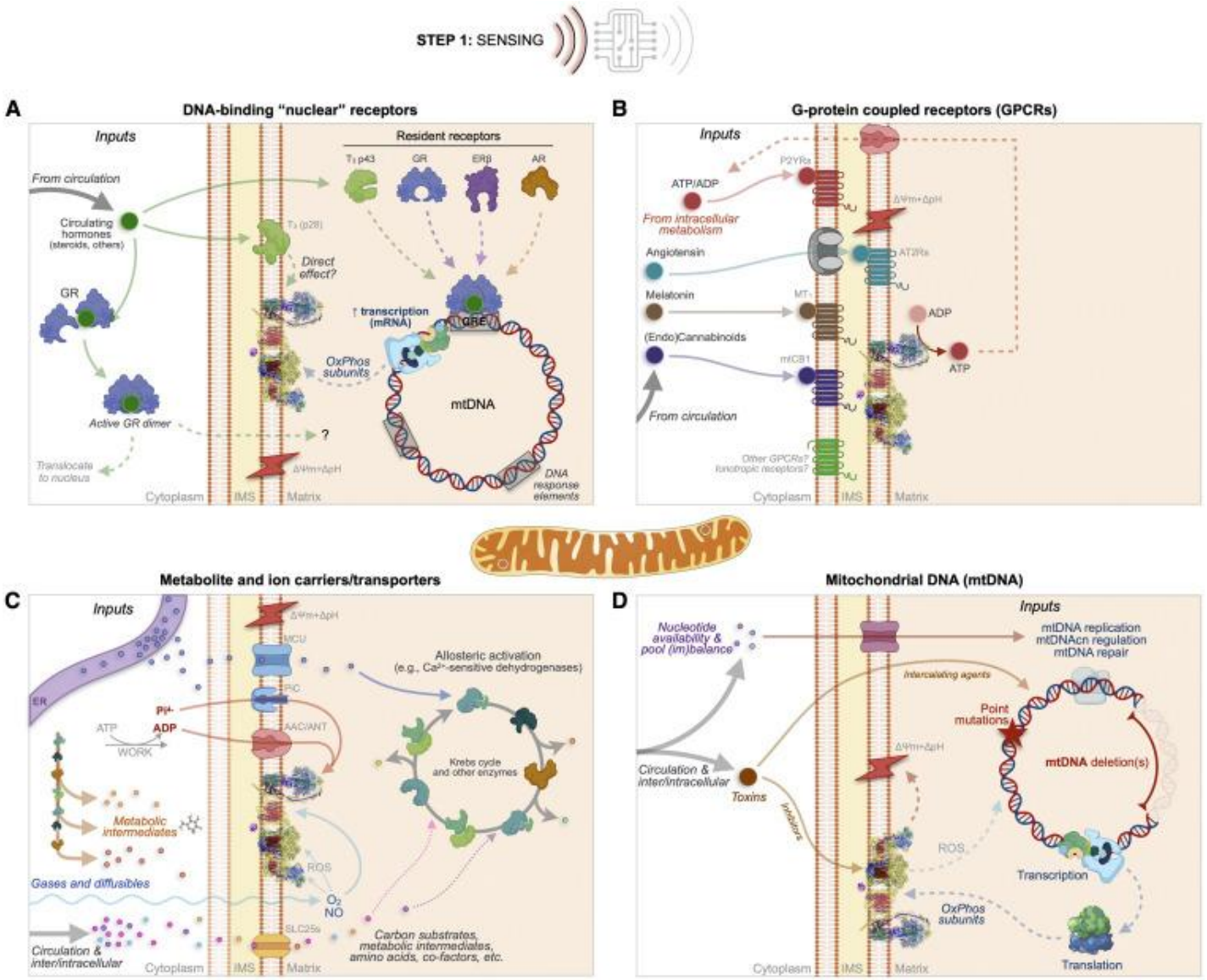

Figure 4 MIPS step 1: Sensing

Canonical “nuclear” receptors

Mitochondria contain ligand-activated transcription factors traditionally known as “nuclear” receptors. These receptors are expressed and generally reside in the cytoplasm or directly in mitochondria, homo- or hetero-dimerize upon ligand binding, and then translocate either to the nucleus or to the mitochondrial matrix where they interact with target DNA sequences. Limitations exist around the experimental evidence underlying the localization of these receptors within mitochondria, calling for further research using rigorous designs and sensitive molecular approaches.[56] The most well-documented examples include receptors for thyroid hormones, sex hormones (estrogen and androgen), and stress-related glucocorticoids (Figure 4A).

Thyroid hormones (T_3, T_4, and related metabolites) have potent effects on tissue oxidative capacity and systemic energy expenditure through their dual action on nuclear gene expression and directly on mitochondria. In isolated mitochondria, respiratory chain activity is modulated by triiodothyronine (T_3) without changes in protein synthesis—taking place *in vitro* or “*in organello*”—substantiating the direct sensitivity of mitochondria to circulating thyroid hormones.[57] Two putative resident mitochondrial thyroid hormone receptors have been described. The p28 receptor likely resides in the IMM, lacks a DNA-binding domain, and binds T_3 with high affinity.[58] It appears responsible for the rapidity (within 2 min *in vitro*, <30 min *in vivo*) with which mitochondrial respiration responds to thyroid hormone stimulation.[59,60] The other p43 receptor is a 43 kDa member of the c-Erb α1 DNA-binding family residing in the mitochondrial matrix.[61] Mitochondria respond to T_3 by increasing mitochondrial DNA (mtDNA) transcription and changing the ration of mRNA and rRNA.[62,63] Most studies on mitochondrial T_3 response have been performed on liver mitochondria, but mitochondrial thyroid sensing may exhibit high tissue specificity.[64] In mice, manipulating the expression of the mitochondrial T_3 receptor p43 in different tissues triggers selective transcriptional and enzymatic effects on mtDNA-encoded OxPhos components (e.g., not on complex II proteins or activity),[65] as well as broad cellular and physiological effects,[66] highlighting the likely physiological significance of mitochondrial thyroid hormone sensing.

There are two isoforms of the estrogen receptor related to mitochondria: ERα and ERβ. They have relatively low homology for their ligand-binding domains and *trans*-activational domains, and therefore have strongly divergent functions.[67] ERα primarily influences nuclear gene expression, including activation of mitochondrial biogenesis and other aspects of mitochondrial biology,[68] whereas ERβ translocates to mitochondria and is found at high levels in murine and human mitochondria from neurons and cardiomyocytes.[69] Under baseline conditions in cancer cell lines, the majority of ERβ is primarily located in mitochondria.[70] Activation of mitochondrial ERβ results in anti-apoptotic effects by disrupting Bad-Bcl-X(L) and Bad-Bcl-2 interactions.[71] Estrogen receptor signaling may also increase mitochondrial OxPhos capacity in genetically compromised cells from patients with Leber’s hereditary optic neuropathy (LHON), either directly by acting on the mitochondrial OxPhos system or indirectly by reducing oxidative stress.[72]

Mitochondria sense androgenic hormones via the canonical androgen receptor (AR). In cultured prostate cells, a substantial fraction of total AR may localize to mitochondria.[73] The mitochondrial AR influences mtDNA levels, mtDNA transcription and translation, and RC protein abundance and complex activity.[73] This enables both genetic and functional mitochondrial responses to circulating androgen levels. In the human sperm midpiece, both the

AR and ERβ localize to mitochondria.[74] Mitochondrial responses to estrogens and androgens via these DNA-binding receptors may in part account for sexually dimorphic mitochondrial features and functions.[75,76]

Mitochondria also contain the glucocorticoid receptor (GR) and thus can respond to glucocorticoid hormones, including the psychological stress mediator cortisol and corticosterone. Two major GR isoforms have been defined, GRα (predominant, ~90% of transcripts) and GRβ (minor, ~10%), which differ only in their distal domain from exon 9 alternative splicing.[77] Another isoform, GRγ, is produced through alternative splicing (includes an intronic codon between exon 3 and 4) and differs from GRα and GRβ isoforms by a single amino acid.[78] Within mitochondria, the active GR receptors interact with mtDNA glucocorticoid response element (GRE) sequence motifs to influence mitochondrial rRNA synthesis[79] and gene expression. The mtDNA contains 8 putative GREs: 2 within the D loop,[80] 1 in the 12S rRNA, 1 in tRNALeu$^{(UUR)}$, 3 in COX I, and 1 in COX III.[81] Compared to the nuclear genome, which contains approximately 680 GREs (1 GRE for every ~37 protein coding gene), the abundance of GREs in mtDNA is substantially higher, at 1 mtDNA GRE for every ~1.6 protein coding gene.[82] Mitochondrial glucocorticoid sensing is likely primarily mediated by GRγ,[83] acting on D loop GREs to promote expression of all polycistronic rRNA and mRNA genes.[84] It is worth noting that reduced mitochondrial GR localization may occur under certain pathological states, potentially hindering the mitochondrial sensing of glucocorticoid levels.[85]

Thus, conserved DNA-binding receptors allow mitochondria to sense the broad class of metabolism-regulating, sex- and stress-related hormones conveying systemic information about the state of the organism to core biochemical and genetic elements within the MIPS.

G protein-coupled receptors

The mitochondrial sensory system also includes one of the evolutionarily more recent innovations, the G protein-coupled receptors (GPCRs). Mitochondrial GPCRs sit in the OMM and IMM and are specific to hormones such as angiotensin II,[86] melatonin,[87] endocannabinoids,[88] and purines.[89] Mitochondria-localized GPCRs influence core mitochondrial functions including ion uptake, OxPhos, nitric oxide synthesis, apoptotic signaling, and reactive oxygen species (ROS) production,[90] illustrating their potentially broad action spectrum (Figure 4B).

Angiotensin type 1 and 2 receptors (AT_1R and AT_2R) are present on both the nuclear membrane and on the IMM.[91] Despite lacking a canonical mitochondrial targeting sequence, transfection of full-length GFP-tagged AT_2R naturally results in their mitochondrial localization.[86] Mitochondrial AT_2R appears to colocalize with its endogenous ligand Angiotensin II (thus forming an endogenous renin-angiotensin system) in several cell types including (from most to least abundant) mouse hepatocytes, cardiomyocytes, and renal tubule cells, and in human monocytes.[91] Functionally, activation of AT_2R on isolated mitochondria was found to increase nitric oxide production by ~25% with a proportional decrease in complex I-driven O_2 consumption capacity,[86] supporting the physiological effects of the angiotensin GPCR on mitochondrial oxidative capacity.

Mitochondria also contain the functional melatonin GPCR MT_1. In mouse brain neuron mitochondria, MT_1 is located on the OMM with its signal transduction apparatus coupled to

cyclic AMP in the intermembrane space.[87] In isolated mitochondria, activation of MT_1 by melatonin could partially inhibit permeability transition and subsequent cytochrome *c* (Cyt *c*) release, and expectedly conferred downstream protection from ischemic injury, permeability transition pore (PTP) opening, and subsequent cell death.[87] Other potential functions of mitochondrial melatonin signaling involve redox modulation as melatonin is a potent antioxidant,[92] and may also include stimulation of mitochondrial biogenesis.[93] However, further research in neurons and other cell types is needed to disentangle the effects of MT_1 signaling on mitochondria versus on the plasma membrane.

Another functional GPCR localized to mitochondria is the type I cannabinoid receptor (mtCB1). mtCB1 is expressed in neurons,[88] astrocytes,[94] and skeletal muscle myofibers.[95] Similar to CB1 localized at the plasma membrane of neuronal synapses where their signaling inhibits neurotransmitter release, mtCB1 receptors on the OMM signal through intra-mitochondrial Gαi protein activation and inhibition of soluble-adenylyl cyclase (sAC),[34] which inhibits protein kinase A (PKA)-dependent phosphorylation of target OxPhos subunits.[34] Functionally, mitochondrial endocannabinoid sensing through CB1 reduces complex I activity and mitochondrial respiration.[88] In mice, the effects of mtCB1 signaling affect neuronal function and memory formation,[34] suggesting that mitochondrial endocannabinoid sensing also has downstream effects on the behavior of the organism.

Mitochondria sense and respond to cytoplasmic purine (ATP, ADP, and AMP) levels via the purine GPCRs $P2Y_1$ and $P2Y_2$. These receptors, whose precise sub-organellar location remains unclear, have been suggested to be coupled to phospholipase C (PLC) and downstream regulation of the mitochondrial calcium uniporter (MCU).[89] In hepatocytes, activation of mitochondrial $P2Y_1$ stimulates Ca^{2+} uptake whereas activation of $P2Y_2$ inhibits uptake.[96] A receptor of the same family, the $P2X_7$ ionotropic purinoceptor (P2Y7R), also appears to be present in both the plasma membrane and in the OMM of cultured mouse and human cells.[97] Deletion of $P2X_7$ reduces transmembrane potential and respiratory capacity and leads to the accumulation of NADH (i.e., reductive stress) likely secondary to complex I inhibition.[97] The presence of surface ADP-sending GPCRs in mitochondria, along with the ADP/ATP carrier and F_1/F_0 ATP synthase system (discussed below), illustrates the potential value of redundant mechanisms allowing the MIPS to sense particularly critical cytoplasmic signals such as the cytoplasmic ADP:ATP ratio.

Other receptors may also localize to the MIPS. For example, GPCRs internalized from the plasma membrane, such as the kynurenic acid-activated GPR35, may translocate to the OMM and modulate the OxPhos system under stress conditions.[98] The ligand-gated ion channel α7 nicotinic acetylcholine receptor (nAChR) on the OMM may also enable mitochondria to sense acetylcholine (and nicotine) to modulate Ca^{2+} transients, permeability transition, and mtDNA release.[99,100] Additional work is required to discover and validate additional mitochondrial receptors, and to determine the ligand specificity and functional significance of mitochondrial GPCRs as components of the mitochondrial sensing machinery.

Metabolite signaling

In a process highly integrated with cytoplasmic micronutrient sensors such as mTORC1 and AMPK, mitochondria sense and respond to metabolite levels and availability through specific carriers and transporters embedded within the IMM (Figure 4C). One of the classic MIPS inputs

that triggers responses among the OxPhos system and multiple downstream mitochondrial processes is the phosphorylation potential (ΔGp), reflected simplistically in ADP levels.[101] An increase in cytoplasmic ADP concentration (or more accurately a decrease in ΔGp, or ATP:ADP ratio) is rapidly transmitted to the mitochondrial matrix via monomers of the ADP/ATP carrier spanning the IMM.[102] This sets the rotary F_oF_1 ATP synthase into motion, transiently dissipating the protonmotive force ($\Delta pH+\Delta\Psi_m$: pH gradient + mitochondrial membrane potential).[103] In this single step, the shift in ATP/ADP levels causes a consequential thermodynamic shift that sends biochemical ripples sequentially accelerating (1) proton pumping and electron flow by respiratory chain complexes I, III, and IV; (2) the reduction of O_2 to H_2O by Cyt *c* oxidase (complex IV); and (3) the oxidation of reducing equivalents NADH and $FADH_2$ at complexes I and II, respectively, thus (4) driving the oxidation of metabolic intermediates in the TCA/Krebs cycle, which in turn (5) increases CO_2 production and (6) increases the diffusion gradient for the uptake of cytoplasmic substrates/metabolites into the matrix.[101] In isolated mitochondria, this ADP-induced change in state from low flux to actively respiring mitochondria is associated with profound conformation changes of the mitochondrial cristae membranes—from the orthodox to condensed state.[104] This simple example illustrates the breadth and complexity of ultrastructural and biochemical responses that a single input, such as ADP, can elicit within the MIPS.

Mitochondrial metabolite uptake and sensing are broadly enabled by >50 proteins from the SLC25 family of transporters, known as the mitochondrial carrier system (MCS).[105] These transmembrane IMM proteins are essential to both MIPS sensing and also to fulfill the biosynthetic functions of mitochondria, allowing the export of the ingredients for growth and repair, i.e., several amino acids and one-carbon carrying folate forms, carboxylic acids, fatty acids, cofactors, inorganic ions, and nucleotides to the whole cell.[106] In relation to mitochondrial sensing, the MCS provides sensory capacity to small molecule metabolite carriers including pyruvate (MPC1/2),[107,108] dicarboxylate (malate-phosphate, DIC) and tricarboxylate (citrate-malate, CTP) carriers, aspartate-glutamate (AGC1/2), the phosphate carrier[105] and NAD carrier,[109] and many others. Some mitochondrial transporters are often alternatively expressed variants of genes encoding plasma membrane carriers, as for the mitochondrial glutamine transporter that allow mitochondria to respond directly to cytoplasmic glutamine levels.[110] In cancer cells, the diverse MCS enables mitochondria to sense cytoplasmic levels of key amino acids via the TCA cycle, and to undergo secondary morphological changes.[111] Thus, metabolite carriers and transporters allow the MIPS to sense and respond to inputs from numerous metabolic pathways.

We also note that the bioenergetic state of the cell exerts regulatory control on dozens of mitochondrial enzymatic reactions. As a result, high ATP:ADP and NADH:NAD^+ ratios favor anabolism and promote export of metabolites, shifting metabolism toward non-oxygen-dependent glycolysis and biosynthesis.[112] In cases of OxPhos defects, NADH accumulates and reduce the availability of NAD^+, causing reductive stress,[113,114] driving the flux of metabolic pathways toward mitochondrial anabolic pathways contributing to disease.[115,116] The collective action of metabolic inputs on mitochondrial OxPhos and the NADH:NAD^+ ratio also translates into the availability of downstream substrates, including coenzyme A (CoA) and NADP(H). Changes in CoA availability affect the conversion of acetyl to acyl-CoA used to post-translationally acetylate and functionally modulate not only cytoplasmic enzymes and nuclear chromatin,[117] but also dozens of mitochondrial proteins.[118] Together, these biochemical dial systems provide a set of molecular cascades that dynamically integrate and convert biochemical

inputs into functional mitochondrial recalibrations,[119] thereby allowing the MIPS to sense a broad array of biochemical inputs about the dynamic bioenergetic state of the cell.

Electrophysiology of mitochondria: Ion signaling

Mitochondria sense and respond to ions, which is a logical consequence of the relatively high membrane potential across the IMM, generating a large diffusion potential for charged atoms and molecules (Figure 4C). One of the most studied examples of ionic mitochondrial sensing is calcium (Ca^{2+}). The MCU enables rapid Ca^{2+} uptake within seconds.[120,121] Mitochondrial Ca^{2+} uptake from the cytoplasm and ER triggers rapid changes in mitochondrial physiology through post-translational modifications (PTMs) of dehydrogenases that increase TCA cycle activity[122] and results in membrane potential changes.[123] Although genetic ablation of the MCU is not lethal in most mouse strains, its loss prevents mitochondria from sensing surrounding Ca^{2+} levels[123] and may impair mitochondrial fusion during cell-cycle division,[124] highlighting the significance of mitochondrial Ca^{2+} sensing on the MIPS.

Mitochondrial Ca^{2+} is also linked with sodium (Na^+) signaling. The organellar Ca^{2+} levels are affected by the activity of the mitochondrial Na^+/Ca^{2+} exchanger (NCLX). NCLX sits in the IMM and extrudes matrix Ca^{2+} in exchange for cytoplasmic Na^+.[125] Entry of sodium into the cytosol during an action potential in neurons, or in response to glucose stimulation in the pancreatic beta cell, triggers the extrusion of calcium from the mitochondria, preventing mitochondrial calcium overload and subsequent cell death.[126] By lowering the intra-mitochondrial Ca^{2+} levels ($[Ca^{2+}]_{mito}$) in cardiomyocytes and brown adipocytes, NCLX activity thereby decreases intra-mitochondrial calcium levels and directly regulates mitochondrial PTP (mPTP) dynamics and downstream signaling.[127,128] But in addition to decreasing $[Ca^{2+}]_{mito}$ levels, NCLX activity rapidly elevates matrix $[Na^+]$ levels,[129] likely preventing collapse of the MIPS through the flux of Ca^{2+} and Na^+ ions.

Mitochondria sense and also respond to surrounding concentrations of various atoms and ions including magnesium (Mn), inorganic phosphate (Pi), chloride (Cl), iron (Fe), and possibly others including lithium (Li),[130] although the underlying mechanisms for the most part are not resolved. Mitochondria are also sensitive to divalent gases such as nitric oxide (NO), which acts directly on complexes I and IV by chemically modifying sensitive residues, thereby modulating respiration.[131] One fairly well-studied input is molecular oxygen (O_2), which is sensed directly by a combination of complex I-[132,133] and complex III-derived[134] bursts of ROS during hypoxia. In low-oxygen conditions (hypoxia), acidification of the mitochondrial matrix in a complex I-dependent manner solubilizes intra-mitochondrial calcium-phosphate deposits, which increases soluble $[Ca^{2+}]_{mito}$ (even in the absence of MCU). In mouse embryonic fibroblasts, hypoxia activates NCLX and causes a 2- to 3-fold increase in mitochondrial matrix Na^+, which interacts with IMM phospholipids to decrease membrane fluidity and promote superoxide formation by semiquinone,[129] transforming information about oxygen availability into molecular information within the MIPS. Mitochondrial O_2 sensing undoubtedly complements cytoplasmic sensors such the hypoxia-inducible factor 1 alpha (HIF-1α) pathway that primarily act on the nucleus.[135] Overall, several evolutionarily ancient ion channels, transporters, and mechanisms based on chemical modifications thus ensure that mitochondria can sense and rapidly respond to their surrounding intracellular ionic environment.

Intrinsic mtDNA defects

In addition to cytoplasmic signals sensed through canonical receptors and carriers, mitochondria also dynamically recalibrate their structure and internal processes in response to *intrinsic* signals, such as those arising from the mitochondrial genome (Figure 4D). The mtDNA codes for 37 canonical genes, including 13 protein-coding mRNA sequences,[136] plus small mitochondria-derived peptides (MDPs).[137] As the mtDNA can be affected by external factors (e.g., mutagens, nucleotide availability) and produce outputs (RNA, proteins) that influence and shape the OxPhos system and downstream mitochondrial behaviors, the mtDNA is a component of the mitochondrial sensing system.

Defects in the mtDNA sequence, which are either inherited[138] or acquired,[139] alter the synthesis of OxPhos subunits, which consequently impair respiratory capacity, OxPhos function, and $\Delta\Psi_m$, culminating in disease.[140,141] Because most biochemical reactions taking place within mitochondria are directly or indirectly linked to OxPhos and $\Delta\Psi_m$, including substrate and ion uptake, mtDNA perturbations have widespread consequences for several metabolic pathways.[113,142] Within skeletal muscle, for example, acquired somatic mtDNA deletions can disrupt OxPhos enzyme activities and trigger local mitochondrial proliferation when in proximity to a nucleus[143] (see section on mitochondrial signaling). Milder mtDNA variants are also sensed, are translated in metabolite levels,[144] and result in variation in cellular and organismal phenotypes that influence lifespan and disease risk.[145,146] Moreover, because some mutagens and toxins may preferentially affect the mtDNA relative to the nuclear DNA—in part owing to the negatively charged matrix compartment (which attracts positively charged molecules), rapid replication, poor repair, or other factors—the mitochondrial genome maintenance and expression systems may act as a cellular "sentinel" of genotoxic stress.[147]

Certain intrinsic mitochondrial inputs such as nucleotide availability and genotoxic molecules may not influence any of the mitochondrial biochemical processes directly, and may in fact only be sensed through the (replicating) mtDNA. For example, low nucleotide availability impairs OxPhos function specifically through the decline in mtDNA copy number,[148] which may or may not induce nucleotide salvage or cytoplasmic nucleotide synthesis pathways. We propose that the mtDNA replisome is an actively communicating structure, which tunes its function based on cellular nucleotide pools and the local mtDNA expression machinery. The actual signals contributing to mtDNA communication within the MIPS are still poorly understood.

Summary of mitochondrial sensing

Mitochondria are equipped with a surprisingly wide variety of receptors and molecular features that give them the ability to sense hormonal, metabolic, ionic, genetic, and other inputs. With such sensitivity to a broad spectrum of inputs, the MIPS senses both the local biochemical conditions surrounding each organelle and systemic neuroendocrine signals produced in distant anatomical locations of the organism: by other cells, within other organs. Mitochondrial behavior is therefore not only driven by changes in nuclear gene expression—which produce the sensing components—but also more acutely and reversibly by biochemical and endocrine inputs that dynamically modulate their biochemical, genetic, ultrastructural, and physiological properties.

The evolutionary co-opting of a variety of DNA-binding receptors, GPCRs, and transporters suggests that increasing the range of inputs that mitochondria were capable of sensing must have positively contributed to the organism's adaptive capacity. As a result, the diverse mitochondrial sensing machinery has been evolutionarily selected and likely also enriched in mitochondrial membranes relative to other organelles. Defining the full spectrum of inputs directly sensed by the MIPS across different cell types is an outstanding research challenge. Expanding our understanding of the inputs that directly shape mitochondrial biology could illuminate new disease pathways, independent or upstream of OxPhos or other well-defined disease-causing mechanisms.

Next, we turn our attention to dynamic factors that physically and functionally connect sensing mitochondria as interactive networks capable of signal processing and integration.

Mitochondrial signal integration

In its simplest form, signal integration is the process by which inputs are converted into common second messengers containing transformed information about the inputs. For example, within cells, multiple cell surface receptors converge on the production of common chemical secondary messenger molecules such as cyclic AMP or Ca^{2+}, which in turn trigger broad-acting downstream response(s).[149] Because secondary messengers are shared products for multiple receptors, multiple stimuli converge on the same signaling hubs. Another good example of this concept takes place in neurons: dozens of neurotransmitters and modulators signal via ionotropic and metabotropic receptors to converge on a single cellular property—the plasma membrane potential. The temporal combination of inputs determines whether or not an action potential is generated.[150] As a result, in neural networks (as in mitochondrial networks) membrane potential serves as an integrating hub for signal transduction. The convergence of inputs onto chemical second messengers and membrane potential thus allows cells to produce coherent, integrated, and robust responses simultaneously shaped by multiple inputs.

Another core concept for signal integration is that large-scale functional networks bind small competent units into larger scale computational agents.[51] Cells and organs integrate and compute information as cell collectives.[151] For instance, in the brain no single neuron (unit) can accomplish the sophisticated brain computations required to coordinate and sustain the rest of the body. Glial cells and neurons accomplish remarkable feats of integration through cell-to-cell communication, creating a functional collective (the brain) that naturally integrates or computes information.[48] Similarly, mitochondria are functionally linked and operate as "social" collectives within the cell cytoplasm.[152] For our purposes, integration refers to the functional computations (i.e., the transformation of inputs into outputs) that take place within the MIPS between the sensing and signaling steps.

A third and final relevant concept to signal integration states that computational processes are influenced by the structural properties of the network itself—i.e., how individual units are arranged and connected relative to other ones.[153,154] The interactions between mitochondria, defined as the probability of direct information exchange between individual organelles, is termed "connectivity." Across physical, biological, and social networks, the extent and nature of the connectivity between units largely define the network properties[155,156] (Figure 5). Thus, the information processing capacity of the MIPS, created by networks of coexisting mitochondria,

must be determined jointly by both the intrinsic properties of mitochondria (their sensing machinery, mtDNA, OxPhos system, etc.) and their functional connectivity with one another.

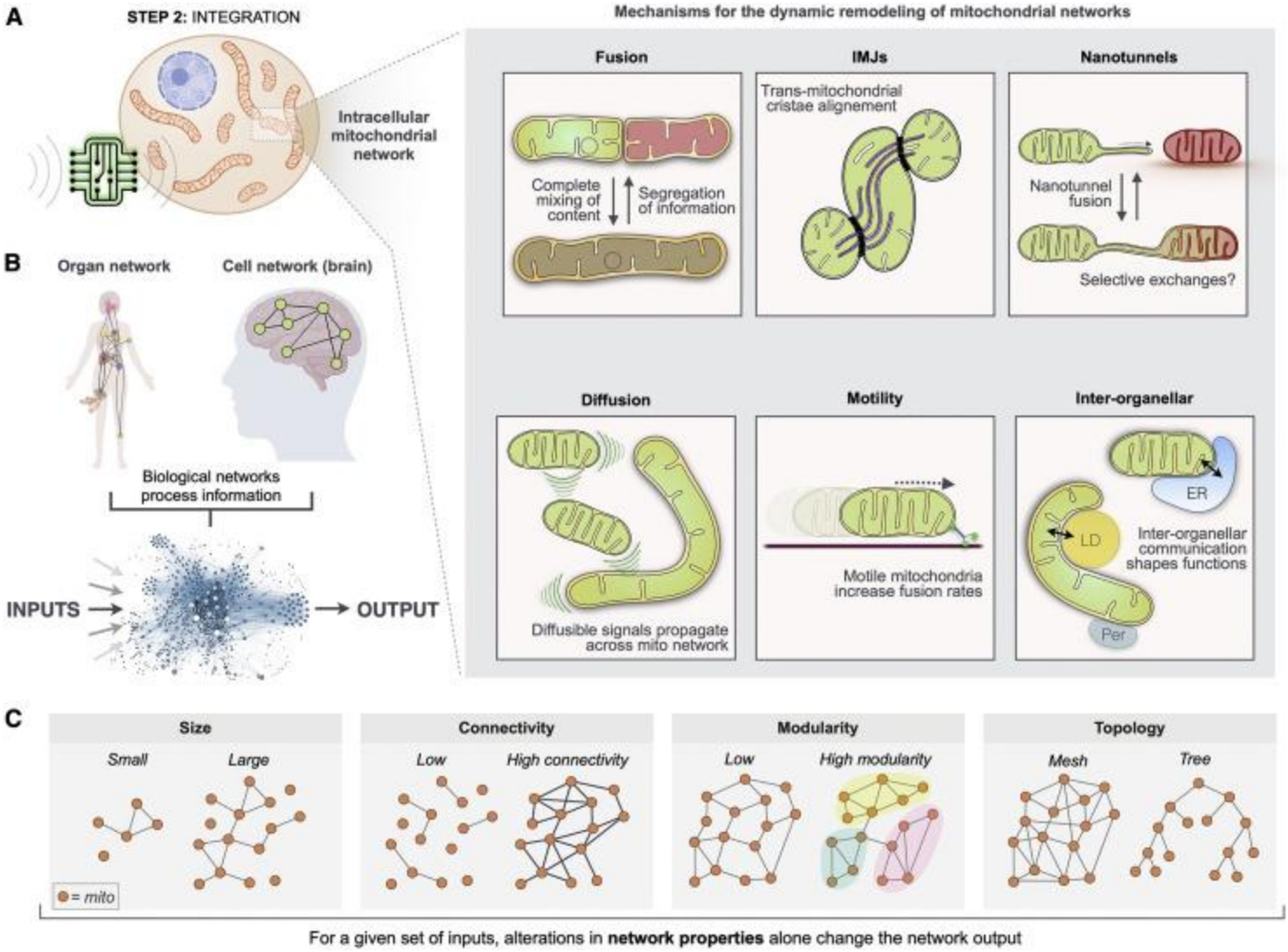

Figure 5 MIPS step 2: Signal integration

Show full captionFigure viewer

Below we discuss how physical inter-organellar interactions, diffusible signals, dynamic morphological transitions, motility, and sub-cellular positioning dynamically define the architecture and connectivity of mitochondrial networks, which are the basis for mitochondrial signal integration (MIPS step 2 of 3).

Mechanisms of homologous mitochondrial communication

Several types of physical interactions enable transient information exchanges among mitochondria. Mitochondrial “kiss-and-run” involves the partial fusion of mitochondrial membranes among motile mitochondria in plants[157] and cultured mammalian cells.[13,158] These rapid interactions occur in the span of seconds to minutes and require the OMM mitofusins

(MFN1/2) and IMM optic atrophy 1 (OPA1). Kiss-and-run events enable the exchange of proteins and membrane potential,[158] and possibly mtDNA nucleoids, although likely only in some cell types.[159]

Inter-mitochondrial junctions (IMJs) are close OMM-OMM contact sites anatomically similar to cell-cell gap junctions. The juxtaposition of highly electron-dense mitochondrial membranes, originally visualized in cardiomyocytes[160] between electrically connected mitochondria,[161] increases in frequency with cellular energy demand (e.g., exercise[162]) and with mitochondrial volume density.[163] At IMJs, which are evolutionarily conserved from mollusks to mammals, internal cristae membranes exhibit a remarkable degree of coordination (i.e., cristae alignment) across the two juxtaposed mitochondria, revealing the exchange of information between the two linked organelles.[163] Artificially linking energized mitochondria *in vitro* via synthetic linkers was sufficient to recapitulate IMJs and trigger cristae remodeling,[163] and the iron-sulfur cluster containing OMM protein MitoNEET may be one of the IMJ tethering proteins.[164] Functionally, IMJs may provide the physical basis for the propagation of membrane potential and other physicochemical signals even in the absence of protein exchanges and complete mitochondrial fusion.[165,166]

Mitochondrial nanotunnels are thin ~100-nm-wide double-membrane protrusions that arise from donor mitochondria, extend over distances up to several microns, and can interact and fuse with a receiver mitochondrion.[167] Nanotunnels transport matrix proteins and therefore represent a mechanism of protein sharing and communication even between non-adjacent mitochondria.[168] In cultured cells, nanotunnels can be induced by the pulling action of the kinesin motor protein Kif5b.[169] *In vivo*, the existence of nanotunnels has been limited to tissues where mitochondrial motility is restricted such as in the densely packed cytoplasm of human skeletal muscles[170] and rat cardiomyocytes,[171] suggesting that physically constrained mitochondria that cannot encounter diverse fusion partners reach out to other functional mitochondria via nanotunnels. In patients with mitochondrial disease, mitochondria with compromised OxPhos function due to mtDNA mutations were found to have ~6-fold more nanotunnels than in healthy controls.[170] This suggests that mitochondrial nanotunnels may preferentially arise or stabilize between mitochondria with impaired OxPhos capacity as a mean of functional complementation,[167] or as a mean of increasing the effective functional connectivity among the mitochondrial network of the MIPS. Among other biological networks, enhancing the structural connectivity between individual units alters global network properties and can enhance robustness and computational/cognitive properties.[172,173]

Mitochondria also communicate via diffusible signals. One well-described example of diffusion-based mito-mito communication is ROS-induced ROS release (RIRR). Among the relatively uncluttered cytoplasm of cultured cells, mitochondria can generate and propagate waves of ROS production progressing through sequential PTP opening at rates of ~5 μm/min.[174] This soluble form of signaling relies mostly on the physical proximity of mitochondria. In cardiomyocytes, proximity-based propagation depends on the production and diffusion of superoxide anions ($O_{2}^{\cdot -}$) and H_2O_2.[175] Similarly, mitochondria can propagate waves of apoptotic signaling by sequentially undergoing permeability transition: waves are propagated by groups of mitochondria that sequentially uptake and release Ca^{2+}, which neighboring mitochondria then uptake and release, and so on.[10] The mito-mito transmission of information via diffusible signals within the MIPS may also be facilitated by some of the physical structures described above, particularly inter-organellar tethers.

Mitochondrial dynamics: Fusion and fission

Mitochondrial fusion is a well-described process whereby two adjacent and generally motile mitochondria encounter each other and interact via the outwardly protruding domains of mitofusins (MFN1/2) and accessory proteins, leading to the sequential merging of the OMM and IMM of both organelles.[176] After fusion, the two original mitochondria form a unified organelle with a continuous matrix and membrane system. Organelle fusion allows the exchange of all matrix, IMM, IMS, and OMM components, including mtDNA, proteins and RC complexes, lipids, metabolites, ions, and membrane potential.

Experiments tracking the diffusion of photo-activable green fluorescent protein (mtPAGFP) in cultured mammalian cells[177] and *in vivo*[178] show that fusing mitochondria readily exchange molecular material.[179] In cardiomyocytes cultured *ex vivo*, mtPAGFP is exchanged through kiss-and-run fusion and nanotunnels and becomes distributed to the entire mitochondrial network within ∼10 h.[168] In immortalized cell lines, the rate of mitochondrial fusion for each organelle is significantly faster, at one fusion event every ∼5–20 min.[13] Mitochondrial membrane fusion therefore leads to the mixture and homogenization of mitochondrial protein distribution (i.e., mitochondria are more similar to each other). On the other hand, ablation of mitochondrial fusion by double Mfn1/2 silencing in mouse embryonic fibroblasts drastically increases mitochondrial heterogeneity (some mitochondria have a lot of protein x, others have little of it) within the MIPS.[12] *Ex vivo* studies of post-mitotic tissues and cells have made it clear that mitochondria in post-mitotic cells have lower fusion rates than cancer cells and immortalized cell lines (e.g., Eisner et al.[180]). Moreover, the cytoplasm of certain tissues can inhibit *ex vivo* mitochondrial fusion rates.[181] But in post-mitotic cells in which mitochondrial movement is restricted by cytoskeletal elements, fusion and fission can take place without displacement of mitochondria. This can be viewed as fire-doors in a long corridor—rapidly and reversibly modulating the network connectivity.

The functional relevance of dynamics to mitochondrial signal transduction is that larger mitochondria with larger matrix volume and lower surface-area-to-volume ratio respond differently to incoming signals. One example is the ability of mitochondria to handle histamine-induced rises in cytoplasmic [Ca^{2+}]. Relative to small fragmented mitochondria, larger tubular mitochondria in the same cell uptake Ca^{2+} at a similar rate but recover more quickly (within 30 s).[182] In response to hyperglycemia, mitochondrial fragmentation precedes hyperglycemia-induced ROS production.[183,184] Hyperglycemia increases ROS production within ∼30 min, and fragmented mitochondria produce ∼50% more ROS than filamentous mitochondria in the same cell.[182] Again, the sequential events of sensing and responses illustrate how the functional responses of mitochondria to environmental inputs and stimuli are not rigidly set by genetically encoded states, but rather dynamically regulated by shape changes that remodel the network properties of the MIPS. Distinct fission signatures (i.e., where the fission event occurs along the mitochondrial tubule) are associated with the fate—degradation or biogenesis—of the resulting mitochondrial fragments,[185] possibly influencing long-term network properties.

The mitochondrial network also responds to metabolic signals. Mitochondrial fusion and fission are modulated by the cellular metabolic state,[186] and in turn regulate mtDNA stability *in vitro* and *in vivo*.[187] For example, the MIPS responds to substrate deprivation by undergoing MFN-dependent fusion,[188,189] whereas metabolic oversupply can inhibit mitochondrial fusion and lead to higher DRP1-dependent fragmentation in cultured cells[184,190,191] and in skeletal

muscle *in vivo*.[192] Morphological changes underlie intra-mitochondrial functional changes that optimize coupling efficiency (i.e., the coupling of oxygen consumption to ATP synthesis) to best match the dynamic metabolic state.[186,193] In brown adipocytes, mitochondrial fission decreases coupling efficiency in a DRP-1 and free fatty acid-dependent mechanism,[194] reflecting an intra-mitochondrial morpho-functional response that increases fatty acid utilization and heat production. Like neural connections that come and go through activity-dependent sprouting and pruning,[195] mitochondrial interactions and connections also persist and vanish over variable time periods, modulating information flow within the MIPS network.

Motility

Mitochondrial motility refers to the ability of mitochondria to travel to and from different parts of the cell. Motility influences MIPS structure as mitochondria stretch into their common tubular structure by adhering to cytoskeletal elements such as microtubules and actin filaments. When mitochondria fall off the cytoskeleton, they lose their tubular shape. Motility of an individual mitochondrion is also the strongest predictor of mitochondrial fusion.[196] Remarkably, the highest probability for a successful meeting between two mitochondria to develop into a fusion event is when one mitochondrion is moving while the other is stationary. The lowest probability is when both mitochondria have been stationary, even if they are juxtaposed.[177] On the other hand, fission is commonly followed with movement of the two daughter mitochondria so that they are not juxtaposed anymore (e.g., Kleele et al.[185]). The two fission products can therefore subsequently interact, possibly fuse, and thus share their content and more labile states with other units within the network. Both microtubules and actin filaments play a role in mitochondrial fission; for example, forcing the depolymerization of microtubules prevents the cytoplasmic redistribution of mitochondria in response to stress.[197] Directional motility is facilitated by cytoskeletal elements, but non-directional Brownian movement also appears to be a contributor to mitochondrial motility.[198]

Motility is influenced by the sensing of environmental signals.[199] The molecular sensors responsible for transducing metabolic and biochemical signals into motility implicate a complex of proteins that connect mitochondria to the motor machinery, the dynein and kinesin. Dynein and kinesin-1 walk the mitochondria on microtubules and thus any movement requires their attachment to the mitochondrial surface.[200] The molecular complex connecting mitochondria to these motor proteins includes Miro and Milton, whose regulations have been well defined in neurons.[201] When mitochondria enter an area with high calcium concentrations, Miro detaches from the motor proteins, resulting in the mitochondria falling off the cytoskeleton and becoming stationary; as a result, mitochondria stop their movement and accumulate in areas with increased calcium, where they can contribute to calcium buffering.[202] Similarly, Milton (Trak1) is inactivated by GlucNAC when glucose concentrations increase, leading to a similar arrest of mitochondrial movement in neurons in response to hyperglycemia.[203] In cultured cells, inter-mitochondrial tethering events similar to IMJs (without fusion) regulated by lysosomes[204] occur ~10× more frequently than fusion/fission events, limiting mitochondrial motility and therefore regulating mitochondrial distribution within the cytoplasm.[205] Overall, motility is a mechanism that dynamically redistributes mitochondria and together with fusion and fission determines the network structure of the intracellular mitochondrial collective.

Communication with other organelles

The MIPS engages in functional interactions with the ER lysosomes, peroxisomes, lipid droplets, and likely other organelles. This topic has been elegantly reviewed elsewhere.[206,207] Mitochondrial metabolism is directly supported by surrounding organelles that provide various substrates, lipid intermediates, and ionic signals that not only supply substrates, but also communicate information about the overall state of the cell. In particular, input from the nucleus provides hundreds of proteins that sustain and confer mitochondria with both their molecular sensory machinery and the machinery for fusion/fission dynamics and motility that influence their propensity to adopt certain network configurations.

Mitochondrial cortisol synthesis is exemplary of this inter-organelle inter-dependence, requiring the transfer of cholesterol from lipid droplets to mitochondria and its import across mitochondrial membranes, followed by shuttling of steroidogenic intermediates from mitochondria to the ER, and from the ER back to the mitochondrial matrix, where cortisol is finally synthesized.[208] The synthesis of the mitochondrial IMM phospholipid cardiolipin similarly involves the shuttling of lipid intermediates between mitochondria and ER at mitochondria-associated membranes (MAMs) through the ERMES[209] and ER-mitochondria complex (EMC).[210] Punctual, localized, and pulsatile redox-based communication between mitochondria and the ER can also propagate signals from single mitochondria to the ER and other mitochondria.[211] These examples illustrate the functional inter-dependence of mitochondria and other organelles, and the existence of conserved mechanisms for information exchange, propagating the state of the MIPS to other organelles, and vice versa.

Summary of mitochondrial signal integration

After describing the molecular machinery allowing mitochondria to sense and dynamically respond to intracellular and systemic inputs, here we have discussed the mechanisms allowing mitochondria to communicate and exchange information among each other and with other organelles. As the MIPS physically and functionally interacts as a mitochondrial collective with other organelles, it generates distributed representations of the biochemical and energetic conditions of the cells and organism. In turn, these capacities to sense and integrate information are adaptive, allowing mitochondria to tune and optimize their morpho-functional states to changing intracellular and environmental conditions.

Note that soluble communication mechanisms undoubtedly complement more complete forms of mitochondrial communication involving the merging and more-or-less complete union of mitochondria through membrane fusion. If diffusible signaling and transient protein exchange are analogous to “kiss-and-run,” more stable physical mitochondrial contacts such as IMJs and nanotunnels may reflect “engage-and-hold,” whereas complete mitochondrial fusion is analogous to “marry-and-mix.” Thus, mitochondrial interactions can be relatively transient (ion efflux lasts a few milliseconds), selective (nanotunnels connect with only one acceptor mito), and reversible (inter-organellar tethers can dissociate). The nature of these interactions is consistent with other plasticity mechanisms in biology, such as those modulating synaptic function within neural networks, which similarly integrate inputs and compute information.[212]

However, the ultimate unit of evolution and adaptation is not the mitochondrial network or the individual cell. It is the cell collective that constitutes the organism. Therefore, the goal of mitochondrial sensing and integrating information must be to optimize adaptation and health of the organism itself. Biologically, this becomes possible if the information sensed and integrated by the MIPS is then communicated to the cell and to the rest of the organism. This logic brings us to consider how mitochondrial inputs are converted and transmitted into meaningful cellular and organismal outputs or signals, through mitochondrial signaling (MIPS step 3 of 3).

Mitochondrial signaling

Several well-established and emerging signaling pathways link mitochondrial behavior to gene expression within the cell nucleus. Moreover, beyond the cell, the MIPS releases signals in the systemic circulation, influencing metabolic processes in neighboring cells and distant target organs. Several elements of mitochondrial signaling have been extensively covered elsewhere, such as apoptotic signaling,[213] ROS-mediated signaling,[214,215] and metabolic intermediates.[216] Here we only briefly cover these areas and expand the discussion of mitochondrial signaling to a broader spectrum of mitochondrial outputs that serve as intracellular and/or systemic outputs, including small metabolites, proteins, DNA, steroid hormones, and non-molecular signals including heat (Figure 6). We also discuss how the potency and specificity of signal transduction may be influenced by the sub-cellular localization of signaling mitochondria.

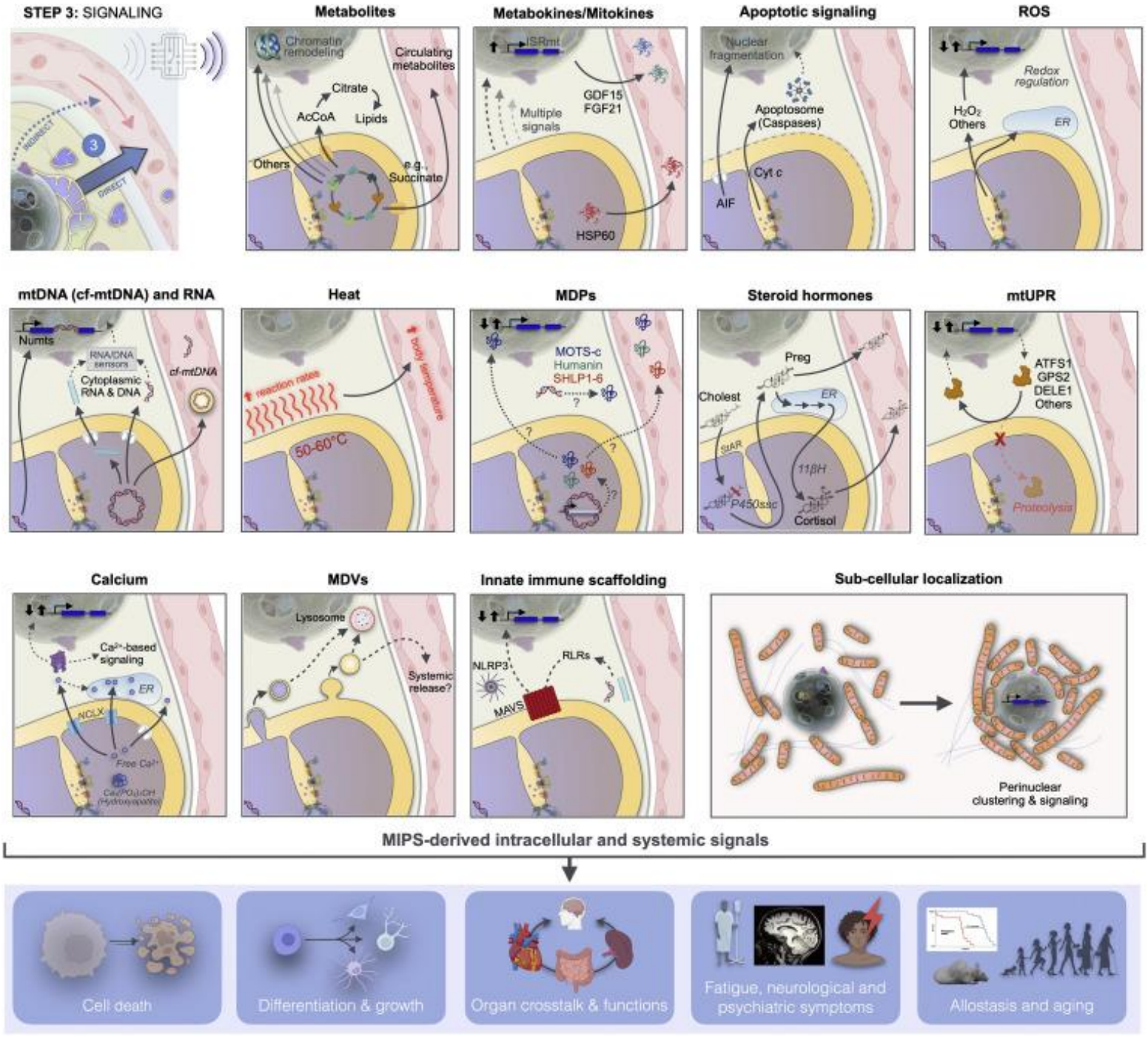

Figure 6 MIPS step 3: Signaling

Apoptotic signaling

The first use of the term "mitochondrial signaling" appeared in 1999 in relation to the release of the pro-apoptotic mitochondrial output Cyt *c*.[217] Cyt *c* is a small heme protein normally residing in the IMS where it shuttles electrons between OxPhos complexes III and IV. However, in

response to the convergence of specific inputs such as ROS, high [Ca^{2+}], and low [ATP], especially among a fragmented and poorly connected mitochondrial network,[218] mitochondria undergo permeability transition through PTP opening.[219] PTP opening triggers the cytoplasmic release of Cyt *c* where it interacts with and activates pro-caspases,[9] as well as other mediators of the intrinsic apoptotic pathway, including the apoptosis inducing factor (AIF) and the endonuclease EndoG that translocates to the nucleus and fragments the nuclear genome, and Smac/Diablo (reviewed in Wang and Youle[220]). In cancer cells, Cyt *c* released during non-lethal permeability transition (i.e., "flickering mode") can also play non-apoptotic signaling roles involving the activation of the nuclear ATF4-dependent integrated stress responses (ISRs; see below).[221] To prevent the assembly of pro-apoptotic molecular complexes at the OMM, mitochondria can also recruit anti-apoptotic proteins from the Bcl2 family. Functionally, PTP opening is closely linked to mitochondrial Ca^{2+} release and signaling, which is under the control of increasingly well-defined cristae-regulating mechanisms.[222] Thus, the MIPS contains a number of powerful cellular life-or-death signals coordinately released based on their integrated representation of biochemical conditions both within mitochondria and the cytoplasm.[223]

Mitochondrial metabolite signaling

Mitochondria speak the language of the epigenome. It is likely that the endosymbiosis of mitochondria and the MIPS preceded the development of the histone code, such that current epigenetic nuclear mechanisms have developed to couple gene expression to the metabolic state of the cell in the context of mito-nuclear communication.[224] As a result, the nuclear genome is densely wrapped with abundant histone proteins (mainly H2A, H2B, H3, and H4) that contain hydrophilic tails, which are heavily post-translationally modified by the metabo-chemical perinuclear and nuclear environment.[225]

Most substrates or cofactors required by histone-modifying enzymes to alter histone structure and downstream gene expression are direct products of mitochondrial metabolism.[226,227] These include metabolites from the TCA cycle[216] and from one-carbon metabolism.[228] For example, the methylation of histones and DNA by histone methyltransferases (HMTs) and DNA methyltransferases (DMTs), respectively, requires S-adenosylmethionine (SAM) derived from serine metabolism as part of the folate cycle and one-carbon metabolism pathway.[116,229] On the other hand, the reverse demethylation reaction requires the cofactor α-ketoglutarate (αKG), a TCA cycle metabolite. Several mitochondrial-derived metabolites are involved in PTMs of histones (and other proteins). These include lactate (i.e., lactylation),[230] a metabolite derived from glycolysis that increases in concentration when mitochondrial OxPhos is impaired; dopamine (i.e., dopaminylation),[231] whose catabolism via the OMM-bound monoamine oxidase involves the respiratory chain;[232] β-hydroxybutyrate (i.e., β-hydroxybutyration),[233] a ketone body synthesized in the mitochondrial matrix under low carbohydrate conditions; and many others.

Mitochondrial metabolites are epigenome-modifying MIPS outputs. mtDNA-depleted Rho0 cells were initially used to demonstrate that mitochondrial outputs alter nuclear DNA methylation.[26] In a similar model comparing a series of human cell lines with varying mutation load (i.e., heteroplasmy) of the pathogenic mtDNA 3243A>G mutation, heteroplasmy ranging from 0% to 100% influenced in a dose-response manner DMT gene expression and global transcriptional signatures.[23] In the same model, mtDNA heteroplasmy altered acetyl-CoA and αKG levels and yielded downstream changes in H4K16ac and H3K9me3 status.[234] Acute mtDNA depletion in

immortalized cells also triggered a physiologically meaningful decrease in the mitochondrial acetyl-CoA pool and downstream histone acetylation,[235] illustrating the range of epigenomic effects of the MIPS. Finally, a longitudinal study in primary human fibroblasts tracking DNA methylation changes over several months showed that both genetic and pharmacological OxPhos defects caused conserved, age-related hyper- and hypomethylation at thousands of genomic locations encoding developmental programs and cell-cell signaling components.[236] A publicly available multi-omic, longitudinal dataset is available to explore the influence of bioenergetic perturbations on the epigenome and transcriptome of aging human fibroblasts.[237] Together, these findings illustrate some mechanisms whereby intrinsic mtDNA-related and OxPhos inputs are transduced into epigenome-remodeling outputs.

However, one point that remains largely unclear is how MIPS-induced molecular and epigenetic modifications are temporally, spatially, and molecularly targeted, as well as their functional consequences on gene expression and cellular phenotypes.[226] Furthermore, this scientific challenge is compounded by the existence of multiple active TCA cycle enzymes directly in the nucleus.[238] The presence of mitochondrial enzymes in the nucleus, mostly documented to date in cancer cell lines, suggests that at least in some cell types, mitochondria may not be the only source of chromatin-modifying metabolites.

In recent years, other mitochondrial metabolites and molecular features have emerged as broad-acting intracellular signals. For example, the levels of TCA cycle metabolites succinate and fumarate are regulated by electron flux through the OxPhos system and more directly by the enzymes fumarate hydratase and succinate dehydrogenase (comprehensively reviewed in Martinez-Reyes and Chandel[216]). These metabolites are released in the cytoplasm, where they regulate signaling pathways involved in hypoxia sensing, immune activation, inflammation, and oncogenic transformation. TCA cycle metabolites also are enzymatically converted to metabolic derivatives such as itaconate and 2-hydroxyglutarate, among others. Itaconate is produced from the TCA cycle metabolite aconitate by aconitate decarboxylase and then acts either on intra-mitochondrial enzymes, for example by inhibiting succinate dehydrogenase,[239] or on transcription factors in the cytoplasm/nucleus, for example by inhibiting NF-κB signaling.[240] Two isomers of 2-hydroxyglutarate (2-HG) are produced from αKG by the mitochondrial or cytoplasmic malate dehydrogenases (MDH2, MDH1, respectively) in an NADH-dependent manner, and also promoted by acidic pH.[241] In the nucleus, 2-HG then inhibits the demethylation of histone tails and DNA by the ten-eleven translocation hydroxylases (TET1-3) and plays important roles in cell fate transitions that affect oncogenesis[242] and immune activation.[243] Besides soluble metabolites, larger mitochondrial lipids also play important signaling roles.[244] For example, the IMM lipid cardiolipin participates in a variety of cell signaling events, translocating to the OMM during stress and serving as a signaling platform relevant to mitophagy, apoptotic signaling, and other functions.[245]

In addition to TCA cycle flux, NADH/NAD^+ ratio, and pH, the presence of carrier proteins on the IMM can influence MIPS metabolite signaling. For example, in mesenchymal stem cells age-related changes in the citrate carrier expression regulate the cytoplasmic export of acetyl-CoA to drive histone acetylation levels, increase chromatin accessibility, and influence stem cell differentiation.[246] Thus, the nature and strength of mitochondrial outputs are likely regulated not only by rapidly changing fluxes through specific intra-mitochondrial metabolic pathways, but also by the relatively stable, albeit malleable, composition and abundance of IMM carriers and transporters.

Beyond the cell, metabolites also act in a cell-non-autonomous manner. A well-studied example is succinate, an obligatory mitochondrial TCA cycle intermediate that accumulates in equilibrium with the coenzyme Q redox state influenced by oxygen tension, $\Delta pH+\Delta\Psi_m$, and ATP demand.[247] Succinate has been reported to signal extracellularly and perhaps systemically through at least one cell surface GPCR, the succinate receptor 1 (SUCNR1), on immune and other cell types to regulate inflammatory processes.[248] On target immune (and possibly other) cell types, succinate may also be imported via the monocarboxylate transporter 1 (MCT1), where it acts intracellularly to inhibit TCA cycle activity and signal transduction pathways inhibiting interferon secretion.[249] Thus, metabolite outputs from the MIPS collectively have broad-acting cell-autonomous and cell-non-autonomous effects on the epigenome, nuclear gene expression, and cell behavior.

One other mitochondrial metabolite is worth special mention for its well-known role in circadian biology: melatonin (N-acetyl-*t*-methoxytryptamine). Melatonin is an evolutionarily ancient bacterial molecule preceding endosymbiosis that has strong antioxidant properties (reviewed in Reiter et al.[92]). Mitochondria not only contain the MT1 melatonin GPCR, but also synthesize melatonin from the amino acid L-tryptophan (with serotonin as an intermediate) via two enzymatic reactions catalyzed by enzymes in the mitochondrial matrix (arylalkylamine N-acetyltransferase [AANAT] and acetyl serotonin methyltransferase [ASMT]).[87] Like other mitochondrial metabolites, systemic melatonin concentration exhibits strong diurnal variation (almost undetectable during the day, peaking at night; e.g., Paul et al.[250]). It modulates sleep/wake cycles in some animals,[251] and its oral consumption in humans may modulate sleep onset.[252] Thus, mitochondria-derived melatonin potentially acts locally in an “automitocrine” and cell-autonomous manner, in a paracrine manner between cells/neurons, as well as systemically via the bloodstream,[253] illustrating the broad reach of MIPS-derived metabolites/hormones in mammalian physiology.

Together, mitochondria-derived metabolic outputs represent complementary signals that integrate and transduce the bioenergetic state of the MIPS into signals intelligible to core cellular signal transduction machinery that orchestrate a broad array of cellular and organismal behaviors.

Mitochondrial ROS signaling

ROS are diffusible molecules, particularly hydrogen peroxide (H_2O_2) produced from the dismutation of superoxide anion ($O_2^{\cdot-}$) by the matrix and IMS antioxidant systems. Mitochondrial ROS originate predominately from OxPhos complexes I and III[254] and travel to the cytoplasm and nucleus where they trigger redox-sensitive gene-regulatory processes.[197,255] Mitochondrial ROS signaling[215] and guidelines for their measurements[256] have previously been reviewed in detail, so here we mainly focus on recent developments in this area.

Mitochondrial ROS regulate various internal mitochondrial states and systemic signaling. For example, in brown adipose tissue mitochondrial ROS production post-translationally modifies UCP1 at Cys253 to increase uncoupling and enable thermoregulation, whereas pharmacological depletion of mitochondrial ROS with MitoQ prevented IMM uncoupling and heat production.[257] In the mitochondrial matrix of heme-synthesizing mitochondria in adipocytes, H_2O_2 oxidizes bilirubin to form biliverdin, which is exported from mitochondria by the ATP binding cassette (ABC) transporter ABCB10.[258] And in secretory pancreatic beta cells, glucose-

stimulated insulin secretion is similarly driven by H_2O_2 accumulation,[259] illustrating how mitochondrial ROS signals within the mitochondrion and intracellularly to trigger the release of systemic endocrine signals such as insulin.

Likely owing to the central role of oxygen in the evolution of aerobic creatures, mitochondria-derived ROS have broad effects on nuclear transcriptional regulation. In cultured cells, elevated ROS production secondary to respiratory chain dysfunction, or mimicked with the addition of the mitochondria-targeted redox cycling agent paraquat (MitoPQ), was sufficient to activate proteins of the mitogen-activated protein kinase (MAPK), including JNK signaling, which induces a secondary signal, namely nuclear chromatin release into the cytoplasm.[260] Similarly, eliciting high levels of temporally controlled ROS specifically in mitochondria using a chemoptogenetic tool elevated nuclear hydrogen peroxide levels and induced telomere damage.[261] In mice, silencing the mitochondrial matrix antioxidant enzyme manganese superoxide dismutase (MnSOD) during development showed that mitochondria-derived ROS activated the cytoplasmic/nuclear Nrf2 and PPARγ/PGC-1α pathway, leading to lasting adaptive hormetic responses that persist in adult animals.[262] Similar results were obtained in mice treated with low-dose rotenone (a complex I inhibitor that increases mitochondrial ROS emission) during embryonic and post-natal development, which altered nuclear DNA methylation and modified coat color.[263] In aging human fibroblasts, mitochondrial signaling via ROS is also necessary and sufficient to activate the Nf-kB pathway and senescence features, including the senescence-associated secretory profile (SASP).[264] In fact, experimentally depleting mitochondria from human fibroblasts by using a Parkin-overexpression/FCCP treatment prevented the acquisition of senescence characteristics,[265] providing compelling evidence that MIPS signaling—including but likely not limited to ROS—is required to trigger complex cellular states like senescence. Moreover, the SASP can propagate senescence phenotypes to neighboring bystander cells both *in vitro*[264] and *in vivo*,[266] illustrating one of many pathways whereby mitochondrial signaling propagates systemically in a cell-non-autonomous manner to influence organismal behavior and lifespan.[17,267]

Besides mito-nuclear signaling, ROS production by individual mitochondria also locally contributes to communication with the ER.[211] Even in distant neural arborizations, far from the nucleated cell body, mitochondrial ROS contribute to local synaptic activity.[268] In response to plasma membrane photodamage, mitochondria at the site of injury were also shown to respond in a DRP1-dependent manner by increasing repair-promoting ROS production.[269] Thus, the site-specific roles of mitochondrial ROS across sub-cellular locations illustrate the significance and potential specificity of localized ROS outputs from the MIPS as drivers of gene regulation and cellular functions.

Mitochondria synthesize sex and stress hormones

One of the most powerful types of mammalian hormones are steroid molecules, broadly categorized into three major classes: (1) the sex-defining testosterone, estrogens, and progestins produced in the gonads; (2) the stress hormones that promote stress adaptation via metabolic and salt balance regulation including glucocorticoids and mineralocorticoids produced in the adrenal glands; and (3) neurosteroids produced in the nervous system.[270,271] Their release is regulated by trophic pituitary hormones from the brain (adrenocorticotropic hormone, ACTH; follicular stimulatory hormone, FSH; and luteineizing, LH) mediated by GPCR-coupled cyclic AMP-

protein kinase A (cAMP-PKA) or Ca^{2+}-PKC signaling in steroid-producing cells.[208] In steroidogenic tissues, the rate-limiting step to synthesize all steroid hormones takes place within mitochondria.

Mitochondria produce steroid hormones from cholesterol, the initial substrate to all steroids. The import of cholesterol through the OMM and IMM requires microtubule and microfilament dynamics as well as protein synthesis[272] and is accomplished by the steroidogenic acute regulatory protein (StAR, from the *STARD1* gene) in the OMM.[273] Whereas mitochondrial import of StAR through the TIM/TOMM translocator complex leads to its proteolytic degradation, stabilization of StAR at the OMM,[274] in association with Tom22 and VDAC2,[275,276] delivers cholesterol to the matrix-facing IMM side chain cleavage enzyme cytochrome P450 (CYP450scc) protein. CYP450scc then catalyzes the rate-limiting reaction for steroidogenesis, which convert cholesterol into pregnanolone, the common precursor to all steroid hormones.[33] Pregnanolone synthesized in the matrix is then exported to the ER where other enzymes sequentially catalyze its transformation into progesterone and other steroid intermediates.[208] In steroidogenic mitochondria from the adrenal cortex zona fasciculata cells, the downstream steroid intermediate returns to the mitochondrial matrix, possibly through the MAM, where the terminal reaction is catalyzed by the mitochondrial matrix enzyme 11β-hydroxylase (11βH, also "mitochondrial cytochrome P450 11B1" encoded by *CYP11B1* in humans) that produces cortisol.[277] Mitochondrial synthesis of systemically acting steroids occurs rapidly within minutes, and its synthesis arrest is equally rapid.[208] The rapid, redox-sensitive, protein import-dependent regulation of this process illustrates how multiple intrinsic factors can influence mitochondrial steroidogenic outputs.

The evolutionary basis for positioning steroidogenesis in mitochondria remains uncertain but may have involved the uniquely reducing conditions of the mitochondrial matrix.[278] The conversion of cholesterol to pregnanolone by P450scc requires the reductive action of 3 high-energy NADPH molecules. As a result, the loss of the matrix-facing NADPH-generating enzyme nicotinamide nucleotide transhydrogenase (NNT) inhibits steroidogenesis, causing hypocortisolemia in mice and humans.[279] Developmentally, steroid hormones drive energetically expensive transcriptional and physiological programs that must incur substantial cellular energetic costs in target tissues. As a result, it is possible that to optimize fitness, these hormones should only be produced in proportion with the energetic capacity of target tissues. Assuming that the function of mitochondria is partially harmonized across both source steroidogenic and target catabolic energy-consuming tissues, we postulate that the mitochondrial localization of steroidogenesis enzymes may reflect the product of system-level adaptation aiming to couple mitochondrial bioenergetic capacity and steroid hormone signaling across the organism.

Mitochondrial genome signaling: Intracellularly

The circular mtDNA is typically contained in the mitochondrial matrix, insulated from the cytoplasm by two membranes. However, the enclosure of mtDNA within the mitochondrial IMM and OMM is naturally disrupted under certain physiological conditions. This includes mtDNA instability caused by the partial loss of the mtDNA-associated protein TFAM, which triggers mtDNA-dependent antiviral gene expression programs in the nucleus.[22] mtDNA release is a relevant signaling mechanism because both the cytoplasm and the extracellular surface of immune and non-immune cells harbor DNA sensors that recognize mtDNA fragments as a

damage-associated molecular pattern (DAMP).[280] DNA (viral, bacterial, and mtDNA) is sensed by multiple innate immune receptors including cGAS (cyclic GMP-AMP synthase), TLR9 (toll-like receptor 9), and the NLRP3 (NOD-, LRR-, and pyrin domain-containing protein 3) and AIM2 (absent in melanoma) inflammasomes. Sensing of mtDNA triggers signaling cascades that either converge on cytokine- and interferon-producing transcription factors including IRF3/7, MAPK, and NF-κB or engage Caspase-1 for processing and secretion of IL-1β and IL-18.[281] The cytosolic release of mitochondrial double-stranded RNA (mt-dsRNA) can also act as a DAMP and is detected by the RIG-I-like (RLR) receptors RIG-I and MDA5. Once engaged, these sensors translocate to mitochondria and activate the mitochondrial antiviral signaling protein (MAVS), which assembles as filaments on the mitochondrial surface[282] in a membrane potential-dependent manner to act as an antiviral signaling platform.[283,284]

Current thinking around innate immune signaling suggests that the mitochondrial network is both a source of stimulatory ligands and acts as the major signaling hub for the four major pattern recognition receptor families (TLRs, NOD, RLRs, and cytosolic DNA sensors [CDSs]).[285] Most of the effects of both exogenous (bacterial, viral) nucleic acids and endogenous mtDNA/mtRNA signaling are likely mediated via these pathways. As an example of mitochondrial signal transduction, when mitochondria in human fibroblasts and cancer cells detect the genotoxic agent doxorubicin, mtDNA damage (sensing) eventually leads to the cytoplasmic release of mtDNA fragments (signaling), which trigger nuclear DNA repair mechanisms in the nucleus and cGAS-STING-dependent activation of interferon-stimulated gene (ISG) expression.[147]

Regarding the mechanism(s) responsible for facilitating mtDNA extrusion into the cytoplasm, two molecular pathways have been described. One mechanism tested in mouse embryonic fibroblasts and mice with lupus-like disease involves VDAC oligomerization in the OMM, stabilized by short mtDNA fragments, forming a large-scale pore that enables the cytoplasmic extrusion of 100- to 400-bp-long mtDNA fragments.[286] Similarly, in bone marrow-derived macrophages 500- to 650-bp-long mtDNA fragments are cleaved from the circular genome by the mitochondrial protein flap-structure-specific endonuclease 1 (FEN1) and released in a VDAC-dependent manner into the cytoplasm where it activates the inflammasome and cGAS-STING signaling.[287] The other described mechanism of cytoplasmic mtDNA extrusion consists of BAX/BAK-mediated pore formation in the OMM, followed by herniation of the IMM at the surface of mitochondria during apoptosis.[288] Under conditions of genotoxic stress, BAX/BAK-mediated herniation also appears to release ds-mtRNAs to activate ISGs in the nucleus.[289,290] A third non-specific mechanism may involve the rupture of mitochondrial membranes, possibly secondary to swelling, which, for example, may occur in skeletal muscle of patients with primary mtDNA mutations.[291]

Another, more permanent way in which the mitochondrial genome can carry information to the nucleus is via the translocation of mtDNA segments to the nucleus followed by their insertion within the coding sequence as nuclear mtDNA insertions (NUMTs, pronounced "*nu-mites*").[292] This process, termed "numtogenesis," has traditionally been understood as horizontal gene transfer, having occurred multiple times during the evolution of single-celled and multicellular organisms.[293,294] As a result, multiple germline NUMTs are shared across individuals. In the case of mitochondria, mtDNA gene transfer is also likely to explain how the majority of the genes from the original proteobacterium's genome have migrated to the nucleus such that >98% of the mitochondrial proteome is now encoded in the nucleus.[295]

But the transfer of mtDNA sequences to the nucleus may also occur over a cell's lifespan. In yeast, mitochondria lacking the mitochondrial protease Yme1 (yeast mtDNA escape 1), a member of the AAA family of ATPase that degrades IMS/IMM proteins to regulate mitochondrial cristae dynamics,[296] produce 77-fold more mito-nuclear transfer of NUMTs along with a 50% reduction in lifespan.[297] Similarly, in cancerous mammalian cells, mitochondria without the human homolog YME1L1 generate ~4-fold more NUMTs, recapitulating the abnormally elevated number of NUMTs in ovarian tumors[298] and other cancer types.[299] Numtogenesis may also occur at a steady rate over days to weeks in healthy replicating primary human fibroblasts *in vitro*, and over a person's lifespan in brain tissue (unpublished data). Whether the effects of NUMTs on nuclear genome instability and cellular aging is a bona fide, regulated form of MIPS signaling remains to be established.

Mitochondrial genome signaling as extracellular, cell-free mtDNA

mtDNA copies are often well in excess of the number of copies required to transcriptionally sustain OxPhos.[300] An emerging notion suggested by Shadel et al. is that the mtDNA molecules do not only supply RNA and OxPhos subunits but in fact exist as sentinels of genotoxic stress and other insults.[147] This suggests that the hundreds of mtDNA genomes in each cell may represent a pool of signaling molecules—in the same way the neurotransmitters are produced and stored in presynaptic boutons, awaiting release.

Beyond mtDNA detected in the cytoplasm and nucleus, a substantial amount of circulating cell-free mtDNA (cf-mtDNA; as well as nuclear DNA, cf-nDNA) is released extracellularly, detectable in various biofluids from healthy individuals (reviewed in Trumpff et al.[301]). In blood (serum or plasma, which contain different cf-mtDNA levels[302]) and cerebrospinal fluid, cf-mtDNA is elevated in some although not all individuals with primary OxPhos defects,[303,304,305] during pregnancy,[306] after physiological stress such as exercise,[307] minutes after acute psychological stress,[307,308] and hours to days after intensely stressful life events,[309] highlighting the dynamic release of cf-mtDNA. In saliva, cf-mtDNA also increases several-fold during the morning sleep-wake transition.[310] Notably, in critically ill individuals cf-mtDNA levels are also dramatically elevated, and cf-mtDNA abundance (copies per mL) is a strong predictor of mortality,[311] highlighting the potential physiological significance of cf-mtDNA in humans.

Because the majority of the initial work on cf-mtDNA was conducted in the context of sepsis and inflammatory disorders, and given that the molecular features of the mitochondrial genome and associated proteins are bacterial in origin, the pro-inflammatory aspects of cf-mtDNA signaling have been emphasized.[312] The role of mitochondrial signaling in the control of inflammation has been expertly reviewed elsewhere[285] and leaves little doubt that intracellularly, cf-mtDNA is immunogenic.

However, in relation to extracellular cf-mtDNA in biofluids, emerging evidence suggests that (1) the majority of blood and saliva circulating cf-mtDNA in human plasma may not be naked (required to be accessible to DNA receptors) but rather contained within sedimentable cargo, possibly as circulating whole mitochondria,[310,313,314] and (2) cf-mtDNA is abundant in healthy individuals who do not show signs of systemic inflammation. Therefore, a critical re-appraisal of the evidence reveals that by itself, circulating cf-mtDNA in its physiological forms in human blood is unlikely pro-inflammatory.[301] Cf-mtDNA levels in blood, cerebrospinal fluid,[315] and

saliva[310] also do not consistently correlate with inflammatory markers. The physiological role of cf-mtDNA in general remains unclear. Technically, how mtDNA fragments are physiologically released from the matrix to the cytoplasm, into the extracellular space, and into biofluids also remains to be established.

Together, these findings highlight the influence of mtDNA signaling beyond autocrine/cytoplasmic mito-nuclear signaling. Emerging work in multiple biofluids implicates paracrine (cell-to-cell) and potential endocrine (systemic) roles of cf-mtDNA signaling among the repertoire of signaling mechanisms available to transduce information from the MIPS to the organism.

Non-apoptotic nuclear-encoded proteins sequestered in mitochondria

A different class of mitochondrial outputs includes a group of nuclear-encoded proteins that are normally imported and degraded by functional energized mitochondria but fail to be imported when mitochondria are de-energized (i.e., depolarized). In non-mammalian systems and cultured cells, stress conditions that induce mitochondrial depolarization inhibit protein uptake and cause their accumulation in the cytoplasm where they act as transcription factors.[27] Based on initial studies using unfolded protein stress in the mitochondrial matrix,[316] this response was coined the mitochondrial unfolded protein response (mtUPR). The mtUPR involves close physical contact and functional interactions between mitochondria and the ER.[317]

Known pathways involving nuclear-encoded proteins include ATFS-1 (activating transcription factor associated with stress-1, in *C. elegans*),[19] GPS2 (G-protein pathway suppressor 2, in mammalian cells),[20] and DELE1 (DAP3-binding cell death enhancer 1, in mammalian cells).[318,319] In an OMA1 protease-dependent manner, the mitochondrial network acts as an active sink that normally shunts these proteins and prevents their interactions with nuclear transcription factors including EIF2α.[318,319] Via these proteins, mitochondrial depolarization promotes ATF4 and ATF5 expression, the master regulators of the mtUPR.[320,321] Interestingly, inhibiting mitochondrial translation interferes with cytoplasmic translation and triggers ATF4/ATF5-dependent signaling, marking the interconnectedness of intra-mitochondrial and cytoplasmic protein homeostasis.[322] The ATF4/ATF5 transcription factors overlap with those of the mitochondrial ISR (ISRmt) well defined in mammals. However, in cultured human cells at least, different mitochondrial perturbations selectively induce the mtUPR and ISRmt in a relatively mutually exclusive manner.[323] This result suggests that the mtUPR and ISRmt stress response pathways have either evolved separately or diverged in their specificity, highlighting the existence of at least two well-defined nuclear transcriptional programs induced by MIPS signaling in mammals.

Systemic mitochondrial signaling via the nucleus

MIPS signaling induces nuclear programs that remodel catabolic and anabolic biosynthetic pathways within the cell, and also shapes metabolism systemically. In mammalian models, intrinsic mtDNA transcriptional and translational defects,[16,115,324] inhibition of autophagy,[325] IMM uncoupling,[326] and both pharmacological and genetic OxPhos defects[236,327] are transduced to the nucleus via mechanisms that at least in part involve mitochondria-derived signals inducing the

ATF4- and ATF5-regulated ISRmt. In cultured human cells, loss of hundreds of nuclear-encoded mitochondrial genes, although not all, selectively triggers the ISRmt.[323]

In animals, the ISRmt produces two main nuclear-encoded systemic signals: fibroblast growth factor 21 (FGF21) and growth differentiation factor 15 (GDF15)—two proteins with overlapping but distinct systemic metabolic effects.[328] In mouse models with molecular alterations in skeletal muscle mitochondria, the muscle-derived FGF21 protein travels to distant tissues where it is necessary for some tissue-specific effects such as white adipose tissue browning[329] and glucose uptake and mitochondrial biogenesis in the dorsal hippocampus.[18] However, FGF21 is dispensable for other systemic effects such as glucose tolerance, insulin resistance, anorexia, and weight regulation.[329,330,331] The other well-studied metabokine GDF15 is most highly expressed in secretory tissues (syncytiotrophoblasts, epithelial cells, and glandular cells; https://www.proteinatlas.org/) and has wide-ranging systemic effects linking mitochondrial OxPhos dysfunction, metabolism, and inflammation.[332] Mitochondrial translation defects (Crif1KO) in skeletal muscle[330] or in adipocytes,[333] or chronic skeletal muscle mitochondrial uncoupling (uncoupling protein 1 [UCP1] overexpression),[334] induce both FGF21 and GDF15 secretion from the affected tissues, where GDF15 is required to increase systemic energy expenditure and other behavioral and physiological recalibrations.

Consistent with the functional interplay of the MIPS and the organism, ISRmt signaling occurs at least in part via a periphery-to-brain signaling axis. Mice and humans express the receptor for GDF15 GFRAL most highly in brain tissue (e.g., Mullican et al.[335]), but GFRAL may be expressed in many tissues at low levels (https://www.proteinatlas.org/) and is stress inducible in other cell types including macrophages.[336] Therefore, GDF15-GFRAL signaling provides a mechanism whereby mitochondrial outputs from peripheral tissues use the brain—an organismal integration center—to transduce the functional state of a tissue's mitochondria to regulate systemic metabolism.[337,338] Adding to this systemic signaling picture, in mice GDF15 signaling upregulates hypothalamic corticotropin-releasing hormone (CRH)[339] and activates the downstream HPA axis and secretion of corticosterone, a mitochondria-derived hormone released in response to psychosocial stress.[340] Consistent with the production of metabokines in response to intra-mitochondrial defects converging on OxPhos capacity, FGF21 and GDF15 are circulating biomarkers of subgroups of mitochondrial diseases in adults and children.[113,305,341,342,343]

Thus, the secreted nuclear-encoded metabokines FGF21 and GDF15 convey information about the state of the MIPS in one tissue/organ to the whole organism. However, the contributions of these stress-induced, nuclear-encoded mitochondrial signaling outputs to the maintenance of human health or to disease progression remain only partially explored.

Mitochondria-derived peptides

The discovery of alternative open reading frames (ORFs) within the mtDNA sequence led to the identification of MDPs released within the cell systemic circulation (for a comprehensive review, see Reynolds et al.[344]). Eight MDPs have been reported: Humanin, a 24-amino-acid peptide encoded within the 16S rRNA gene initially discovered to have neuroprotective effects in neuronal cultures[345] and subsequently linked to longevity across invertebrates, small mammals, and humans;[346] 6 small humanin-like peptides (SHLP1–6) that functionally overlap with humanin;[347] and MOTS-c (mitochondrial ORF within the twelve S rRNA type-c), a 16-amino-acid peptide initially identified to promote insulin sensitivity and prevent age-related insulin

resistance in mice.[348] When the mtDNA is selectively depleted with chronic ethidium bromide treatment, or mtDNA transcription is selectively inhibited with actinonin, the expression of MDPs is lost, confirming their origin in the mitochondrial genome.[348] However, where MPDs are transcribed and translated (mitochondrial matrix or cytoplasm) remains uncertain.

Functionally, once in the cytoplasm, MOTS-c translocates to the nucleus in an AMP-activated protein kinase (AMPK)-dependent manner, where it regulates stress-induced gene expression and promotes cell survival.[21] In mice, MOTS-c and Humanin are also found in blood and act in a cell-non-autonomous manner to apparently regulate systemic metabolism.[349] In humans, like other mitochondrial outputs, MOTS-c[350] and Humanin[351] levels increase dynamically in skeletal muscle and in circulation upon exercise. Thus, in addition to nDNA-encoded metabokine proteins FGF21 and GDF15, mitochondria release mtDNA-encoded peptides that act as both intracellular and systemic signaling mediators. The range of physiological functions for MDPs is only beginning to be uncovered, but MOTS-c may increase running capacity (i.e., endurance) in mice and improve resilience to metabolic starvation in cultured myotubes.[350] Other mitochondrial resident proteins, including heat shock protein 60 (HSP60)[352] and TFAM,[353,354] have been identified in blood, suggesting that several canonical mitochondrial proteins are released systemically by the MIPS where they have metabolic, inflammatory, or other systemic signaling roles.

Mitochondrial heat signaling and thermodynamic gradients

Temperature is a powerful effector of biological change. Without heat, biological processes do not proceed. For instance, growth and degradation are greatly reduced at 4°C, whereas optimal temperatures accelerate enzyme kinetics, membrane fluidity, and organismal development.[355] Therefore, the diffusion of heat and the ensuing changes in biochemical activities represent a form of signaling, where information about the state of an organelle is transferred from one sub-cellular compartment to another. Because—according to the second law of thermodynamics—the flow of heat always proceeds from warmer to colder locations, the flow of information also must preferentially (although not exclusively) occur from warmer to colder structures.

Among the cell and the organism, mitochondria are the warmest compartment and the major heat source. Body temperature in endotherms is primarily derived from respiratory chain activity.[356] Exemplary of this phenomenon, mitochondria in brown adipocytes express high levels of UCP1 that increases proton leak across the IMM, accelerating upstream heat-producing biochemical reactions in a Ca^{2+}-dependent manner.[357] Using temperature-sensitive fluorescent probes, initial studies found that the warmest cellular compartments in cultured cells were the nucleus (which is surrounded by perinuclear mitochondria) and mitochondria.[358] Uncoupling of OxPhos with the uncoupler FCCP increases mitochondrial matrix temperature by 6°C–9°C, as would be expected from relieving the electrochemical energy gradient across the IMM and subsequent cascading acceleration of biochemical reactions upstream from the OxPhos system.[359] Accordingly, the biochemical activity of mammalian mitochondrial respiratory chain enzymes was found to be maximal around 50°C.[360] Consistent with this finding, refined live-cell imaging with mitochondria-targeted temperature-sensitive probe showed that mitochondria function at internal temperatures around 50°C, well above the core body temperature of 37°C,[360] suggesting that the MIPS radiates heat-based signals into the cell. Thus, the temperature

gradient between mitochondria (warmest compartment) and other sub-cellular structures likely provides mitochondria with a thermodynamically privileged position in signal transduction.

Sub-cellular mitochondrial localization

The sub-cellular positioning of cellular structures influences their functions and ability to signal to other organelles. Within the cytoplasm, the MIPS is topologically positioned at the interface between the naturally inert nuclear genome and the dynamic extracellular environment. In many cell types, mitochondria directly contact or hover only hundreds of nanometers away from the nucleus. At the nuclear surface, diffusible mitochondrial signals can travel through nuclear pores to reach the nucleoprotein complex of the chromatin.[361] To travel 1 μm—from the mitochondrial IMS to the chromatin—the theoretical isotropic diffusion time for a small 40 kDa protein is 0.02 s,[362] whereas small metabolites like ATP[363] or amino acids[364] travel ~20–100 times faster, closing the 1 μm gap in less than 1 ms. Physical proximity, particularly at high temperature, favors rapid communication.

The position of the mitochondrial network within the cytoplasm can influence signaling behavior. In response to stressors such as hypoxia in cultured endothelial cells, mitochondria redistribute and cluster around the nucleus within <3 h where they promote a pro-oxidant intranuclear state.[197] Inhibiting mitochondrial motility with the microtubule depolymerizing agent nocodazole or dynein knockdown effectively prevents perinuclear clustering.[197] In this case, the reduced physical proximity appeared to decrease the potency of mito-nuclear signaling, hindering HIF-1α binding to the nDNA hypoxia response element nucleotide sequence. The formation of physical contact sites between mitochondria and the nuclear envelope by the OMM-based translocator protein (TSPO) also enables cholesterol redistribution to the nucleus and initiates pro-survival nuclear transcriptional programs that are blunted without mito-nuclear proximity,[255] highlighting the influence of proximity and physical interactions in mito-nuclear signaling.

Mitochondrial positioning also shapes cell behavior away from the nucleus. In developing neurons, mitochondrial positioning at specific locations along axons determines the location of branch points.[365] In ganglion cell dendrites of the retina, mitochondria positioning at terminal branch points and presynaptic sites also stabilizes mature dendritic structures.[366] In neurons, both within presynaptic boutons[31] and at specific locations near dendritic synapses, mitochondria contribute both to local ATP synthesis and Ca^{2+} handling, locally influencing neurotransmitter release and, as a direct result, cell-cell communication.[367] Thus, the regulated topological positioning of mitochondria within the cell can minimize diffusion distances and likely optimize the potency and/or nature of MIPS outputs, illustrating how mitochondrial positioning guides signaling and various cellular functions.

Summary of mitochondrial signaling

In addition to their elaborate sensing (step 1) and networking (step 2) capabilities, mitochondria also possess a wide array of signaling (step 3) mechanisms that transduce mitochondrial states to the cell and organism. The nature of these signals includes ions, metabolites, chemical species (e.g., ROS), DNA, and proteins. These outputs carry—possibly with a fairly high degree of specificity based on their circumstantial combinations—information about various aspects of

mitochondrial biology to the cell nucleus and other organelles. At specific sub-cellular locations and in specific cell types, adaptive mitochondrial signals are transformed into transcriptional, cellular, and humoral physiological responses that inform and influence organismal functions. Less specific factors, including temperature and physical distances, may modulate the potency of these signals. Emerging evidence also suggest that systemic MIPS outputs may include mitochondria-derived vesicles (MDVs),[368] extracellular vesicles with mitochondrial cargo,[369,370] and even whole mitochondria[314] that travel from source cells/tissues to functionally impact distant target organ systems. Finally, the description of overlapping molecular connections between mitochondria and target nuclear genetic programs, such as the mtUPR and ISRmt, emphasizes the evolved sensitivity of the mammalian genome to MIPS outputs. Notably, several mitochondrial outputs reach the bloodstream, the biofluid that metabolically connects all cells and organs, giving systemic organismal access to MIPS signaling.

Tissue specificity in mitochondrial functions and behaviors

Although we have so far considered mitochondria as a more-or-less uniform family of organelles, mitochondria are not all created equal. From their shared origin in the oocyte,[371] mitochondria undergo profound specialization as different cell types and tissues mature during embryonic development. This gives rise to somatic mitochondria that differ in their protein composition[372,373] and functions (respiratory properties, ROS production, PTP sensitivity, β-oxidation capacity).[374] These developmentally acquired characteristics represent tissue-specific mitochondrial phenotypes. Analogous to functionally and molecularly distinct cell types, there are functionally and molecularly distinct mitochondrial types, or "mitotypes."[375]

Different tissues and cell types contain markedly different mitotypes that likely influence MIPS signal transduction. For example, cardiomyocyte mitotypes in the heart are optimized for ATP synthesis, adrenal cortex mitotypes specialize for steroidogenesis, and liver mitotypes specialize for ketogenesis, serine metabolism, and anaplerosis. Even within a given organ, neighboring cell types can acquire distinct mitotypes. For example, mitochondria from adjacent oxidative versus glycolytic skeletal muscle fiber types acquire vastly different proteomes that match their functional specialization.[376] Likewise, circulating human immune cell subtypes (B cells, naive or activated T cells, monocytes, neutrophils, etc.) exhibit markedly different OxPhos profiles and mtDNA copies per cell.[375] And in the mouse brain, mitochondria exhibit regional[377] as well cell-type-specific functional and molecular diversity.[373] These divergent cell-type-specific mitochondrial features, along with cell-specific metabolic requirements, may explain why in mice spongiform neurodegeneration is caused by the loss of mtDNA specifically in astrocytes but not in neurons, for example.[378] In mitochondrial disease, large intracellular and cell-to-cell heterogeneity in mitochondrial phenotypes also develops as mutant mitochondria proliferate,[379] such that adjacent muscle fibers can show different stages or even opposite responses to OxPhos defects.[380]

Diverse mitotypes also populate different sub-cellular compartments within individual cells.[201] In neurons, the cell body (i.e., soma) and synaptic boutons have remarkably different mitochondrial proteomes.[381] Similarly, muscle fibers contain two mitotype sub-populations (subsarcolemmal [SS] and intermyofibfillar [IMF]) with quantitatively distinct proteomes.[382] Adipocytes also are populated by at least two main mitotypes: mitochondria proximal to lipid droplets (i.e., peridroplet, or PDMs) and mitochondria not in immediate contact with lipid droplets.[383] These

two adipocyte-specific mitotypes exhibit distinct bioenergetic, proteomic, and fusion dynamics. Thus, the organism is composed of a wide spectrum of molecularly and functionally specialized mitotypes.

Relevance of mitochondrial functional specialization to sensing, integration, and signaling

Mitochondrial sensing (MIPS step 1): in multicellular organisms, individual cell types express a narrow set of cell-type-specific receptors and are therefore sensitive to a narrow set of inputs. For example, the sensory organs in animals exhibit specific sensitivities to a narrow set of inputs: the eyes sense light but do not perceive sound nor taste, and neither the inner ear nor the tongue respond to light. Each set of neurons within sense organs specifically responds to select inputs. Similarly, the expression levels of dozens of mitochondrial genes and proteins[35,384] including mitochondrial sensory components—transporters, receptors, enzymes—are relatively specialized across both mouse and human tissues (A.S. Monzel, personal communication). The functional specialization of mitotypes across tissues and cell types may thus produce unique mitochondrial sensory systems tailored for specific inputs in different cell types.

Mitochondrial signal integration (MIPS step 2): several aspects of mitochondrial morphology, dynamics, and motility vary between tissues and cell types.[201] In human and mouse skeletal muscle, SS/perinuclear mitotypes are spheroids whereas IMF mitotypes that intersperse sarcomeres have a branched, elongated morphology.[170] In neurons, despite sharing a continuous cytoplasm, somatic mitochondria form a partially connected network surround the cell nucleus, elongated branched dendritic mitochondria extend for tens of microns, whereas axonal and synaptic mitochondria are mostly punctate.[385] In relation to motility, skeletal muscle mitochondria are remarkably stationary[180] compared to neuron axonal and dendritic mitochondria that exhibit greater motility.[386] From first principles, these profound differences in the morphology, topology, and dynamic properties of the MIPS predict that mitochondrial information transfer, integration, and computation differ between tissues and cell types. Although currently technically challenging, improving imaging (e.g., Wolf et al.[387]) and experimental (e.g., Berry et al.[388]) technologies combining spatial and temporal resolution should eventually allow us to map and empirically manipulate information flow through mitochondrial networks.

Mitochondrial signaling (MIPS step 3): tissue-specific mitotypes influence both the nature and magnitude of MIPS outputs and cellular responses. For example, susceptibility to PTP opening, Ca^{2+} buffering capacity, and ROS emission characteristics differ remarkably between glycolytic and oxidative skeletal muscle mitotypes.[374] This has implications for inter-organelle crosstalk. The ISRmt response also is induced cell-specifically; proliferating myoblasts and myotubes exhibit different ISRmt responses to the same mitochondrial perturbations.[327] In the mouse brain, progressive mtDNA depletion in Twinkle-KO astrocytes but not neurons induces the ISRmt.[378,389] Mitochondrial activation of the ISRmt and its interaction with other pathways, such as the mTORC1, is also tissue-specific.[115,380,389,390] Thus, MIPS signaling as well as the cellular responses to MIPS signals both differ between cell types and tissues. Our current understanding of how mitotypes from different tissues differentially signal intracellularly and systemically is in its infancy.

Outstanding questions

To understand how mitochondria contribute to organismal health and disease, several important challenges remain. As reviewed above, the MIPS performs several functions that ensure rapid cellular and systemic responses commensurate with the energetic and biochemical state of the organism. As a result, mitochondria contribute to healthy cellular and physiological adaptation. Clinically, it is clear that mitochondrial diseases involve primary genetic defects affecting molecular processes other than the OxPhos machinery (i.e., not all mitochondrial diseases are disorders of ATP deficiency).[391] Certain tissues and organs also specifically become affected, whereas others are relatively spared.[392] How do non-energetic mitochondrial functions influence health and disease?

The three-step mitochondrial signal transduction framework described here raises several questions, some of which are listed below. Providing answers to these and other emerging questions would advance our understanding of the instructive role that the mitochondria play in human health. Because tissue-specific mitochondrial phenotypes (i.e., mitotypes) are the integrators of cell, tissue, and organismal metabolic inputs, and because MIPS outputs modulate not only a large fraction of the human genome but also complex animal behaviors, the following questions broadly concern the biological and biomedical sciences.

- Are defects in the sensing, integration, and signaling functions of the MIPS sufficient to perturb physiological adaptation in the organism, leading to disease? Communication between cells is essential to maintaining organismal integrity, and perturbing communication alone is sufficient to cause health disorders.[393,394] For example, impaired mitochondrial fusion (and/or inter-organellar interactions) causes human disease.[395,396] Is impaired mitochondrial signal transduction—in the absence of OxPhos defects—a cause of metabolic and other types of health disorders?
- How are specific mitochondrial functional impairments communicated to the cell? Different molecular defects converging on downstream OxPhos deficiency can cause different gene-regulatory signals,[323] cellular responses,[23] and disease manifestations.[140] In general, critical biological processes tend to exhibit redundancy (several effectors exist to sense or communicate the same inputs), which, coupled to a diversity of downstream interacting genetic programs (e.g., innate immunity, ISRmt, mtUPR), affords a diversity of potential cellular and organismal responses. Are MIPS output signals, or combinations thereof, cell- or tissue-specific? What determines the exact transcriptional responses they elicit?
- How generalizable or species-specific are mitochondrial signal transduction mechanisms? Biological mechanisms and therapeutic processes in rodents and invertebrates often align only partially with humans,[397,398] and important differences also exist between mouse strains,[399] for example. Furthermore, different cell types harboring distinct mitotypes may exhibit different responses to metabolic stressors.[380] Systematic exploration of human health and disease states, as well as experimental models for specific molecular features that mimic as closely as possible human physiology or pathology, will increase the likelihood that our findings in model systems will be of biologic, diagnostic, or therapeutic value in humans.

Did the role of mitochondria as an information processing system contribute to the evolutionary turning point of endosymbiosis? Argument accounting for the role of mitochondria as a harbinger of multicellular, complex life includes the protection from oxygen[400] and a rise in energy supply,[401] although these possibilities have been challenged.[402] Communication and information exchange via optimized biological structures—epitomized at the scale of the organism by the nervous system[361]—afforded an unprecedented acceleration and complexification of social behaviors among animals. This raises the possibility that the acquired ability of cells to sense their environment, efficiently transduce information, and communicate with each other via the MIPS may have been a decisive factor in the evolution and diversification of multicellular life.

Summary

The past decades of mitochondrial research have produced remarkable advances in our knowledge of how mitochondria function and behave within the cell. More recently, accumulating evidence revealed how mitochondria communicate extensively with other organelles, between cells, and even across organ systems. Integrating these notions under a common framework suggests that a central role of mitochondria is to transduce information, functioning as a distributed information processing system. The most advanced known form of signal transduction occurs in the brain, which efficiently integrates sensory inputs to develop precise internal representations of the outside world, and secondarily deploys optimal organismal responses and behaviors that promote adaptation and survival. We propose that mitochondria perform a similar, albeit more primitive, form of signal transduction. The MIPS integrates the constant flow of molecular and non-molecular inputs about the energetic and metabolic states of the system, and secondarily deploys in collaboration with the nucleus an array of outputs that guide cellular and organismal adaptation (Figure 7).

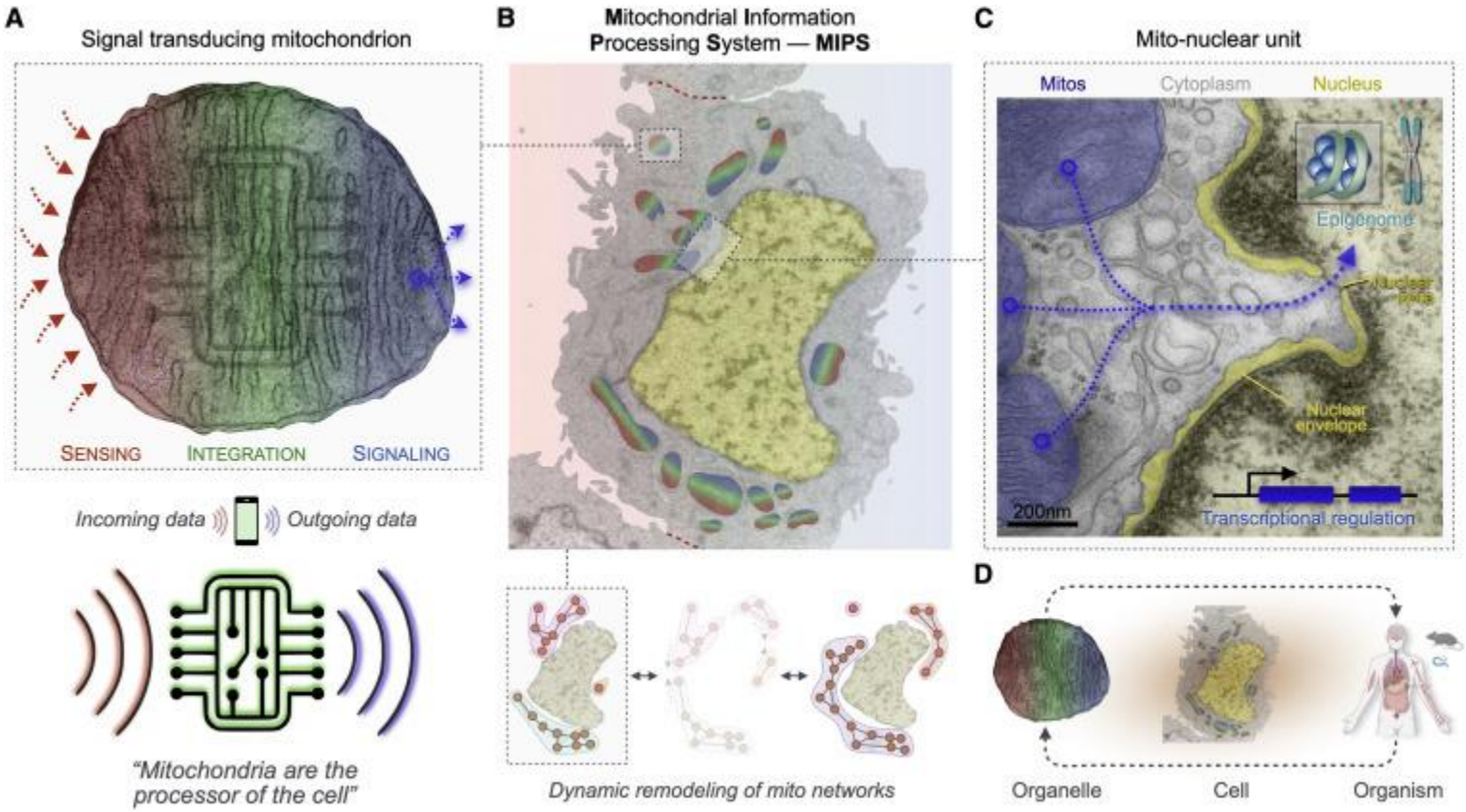

Figure 7 Core MIPS components for mitochondrial signal transduction

Show full captionFigure viewer

The mitochondrial signal transduction framework highlights how mitochondria simultaneously contribute central roles to energy transformation and biosynthesis, as well as to signal transduction. This framework also helps to situate our increasingly precise, mechanistic, and reductionistic investigations of mitochondrial features, activities, functions, and behaviors within the context of the organism and its environment. The view of mitochondria as a distributed information processing system—or as a "portal" positioned at the interface of the outside environment and the inner world of the cell's (epi)genome—integrates all historical domains of mitochondrial biology. As a result, the mitochondrial signal transduction framework emphasizes the need for knowledge integration across sub-fields of mitochondrial science. This also highlights the many ways in which multiple domains of mitochondrial biology beyond energetics may be linked to organismal health.

Improving human health is the shared goal of the biomedical community. This collective effort involves building increasingly accurate theories, models, and testable hypotheses about the processes that not only falter in advanced stages of diseases, but also those that enable optimal adaptation so that health is achieved. Health is the ability to deploy optimal responses to challenges.[55] Organismal health emerges from the functional interconnections and crosstalk between cellular and physiological systems, behaviors, and psychosocial states that regulate biology, and vice versa.[403,404,405,406] As we begin to map the basis of health beyond the absence of disease,[394,407] it appears crucial to mechanistically decipher two prominent forces related to mitochondria. The first is energy, which brings otherwise inert genes to life and powers the

functions of cells and organs. The second is communication or signal transduction, which connects and thus turns parts into wholes. Signal transduction turns cells into cell collectives and binds organs together as an organism. The organism—not the cell—is the ultimate evolutionary unit upon which selection pressures act and where health manifests.

Therefore, articulating the role of multifaceted mitochondria in signal transduction across the organism can help us achieve our shared goal of improving human health in three main ways: (1) by broadening and prioritizing the health-relevant mitochondrial biology questions to test, (2) by selecting the ideal human study design or animal model systems in which to address them, and (3) by connecting more effectively new molecular, cellular, and physiological discoveries in mitochondrial biology to human health.

Acknowledgments

The authors are grateful to Anu Suomalainen for extensive input to this manuscript; Jodi Nunnari and Vamsi Mootha for discussions and Phillip West for edits that helped shape parts of this review; Mary Elizabeth Sutherland, Eugene Mosharov, Guy Las, Daniel Dagan, Mario Ost, Alex Junker, Otto Kalliokoski, Robert Taylor, Stavros Fanourakis, and Gilles Gouspillou for comments, suggestions, or edits; and members of the Mitochondrial Psychobiology Laboratory for stimulating discussions. The authors' work was supported by NIH grants R35GM119793, R01MH119336, R01MH122706, R01AG066828, and R21MH123927 and the Baszucki Brain Research Fund to M.P.

Biophotons as Subtle Energy Carriers

TM Srinivasan [1]

PMCID: PMC5433113 PMID: 28546674

Introduction

Subtle energy research in Qi and prana is leading us into myriad labyrinths of scientific trails. Qi, the Chinese energy equivalent of Prana, is measured in acupuncture systems and its flow is directed for promoting health. We even know some of the channels through which Qi energy seems to flow. The channels are called Bonghan system, seen in some parts of the body.[1] Still, we are not sure what kind of physical energy flows through these ducts; is it electromagnetic or some particles that roll through these interlinking systems of channels? Although scientists have postulated laser-like electromagnetic radiations flowing through these links, it is still early to say if this is indeed the case in all acupuncture meridians.

In the tangible domain, two subtle energy carriers come to mind: biophotons and bioelectrons. Biophotons are photons (light particles) that are generated within the body, and these could be measured as they emanate from the skin. Similarly, bioelectrons are available from within the body; these are measured in instruments such as electro-photonic imaging. This aspect will be taken in a later presentation.

Biophotons

Bioluminescence is produced in living organisms such as fireflies and this should not be confused with biophotons. Bioluminescence is produced due to the presence of specific biochemicals in these organisms. The vivid colors emanating from these organisms are for attracting a prey or for species propagation. These biochemicals are not available in all organisms (for example, not in humans). Hence, bioluminescence is observed only in some species. Biophotons, however, are light particles that are generated within the body and are constantly radiated from the body surface. These spontaneous emissions are thought to be associated with generation of free radicals due to energy metabolic processes.[2,3] Since these dynamic metabolic processes are common to most living systems, it is likely all living beings give rise to biophotons. Further, these light emissions are extremely weak and hence cannot be observed by the naked eye. Detections of biophotons need special photon counters which are sensitive to pick up even a single photon in the environment.

In one experiment, photomultiplier tubes were used along with a charge-coupled camera.[3] Any stress to the skin in the form of exposure to ultraviolet radiation or cigarette smoke enhances the emission of biophotons while topical application of ascorbic acid or antioxidant solutions reduces such radiation. It is thought that studies of spontaneous ultraweak photon emission could be used for assessing aging in humans as well as for determining oxidative processes in humans.[3]

It is known further, that after practice of meditation, biophoton emissions from the body decrease; this could be due to reduced free radicals in meditating subjects.[4] Communication and control are two required activities within and between cells to maintain homeostasis. Normally, it is thought that both these functions are achieved through biochemical and neurological means. The coherent light source is now thought to be another arm through which both control and communication are achieved. This may be true especially in long-range communications in the body.[5]

Coherent biophotons as a control signal are proposed in acupuncture theory also.[6] Coherence is a property when the phases of the signals are related precisely as in a laser which gives the laser beam its unique properties. It is tempting at this point to think of biophotons as equivalent to Qi energy as modeled in Traditional Chinese Medicine or to prana in Ayurveda and Yoga. However, it is too early to draw this conclusion. Perhaps, there is a dynamic exchange between Qi/prana and biophotons; the photons in the body in their turn, take part in biocommunication and signaling. Since biophotons are a result of oxidative processes also, there could be complex interrelation between oxidative processes, biophotons, and Qi energy.

Conclusion

As early as in 1923, Gurwitsch, a Russian scientist, observed optical radiation during mitosis in onion roots and called it mitogenetic radiation. Modern biofield theory has extended this hypothesis to postulate electromagnetic interactions between cells for control and for information transfer. These have been called “nonchemical, noncontact cell-to-cell communication.”[7] Action at a distance was introduced in physics more than 150 years ago when Maxwell derived his famous electromagnetic equations. Now, the notion of action at a distance has permeated biophysics also conferring possibilities and problems in living systems that are more difficult to locate and measure.

It is known that oxidative stress is harbinger of many metabolic syndrome disorders.[8] This also seems to contribute to aging and related degeneration in the body. Hence, measuring metabolic syndrome through a consistent method is of importance. It is likely that biophoton emission is a fundamental process and its measurement could portend a stable method; however, measurement method itself is expensive and complex. It is possible that the photon measurements could be substituted or complemented with electron availability in the biosystems. This could become an easy and noninvasive method of measuring oxidative process in the body. This aspect will be taken up later.

While the problems of aging and oxidative stress are inherent in any living system, it is also possible to reverse these processes through practice of Yogaasanas and meditation. Work is also emerging in this area; if life style confers these problems obviously changing lifestyle and reversing and mitigating these degenerative processes is also possible.

Mitochondrial-targeted nanoparticles: Delivery and therapeutic agents in cancer

Author links open overlay
panelChaithanya Ganji [a], Veda Muppala [a], Musaab Khan [a], Ganji Purnachandra Nagaraju [a], Batoul Farran [b]

Highlights

- •
  Dysregulation of mitochondrial metabolism is a hallmark of cancer development.
- •
  Nanoparticles (NPs) enable the efficient and targeted delivery of mitochondrial agents.
- •
  NPs can target key mitochondrial pathways, such as mitochondrial respiration and production of reactive oxygen species.
- •
  Theranostic NPs can enhance the efficiency of photodynamic therapy (PDT), photothermal therapy (PTT) and chemotherapy.

Mitochondria are the powerhouses of cells and modulate the essential metabolic functions required for cellular survival. Various mitochondrial pathways, such as oxidative phosphorylation or production of reactive oxygen species (ROS) are dysregulated during cancer growth and development, rendering them attractive targets against cancer. Thus, the delivery of antitumor agents to mitochondria has emerged as a potential approach for treating cancer. Recent advances in nanotechnology have provided innovative solutions for overcoming the physical barriers posed by the structure of mitochondrial organelles, and have enabled the development of efficient mitochondrial nanoplatforms. In this review, we examine the importance of mitochondria during neoplastic development, explore the most recent smart designs of nano-based systems aimed at targeting mitochondria, and highlight key mitochondrial pathways in cancer cells.

Graphical abstract

Antitumor agents are delivered via nanoparticles (NPs) to the mitochondria. The drugs attack the mitochondria resulting in mitochondrial damage and the release of cytochrome C (Cyto-C). Cyto-C binds with Apaf1 and Caspase-9 to form an apoptosome. The apoptosome activates Caspase 3, which ultimately results in the death of cancer cells.

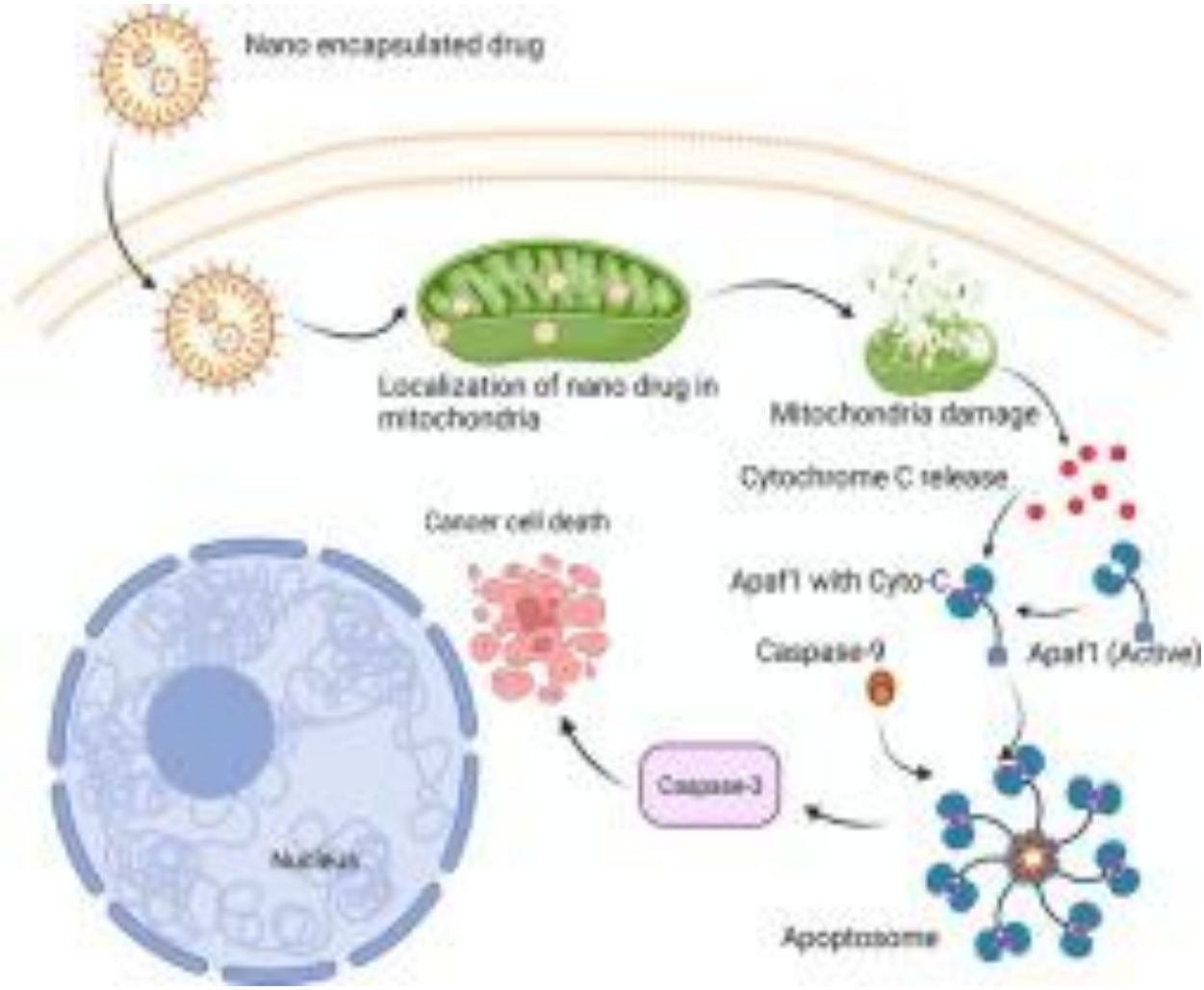

Introduction

Mitochondria are semi-independent organelles that are implicated in energy production, signal transmission, apoptosis modulation, and cell differentiation. They are considered the energy factories or powerhouses of cells, responsible for providing a constant ATP supply [1], [2], [3]. As mitochondria are key components of the cell, their dysregulation largely contributes to tumor development, cancer cell anabolism, uncontrolled tumor replication, resistance to anticancer treatment, and apoptosis. Given their inherent properties, mitochondria promote cancer survival. For instance, mitochondrial glycolysis supplies tumor cells with the ATP required for their survival [4]. In addition, fatty acids undergo oxidation to drive mitochondrial ATP production, further promoting tumor cell survival [4]. Mitochondria support cancer cell invasion and metastatic spread through oxidative phosphorylation (OxPhos), which is mediated by the peroxisome-proliferator regulator [5], [6], [7]. Furthermore, mitochondrial energy metabolism increases the production of reactive oxygen species (ROS), thereby activating SRC protein tyrosine kinases (TKs) and PYK2, and further stimulating metastasis [8]. Recent research indicates that mitochondria-associated membranes are key to determining cancer prosperity versus death. By successfully leveraging

mitochondrial calcium uptake and fine-tuning ER and mitochondrial tethering, cancer cells can modulate Ca^{2+}-driven mitochondrial metabolism and can evade Ca^{2+}-induced cell death [9]. In addition, mitochondria contribute to tumor proliferation and treatment resistance in cancer cells, which upregulate glutamine generation by oxidizing glucose through mechanisms associated with mitochondrial pyruvate dehydrogenase [4]. Hence, the key roles of mitochondria in cancer development render them an attractive therapeutic target. Various mitochondrial agents have been developed and investigated in the pre-clinical setting, with limited success. The failure of these strategies is due to the phospholipid bilayer that surrounds the mitochondria and that hampers effective drug targeting and delivery. These failed experiments highlight the need for smarter delivery platforms that are tailored to overcome the drug delivery challenges.

Advances in nanoparticle (NP) design offer a unique avenue for developing highly innovative customized nanosystems with increased flexibility and biocompatibility in order to bypass the drug delivery hurdles. In this paper, we explore some of the most-studied mitochondrial nanoplatforms and the various mitochondrial pathways that they target, ranging from mitochondrial respiration to ROS production [10]. We also discuss how these nano-mitochondrial agents can inform the design of theranostic platforms that enhance the efficiency of conventional therapeutic modalities such as chemotherapy.

Mitochondria in the pathophysiology of cancer

Defining the function of mitochondria is key to understanding their role in the pathophysiology and development of diseases such as cancer. The first observation of a metabolic change in cancerous cells, the Warburg effect of aerobic glycolysis, was reported a century ago [11]. Otto Warburg noticed that cancers harbor the aberrant ability to take up then ferment glucose into lactate in the presence of oxygen. On the basis of this observation, Warburg hypothesized that defects in mitochondrial

Mitochondrial respiration as a tumor suppressor

Various lethal signaling pathways converge at the mitochondria, inducing mitochondrial outer membrane (MOM) permeabilization and causing the cytosolic secretion of pro-apoptotic factors and the impairment of mitochondrial bioenergetics functions [17]. Unlike healthy cells, tumor cells display anaerobic glycolytic ‘fermentative’ metabolism in the cytoplasm, which is independent of oxygen abundance (the Warburg effect) [18]. The importance of glycolysis in supporting cancer cell proliferation and

Nano-sized mitochondrial delivery systems

Mitochondria represent a key hub for aberrant tumor pathways and a promising therapeutic target for cancer. This concept has led to the design of modulators of apoptosis, a function controlled by the outer mitochondrial membrane (OMM) [17], [20]. Despite these advances, the idea of targeting mitochondrial metabolism remains a

novel concept. Examples of drugs that target the mitochondria include hexokinase isoenzyme inhibitors designed to block the first glycolysis reaction, such as lonidamine,

Targeting the mitochondrial membrane potential

The mitochondria of cancer cells display completely altered bioenergetics and physiological profiles that distinguish them from normal cells. Cancer cells are characterized by altered redox states, higher pH, ROS levels and temperature, increased glutathione (GSH) production, decreased oxygen consumption, aberrant mitochondrial dynamics, and hexokinase II (HK II) upregulation (Figure 1) [48]. The mitochondrial membrane potential (MMP) in malignant cells is hyperpolarized compared to that in

Mitochondrial NPs and PDT

PDT is mediated through ROS generation by photosensitizers (PS) under light irradiation to annihilate tumor niches (Table 1) [84]. Unfortunately, PDT is limited by: (i) short ROS diffusion distance from the PS, (ii) insufficient oxygen in hypoxic TME, and (iii) short penetration depth of the light used in PDT [85]. UCNPs, which can convert NIR light into visible light and stimulate PS to generate ROS and increase tissue penetration, can circumvent those limitations (Figure 3). On the basis of

Mitochondrial NPs for enhanced PTT and chemotherapy

PTT destroys tumor cells by converting the electromagnetic energy of light to thermal energy through a PS that warms cells. Although it specifically generates heat in areas targeted with a photosensitizer, PTT can cause non-specific killing of neighboring tissue as the result of non-specific photosensitizer delivery or heat diffusion. Mitochondria-targeting NPs represent an effective strategy for minimizing this side effect [84]. The nanomaterials that are used for PTT can be subdivided into

Conclusions

Mitochondria contribute to various physiological processes and are promising drug targets for cancer therapy. Nevertheless, their unique structures, characterized by a negatively charged IMM, render them difficult to target. To resolve these limitations, mitochondrial NPs have been engineered specifically to target drug-loaded NPs to the mitochondria, thus achieving rapid localization and accumulation in the mitochondria and improved therapeutic outcomes. Mitochondria-targeting NPs can

Author contributions

Ganji C: writing – original draft. Muppala: writing – original draft. Nagaraju GP: conceptualization, figures, review and editing. Farran B: conceptualization, review and editing.

Chaithanya Ganji is an observer at the Heersink School of Medicine, University of Alabama at Birmingham. He is a student at Harrison High School, Kennesaw, GA, USA.

Ganji's research focuses on meta-analysis and genetic polymorphism in gastrointestinal malignancies. Ganji has received several academic awards at school, county and state level. He is a member of the American Association of Cancer Research (AACR). Recently, he presented his research at the AACR conference in New Orleans, LA, USA.

Low-level laser therapy

Low-level laser therapy (**LLLT**), **cold laser therapy**, **photobiomodulation** (**PBM**)[1][2][3][4] or **red light therapy**[5] is a form of medicine that applies low-level (low-power) lasers or light-emitting diodes (LEDs) to the surface of the body. Whereas high-power lasers are used in laser medicine to cut or destroy tissue, it is claimed that application of low-power lasers relieves pain or stimulates and enhances cell function. The effects appear to be limited to a specified set of wavelengths and new research has demonstrated effectiveness at myopia control.[6] Several such devices are cleared by the United States Food and Drug Administration (FDA), and research shows potential for treating a range of medical problems including rheumatoid arthritis[7] and oral mucositis.[8]

Mechanism

Research is ongoing about the mechanism of LLLT. The effects of LLLT appear to be limited to a specified set of wavelengths of laser,[9] and administering LLLT below the dose range does not appear to be effective.[10] Photochemical reactions are well known in biological research, and LLLT make use of the first law in photochemistry (Grotthuss-Draper law): light must be absorbed by a chemical substance in order for a photochemical reaction to take place. In LLLT that chemical substance is represented by the respiratory enzyme cytochrome c oxidase which is involved in the electron transport chain in mitochondria,[11][12] which is the generally accepted theory.

Medical uses

Various LLLT devices have been promoted for use in treatment of several musculoskeletal conditions including carpal tunnel syndrome (CTS), fibromyalgia, osteoarthritis, and rheumatoid arthritis. They have also been promoted for temporomandibular joint disorders, wound healing, smoking cessation, and tuberculosis. LLLT appears to be effective for preventing oral mucositis in recipients of a stem cell transplant with chemotherapy.[8][13] In other areas, evidence for LLLT remains conflicted. Some studies suggest that LLLT may be modestly effective in relieving short-term pain for rheumatoid arthritis,[7] osteoarthritis,[14] chronic low back pain,[15] acute and chronic neck pain,[16] tendinopathy,[9][17] and chronic joint disorders.[10] The evidence for LLLT being useful in dentistry,[18][19] and in the treatment of wound healing[20] is unclear.

Concerns have been raised in the literature about brain stimulation techniques that rely upon low-level (low-power) lasers and light-emitting diodes (LEDs). The transcranial

photobiomodulation or transcranial low level light therapy is limited in neuromodulation due to several reasons:

- An excessive dose of radiation can be harmful.[21] Therefore, at adequate doses of light there may be stimulation of growth, but at high doses excessive singlet oxygen may be produced and its chemical action may be harmful to cells.[22][21]

- Regarding LED light therapy, this neurostimulation method based on the light-emitting diodes stimulation cannot pass through the skin, only laser can penetrate deeper tissues and stimulate brain areas accordingly. The penetration depth of white light and LED light into the skin increases with increasing wavelength from the UV to the visible light range, and then decreases again in the IR range depending on the selected optical properties. This depth further increases if the thickness of the stratum corneum decreases.[23] Broadband polychromatic light (white light) and LED radiation can only penetrate 0.0017 mm to 5 mm of tissue.[24] For example, research shows that at wavelengths of 450 nm and 650 nm only 1% of the light reaches approximately 1.6 mm and very little reaches 5 mm.[25][26] Only laser radiation can propagate into deeper tissues.

- Since the action spectrum for tissue regeneration and repair consist of more than one wavelength,[27][21] laser and LED light sources may offer some disadvantages,[28] destroying healthy cells.[21] We still lack knowledge of mental processes at the cellular level. The link between neuronal activity and mental processes is still an intriguing research question and a problem in treatment targeting. Therefore, no one can be sure whether the laser beam only reaches the neuronal structures in the brain that need treatment. An undetermined dose of radiation and the target of radiation can destroy healthy cells during the treatment procedure.[21]

Veterinary use

Veterinary clinics use cold laser devices to treat a wide variety of ailments, from arthritis to wounds, on dogs and cats.[29][30] Very little research has been done on the effects of this treatment on animals. Brennen McKenzie, president of the Evidence-Based Veterinary Medicine Association, has stated that "research into cold laser in dogs and cats is sparse and generally low quality. Most studies are small and have minimal or uncertain controls for bias and error".[31][32] While allowing that some studies show promising results, he reports that others do not. While believing that there is enough evidence to warrant further study, he concludes that there is not enough evidence to support routine clinical use of cold laser in animals.

Society and culture

Faroese physician Niels Finsen is believed to be the father of modern light therapy.[33] He used red light to treat smallpox lesions. He received the Nobel Prize in Physiology or Medicine in 1903.[34] Scientific evidence for some of his treatments is

lacking, and later eradication of smallpox and development of antibiotics for tuberculosis rendered light therapy obsolete for these diseases.[35]

Hungarian physician and surgeon Endre Mester (1903–1984) is credited with the discovery of the biological effects of low power lasers,[36] which occurred a few years after the 1960 invention of the ruby laser and the 1961 invention of the helium–neon (HeNe) laser.[11] Mester accidentally discovered that low-level ruby laser light could regrow hair during an attempt to replicate an experiment that showed that such lasers could reduce tumors in mice. The laser he was using was faulty and was not as powerful as he thought. It failed to affect the tumors, but he noticed that in the places where he had shaved the mice in order to do the experiments, the hair grew back more quickly on the treated mice than on those among the control group.[2] He published those results in 1967.[11] He went on to show that low level HeNe light could accelerate wound healing in mice.[11]

By the 1970s, he was applying low level laser light to treat people with skin ulcers.[11] In 1974, he founded the Laser Research Center at the Semmelweis Medical University in Budapest, and continued working there for the remainder of his life.[37] His sons carried on his work and brought it to the United States.[36] By 1987, companies selling lasers were claiming that they could treat pain, accelerate healing of sports injuries, and treat arthritis, but there was little evidence for this at that time.[36] Mester originally called this approach "laser biostimulation"', but it soon became known as “low-level laser therapy" and with the adaptation of light emitting diodes by those studying this approach, it became known as "low-level light therapy", and to resolve confusion around the exact meaning of "low level", the term "photobiomodulation" arose.[2]

Names

The following terms are accepted as alternatives of *low level light therapy* term: LLLT, laser biostimulation, laser phototherapy, low-level laser therapy, low-power laser irradiation, low-power laser therapy, and photobiomodulation therapy. The term *photobiomodulation therapy* is considered the preferred term by industry professionals.[3][4] However LLLT has been marketed and researched under a number of other terms, including red light therapy,[38] low-power laser therapy (LPLT), soft laser therapy, low-intensity laser therapy, low-energy laser therapy, cold laser therapy, bio-stimulation laser therapy, photo-biotherapy, therapeutic laser, and monochromatic infrared light energy (MIRE) therapy.[39] More specific applications sometimes have their own terms, for example when administered to acupuncture points, the procedure is called laser acupuncture. When applied to the head, LLLT may be known as transcranial photobiomodulation, transcranial near-infrared laser therapy (NILT),[40] or transcranial low level light therapy.

Government action

The FDA filed a complaint for injunction in 2014, alleging that company QLaser PMA were marketing their devices as being able to treat “over 200 different diseases and disorders,” including cancer, cardiac arrest, deafness, diabetes, HIV/AIDS, macular

degeneration, and venereal disease. This case resulted in a permanent injunction against the manufacture, marketing, sale, and distribution of those devices in 2015.[41]

In 2017, the owner of QLaser, Robert Lytle, and two of QLaser's distributors were charged with a criminal conspiracy to commit fraud. Lytle pleaded guilty to one count of conspiracy to introduce misbranded medical devices into interstate commerce with the intent to defraud and mislead, and one count of criminal contempt in January 2018. Lytle was sentenced to serve 12 years in prison and made an initial restitution payment of $637,000. Lytle's conspirators were sentenced to 24 months and 15 months, respectively.[42][43]

Research

Demonstration of LLLT with intranasal irradiation

Musculoskeletal

Evidence does not support a benefit in delayed-onset muscle soreness.[48] It may be useful for muscle pain and injuries.[49] A 2008 Cochrane Library review concluded that LLLT has insufficient evidence for treatment of nonspecific low back pain,[50] a finding echoed in a 2010 review of chronic low back pain.[51] A 2015 review found benefit in nonspecific chronic low-back pain.[15] LLLT may be useful in the treatment of both acute and chronic neck pain.[16] In 2013, however, a systematic review and meta-analysis of LLLT for neck pain indicated that the benefit was not of significant importance and that the evidence had a high risk of bias.[52] In a study testing the efficacy of low-level laser therapy treating plantar fasciitis found that LLLT significantly reduces pain in lower extremity tendinopathy and plantar fasciitis in the short and medium terms. [53] The same study also stated that while comparing the effect of LLLT to that of therapeutic ultrasound in persons with patellar tendinopathy, and they found a statistically significant effect in favour of LLLT, both on pain reduction and function.[54]

There are tentative data that LLLT is useful in the short-term treatment of pain caused by rheumatoid arthritis,[7] and possibly chronic joint disorders.[10] Research that compared the effects of LLLT against other treatments, sham treatments, or no treatment at all, and randomized adult patients with rheumatoid arthritis to receive it were considered. These outcomes included pain, functional capacity, adverse events, inflammation, disease activity, range of motion, stiffness in the morning, muscle strength, and quality of life.[55] The findings indicate that the differences between utilizing a sham and an

infrared laser may be negligible or nonexistent in terms of pain, stiffness in the morning, grip strength, functional ability, inflammation, range of motion, disease activity, and side events. We also discovered that the data about the effects of laser acupuncture against reflexology in terms of functional ability, quality of life, and inflammation is quite hazy, and about the effects of red laser versus sham in terms of pain, morning stiffness, and side events.[56] The usefulness of red laser, laser acupuncture, and reflexology in the treatment of RA patients is not well enough demonstrated. [57] A 2019 systematic review and meta-analysis found evidence for pain reduction in osteoarthritis.[14] While it does not appear to improve pain in temporomandibular disorders, it may improve function.[58]

There is tentative evidence of benefit in tendinopathy.[9][17] A 2014 review found benefit in shoulder tendinopathy.[59] A 2014 Cochrane review found tentative evidence that it may help in frozen shoulders.[60]

Mouth

Similarly, the use of lasers to treat chronic periodontitis[18] and to speed healing of infections around dental implants[19] is suggested, but there is insufficient evidence to indicate a use superior to traditional practices.[61] There is tentative evidence for dentin hypersensitivity.[62] It does not appear to be useful for orthodontic pain[63][64] LLLT might be useful for wisdom tooth extraction (complications).[65]

Hair loss

LLLT has been studied as a treatment for hair loss; a review in 2012 found little evidence to support the use of lasers to treat hair loss.[66] A 2014 review found tentative evidence for benefit for lasers,[67] while another 2014 review concluded that the results were mixed, had a high risk of bias, and that its effectiveness was unclear.[68] A 2015 review found tentative evidence of benefit.[69] Additionally, a 2017 review of clinical trials found 10 of 11 trials reviewed "demonstrated significant improvement of androgenic alopecia in comparison to baseline or controls when treated with LLLT."[70]

LLLT is shown to increase hair density and growth in both genders. The types of devices (hat, comb, helmet) and duration did not alter the effectiveness,[71] with more emphasis to be placed on lasers compared to LEDs.[72] Ultraviolet and infrared light are more effective for alopecia areata, while red light and infrared light is more effective for androgenetic alopecia.[73]

Medical reviews suggest that LLLT is as effective or potentially more than other non invasive and traditional therapies like minoxidil and finasteride but further studies such as RCTs, long term follow up studies, and larger double blinded trials need to be conducted to confirm the initial findings.[74][75][76]

Brain injuries

LLLT has been studied for traumatic brain injury (TBI) and stroke among other conditions.[11] When applied to the head it is known as transcranial photobiomodulation or transcranial low level light therapy.

Cancer treatment side effects

LLLT has been studied as a way to reduce pain and swelling in breast-cancer related lymphedema.[77][20] The 2015 systematic review & meta-analysis by Smoot, Chiavola-Larson, et al found: "Moderate-strength evidence supports LLLT in the management of [breast cancer related lymphoedema], with […] reductions in volume and pain immediately after conclusion of LLLT treatments. Greater reductions in volume [of lymph nodes or surrounding tissues] were found with the use of LLLT than in treatments without it."[78]

Stem cells

An ongoing area of research is the application of LLLT for increasing cell proliferation, including stem cells.[79]

Wound healing

Low level laser therapy has been studied as a potential treatment for chronic wounds, and higher-power lasers have sometimes been successfully used to close acute wounds as an alternative to stitching.[80] However, as of 2012 and due to inconsistent results and the low quality of extant research, reviews in the scientific literature have not supported its widespread application.[80][81]

See also

- Blood irradiation therapy – Alternative medical procedure
- Light therapy – Therapy involving intentional exposure to sunlight
- Neurotechnology
- Photomedicine – interdisciplinary field examining the effects of light on human health
- Photorejuvenation – Skin treatment

Green light therapy vs red light therapy – which LED treatment is right for you?

As sales of at-home LED light devices continue to rise, searches for "green light therapy vs red light therapy" are up on Google, too. Targeting different layers of the skin, these two wavelengths work in slightly different ways to deliver distinct results. While one is incredibly beneficial for photodamaged skin, the other is ideal for sensitive skin conditions.

If you're into beauty tech, you're likely familiar with the myriad red light therapy benefits. But what about *green* light therapy? Not as popular as its red light sister, green light is slowly starting to gain traction as more and more people become privy to its skincare benefits. Focusing on the surface of the skin, this light "mode" is said to help reduce redness and improve pigmentation (among other things).

Now a featured light setting in several of the best light therapy devices, users are keen to find out which one is right for them. Ahead, we share answers from the experts to break down the key differences between green light therapy vs red light therapy, including everything you should know before buying a light therapy device.

An expert guide to green light therapy vs red light therapy

How do green light and red light differ?

"Think of red light as the skin revitaliser, reaching deep into the dermis to stimulate collagen production, improve elasticity and repair cells," says Dr. Derrick Phillips, consultant dermatologist. This wavelength, which is extremely popular among the celebrity circuit, is ideal for anyone looking to rejuvenate their skin from within.

"Green light, on the other hand, is the 'calm' wavelength, focusing on the skin's surface to soothe irritation, reduce redness, and even out pigmentation," Dr.

Phillips continues. This means green light is perfect for anyone following a skincare routine for sensitive skin that needs gentle balancing.

What are the benefits of green light vs red light therapy?

“Red light therapy can be beneficial for overall skin health; it can support collagen production and help both calm and heal inflammation – ideal for conditions like acne and rosacea,” explains Dr. Hiba Injibar, consultant dermatologist and founder of the Dermasurge Clinic. “It's essentially a way to press ‘reset’ on stressed skin to restore a healthy glow and is a great non-invasive option for ageing skin to assist in overall skin quality.”

Meanwhile, “green light therapy is typically used to tackle pigmentation, such as the appearance of age spots or post-acne hyperpigmentation, by decreasing the production of melanin,” notes Dr. Maryam Zamani, oculoplastic surgeon and leading facial aesthetics doctor. She adds that green light can also help to reduce inflammation and redness and revitalise the skin around the eyes.

Which skin types do green light and red light suit?

- "**Red light therapy** is gentle enough for most skin types, but it is especially beneficial for mature or photodamaged skin,” explains Dr. Phillips.
- **Green light therapy** is ideal for sensitive skin. “Its calming effect soothes redness without causing irritation, making it a great option for those with sensitive skin conditions like rosacea,” says Dr. Phillips.

Do green light and red light have any downsides?

According to Dr. Injibar, both therapies are typically safe and gentle. She does flag, however, that it’s wise to avoid overuse, which can cause mild irritation or

dryness. “If you have reactive skin, start slowly, allowing your skin to adjust," she recommends. "And, because these treatments can heighten sun sensitivity, always apply your best facial sunscreen afterwards to keep your skin protected and glowing."

“People who are sensitive to light or have a condition that makes their skin hypersensitive to light, such as porphyria, should avoid LED light therapy as it can exacerbate the condition,” warns Dr. Zamani. She adds that certain medications can increase photosensitivity, too (such as tetracycline antibiotics). “Individuals taking these medications should exercise caution when using light therapy," she confirms.

Can green light and red light therapy be used together?

“You can use both in conjunction as they target different layers of the skin; each frequency of wavelength penetrates a different depth of skin – the shorter the wavelength, the deeper it can penetrate,” explains Dr. Zamani. So, while red light works deeper to stimulate collagen and elastin production, green light works on the superficial skin layers to improve pigmentation. “Together, red and green lights bring a restorative harmony for a vibrant, healthy complexion,” agrees Dr. Phillips.

Three of our favourite green and red light therapy devices

Déesse Pro LED Phototherapy Mask
RRP: £1,440

Trusted by professionals and loved by A-listers, this game-changing mask features 770 medical-grade LEDs (that’s *a lot* more than most other LED masks). Spanning four different wavelengths, reap the rewards of red light, blue light, green light and near infrared light. Treatment sessions last 20-minutes and results can be seen in a matter of weeks.

Skin Gym Revilit LED Light Therapy
RRP: £77

For a more affordable LED light therapy device, turn your attention to this skin tool from Skin Gym. A great entry-level gadget, this handheld tool emits red, blue and green light to help tackle redness, acne and pigmentation in just three-minute treatment sessions.

MZ Skin LED 2.0 LightMAX Supercharged LED Mask
RRP: £750

Incredibly comfortable and user-friendly, this luxurious LED face mask from MZ Skin can be used to treat inflammation, breakouts and signs of ageing with its choice of two settings - Red + Infrared or Red + Blue. Use regularly (at least twice a week) for a more radiant and clearer complexion in just eight weeks.

Effects of 6-10 Hz ELF on Brain Waves

David S. Walonick
Minneapolis, MN, May 1990

Introduction • Equipment • Experimental Design • Results • Summary • Additional Observations • The Story of Maynooth • Andrija Puharich's Watch • Electromagnetic Pollution

---

There is evidence that ELF magnetic waves can affect brain waves. This set of experiments was designed to study the effects of ELF rotating magnetic fields on the brain.

The specific ELF frequencies I was interested in studying are 6-10 Hertz. These frequencies are the same as those produced by the human brain in the theta and alpha states. Generally, specific brain wave frequency ranges can be associated with mood or thought patterns. Frequencies below 8 Hertz are considered theta waves. While these seem

to be some of the least understood frequencies, they also seem to be associated with creative, insightful thought. When an artist or scientist has the "aha" experience, there's a good chance he or she is in theta. Alpha frequencies are from 8 to 12 Hertz and are commonly associated with relaxed, meditative states. Most people are in an alpha state during the short time immediately before they fall asleep. Alpha waves are strongest during that twilight state when we're half asleep and half awake. Beta frequencies (above 12 Hertz) coincide with our most "awake" analytical thinking. If you are solving a math problem, your brain is working at beta frequencies. Most of our waking hours as adults are spent in the beta state.

A question of importance is: "If we can electronically shift the brain wave frequencies to alpha or theta, will a person's moods or thought patterns change to those commonly associated with those frequencies?" In other words, if we can electronically move a person's brain waves to the alpha frequencies, will they become more relaxed? Will their state of consciousness change to coincide with their brain waves, even if those brain waves were electronically induced? These are important questions with far reaching implications.

When I began these experiments, I was well aware of the possible ethical implications involved in ELF research. For example, if I were carrying an ELF transmitter operating at alpha frequencies, would the people around me be affected as well? Would they unconsciously gravitate toward me because they'd become more relaxed as they moved closer to me? Would they like me more because they felt "good" when they were around me? What if a salesman were carrying an ELF transmitter? Would people be influenced to buy something because they were more relaxed around the salesman? Could entire populations be influenced to be comfortable with ideas they would normally reject? These, and many others, are serious ethical considerations involved with ELF research. They cannot be taken lightly.

I decided to undertake this research with full knowledge of the ethical implications. While there is the potential for misuse, a desire for knowledge and understanding are part of being human, and the potential benefits to humanity are great. What if we could treat depression, insomnia, anxiety, stress and tension with ELF magnetic fields? What if we could increase intelligence or improve learning? As in any scientific endeavor, there are both positive and negative potential uses for any discovery. One only need look at the development of atomic energy to

understand the benefits/misuse dichotomy. It is my personal belief that the potential benefits to humanity justify the research.

I began by collecting all the available research on ELF fields. Lana Harris, a secondary research specialist, did an excellent job in acquiring virtually all the available research in this area. In addition to a multitude of published journal articles, several military and NASA research reports were ordered. A review of the research showed that most studies had been performed to determine the effects of 50-60 Hertz high voltage power-line fields. Since these are the frequencies of most of the world's electrical power distribution systems, the importance of understanding the effects on plant and animal life are evident. To a much lesser degree, a few researchers had concentrated on lower power and lower frequencies (the focus of this study).

EQUIPMENT

The equipment required for this research was easily attainable, with the notable exception of a stable frequency counter with .01 Hertz resolution. Accurate frequency measurements were essential for this research, so I designed and built a digital frequency counter capable of measuring frequency to the hundredth of a Hertz (plus or minus .005 Hertz). A 100 KHz crystal Colpitt's oscillator (calibrated with WWV) was used as a time base and divided by ten to the seventh power to attain the desired resolution.

Other equipment used is: a Biosone II Brainwave Monitor and Myosone 404 EMG Monitor (Bio-Logic Devices, Inc., 81 Plymouth Rd., Plainview, NY 11803); a Model 3011 Digital Display Function Generator (BK Precision Dynascan Corp., 6460 West Cortland St., Chicago, IL 60635); and IBM PC compatible computer with a clock speed of 7.16 MHz (the faster the clock speed the better); a SAC-12 A to D signal acquisition board (Qua Tech, Inc., 478 E. Exchange St., Akron, OH 44308); a Codas II video board and software release 3 (Dataq Instruments, Inc., 825 Sweitzer Ave., Akron OH 44311); a Fluke 77 digital multimeter (John Fluke Mfg. Co., Inc., PO Box C9090, Everett, WA 98260); and StatPac Gold statistical analysis software (Walonick Associates, Inc., 6500 Nicollet Ave. S., Minneapolis, MN 55423).

The transducer was a 24" diameter hand-wound coil, consisting of 1000′ of #25 magnetic wire. The coil had a DC resistance of 32.4 ohms. It was mounted on a 26" square piece of Bakelite board for stability. Two

dowels were mounted with plastic ties onto the board so they extended 24" from opposite sides of the board and the entire apparatus was secured by two microphone stands.

[33]

EXPERIMENTAL DESIGN

All twenty-two subjects were friends or acquaintances of the author. There was no remuneration to participants. The excitement or novelty of participating in a brain wave research experiment seemed to provide sufficient reward in and of itself.

Subjects were sent a pre-experiment letter briefly describing the intent of the experiment and what they could expect. They were asked not to use any drugs or alcohol for 24 hours before their appointment, and not to wear any metal jewelry. (It was thought that metal jewelry might distort the magnetic field, thus creating uncontrolled inconsistencies between subjects.)

Upon arrival at the laboratory, participants were given a short orientation to the procedure and any questions they had were answered. They were hooked up to the EEG monitor (frontal to occipital, midline) and then allowed to listen to a relaxation tape for five minutes. The purpose of the relaxation tape was to establish a "relaxation level" baseline and to relieve some of the anxiety associated with the experiment. At the end of five minutes, the headphones were removed and the subject was told they were at a relaxation level of 5 on a scale from zero to ten (0 being very tense and 10 being very relaxed). This was the baseline they were to use for reporting their relaxation level following each ELF exposure. Subjects were told that they could choose to stop the experiment at any time.

Each ELF exposure consisted of a ten second, sine-wave transmission separated from one another by 45 - 60 seconds of no exposure. The voltage fed to the coil was 3.1 VAC (RMS).

The coil was positioned 18" in front of the subjects head. The outputs from the ELF transmitter (function generator) and the brain wave monitor were fed directly into the computer A to D board, allowing both to be displayed on the computer monitor (and recorded on disk) simultaneously. The sampling rate of the A to D converter was set at 2000 samples per second for the entire experiment. This was sufficient to

visually detect differences of .1 Hertz between the ELF and brain wave frequencies. Subjects were not told when a transmission was beginning. However, at the end of each transmission, they were asked to "report". This was their current relaxation level based on the zero to ten scale. They also reported any feelings they had experienced and these were recorded verbatim.

Twenty-one frequencies were presented to each subject (from 6 to 10 Hertz in increments of .2 Hertz. For half the subjects, these frequencies were randomly selected. For the other subjects, they began at 10 Hertz and were decreased by .2 Hertz with each transmission. Subjects were not told the order of frequencies that would be presented to them.

Post acquisition software was used to visually examine the coherence (frequencies) and synchronously (phase relationship) between the transmitted ELF and prominent brain waves.

RESULTS

Examination of the computer data revealed substantial differences between subjects. Some subjects showed lock-on (entrainment) over a wide frequency range, while other subjects showed no lock-on whatsoever. In general, lock-on occurred most frequently from 8.6 to 10 Hertz and less frequently below 8.6 Hertz.

One subject displayed lock-on for all frequencies from 7.4 to 10 Hertz. Two subjects displayed no lock-on over the entire frequency range. While I did not test a sufficient number of subjects to be statistically significant, I suspect that susceptibility to ELF entrainment follows the normal (bell-shaped) curve. At this time, I do not have any hypothesis that would allow us to predict who is susceptible and who is not.

Several interesting observations were readily apparent. Lock-on generally occurred very rapidly . . . within a quarter of a second in most cases. If lock-on did not occur at a specific frequency in the first second, it didn't at all. When the brain did lock on, the amplitude of the brain waves increased to nearly double their normal size. This is typical for naturally (non-ELF) produced alpha patterns. The brain locked on to higher frequencies (9-10 Hertz) more readily, and maintained the lock-on for the entire duration of the transmission. As the frequency was lowered (below 8.6 Hertz), lock-on for most subjects occurred in bursts, rather than being continuous. For example, there might be immediate lock-on for two

seconds; then the brain would "fight" the ELF frequency for a quarter of a second, and then lock-on again for another few seconds, etc.. I use the word "fight" because it looked like the brain was fighting the ELF to maintain its own frequency. The "fight" was characterized by low amplitude beta frequencies in the 15-20 Hertz range. These may, of course, have simply been analytical type thoughts, but they were not observed when the frequency was in the 9-10 Hertz range. This "fight" became more frequent as the frequency was lowered, until no lock-on was observed at all.

None of the subjects were able to consciously detect the presence of the ELF field. One female subject was able to detect whenever the field started or ended, but could not accurately say when if it was on or off at any given time. In other words, she was able to detect the change in the magnetic field, but not the presence or absence of the magnetic field itself. She thought she felt it because it aggravated her sinuses. When lock-on occurred, the brain waves lagged behind the transmitted ELF. This appeared to have been the "reaction time" of the brain to the ELF waves (approximately 60-80 milliseconds). More accurate experimentation is needed to explore this relationship.

Subjects verbatim reports were quite revealing. (Keep in mind that none of the subjects actually said they felt the ELFs.) The most common verbatim reports occurred between 8.6 and 9.6 Hertz. Common statements were subtle [34]"tingling" sensations in the fingers, arms, legs, teeth, and roof of the mouth. Two subjects reported a "metallic" feeling in their mouth. One subject reported a "tightness" in the chest and another subject reported a "tightness" in the stomach. Several subjects also reported sensations when the ELF frequency was between 6 and 7 Hertz. The verbatim responses in this range were "ringing" in the ears, "flushed" face, "fatigued", "tightening" in the chest and "increasing" pulse.

Lock-on occurred at lower frequencies more often when the transmitted frequencies were progressively lowered, rather than randomly presented. It would seem that the brain prefers a gradual lowering of frequency rather than a sudden or abrupt change in frequency. This may have been due to the extremely short duration of each transmission (10 seconds). It may be that this effect would disappear if longer transmission times were used.

There was no significant correlation between subjects reported level of relaxation and the ELF frequency or the occurrence of lock-on.

Again, this may have been due to the extremely short duration of each transmission.

Summary

It is clear from these experiments that brain waves do in fact lock on to artificially produced ELFs in the 6 - 10 Hertz range. It is equally clear that the 10 second transmission was not sufficient to alter subjects moods to any consistent degree.

Additional Observations

Since my original experiment, I have continued to study the interaction of ELF's and brain waves. These mini-experiments were conducted more informally than my original experiment and the observations are based on only one or two subjects. They should be considered only observations until confirmed by additional study.

1. A sine wave produces lock-on more readily than a square wave or a triangle wave. A sine wave output produces a rotating magnetic field where there is a gradual build up, collapse and reversal of the field intensity. A square wave output produces a pulsed alternating magnetic field where the build-up, collapse and reversal of the magnetic field is more abrupt.

2. The brain is sensitive to a wide range of intensities. I have observed lock-on with power settings down to one half of a milliwatt.

3. Psychics and "sensitives" are neither more or less prone to lock-on than anyone else. I have tested two well-known psychics and a Kahuna from Hawaii. While all three subjects produced more alpha that usual, it was not related to the ELF generator and they did not show unusual lock-on. It is interesting to note, that the woman who could "feel" when the field switched off and on (in my first experiment) was one of these psychics.

4. Extended exposure to ELF's does alter moods, but the effect is subtle. I was not able to duplicate the "dramatic psychoactive" effect that Robert Beck has reported. Low frequencies (below 8 Hz) seem to produce a general agitation or uneasiness, while higher frequencies (8.6-10 Hz) produce a general feeling of relaxation. These are not profound effects like drug induced mood changes. The subject is not aware of any change in his consciousness or mood. From his perspective, nothing has changed. However, an outside observer can detect subtle changes (e.g. body

movement). I have confirmed this by monitoring muscle activity with an EMG monitor.

5. I have exposed myself to ELFs for one and two hour durations and have found that the frequencies from 8.6 to 9.8 Hertz to be sleep inducing; however, it is impossible to eliminate the placebo effect from experiments I performed on myself.

6. I built and distributed several portable ELF generators for testing. I have received many reports that indicate that falling asleep with the ELF generator operating is probably not a good idea. People don't feel rested when they sleep with the ELF generator on. My personal experience supports this. ELF's may inhibit dreaming which is necessary for normal brain functioning.

7. I have found three definite beneficial uses for the ELF generator: a) for relaxation, b) to eliminate jet lag, and c) the elimination of seizures in a dog.

THE STORY OF MAYNOOTH

Shortly after completing my first experiments, my neighbor's dog began to have seizures. Maynooth was a one year old, 190 pound Irish Wolfhound. His seizures were occurring four to five times a week. A seizure by a 190 pound dog is not a small affair. He would trash around wildly with no awareness of his surroundings. The seizures would last 10-30 minutes. My neighbors took Maynooth to the vet, who prescribed phenobarbital to control the seizures. The drug was not effective and Maynooth continued to have regular seizures.

After discussing Maynooth's condition with my neighbor, we decided to try a portable ELF generator that Maynooth could wear to control his seizures. Seizures are accompanied by wild fluctuations in brain wave activity. We hypothesized that a portable ELF generator could control the seizures by stabilizing Maynooth's brain waves. If we could get Maynooth's brain to lock-on to an ELF frequency, we could in effect, eliminate the seizures.

I constructed a portable ELF generator about the size of a pack of cigarettes. The ELF generator was powered by a nine volt battery and had two frequencies, selectable by a toggle switch (10.0 Hz and 7.83 Hz). The 10 Hz frequency was chosen because previous experiments had shown that lock-on was more likely to occur at higher frequencies (i.e., closer to the prominent frequency of the brain). The 7.83 Hz frequency was chosen

because it is the resonant frequency of the Earth and naturally occurring low intensity magnetic [35]radiation can be detected at this frequency (Schumann, 1952).

The schematic for the portable ELF generator is illustrated. It is a twin-T oscillator followed by a high power 386 amplifier. The twin-T was chosen because of its high stability and low distortion sign wave. Construction is straight forward and the placement of parts is not critical. All parts are readily available. The two 10K frequency adjustment pots should be 10-20 turn trim pots to allow precise frequency adjustment. The 10K output level adjustment pot should be set so that the output feeding the coil is less that 100 milliwatts to comply with FCC regulations (I set Maynooth's to 10 milliwatts). The coil itself is not critical and can be wound on any iron core. Use only an alkaline or nickel-cadmium battery.

Maynooth began wearing the generator in the spring of 1988. We tried the 10 Hz frequency first. The results of the experiment were astounding to say the least. Maynooth's seizures stopped immediately when he began wearing the generator. Furthermore, Maynooth was able to completely stop taking the phenobarbital and the seizures have remained in remission. For the first three months, Maynooth wore the generator all the time in a cloth pouch from his collar. After that, the generator was only used at night and simply placed near his sleeping area.

Maynooth has had a total of three seizures following his first use of the generator. Two of these could be traced to malfunctions with the generator. The first was a broken wire from the battery connector and the second was a dead battery. The third seizure could not be explained by a hardware malfunction, although Maynooth was only using the generator during the night and the seizure occurred during the day. It should be noted, however, that this seizure was mild in comparison to his prior episodes.

Maynooth's owners were so convinced of the efficacy of the ELF generator, that they asked me to make a spare generator in case the one they had broke. Maynooth's vet (at the University of Minnesota) showed curiosity in the generator, but not enough to explore it further. They preferred to remain with a drug treatment, even though it had proven to be ineffective. Fortunately, Maynooth's owners had more sense.

Maynooth still uses the ELF generator in his sleeping area at night. The rechargeable battery is charged during the day so it is fresh each night. (The battery lasts about 6-8 hours at a 10 milliwatt power setting).

Andrija Puharich's Watch

Dr. Andrija Puharich sells a watch that he claims will work a shield for ambient high frequency ELF's (40-100 Hz). An important feature of this watch would include shielding from 60 Hz power lines. I had the opportunity to try one of his watches for a few days. The owner was quite reluctant to part with it so I had to run all tests over just one weekend.

It is quite easy to monitor ambient 60 Hz radiation being absorbed by your body. Simply touch the probe of any oscilloscope and you can watch the 60 Hz wave. Your body is acting as an antenna and the amplitude on the oscilloscope is an indication of the amount of radiation you're absorbing. I found no difference in the amplitude when I was wearing the watch or when it was removed by a distance of four miles.

I attempted to determine if there was any measurable magnetic output from the watch. I used a large roll of magnetic wire as a pickup coil and connected it to the input of an EEG monitor with five microvolt sensitivity. The EEG voltage was fed directly to the A to D board of the computer. The equipment was tested for proper functioning by bringing a magnet in proximity to the pickup coil. A weak magnet moving within six inches of the pickup coil would drive the EEG monitor into saturation. The watch was placed against the coil but I could not pick up any magnetic fields from the watch. This surprised me because I was using very sensitive equipment and the watch had to be producing a magnetic field because it was using a battery. Anytime there is a current flowing (even the small current required to power a watch), there is always a magnetic field created. Either the watch was cancelling it's own magnetic field or my equipment was not sensitive enough to measure it. (It turned out to be the latter).

The final test was to hook myself up to the EEG monitor while I was wearing the watch. The output was fed into the computer so that I could do posthoc analysis. I wore the watch for 15 minutes and recorded my brain waves. The incidence of beta and alpha frequencies was not different from my "usual" brain waves. I could not substantiate Puharich's claim that the watch would act as a filter with a center frequency of 10 Hz. This particular finding may not be accurate because my excitement with

the experiment may have inhibited the alpha centering that Puharich refers to.

Since I had told the person I borrowed it from that I'd take good care of the watch, that precluded the idea of disassembling it. I carried the watch with me in my backpack that weekend. As luck would have it, the back cover of the watch fell off and I got to examine the inside.

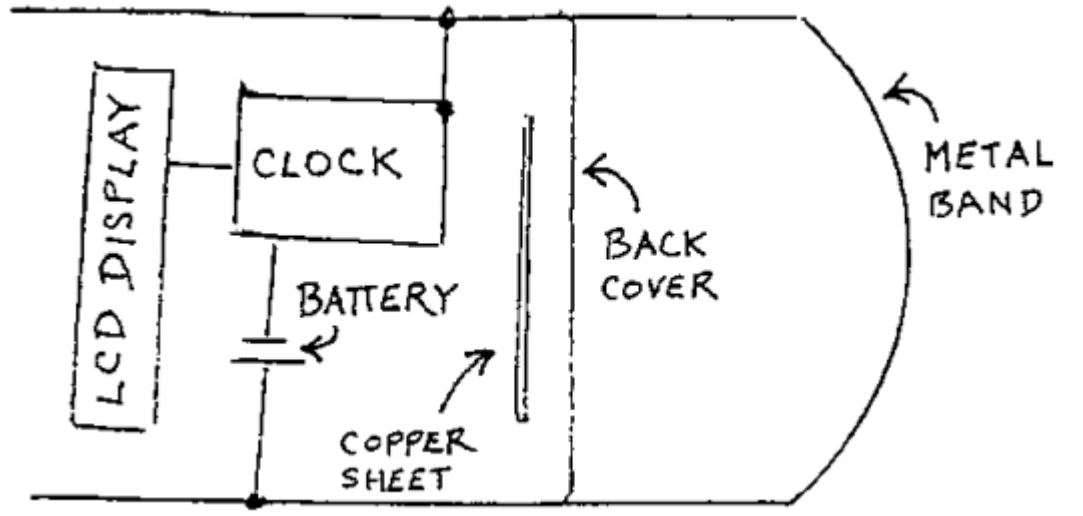

It is a digital "over-the-counter" type watch. As far as I could tell, the watch was normal in every way except that there was a square sheet of copper (about 1 cm square), wrapped in plastic packing tape inside the back cover. The tape was obviously used to insulate the copper from the electronics of the watch and the back cover.

[36]

With the copper removed, my equipment could still not detect the magnetic fluctuations produced by the watch. If the copper sheet does do anything, my equipment was not sensitive enough to measure it. This indicates that the amplitude of the magnetic field produced by the watch was very low, probably around the amplitude of the naturally occurring magnetic fluctuations of the earth.

I do not know whether Puharich's watch works. It did not reduce the electromagnetic radiation that my body was absorbing, nor did it alter my brain wave pattern in any way I could detect. My current understanding of ELF's, electronics and magnetics does not provide a theoretical foundation for the efficacy of the watch.

Electromagnetic Pollution

When I began my research, I was only interested in the effects of ELF's on brain waves. I have since come to believe that ELF's are only the tip of the iceberg. Electromagnetic radiation may be the most harmful pollutant in our society. There is mounting statistical evidence that cancer and other diseases can be triggered by electromagnetic waves.

ELF pulse-modulated radio waves work at the cellular level. Cancer and birth defects have been increasing in this country since about 1950 (as television became popular). The average resonant frequency of the body is around 82 MHz. It is no coincidence that this is near the middle of the VHF TV band.

Even low intensity 60 Hz fields are capable of causing DNA damage and weakening the immune system. Cancer cells exposed to 60 Hz electromagnetic fields for 24 hours show a sixfold increase in their growth rate.

The evidence is becoming overwhelming that cellular functions can be switched on and off through frequency specific electromagnetic radiation that induces nuclear magnetic resonance in the cell. We may find that many diseases can be caused or cured by frequency specific radiation that is ELF pulse modulated.

In our technological society, there are few places to go where you will not be exposed to electromagnetic radiation. Television, radio and microwave radiation are abundant in all metropolitan areas. High voltage 60 Hz power lines crisscross the country. Microwaves (one of the most dangerous) are becoming increasingly common. The FCC has started to grant licences to use microwaves for cellular phones.

The powers that control the energy and communications industries will stop at no end to prevent the public from learning the truth. Their financial health depends on it. Since the military is one of the largest producers of high power electromagnetic radiation, it is not likely that we can count on government intervention.

We have probably reached a point where the only solution is in the form of a portable shield device. ELF generators may be one possible solution. My current research is in this area.

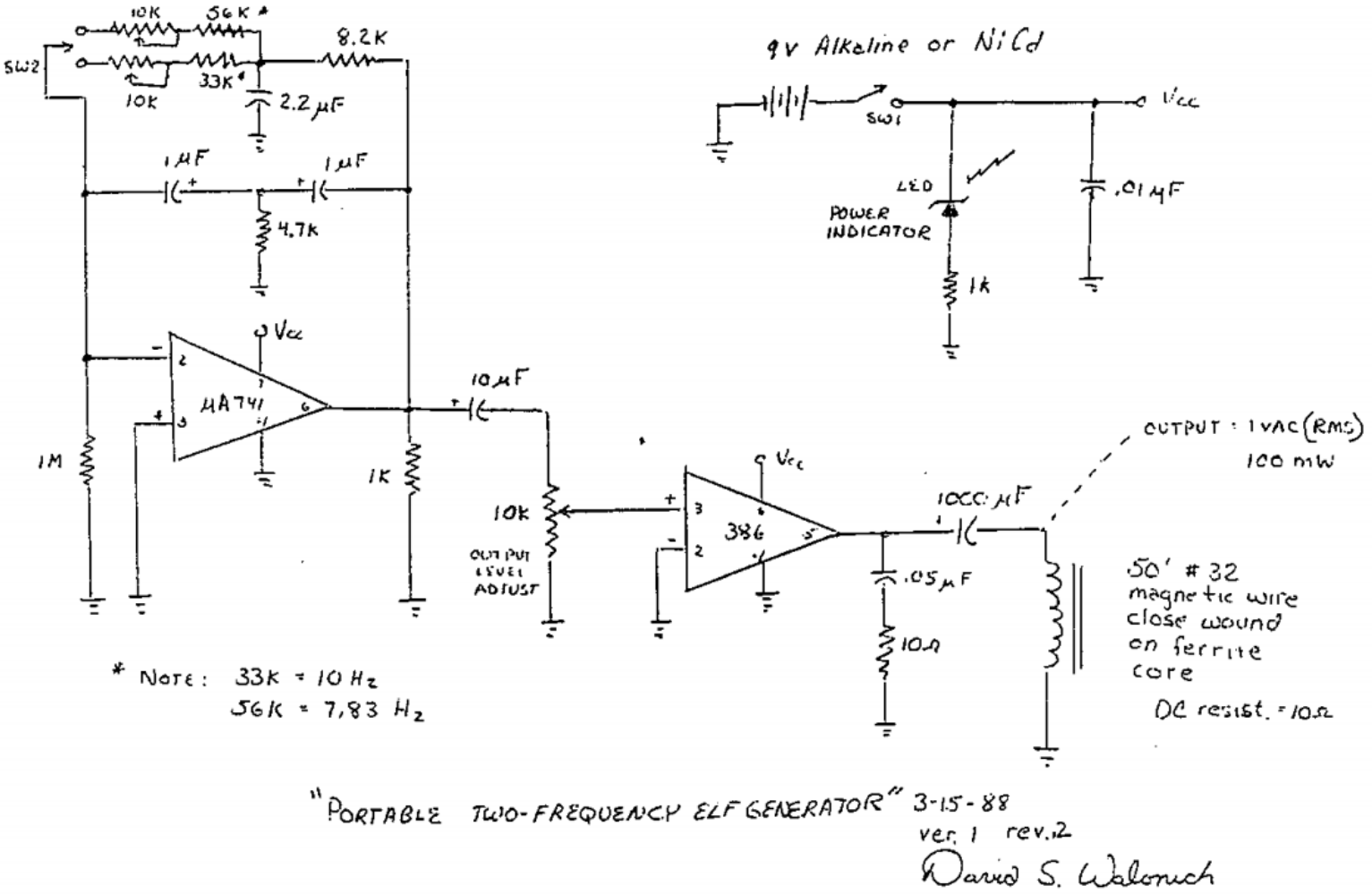

---

*Seeking **more information** on the potential applications of ELF? Explore our growing selection of articles on the use and misuse of ELF (Extremely Low Frequency), as well as other forms of radio research and variable frequency phenomena.*

References

1. Dr. Puharich's watch was branded as **"Teslar"**, named (naturally) for Nikola Tesla, and sold through **ELF Cocoon Corp**. The technology has been reported to have been a small electromagnetic generator that imitates the

Earth's natural magnetic field frequency; refer to Philip Coppens' "The Stargate Conundrum: The US Government's Secret Pursuit of the Psychic Drug" (philipcoppens.com) for Puharich's own words, and and Dr. Anthony Scott-Morley's "The Teslar Wrist Watch" (archive.org). A number of imitators have appeared since the passing of Puharich, though, as one might expect, it is unclear if any of them offer anything resembling the original.
